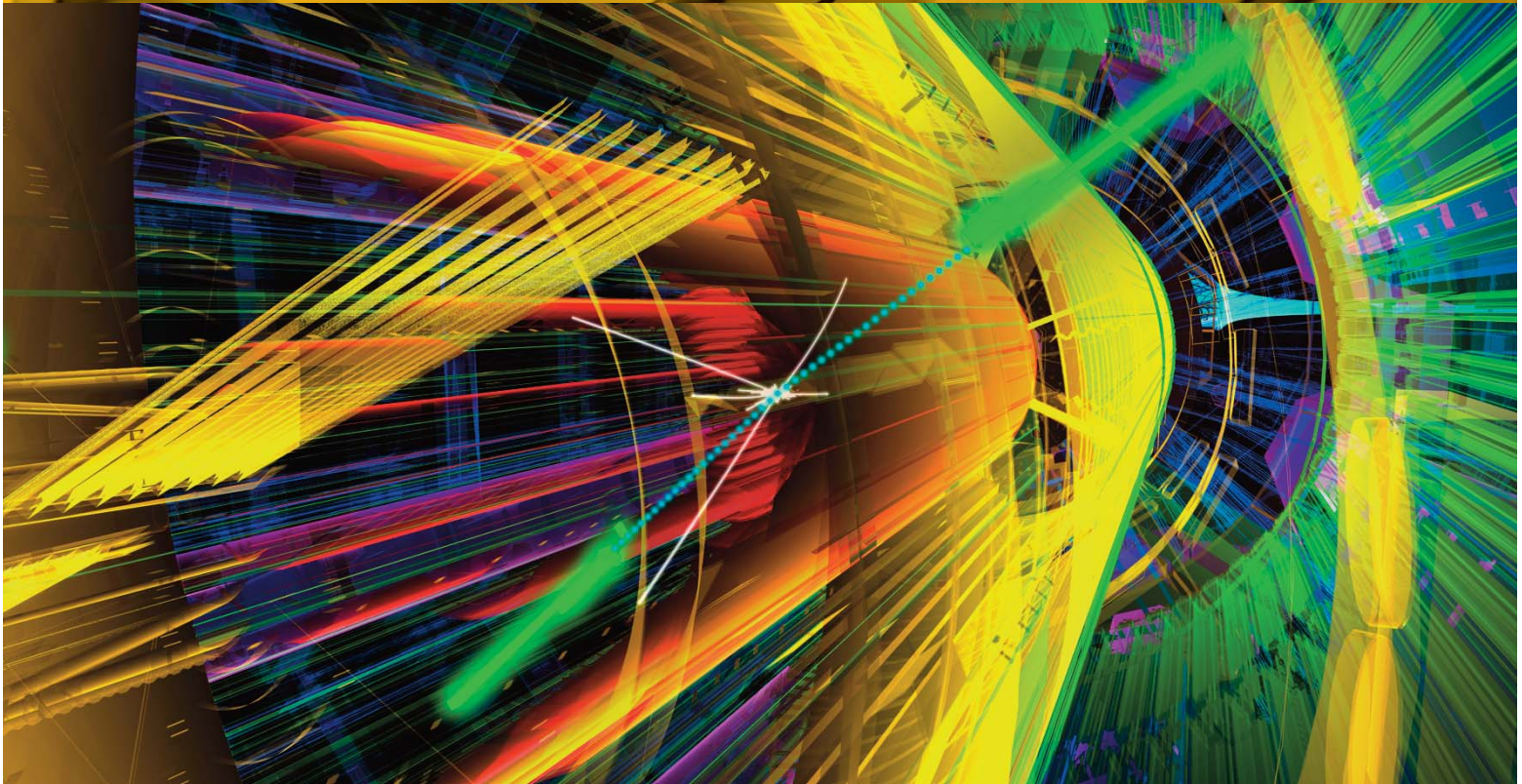


Successes

Highlights from 2008–2012

4



Courtesy: ATLAS Collaboration © 2013 CERN

061	4.1 Introduction
063	4.2 Advancing Knowledge
172	4.3 Creating Future Leaders
182	4.4 Generating Societal and Economic Benefits

CHAPTER 4 | SUCCESSES: HIGHLIGHTS FROM 2008–2012

COMPLETE TABLE OF CONTENTS

4.1 Introduction	061	4.3 Creating Future Leaders	172
4.2 Advancing Knowledge	063	4.3.1 Direct Research Experiences for Young People	173
4.2.1 Fundamental Constituents of Matter and Their Interactions	063	4.3.2 Informal Science Education	176
4.2.1.1 Direct Particle Production Searches	064	4.3.3 Outcomes	181
4.2.1.2 Neutrino and Dark Matter Physics	074	4.4 Generating Societal and Economic Benefits	182
4.2.1.3 Fundamental Symmetries	080	4.4.1 Results from Advanced Applied Physics Solutions, Inc.	183
4.2.1.4 Weak Interaction Studies	089	4.4.2 Results from TRIUMF's Innovation and Industrial Partnerships	187
4.2.2 Strongly Interacting Systems: From Nuclei to Stellar Explosions	095	4.4.3 Results from Modeling Economic Impact	190
4.2.2.1 From QCD to Nuclear Forces	096	4.4.4 Conclusion	194
4.2.2.2 Nuclear Forces and Exotic Nuclei	100		
4.2.2.3 Collective States in Nuclei	107		
4.2.2.4. Nuclear Astrophysics	110		
4.2.3 Nuclear Medicine	119		
4.2.3.1 Introduction	119		
4.2.3.2 Alternative Production Methods for Tc-99m	119		
4.2.3.3 Medical Isotope Production	121		
4.2.3.4 Technological Innovations	124		
4.2.3.5 Advancing Radiopharmaceutical Synthesis and Application	127		
4.2.3.6 Proton Therapy	131		
4.2.4 Molecular and Materials Science	133		
4.2.4.1. Background	133		
4.2.4.2. Magnetism	136		
4.2.4.3 Superconductivity	140		
4.2.4.4 Muon Chemistry	145		
4.2.4.5 β -NMR	151		
4.2.4.6 Radiation Induced Effects in Materials and Electronics	156		
4.2.5 Accelerator Science & Technology	158		
4.2.5.1 System Development and Upgrades	158		
4.2.5.2 Improvements to Machine Performance for Existing Accelerator Complex	160		
4.2.5.3 Design and Modeling	163		
4.2.5.4 Accelerator Science	166		
4.2.5.5 External Collaborations	168		
4.2.5.6 Other Activities	169		
4.2.6 Detector Science and Technology	170		

4.1 INTRODUCTION

The scientific enterprise drives three basic benefits for society: advancing knowledge, creating future leaders, and generating direct societal benefit and economic growth. This chapter is organized to show how TRIUMF has contributed to each of these three areas. The recent successes enjoyed by TRIUMF in all three areas have been noteworthy. This is evidenced by the quantity and quality of publications, by the positive attention received from the press, by the number of invitations TRIUMF scientists receive to speak at conferences, by prestigious awards, and by the success of companies TRIUMF has helped foster.

TRIUMF is working to advance knowledge on many fronts: fundamental constituents of matter and their interactions, strongly interacting systems, from nuclei to stellar explosions, nuclear medicine, molecular and materials science, and accelerator science (please see Figure 1 in Section 2.2. for an overview).

The first three of these fronts can be combined under the rubric: subatomic physics. The study of subatomic physics is the study of the entire spectrum, from nuclear to ever-decreasing sub-nuclear scales. TRIUMF scientists are not only involved in but are leaders at both extremes of the scales, and this is an impressive feat. Understanding the nature and origin of elementary particles and the forces that are responsible for their interaction is a key area of research at TRIUMF. The parameters of the Standard Model of particle physics have been tested to extreme precision and so far attempts to disprove any aspect of it have failed. But while physicists have established with great precision the overall validity of the Standard Model to describe the bulk of matter, the ongoing task is to obtain a deeper understanding of its applicability to a wider range of phenomena. Strong evidence for the Higgs particle, a key component of the Standard Model, has come about recently through the ATLAS experiment, and its properties are being investigated. Canada and TRIUMF have played a well-recognized leadership role within the international collaboration.

Our quest has shifted from testing the Standard Model to looking for chinks in the armour, and this can be done through searches for new particles. These searches involve very high precision measurements of Standard Model observables, or of phenomena forbidden or suppressed in the Standard Model. Indeed, these “indirect” signatures of new physics can probe very large energy scales, i.e., scales that are not accessible in the laboratory. The lightest new particle may be a candidate as dark matter particle and searches are ongoing. Nuclear physics measurements of the electric dipole moment can also probe very large energy scales and provide complementarity, and experiments conducted at TRIUMF are poised to lead the way in this field. Other high-precision tests are being carried out with antihydrogen or by using the atomic nucleus as a laboratory.

Properties of the elusive neutrino have been extensively studied by TRIUMF scientists at experiments based at accelerators (T2K) and deep underground (SNO). The TRIUMF-conceived “off-axis” method for long baseline neutrino measurements is now used worldwide. Massive neutrinos and neutrino oscillations have challenged the Standard Model, and with recent confirmation (T2K) of one type of neutrino transmutation that allows sensitivity to CP violation, this will open the path towards a better understanding of the origin of matter-antimatter asymmetry in the universe from neutrinos.

The theory of strong interactions (QCD) is relevant for a large part of the TRIUMF subatomic program, from ISAC to the Large Hadron Collider at CERN. QCD, through a low-energy effective theory, is the basis for understanding the interactions that bind nuclei. It is used to explain the structure of hadrons, and also to form the theoretical foundation for nuclear physics studies, providing a useful meeting ground between theory and experiment.

Primordial nucleosynthesis is the formation of nuclei that occurred during the cooling immediately following the Big Bang, producing H, He, and Li. All other chemical elements in the universe were produced as a result of nuclear reactions occurring in stars, during supernovae explosions, novae, neutron-star mergers, etc. It is a central goal in physics to explain the origin of matter in the universe, and nuclear astrophysics addresses the many fundamental questions involving nuclear physics.

Studying matter under extreme conditions, such as very high densities and temperatures and/or extreme proton-to-neutron ratios is undertaken at the unique facilities provided by ISAC. Under such conditions, very short-lived exotic nuclei are produced that do not exist under “regular” everyday conditions but that play decisive roles in the understanding of key processes. This latter field has benefited enormously from the ISAC radioactive-beam facility that allows for the measurement of nuclear reactions involving nuclei of relevance to astrophysics. These include measurements of the various nuclear capture processes and the determination of masses, half-lives, and structures of rare nuclei that occur in cataclysmic stellar environments such as novae or supernovae explosions. The TITAN experiment measures the mass of short-lived isotopes with high precision, but also demonstrates the reach of such an experiment to astrophysics, fundamental symmetries, nuclear isomers, and laser and X-ray spectroscopy. Jens Dilling (the leader of TITAN) and Ritu Kanungo (a leading TRIUMF collaborator from Saint Mary’s University) were among the select invitees of the 152nd Nobel Symposium in Gothenburg, Sweden, on *Physics with Radioactive Beams*.

As a multi-program laboratory, TRIUMF also supports interdisciplinary projects that cut across the traditional academic disciplines. The ALPHA project is a perfect example; the Canadian team includes particle physicists, condensed-matter physicists, atomic physicists, and accelerator scientists in a premier experiment to trap and study antihydrogen at CERN. TRIUMF scientists are involved in all aspects of the experiment; electronics and data-acquisition software were developed at TRIUMF and a cryostat was built with TRIUMF expertise.

CMMS is the acronym for the Centre for Molecular and Materials Science at TRIUMF. This TRIUMF facility enables an international community of chemists, condensed matter physicists, and materials scientists to utilize the powerful experimental capabilities of the muon and polarized nuclei as atomic-scale local probes of matter. The research program is multi-faceted, from a broad range of fundamental studies in systems of ever-increasing complexity and sophistication, to the characterization of modern materials and industrial processes. TRIUMF is the sole provider of muon beams in the Americas and one of only four institutions in the world to provide similar experimental capabilities.

Radioactive nuclei from TRIUMF’s ISAC-I can be used to probe materials from 5–400 nm below the surface, using the techniques of β -NMR (beta-detected nuclear magnetic resonance) and β -NQR (beta-detected nuclear quadrupole resonance). The CMMS program now encompasses these techniques. To date, β -NM(Q)R experiments have been successfully carried out on surface and interface proximity effects in normal metals, superconductors, systems with structural and quantum phase transitions, and on the properties of magnetic multi- and mono-layers. β -NQR can also be used to measure the ground state quadrupole moment of a nucleus.

The nuclear medicine program at TRIUMF is supported by the strength and expertise of the accelerator scientists who provide isotopes and radiopharmaceuticals for biological and imaging studies. The power of accelerators and beams for the production of isotopes is particularly noteworthy in this Five-Year Plan because a solution was found to the Tc-99m crisis. Through TRIUMF’s leadership, three institutions in Canada are now capable of producing Tc-99m using cyclotrons, paving the way for a safe, secure supply of this critical isotope for years to come. Many cardiac and cancer patients will continue to receive life-saving medical scans after the cessation of isotope production from Chalk River in 2016.

Training future leaders is an important part of TRIUMF’s mandate. It provides direct research experiences and informal science education for thousands of people, helping them to thrive in the increasingly technology driven world. The training of highly qualified personnel is evident, not only for graduate and postdoctoral students—many of whom have moved on to prestigious positions—but also for technicians, engineers, etc.

The co-op program has been very successful, and the graduate student summer institutes have proven to be popular. The open houses and outreach events at TRIUMF and Science World BC at Telus World of Science, and in the local university communities, are popular and provide a vital link to the community.

Science is supported because it is perceived to be useful and indeed it is. TRIUMF puts great emphasis on not just learning about how the universe works, but on putting that knowledge, and the techniques used to acquire that knowledge, to practical use. One avenue is the medical program, which treats ocular melanoma and provides rare isotopes for medical studies.

A second avenue is the commercialization of TRIUMF's technical knowledge. In 2008, TRIUMF was awarded funds by the Networks of Centres of Excellence Program to launch a Centre of Excellence for Commercialization and Research called Advanced Applied Physics Solutions, Inc., (AAPS). In addition TRIUMF beams are used for a number of applications, including the irradiation of electronics components used in the space and aeronautics industry.

This chapter of the report expands on all these avenues, detailing the results and progress enjoyed over the past five years and sets the stage for the future. In the following chapter (Chapter 5) where the facilities are described, the role of TRIUMF in each of these activities is given along with a list of the national and international partners with whom TRIUMF has teamed up for each topic.

4.2 ADVANCING KNOWLEDGE

TRIUMF is predominantly a basic science laboratory that addresses fundamental questions in nuclear and particle physics, develops next-generation accelerator technology, and advances knowledge in nuclear medicine as well as molecular and material science. As described in this chapter, TRIUMF has made major contributions to this wide range of topics, resulting in numerous new and interesting discoveries and breakthroughs. In this report, the topics have been arranged by science theme, not by device or location. For example, the TITAN mass measurement apparatus produces results that have application in both nuclear structure and nuclear astrophysics. Hence the results from TITAN are discussed in different sections. Similarly the work of the Theory Group is discussed under the relevant science topic not as separate section with all the theory in one place.

4.2.1 FUNDAMENTAL CONSTITUENTS OF MATTER AND THEIR INTERACTIONS

Particle physics is dominated by the Standard Model. This model has been phenomenally successful in passing all experimental tests thrown at it, from the fine structure of the hydrogen atom to the recently discovered Higgs boson. But we know that it is not a complete description of even the known forces, as it does not include gravity. It also has a number of features that are not aesthetically pleasing, like its large number of parameters or the fine-tuning needed for the parameters. So we proceed on two fronts: First, we want to determine the parameters of the Standard Model and secondly, we want to find shortcomings that would drive a revolution in our understanding of the basic properties of nature.

There are two broad experimental approaches to attacking these problems. One is denoted as the energy frontier and the other the precision frontier. The first relies on producing ever more energetic beams of particles and the second on doing ever more precise experiments. The energy frontier produces results that are easier to interpret; the direct production of a particle leaves little doubt of its existence. The precision experiments, on the other hand, allow one to probe energy scales inaccessible even with the highest energy

facilities available. But they leave room for doubt on the interpretation. Previous experiments had ruled out Higgs bosons over a variety of mass ranges. Fits to precision data constrained a Standard Model Higgs boson to a window of about a hundred GeV around the mass where it was eventually found. Although no viable theory existed to explain electroweak symmetry breaking without a Higgs mechanism, it was only by direct observation of a Higgs boson that the mechanism was finally confirmed.

TRIUMF is involved in both of these complimentary approaches to exploring the Standard Model and its extensions; the high-energy approach at CERN and the high precision approach at a number of sites including the TRIUMF laboratory itself. TRIUMF is also actively involved in the theoretical aspects of the problem.

4.2.1.1 DIRECT PARTICLE PRODUCTION SEARCHES

Particle physics is the study of the most fundamental building blocks of the universe. Some are ubiquitous: photons, electrons, the up and down quarks that form the protons and neutrons that make up the bulk of the visible universe, and the ghostly neutrinos that pass almost imperceptibly through it. These particles are effectively stable—a photon emitted in a distant galaxy can travel for billions of years before being absorbed in a human eye. There are other particles, however, which are no less fundamental (or “elementary”) but are not stable: their lifetimes range from attoseconds to microseconds. To study their properties, we must first produce them.

An elementary particle is produced in the decay or annihilation of other elementary particles; in order to produce a child particle more massive than its parents, the original particles must be accelerated so that they have enough kinetic energy to convert into the required mass, $E=mc^2$. There also needs to be a force that couples the parent particle to the one being produced. These two characteristics—the mass and the couplings—determine the kind of accelerator required to search for a given particle. While the existence of particles too massive to be produced at an accelerator may be inferred indirectly in experiments at lower energies, their nature and properties can only be confirmed by producing them directly. The Large Hadron Collider (LHC) collides protons at energies of 7 to 8 TeV (1 trillion electron volts = 1 TeV), to be increased within two years to 13 TeV [1]. The ATLAS detector records the results of these collisions [2]. The following sections describe a number of searches (and one, now-famous discovery) (see Section 5.5.5.2).

The Standard Model (SM) of particle physics was developed about forty years ago to accommodate and explain all the elementary particles then known. It predicted the existence of a number of additional particles, which were subsequently produced and discovered at accelerators. The last of the particles predicted by the Standard Model to remain undiscovered was the Higgs boson. Without postulating the existence of an otherwise unobservable scalar field, of which the Higgs boson would be an observable quantum, it is impossible to construct a consistent (gauge invariant and renormalizable) theory with massive elementary particles. If such a scalar field exists, it can generate masses for the weak vector bosons (the W and Z), and its remaining degrees of freedom manifest themselves as massive scalar particles: the Higgs bosons. In the simplest case, the SM, there is only one of these. Higgs bosons interact through the electroweak force, and couple to fermions in proportion to their masses, as well as to the massive weak vector bosons. In order to produce Higgs bosons, it was necessary to build an accelerator that could produce large numbers of massive, weakly interacting particles that could decay to Higgs bosons.

The LEP (Large Electron-Positron) experiments established that the Higgs boson mass had to be greater than $114 \text{ GeV}/c^2$, and unitarity bounds suggest it should be less than about $1 \text{ TeV}/c^2$. Protons are strongly interacting particles, so most collisions at the LHC produce jets of strongly interacting particles: quarks and gluons. Only a tiny fraction of collisions can produce Higgs bosons; however, the total rate of collisions is so high that substantial numbers will be detected: the advantage of the LHC is in its very high collision rate (luminosity) and in its coverage of the entire mass-range of interest. The strongly interacting massive particles that are produced so copiously at the LHC also interact weakly, and thus sometimes decay to Higgs bosons, either directly or through intermediate decays to W and Z bosons, which can radiate Higgs bosons.

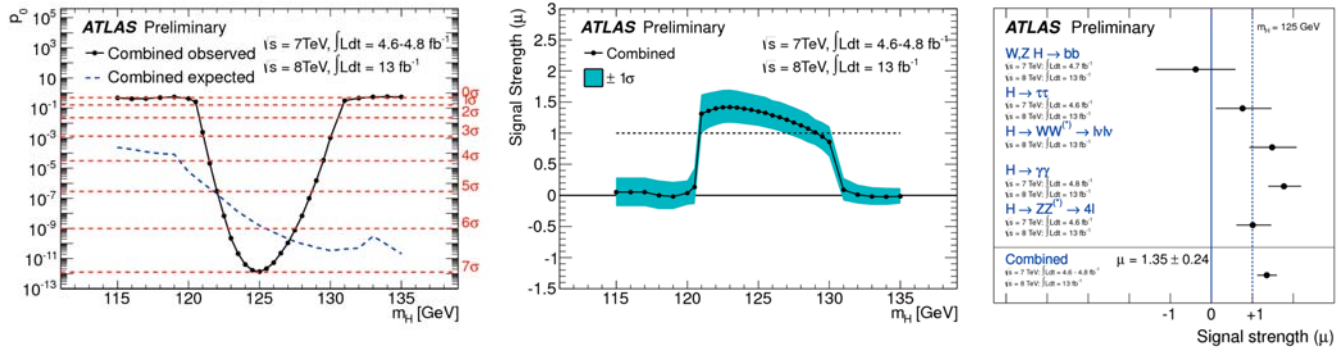


Figure 1: Left-hand plot shows consistency of data with background-only model (no Higgs boson); the middle plot shows the signal strength as a function of assumed Higgs boson mass. A strength of 1 corresponds to the signal strength expected for a Standard Model Higgs boson of the mass indicated on the abscissa—thus, a value near one indicates consistency with a Higgs boson of the corresponding mass, while a value near zero indicates consistency with the background-only hypothesis; the right-hand plot shows the signal strength for each decay channel, as well as for the combination.

Higgs bosons can decay in many different ways, depending on their mass, which is not predicted by the Standard Model. After analyzing 4.8 fb^{-1} of ATLAS data from 7 TeV collisions, and 13 fb^{-1} from 8 TeV collisions, significant excesses of events were observed with two photons in the final state, or with particles consistent with the decays of pairs of W and Z bosons. The numbers of events observed were significantly discrepant with numbers expected from decays of previously known particles, the combined discrepancy being at the level of more than five standard deviations, the gold standard for a discovery [3]. In all cases these excesses were consistent with the decay of a scalar boson with a mass around $125 \text{ GeV}/c^2$. Similar excesses were observed by the CMS experiment, also at the LHC, and the two experiments announced their results simultaneously on July 4, 2012. Since then, each experiment has published their results [4,5] and subsequently accumulated additional data [6], confirming the discovery (see Figure 1, Figure 2). Critical to these results was the superb performance of the ATLAS detector, including the hadronic endcap and forward calorimeters, designed and built at Canadian ATLAS Tier-1 Data Centre at TRIUMF and by TRIUMF personnel at Canadian universities. The timely addition of extra resources at the Canadian Tier-1 computing centre at TRIUMF was essential for the prompt reconstruction and analysis of the data. Canadian researchers, including a number of TRIUMF research scientists and university-based faculty, as well as the post-doctoral researchers and students they supervised, played leading roles in the analysis, review, and production of these results.

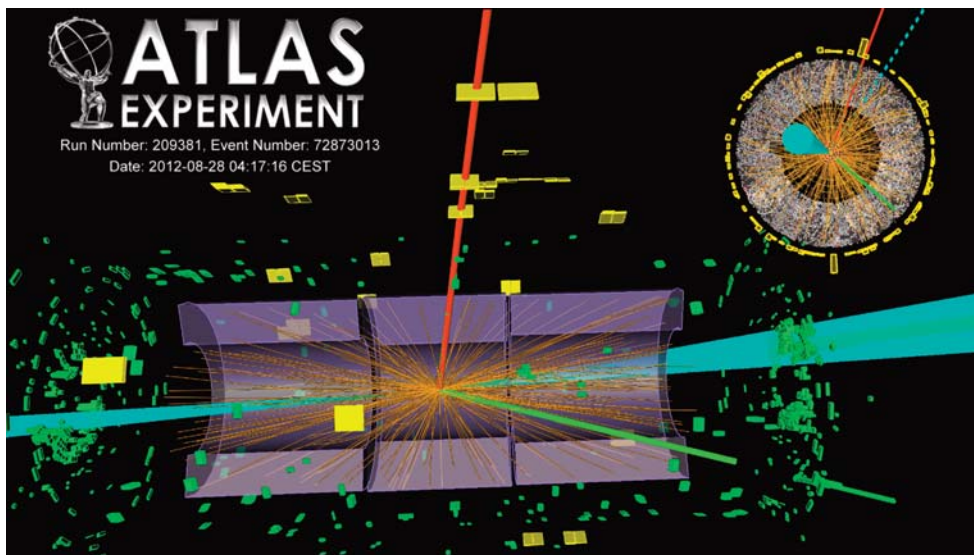


Figure 2: Candidate Higgs event from vector boson fusion, decaying to tau leptons (green and red narrow cones). The forward jets (cyan) in the hadronic end-cap (left) and forward (right) calorimeters are essential to identify vector boson fusion events.

Now that this Higgs boson has been observed it is important to establish its properties with precision. Higgs bosons with a mass in this range are expected to decay to a large number of different final states, with the fraction of each final state predicted by the Standard Model. The highest priority is therefore to search for all the final states predicted and confirm whether they are produced in the proportions expected. So far, the observed properties of the new particle are consistent with the predicted properties of a 125 GeV/c² Higgs boson. The new particle decays to pairs of photons, Z bosons, and W bosons; however, the ATLAS experiment has not yet reported a significant observation of decays to pairs of tau leptons or b-quarks. The observed results in the tau and b-quark channels are thus consistent both with the hypothesis of a Standard Model Higgs boson and with a background-only hypothesis. Other final states, such as Higgs decays to a photon and a Z boson, are so rare that there is as yet no sensitivity. It is also essential to confirm that Higgs bosons are produced in all of the expected processes, at the expected rates, which may be done by looking for Higgs boson production in association with other particles: ttH, ZH, WH.

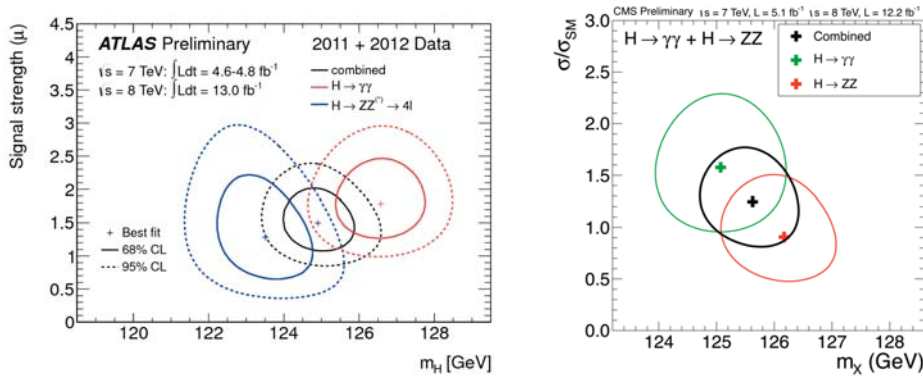


Figure 3: (Left) Mass of Higgs boson from the two high-mass-resolution decay channels; in the preliminary ATLAS results, these are compatible within 2.7 standard deviation; (Right) the CMS preliminary results show the 68% confidence level contours.

Another priority is determining with precision the mass of the new particle (see Figure 3), as this is an important input in fits of existing experimental results to the Standard Model and to other models that can be used to infer the existence of particles too massive to have been observed yet.

It is also possible to distinguish Higgs production through vector boson fusion (see Figure 2 again) from the more common gluon fusion, as the former often produces distinctive event topologies with jets in the detector endcaps (including the Canadian-built hadronic endcap and forward calorimeters), and the decay products of the Higgs boson in the central part of the detector. Canadian groups, including several TRIUMF group members, have been active participants in many of the Higgs boson search analyses, notably the W⁺W⁻ final state, but also ZZ and two-photon signatures, and final states with tau leptons, particularly in the vector boson fusion topology.

While the analysis of the full ATLAS dataset of ~25 fb⁻¹ has already confirmed that the newly discovered particle is indeed a Higgs boson, it remains to be seen if it is in fact *the* Standard Model Higgs boson or the first of a host of particles (including a SM Higgs) not predicted by the Standard Model. It is particularly interesting to study the kinematics of the final-state particles to determine the spin of the new particle, and confirm that it is indeed a scalar (spin 0). This work is in progress for the ZZ and W⁺W⁻ final states [7]. The 0⁺ state is found to be favoured over the 0⁻, 2⁺ and 2⁻ states with 0⁻ excluded by 2.7 standard deviations [8] compared to 0⁺. The full data set should be sufficient to find evidence for Higgs boson decays to tau pairs and b-quark pairs (see Figure 1 again), confirming that the new particle does indeed decay to fermions as well as bosons.

The Higgs boson was the last particle predicted by the Standard Model to be discovered, but the Standard Model is a low-energy effective model that leaves too many open questions to be a complete theory. If there are other strongly interacting particles, so far unknown, and if they are not too massive, these should be produced in very large numbers at the LHC. Several extensions to the Standard Model predict such new

particles: supersymmetry predicts that each quark has a scalar counterpart, a *squark*, which would be strongly produced. The LHC was designed not only to find the Higgs boson and complete the Standard Model but to be sensitive to the broadest possible range of models of new physics, including supersymmetry, models with extra spatial dimensions, and a variety of extensions of the Standard Model with additional gauge bosons or additional quark or lepton families. There are also models where particles currently thought to be elementary are found to have excited states, implying that they are in fact composite particles made up of more fundamental constituents. There are also various effective field theories designed to remedy some of the immediate problems of the TeV scale. In some of these, the role of the Higgs is played by composite particles; such models include Technicolor. Many of these models predict vector boson resonances and new vector-like fermions.

Searches have been made for excesses of events over Standard Model predictions in a wide variety of final states including leptons, jets from quark and gluon production, missing transverse energy consistent with the undetected escape of electrically neutral weakly interacting particles. These searches have increased the previous limits on a broad range of models, in many cases by orders of magnitude, but so far no evidence has been found for particles not predicted in the Standard Model. Only a selection of these searches can be described here.

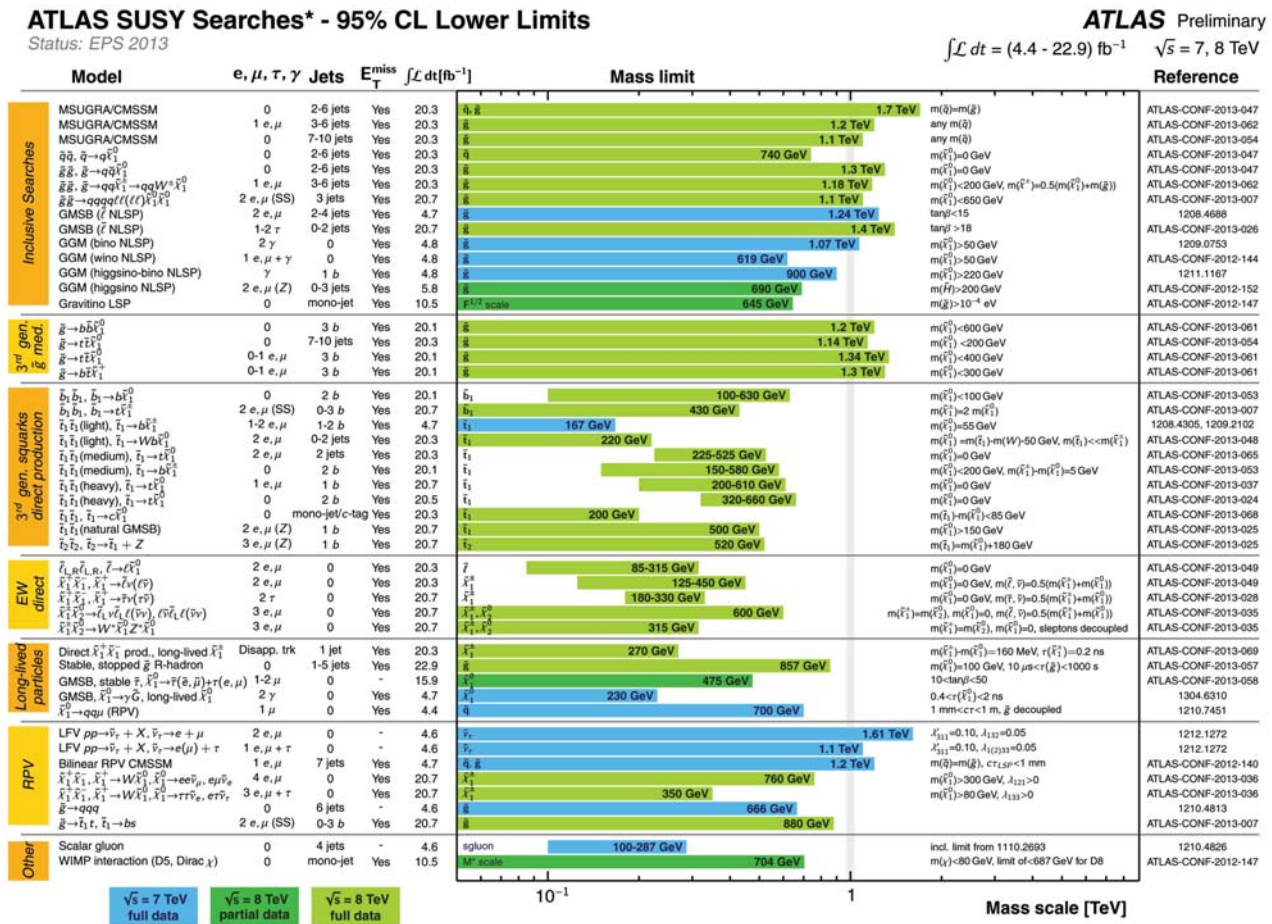


Figure 4: A selection of limits from ATLAS searches for supersymmetry (as of December 2012). The ATLAS-CONF note numbers on the coloured bars can be used to find the documents describing these results in detail.

Supersymmetry

Supersymmetry is an elegant theory which extends the Standard Model by postulating the existence of a scalar bosonic partner for each of the Standard Model fermions, and a fermion for each of its gauge and scalar field components, thus doubling the number of fundamental particles with the hypothetical “superpartners”. Searches for evidence of supersymmetry fall into several broad categories, described in the following paragraphs. Figure 4 shows a selection of limits set by the ATLAS experiment on masses of supersymmetric particles; all of these have some model dependence, but most are now in the 100 GeV – 1 TeV range.

The LHC collides protons, which are made of strongly interacting particles called quarks and gluons. It is thus an ideal place to look for the supersymmetric particles that carry strong-force charges because we expect them to be copiously produced. There are therefore many generic searches for strong production of supersymmetric particles [9]. It is typically assumed that there is a conserved quantity (“R-parity”) corresponding to the supersymmetric particles, and that the lightest supersymmetric particle (LSP) must therefore be stable. If the LSP carries no electric or strong force charge, and interacts only weakly, it is an ideal candidate for dark matter (see Section 4.2.1.2). ATLAS would not directly detect a particle that interacts only weakly, but is designed to be hermetic so that the escape of such a particle would leave a signature of unbalanced momentum in the plane perpendicular to the incident beams (also referred to as “missing transverse energy”); this is the key feature of most searches for R-parity-conserving supersymmetry. These searches for strong production of supersymmetric particles tend to set the strongest limits (see Figure 5) on generic supersymmetry models but are model-dependent and must be treated cautiously.

If supersymmetry were an unbroken symmetry, then the superpartners would have the same masses as the corresponding Standard Model particles. If this were exactly the case, then the divergences in the Higgs mass predicted at high energies due to loop contributions from the massive fermions, especially the top quark, would be cancelled by corresponding contributions from superpartner loops. While it is clear that supersymmetry is broken, because we have not observed scalar partners of the electron, muon, and other light fermions, this cancellation would still be possible if the masses of the top and its scalar partner (*stop*) were close enough. In so-called “natural” supersymmetry [10] considerations such as these imply that supersymmetric partners of the Higgs boson, top, and bottom quarks should not be too far above the weak scale. The rest of the spectrum, including the squarks of the first two generations, can be heavier and beyond the current LHC reach.

The second class of supersymmetry searches look for the direct production of the supersymmetric partners of the gauge and Higgs bosons. These fermions, which can mix with the partners of the Higgs bosons, are collectively referred to as “electroweakinos.” Electroweakinos are produced in weak interactions, with much smaller cross-sections than the strong production referred to previously; however, with the large dataset now collected, we are able to look for these as well. The limits on weak gaugino production show that the LHC is already sensitive to the mass range relevant for demonstrating whether or not supersymmetry can

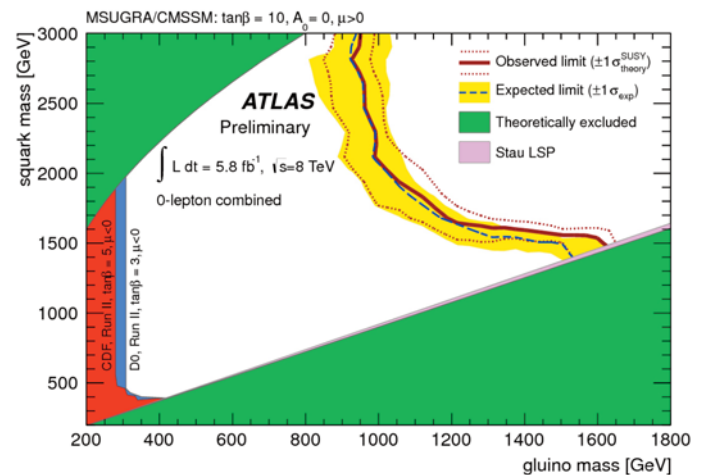


Figure 5: Limits on squark and gluino mass in the classic benchmark MSUGRA model, for the given parameter settings [19].

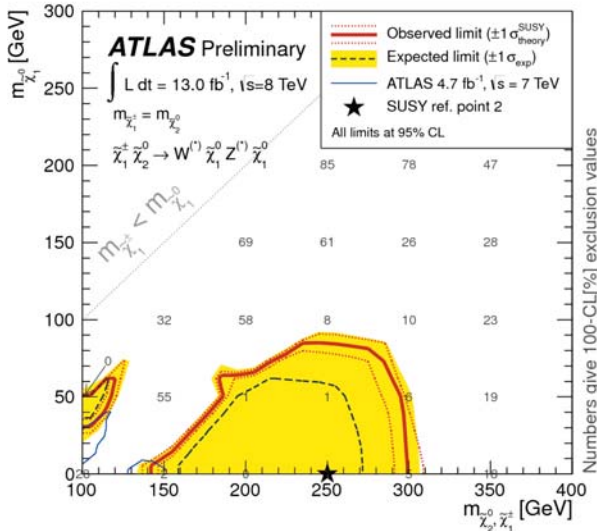


Figure 6: Limits on gaugino production in a simplified model assuming all gauginos decay to Standard Model gauge bosons and the lightest neutralino, which is the LSP.

(if it exists) actually furnish all the solutions to problems of the Standard Model that make it such an attractive theory. Good sensitivity is achieved for the models considered (see Figure 6), although the “interesting” mass region is by no means excluded for all possible models.

Because of the implications of “naturalness” for the partners of the top quark, a third class of searches looks specifically for the scalar partner of the top quark with masses relatively close to the top quark mass (that is, below about 1 TeV). How the stop decays depends chiefly on its mass, so several searches need to be combined; however, it can be seen from Figure 7 that much of the allowed parameter space is excluded for stop masses below about 500 GeV.

A fourth class of supersymmetry searches abandons the assumption of R-parity conservation and includes a number of final states without missing transverse momentum, typically marked by pairs of leptons of the same flavour and charge, arising from the Majorana nature of the scalar partners of the leptons. While R-parity violating (RPV) supersymmetry lacks the stable LSP dark matter candidate that is such an appealing feature of other supersymmetric scenarios, and requires numerous constraints to avoid allowing flavour-changing neutral currents in Standard Model processes where they are already excluded, it is essential to consider that R-parity is simply an *ad hoc* addition to the model and cannot be assumed. Removing the assumption that supersymmetry signatures should include significant missing transverse energy opens up a host of possibilities (see Figure 8 for a particular simplified model). The LHC is able to probe well into the interesting region where supersymmetry could solve the Standard Model hierarchy problem, but the limits are very model-dependent and RPV supersymmetry is by no means excluded.

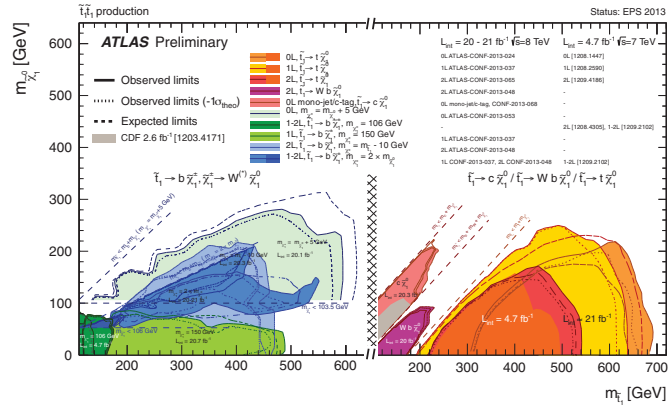


Figure 7: Current status of searches for the supersymmetric partner of the top quark at ATLAS, with several different assumptions about the stop and LSP masses indicated by the different colours. The “natural” preference is for a stop mass not too far from the top quark mass (which is 175 GeV) to cancel divergences in the Higgs mass from top quark loops. The legend refers to the ATLAS-COIN notes documenting these preliminary results.

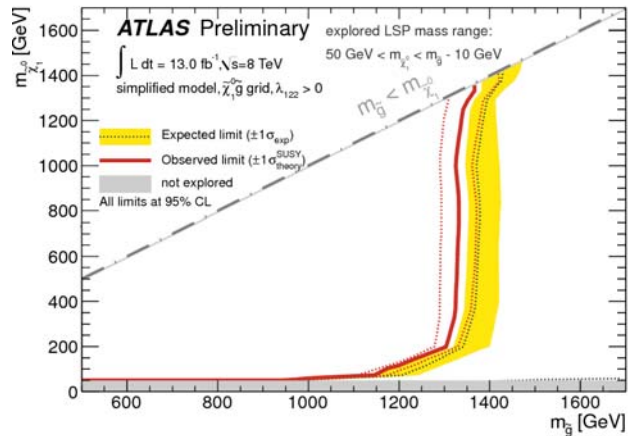


Figure 8: Limits on R-parity violating supersymmetry in a particular simplified model, where the gluino is strongly produced and decays to a final state with four leptons (electrons or muons).

While supersymmetry is perhaps the most appealing theory for extending the Standard Model to higher energies and greater symmetry, it is by no means the only possibility. Other classes of models for “beyond Standard Model” physics can be roughly grouped according to whether they require compositeness of particles currently thought to be elementary, extra dimensions, additional gauge interactions, “hidden” sectors with new interactions that can communicate with the Standard Model particles either through “messenger sectors” or decays tunneling through from “hidden valleys”.

Alternatively, models can be grouped by signature: for example, searches for two oppositely charged leptons and a photon can be interpreted as compositeness searches (for excited leptons), as Technicolor searches (invoking a new strong interaction at high energies), as Higgs boson searches (with the Higgs decaying to a Z boson and a photon), or as generic searches for new components of the electroweak interaction (triple-gauge-coupling measurements). The groups of signatures considered in ATLAS searches include: final states with leptons, final states with jets, final states corresponding to pairs of gauge bosons, final states including top quarks, and final states including long-lived particles (that is, particles which travel at least some measurable distance from the interaction point, and possibly right through the detector, before they can decay into Standard Model particles).

Perhaps the most striking of the lepton final-state signatures is the search for new, very massive neutral particles or narrow resonances (additional gauge bosons, Kaluza-Klein gluons, for example) decaying into oppositely charged pairs of electrons or muons (see Figure 9). Such resonances can be excluded up to masses of over 2 TeV (where the precise exclusion is model-dependent and a function of the couplings of the hypothetical particle to electrons and muons).

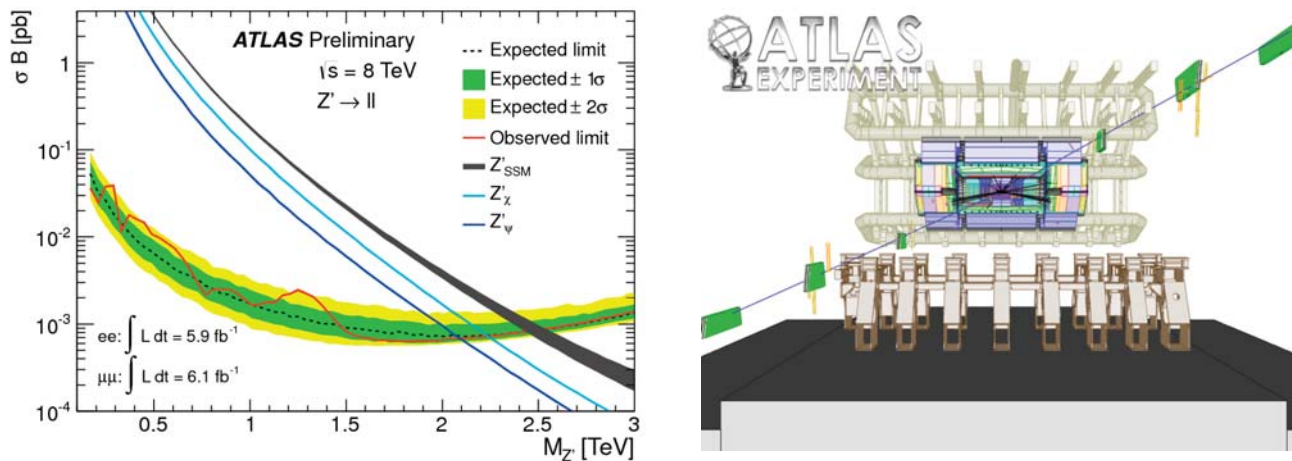


Figure 9: Limits on neutral gauge boson production in various models from searches for resonances in electron- and muon-pair production. The right-hand plot is an event display of a muon pair with an invariant mass of 1.2 TeV.

A closely related search, which includes an energetic photon as well as two oppositely charged electrons or muons in the final state, looks for hints of compositeness by searching for excited leptons emitting a photon as they return to their ground state. Limits are set on the excited lepton mass as a function of the compositeness scale. In the special case where these are equal, both excited electron and excited muon masses below 2.2 TeV are excluded at 95% CL [11].

The simplest possible final state with jets is a single jet (a “monojet”) with nothing else. A monojet is necessarily unbalanced, so there is substantial “missing” momentum in such an event. Searches for this final state set some of the tightest constraints on dark matter candidates and also on the existence of extra

dimensions which could dilute TeV-scale gravity, with a strength comparable to the electroweak and strong forces, down to the ultra-weak force that holds our planet in orbit and keeps our feet on the ground without pulling apart the atoms that make up our bodies. An example of the constraints ATLAS data [12] place on the mass of a weakly interacting massive particle (WIMP) in the context of other spin-independent WIMP searches is shown in Figure 10.

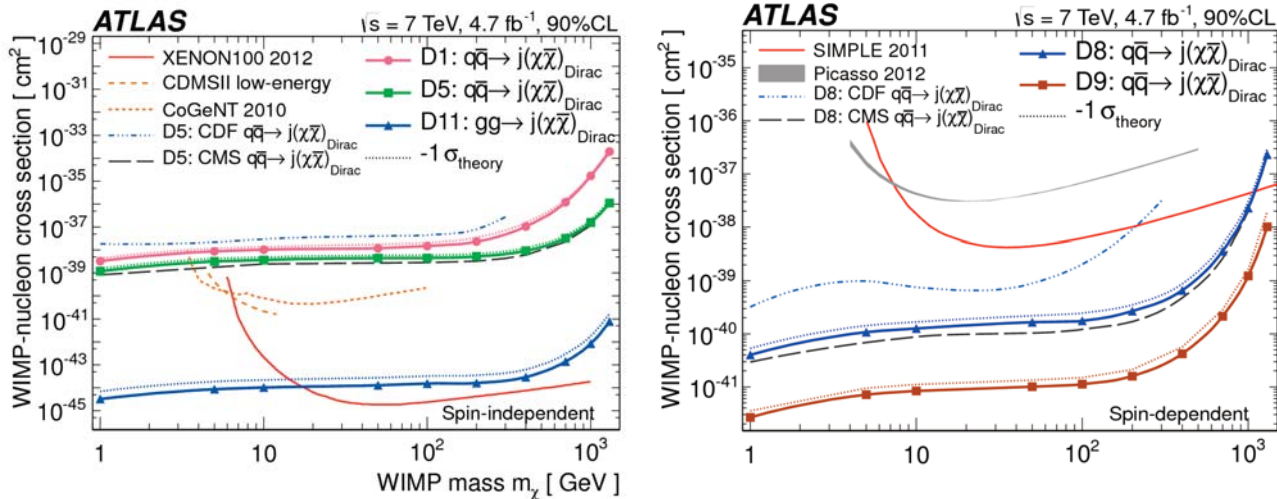


Figure 10: ATLAS 90% confidence-level inferred cross-section limits as a function of WIMP mass for (left) spin-independent and (right) spin-dependent WIMP-nucleon scattering. Cross-sections are shown versus WIMP mass m_χ . In all cases, the thick solid lines are the observed limits excluding theoretical uncertainties; the observed limits are shown as thin dotted lines. The latter limits are conservative because they also include theoretical uncertainties. The ATLAS limits for operators involving quarks are for the four light flavours assuming equal coupling strengths for all quark flavours to the WIMPs.

ATLAS has produced a rich set of analyses of final states consisting of two gauge bosons (WW, WZ, ZZ, Zg, Wg, gg), which are also discussed briefly in Section 4.2.1.4. These can be interpreted in searches for new resonances, including those predicted by models with new strong interactions such as Technicolor [13], or in Higgs boson searches.

Since the top quark is the only quark whose mass is close to those of the W and Z bosons, corresponding to the scale at which the strengths of the electromagnetic and weak interactions become comparable, it does not seem unreasonable to expect it to play a special role, perhaps as the gatekeeper to physics beyond the Standard Model. Searches for resonances in the spectrum of top-anti-top-quark pair production exclude the existence of such resonances up to masses of around a TeV (again, the precise limits are model-dependent).

Searches for long-lived exotic particles make up the final component of “exotic” searches. The methods used in these searches depend on the mass, speed, lifetime, and charge of the particle being sought. If the particle decays inside the beam pipe, these are searches for displaced interaction vertices. If the particle decays inside the ATLAS inner detector, it will produce a kinked, disappearing or non-pointing track. Decays in the calorimeters may produce jets or photons that do not point back to the primary interaction point. Particles that traverse the Inner Tracker or the outer Muon Spectrometer can be identified if they are heavy enough to produce unusual ionization tracks (or if they are multiply charged, which can lead to similar results). Special searches are made for very slow “muon-like” particles [14] and the transition radiation tracker of the inner detector is used to identify long-lived, highly ionizing, penetrating particles with electric charges from twice to six times the electron charge [15]. These are ruled out for masses between 50 GeV/c² and 420-490 GeV/c² (depending on the charge).

Direct Searches and the TRIUMF Theory Group

Direct experimental searches by the ATLAS group are complemented by theoretical investigations by TRIUMF's Theory Group. The Theory Group interprets ATLAS results in the context of the Standard Model and beyond, and connects these findings to other direct-search experiments, lower-energy precision experiments, and astrophysical observations. The Theory Group also develops and studies extensions of the Standard Model that address the many puzzles this model presents [16], and investigates how best to search for new particles and forces in future experiments.

A key research topic of the Theory Group is the Higgs boson. A broad range of extensions of the minimal Higgs sector of the Standard Model have been developed, and their implications for experimental searches for the Higgs boson have been predicted [17]. The Group has also studied the recent discovery of a new Higgs-like particle at the LHC on extensions of the Standard Model. Under the assumption that this particle is indeed the Higgs boson, the Group has studied the implications of the data on the structure of the electroweak phase transition in the early Universe [18], and has used the data to constrain additional scalar particles [19].

The Theory Group also studies new particles and forces beyond the Standard Model that could be discovered in direct experimental searches. The scalar partners of the top quark predicted by supersymmetry were investigated [20]. Existing LHC searches for other types of new physics were found to be sensitive to light stop particles and provide new limits on their masses. A new mechanism was developed to explain both the missing dark matter and the asymmetry of matter over antimatter [21]. The sensitivity of LHC monojet searches to the new particles and interactions required by this mechanism were studied and related to searches for dark matter and nucleon decay [5]. Other topics, which include extended supersymmetric theories [22], attempts to explain the top asymmetry seen at the Tevatron [23], and new light particles and forces that could be discovered in lower-energy high-intensity experiments [24].



CANADIAN RESEARCHERS ON HAND FOR IMPORTANT JAPANESE NEUTRINO OBSERVATION

19 July 2013

At the prestigious European Physical Society meeting in Stockholm, Sweden, TRIUMF's Michael Wilking announced a new breakthrough in understanding neutrinos, nature's most elusive particles. Together with Canadian, Japanese, and other international colleagues as part of the T2K collaboration, Dr. Wilking confirmed the definitive observation of a new type of neutrino oscillation, in which

muon neutrinos transform to electron neutrinos. It has been known that neutrinos transform from one kind into another, but this particular transition had never before been conclusively observed.

Scott Oser, UBC professor of physics and astronomy and spokesperson for the Canadian team known as T2K-Canada, commented, "Canada has been an international leader in neutrino research since the success of the Sudbury Neutrino Observatory (SNO). T2K was the logical next step after SNO in our quest to understand neutrino oscillations, and Canada was in fact the first international partner to join T2K. These new results are the culmination of a decade of work, and open the door to future studies of how both neutrinos and antineutrinos oscillate."

ATLAS has reaped an extraordinary harvest of physics analyses from the unprecedented energy-frontier dataset furnished by the LHC in its first three years of running. In addition to the discovery of a Higgs boson, ATLAS data have been used to explore vast regions of the parameter space of a wide range of extensions to the Standard Model, including supersymmetry, extra dimensions, compositeness, and new gauge interactions. Substantial room remains for discoveries in the dataset already collected, and collaboration between experimenters and theorists allows many fruitful discussions to take place and new directions to be explored. After the 2013–2014 long shutdown, the LHC will turn on again at its design energy, allowing searches for more new particles and push even farther into the unexplored regions.

Selected References

- [1] L. Evans, P. Bryant (Eds.), LHC Machine, JINST 3, S08001 (2008).
- [2] ATLAS Collaboration, JINST 3, S08003 (2008).
- [3] CERN experiments observe particle consistent with long-sought Higgs boson
<http://press.web.cern.ch/press-releases/2012/07/cern-experiments-observe-particle-consistent-long-sought-higgs-boson>, <http://www.interactions.org/cms/?pid=1031893>, July 4, 2012.
- [4] ATLAS Collaboration, Phys. Lett. B716, 1 (2012) ; ATLAS Collaboration, Science 338, 1576 (2012).
- [5] CMS Collaboration, Phys. Lett. B716, 30 (2012).
- [6] ATLAS Collaboration, ATLAS-CONF-2012-170; CMS Collaboration, CMS-PAS-HIG-12-045.
- [7] ATLAS Collaboration, ATLAS-CONF-2012-169; ATLAS Collaboration, ATLAS-CONF-2012-168.
- [8] ATLAS Collaboration, ATLAS-CONF-2012-169.
- [9] ATLAS Collaboration; arXiv:1212.6149.
- [10] C. Brust, A. Katz, S. Lawrence, R. Sundrum, JHEP 1203, 103 (2012) .
- [11] ATLAS Collaboration, ATLAS-CONF-2012-146.
- [12] ATLAS Collaboration, submitted to JHEP, arXiv:1210.4491 (2012).
- [13] ATLAS Collaboration, submitted to Phys. Rev. D arXiv:1302.1283, (2013).
- [14] ATLAS Collaboration, Phys.Lett. B703, 428 (2011) .
- [15] ATLAS Collaboration, submitted to Phys. Lett. B, arXiv:1301.5272 (2013).
- [16] D.E. Morrissey, T. Plehn and T.M.P. Tait, Phys. Rept. 515, 1 (2012).
- [17] D.E. Morrissey and A. Pierce, Phys. Rev. D 78, 075029 (2008); J.D. Mason, D.E. Morrissey and D. Poland, Phys. Rev. D 80, 115015 (2009); W.-F. Chang, J.N. Ng and A.P. Spray, Phys. Rev. D 82, 115022 (2010).
- [18] A. Menon and D.E. Morrissey, Phys. Rev. D 79, 115020 (2009) [arXiv:0903.3038 [hep-ph]]; T. Cohen, D.E. Morrissey and A. Pierce, Phys. Rev. D 86, 013009 (2012).
- [19] W.-F. Chang, J.N. Ng and J.M.S. Wu, Phys. Rev. D 86, 033003 (2012).
- [20] K. Krizka, A. Kumar and D.E. Morrissey, [arXiv:1212.4856 [hep-ph]] (submitted to Phys. Rev. D).
- [21] H. Davoudiasl, D.E. Morrissey, K. Sigurdson and S. Tulin, Phys. Rev. Lett. 105, 211304 (2010); H. Davoudiasl, D.E. Morrissey, K. Sigurdson and S. Tulin, Phys. Rev. D 84, 096008 (2011).
- [22] D.E. Morrissey, D. Poland and K.M. Zurek, JHEP 0907, 050 (2009).
 Y.F. Chan, M. Low, D.E. Morrissey and A.P. Spray, JHEP 1205, 155 (2012).
- [23] J.N. Ng and P.T. Winslow, JHEP 1202, 140 (2012).
- [24] K.L. McDonald and D.E. Morrissey, JHEP 1102, 087 (2011).

4.2.1.2. NEUTRINO AND DARK MATTER PHYSICS

Neutrinos are ghostly particles that feel only the weak nuclear force and can therefore pass through the entire earth with almost no probability of a collision. Due to this elusive nature, some fundamental properties of neutrinos, particularly their tiny but non-zero mass, have only recently been established. Current research is focused on understanding fully the nature of this mass, and the property of “mixing” which, together with the non-zero masses, allows the neutrino to transmute between three “flavours”, i.e. ν_e , ν_μ , and ν_τ , through a process called neutrino oscillations.

Unlike the photon, whose masslessness is dictated by gauge symmetry, there is no *a priori* reason to expect that the neutrino should be massless (as was long believed) or to have such tiny masses—nearly one million times smaller than the next lightest particle, the electron—as we now know. However, neutrino masses do not fit into the Standard Model of particle physics because the normal mechanisms by which fermions acquire mass require coupling right- and left-handed partner states, whereas neutrinos are found in only one of these states in the Standard Model.

Unlike its charged cousins, the quarks and the charged leptons, a neutrino can acquire mass by coupling to its antineutrino state; if this is observed to happen, it implies that the neutrino and antineutrino are the same particle. This form of mass is known as “Majorana,” while the quarks and charged leptons have “Dirac” masses, which necessarily distinguish a particle from its antiparticle.

If neutrinos possess some combination of Majorana and Dirac mass terms, the states will naturally split into two sets of Majorana-neutrinos with observed masses in inverse proportion. This “see-saw” mechanism potentially explains the tiny neutrino masses that we observe. If true, it implies that neutrino mass is of a fundamentally different origin from other forms of mass, and that the neutrino has ultra-heavy siblings with mass $O(10^{15}$ eV). Establishing that the neutrino is its own antiparticle is an essential element of this hypothesis. If this is in fact the case, a process known as “neutrinoless double beta decay” should occur, in which a nucleus undergoes two beta decays simultaneously, with the two neutrinos usually emitted from the process annihilating each other.

The mixing properties of neutrinos, in which the three flavours of neutrinos are combinations of states with definite masses (m_1, m_2, m_3), is governed by three “angles” ($\theta_{12}, \theta_{13}, \theta_{23}$) which parameterize how much of each mass state is present in each flavour state. These angles determine the amplitude of neutrino oscillations, while the mass-squared differences ($\Delta m_{ij}^2 = m_i^2 - m_j^2$) determine the wavelength of the oscillations. We now know that the mixing pattern of neutrinos, where the mixing is very large, is strikingly different from that of quarks, where the mass states nearly align with the flavour states. As with the quarks, the mixing also allows the presence of an irreducible complex phase δ that induces CP violation, giving rise to different oscillation properties for neutrinos and anti-neutrinos. Current neutrino oscillation experiments seek to make precise measurements of the mixing parameters, which may provide some clues to whether there is any underlying pattern or relation between the mixing parameters. Planned experiments such as Hyper-Kamiokande and LBNE will search for the CP violation expected from the δ parameter.

The possible Majorana nature of the neutrino mass, the associated see-saw mechanism and potential CP violation in neutrino oscillations come together in the theory of leptogenesis to explain the matter/antimatter asymmetry of the universe. Leptogenesis posits that the matter domination of the universe originated in the CP-violating decay of the heavy Majorana partner of the neutrino. While no rigorous relationship is known between the mixing parameters of the light neutrinos we observe and these heavy Majorana particles, confirmation of the Majorana nature of the neutrino through neutrinoless double beta decay and the observation of CP violation in neutrino oscillations would establish the key elements of this conjecture. Thus in addition to probing fundamental properties of the neutrino, in particular whether its mass is of a profoundly different nature from other elementary particles, and whether the roots of mixing of flavour and mass states in the Standard Model can be understood at a deeper level to enlighten us about the mysterious

observed pattern, the physics of neutrinos is intimately connected to astrophysics and cosmology. The coming decade will see continued rapid progress in neutrino oscillations and double beta decay experiments, as results from current experiments such as EXO, SNO+ and T2K are reaped and new experiments with high sensitivity start operation.

Neutrino Oscillations

Conclusive evidence for neutrino oscillations came from the observation of the solar neutrino flux with the SNO detector [1,2], in which TRIUMF was involved. Results from all phases of the SNO experiment combined [3,4,5] with results from all other solar experiments and the KamLAND reactor experiment led to best-fit values of the mixing parameters of

$$\Delta m_{21}^2 = 7.59^{+0.19}_{-0.21} \times 10^{-5} \text{ eV}^2 \quad \text{and} \quad \theta_{12} = 34.4^{+1.3}_{-1.2} \text{ degrees}$$

A three-flavour analysis found a best fit value of $\sin^2 \theta_{13}$ to be $2.5^{+1.8}_{-1.5} \times 10^{-2}$, implying an upper bound of $\sin^2 \theta_{13} < 0.053$ (95 % C.L.) [6].

Results from measurements of the through-going muon flux at the SNO observatory were also recently published [7]. For zenith angles $0.4 < \theta_{\text{zenith}} < 1$, for which the muons originate mainly from pion and kaon decays in the atmosphere, the flux was 3.31 ± 0.01 (stat) ± 0.09 (sys) $\times 10^{-10}$ muons/s/cm². The zenith angle distribution was measured for zenith angles $-1 < \theta_{\text{zenith}} < 0.4$, for which the muons originate from atmospheric neutrino-induced interactions in the materials surrounding the detector. This distribution was interpreted [7] in terms of neutrino oscillations with best-fit oscillation parameters of maximal mixing and $\Delta m^2 = 2.6 \times 10^{-3} \text{ eV}^2$, consistent with parameters measured previously in other experiments. An interesting aspect of this latter measurement is that it is the first to observe atmospheric neutrino-induced events from above the horizon, a result of SNO's greater depth than other observatories, for which the neutrinos are not expected to undergo oscillations.

Long baseline neutrino experiments like T2K in Japan [8], in which TRIUMF scientists play a leading role, aim at precisely determining the mixing angles θ_{13} and θ_{23} , and the mass difference Δm_{32}^2 that are not measured by solar neutrino experiments. In particular, T2K studies the $\nu_{\mu} \rightarrow \nu_e$ oscillation that is expected from non-vanishing θ_{13} and makes precision measurements of θ_{23} and Δm_{32}^2 . For the former, there was no evidence until recently for non-zero θ_{13} , and thus establishing this mode of oscillation would constitute the observation of a new form of neutrino oscillations. In the latter case, current measurements point to the peculiar possibility that $\theta_{23} = 45^\circ$, indicating the maximal mixing between the flavour and mass eigenstates. If precise measurements uphold this situation, or if $\theta_{23} > 45^\circ$, this may provide some hints on whether there are any underlying symmetries or patterns in the mixing. As mentioned above, the mixing matrix also contains a CP-violating phase δ , which, if non-vanishing, can be explored by T2K and measured in the next-generation long-baseline experiment Hyper-Kamiokande (HK) in Japan.

T2K uses an intense muon neutrino beam produced at the J-PARC proton accelerator in Tokai, Japan to search for neutrino oscillations, especially for the previously unobserved oscillation of muon neutrinos into electron neutrinos. T2K uses a magnetized near detector, with key components built at TRIUMF [9, 10], and the existing Super-Kamiokande detector, located 295 km west of Tokai, as its far detector. T2K began taking its first data early in 2010.

Unfortunately, data-taking was interrupted by the large earthquake of March 11, 2011. By this point T2K had collected 1.4×10^{20} protons on target, corresponding to about 1/50th of T2K's planned data set, and had achieved beam powers in excess of 150 kW. The 2011 earthquake resulted in no injuries to T2K members and no significant damage to the beam line or detectors. Recovery efforts throughout the year re-established beam operations in December 2011, and neutrino data taking resumed in March 2012. An extended period of operations between October 2012 and July 2013 saw the experiment achieve its highest beam power yet of 220 kW.

In June 2011, T2K released the first oscillation results from the 2010–2011 data, reporting the observation of six candidate ν_e events in the data collected before March 2011, with an expected background of 1.5 ± 0.3 for $\theta_{13} = 0$. [11] This 2.5σ excess suggested that θ_{13} might be large, at or just below the limit established previously by the CHOOZ experiment [12]. This indication was confirmed by the Daya Bay and RENO reactor neutrino experiments, which in early 2012 reported high-significance evidence for the disappearance of reactor antineutrinos at short baselines at rates consistent with T2K’s favoured value of θ_{13} .

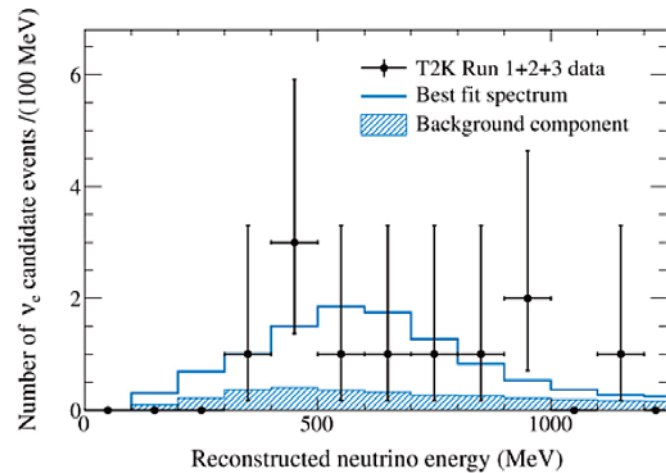


Figure 1: Energy spectrum of candidate electron neutrino events in T2K data taken through summer 2012.

In summer 2012, T2K presented an upgraded analysis, using full spectral information from its near detector and including more than twice as much data as its 2011 analysis. At the ICHEP 2012 conference T2K reported seeing 11 candidate ν_e events on a background of 3.2 ± 0.4 for $\theta_{13} = 0$ (see Figure 1). With a statistical significance of 3.2σ , this is the strongest evidence for the oscillation of muon neutrinos into electron neutrinos in a long-baseline experiment seen to date. TRIUMF-based scientists led the development of improved constraints from T2K’s near detector, which greatly decreased the fractional uncertainty on the background rate. Further improvements are expected as analysis developments permit the measurement of critical neutrino cross-sections. Unlike reactor neutrino experiments, which are sensitive to only θ_{13} , electron neutrino appearance at T2K also depends on the CP-violating phase δ_{CP} of the mixing matrix and on the sign of the neutrino mass hierarchy. Further improvements in T2K’s electron neutrino appearance measurement, in combination with other experiments, may provide the first hint for CP violation in the neutrino sector.

Measuring the disappearance of muon neutrinos probes different neutrino mixing parameters, especially θ_{23} and Δm^2_{32} . In a 2012 paper T2K analyzed its data for muon neutrino disappearance, clearly confirming neutrino oscillation seen in previous experiments [13]. With just $1/50^{\text{th}}$ of its ultimately anticipated data set, this measurement was already competitive for both mixing parameters, thanks to the off-axis neutrino beam tuned at the oscillation maximum. In February 2013, with twice as much data accumulated, T2K announced the world’s best measurement of θ_{23} , which is consistent with maximal mixing. There is considerable theoretical interest surrounding the value of θ_{23} , which appears close to maximal mixing and possibly indicates a flavour symmetry protecting its value.

T2K continues to collect more data, with data taken through summer 2013 expected to give $>5\sigma$ sensitivity to electron neutrino appearance. In August 2013, J-PARC will shut down for a LINAC energy upgrade that will enable a significant increase in the beam power. T2K’s goals for the next several years are to improve the precision for all neutrino mixing parameters, especially θ_{13} and θ_{23} , measure several important neutrino interaction cross-sections, and lay the groundwork for a next-generation upgrade to definitively measure CP violation in the neutrino sector. This will involve the construction of a new megatonne-scale water Cherenkov detector, called Hyper-Kamiokande, near the site of the Super-Kamiokande. Such an upgrade will be proposed in the next few years and, if funded, will not only give sensitivity to CP violation, but will extend sensitivity to proton decay by one order of magnitude.

Neutrinoless Double Beta Decay

While much progress has been made on the mixing angles and squares of mass differences through neutrino oscillations, the exact arrangement of the mass’s differences and the absolute values of the neutrino masses have not been determined so far. As mentioned above, there is a natural explanation for small neutrino

masses if neutrinos have Majorana mass that result in it being its own antiparticle. Proof that neutrinos have Majorana mass would be found if the neutrinoless double beta-decay process could be observed. In addition, it would demonstrate for the first time a violation of total lepton number. Such observations would help in our understanding of the creation of matter in the Big Bang. If such a decay is indeed observed, e.g., by the EXO or the SNO+ experiments, in which TRIUMF is involved, it would mean that neutrinos are their own antiparticles, the so-called Majorana particles, and the decay rate is sensitive to the neutrino masses. A controversial claim of evidence for this process was made in 2001 by some members of the Heidelberg-Moscow experiment with subsequent experiments aiming to confirm or refute this claim.

The EXO experiment is a search for neutrinoless double beta decay in xenon. The work is in two parts. A 200 kg liquid xenon TPC is taking data in the Waste Isolation Pilot Plant (WIPP) facility in New Mexico while R&D for a ton-scale detector is progressing mainly in Canada.

In 2011, EXO published the first observation of the two-neutrino decay mode of Xe-136 [14]. This observation was significant for two reasons. First, it indicated that there is nothing anomalous about the nuclear structure of the decay (as might have been inferred from earlier limit). Secondly, it showed that the care in reducing the backgrounds has been successful as the signal to background through most of the spectrum is better than 10:1. In contrast, the Heidelberg-Moscow group has a signal to background of 1:2 for the equivalent measurement in germanium. The detector is now taking data as one of the world's most sensitive detectors for double beta decay.

In 2012, EXO published the results of its first search for neutrinoless double beta decay in Xe-136 [15]. No evidence for this decay mode was found, and the limit placed on the rate established a new world record for sensitivity. For the first time in over a decade, a serious challenge to the Heidelberg-Moscow claim was produced. The claimed observation is ruled out at 90% confidence for almost all published nuclear matrix elements. There is substantial variation in the nuclear matrix elements calculated for neutrinoless double beta decay and nuclear physics experiments like TITAN-EC at TRIUMF are needed to constrain the nuclear theory calculating these matrix elements.

With the excellent performance of the EXO 200, work is in progress to design the next-generation detector that is envisioned as a five-ton liquid xenon TPC. The preferred location for this detector is at SNOLAB and negotiations have begun with the SNOLAB management to allow a full proposal to go forward. To fully exploit the increase in mass, it will be necessary to either reduce further the radioactivity of the materials of construction or to extract and identify the daughter Ba-136 ion by laser fluorescence [16]. Canadian groups are working on both aspects of this development. If successful, this detector would achieve the next milestone in the field—to explore the inverted mass hierarchy of neutrinos. At the same time, the SNO+ experiment to search for neutrinoless double beta decay of Te-130 is nearing completion at SNOLAB, and is due to start data taking in 2014.

Results and Progress: Neutrinos as Astrophysical Messengers

Neutrinos also play an important role in many astrophysical environments from stellar burning to stellar explosions. The flux of neutrinos resulting from the nuclear burning at the centre of our sun is a sensitive probe of the environment in terms of density, temperature, and chemical composition. The Sudbury Neutrino Observatory (SNO) experiment was unique in that, by using heavy water as the detection medium, it could detect both the ν_e component of the solar neutrino flux via the charged current (CC) reaction $\nu_e d \rightarrow p p e^-$, and all neutrino flavours via the neutral current (NC) reaction $\nu d \rightarrow \nu p n$. In addition, the electron scattering (ES) reaction $\nu e^- \rightarrow \nu e^-$ is sensitive mainly to ν_e . In 2001, the SNO experiment solved the long-standing problem of the missing ν_e 's from the sun by showing that the solar flux contains a non- ν_e component. At TRIUMF, nuclear astrophysics experiments at the ISAC facility for rare-isotope beams have been addressing uncertainties in the production rates of B-8 neutrinos in the sun.

The second and third phases of the SNO experiment incorporated salt and He-3 neutron detectors in the heavy water for additional sensitivity to the neutrons liberated by the ν_μ , and ν_τ . Results from the third

phase of SNO were published in the present reporting period. In the first phase of the experiment neutrons from the neutral current break-up of deuterium were detected by observing the gammas from subsequent (n,γ) reactions on deuterium, while in the second phase detection of these neutrons was enhanced by observing gammas from (n,γ) reactions on Cl-35 following the introduction of 2 kt of NaCl into the heavy water. In the third phase the neutrons were predominantly detected by an array of He-3 proportional counters arranged throughout the detector volume. This independent technique reduced the correlations among CC, NC and ES fluxes extracted in the previous two phases [6].

The equivalent neutrino fluxes derived from the fitted CC, NC, and ES events in the third phase were found to be

$$\begin{aligned}\varphi_{CC} &= 1.67^{+0.05}_{-0.04} \text{ (stat)} \ ^{+0.07}_{-0.08} \text{ (syst)} \times 10^{-6} \text{ cm}^{-2} \text{ s}^{-1}, \\ \varphi_{ES} &= 1.77^{+0.24}_{-0.21} \text{ (stat)} \ ^{+0.09}_{-0.10} \text{ (syst)} \times 10^{-6} \text{ cm}^{-2} \text{ s}^{-1}, \\ \varphi_{NC} &= 5.54^{+0.33}_{-0.31} \text{ (stat)} \ ^{+0.36}_{-0.34} \text{ (syst)} \times 10^{-6} \text{ cm}^{-2} \text{ s}^{-1}.\end{aligned}$$

A paper describing a joint analysis of the data from the first two phases of SNO was also published [3]. A significant development for this analysis was the lowering of the analysis threshold to 3.5 MeV, the lowest yet achieved with a water Cherenkov detector. This was accomplished by including late-arriving scattered and reflected light in the energy estimation, by developing a suite of event-quality cuts based on PMT charge and time information, and by removing known periods of high radon infiltration that occurred during early SNO running. Inclusion of the late-arriving light resulting improved the energy resolution by $\sim 6\%$; this in turn reduced the contamination by low-energy background by $\sim 60\%$.

The total flux of active-flavour neutrinos from B-8 decay in the Sun measured with SNO's neutral current reaction of neutrinos on deuterons was found to be

$$\varphi_{NC} = 5.14^{+0.160}_{-0.158} \text{ (stat)} \ ^{+0.132}_{-0.117} \text{ (syst)} \times 10^{-6} \text{ cm}^{-2} \text{ s}^{-1}.$$

The uncertainties are more than a factor of two smaller than previously published results. A fit to the data in which the free parameters directly describe the total B-8 neutrino flux gave

$$\varphi_B^8 = 5.046^{+0.159}_{-0.152} \text{ (stat)} \ ^{+0.107}_{-0.123} \text{ (syst)} \times 10^{-6} \text{ cm}^{-2} \text{ s}^{-1}.$$

Another publication was based on a search for periodicities in the B-8 solar neutrino flux [2]. SNO has previously reported on searches for periods from 10 years down to 1 day. The present work concentrated on periods from 1 day down to 10 minutes. These high-frequency searches were partly motivated by recent expectations for helioseismological variations on scales of an hour or less, in particular solar "gravity modes." Three searches were carried out, the first looking for any significant peak in the frequency range $1\text{-}144 \text{ day}^{-1}$, the second looking for gravity modes in a more restricted frequency range, and the third looking for any extra power across the entire frequency band. No statistically significant signal was detected in any of these searches.

Results from a low-multiplicity neutrino burst search were also published. Such bursts could indicate the detection of a nearby core-collapse supernova explosion. The data were taken from the first two phases of the experiment. A number of combinations of event multiplicity and resolving times were utilized to maximize the chance of observing a burst from various different supernova mechanisms while at the same time minimizing the chance of a false burst within the given time window. Simulations were used to estimate the backgrounds expected in each window, and less than 0.11 background events were expected in all cases. No evidence for low-multiplicity bursts was observed [4].

Neutrinos also play an important role in the explosions of massive stars, so called core-collapse supernova explosions (CCSN). In this context the TRIUMF Theory Group is studying the neutrino-nucleus interaction, which is an important input for an improved modelling of CCSN.

CCSN are also favourite candidates for the astrophysical site of the so-called r-process that is responsible for the production of about half of the heavy chemical elements. Reactions of neutrinos with nuclei will play a role in this as well. The HALO supernova neutrino detector experiment at SNOLAB, which has just started data taking, is almost unique in that it is primarily sensitive to ν_e rather than anti- ν_e . As a part of the Supernova Early Warning System (SNEWS), HALO will help detect galactic supernovae by their neutrino burst allowing time to notify astronomers.

Searching for Dark Matter

Evidence from large-scale structure formation in the universe and the structure of the cosmic microwave background indicates that non-luminous “dark matter” (DM) not corresponding to any known form of matter is about five times as abundant as regular baryonic matter from which our environment is built. DM exerts a gravitational force but feels neither the electromagnetic nor the strong nuclear force. One conjecture is that DM consists of a vast swarm of weakly interacting massive particles (WIMPs) surrounding each galaxy. If so, they could be observed via collisions with detectors here on earth (e.g., DEAP currently under construction in SNOLAB or SuperCDMS), or they could be produced in very high-energy collisions (e.g., ATLAS at the Large Hadron Collider). Determining the nature of DM is one of the most pressing issues in particle physics today.

The TRIUMF Theory Group investigates and proposes candidates for DM by making use of data from direct, indirect, and collider searches. It also works to develop new methods to discover and measure the properties of DM, to conduct direct searches for DM and opens new experimental directions.

Most direct experimental searches for DM focus on the simplest possibility of a single DM particle scattering elastically with target nuclei. Recent proposals for DM candidates by the Theory Group show that much richer interactions are possible, such as contributions to the scattering from multiple stable dark matter species [16] and inelastic processes [17].

The observed density of DM is also significantly close to the cosmological density of baryons, suggesting a common origin for both. Recently a new mechanism was developed in which the DM consists of hidden exotic antibaryons [18, 19]. The DM candidates in this mechanism can contribute to elastic scattering in direct detection searches, but they can also undergo inelastic collisions with nucleons, producing anti-DM and a meson. This latter process leads to novel signals from DM scattering in searches for nucleon decay, and opens up a new channel for DM discovery.

Selected References

- [1] B. Aharmim et al. (SNO Collaboration), *Phys. Rev. Lett.* 101, 111301 (2008).
- [2] B. Aharmim et al. (SNO Collaboration), *Astrophys. J.* 710, 540 (2010).
- [3] B. Aharmim et al. (SNO Collaboration), *Phys. Rev. C* 81, 055504 (2010).
- [4] B. Aharmim et al. (SNO Collaboration), *Astrophys. J.* 728, 83 (2011).
- [5] B. Aharmim et al. (SNO Collaboration), *Phys. Rev. C* 87, 015502 (2013).
- [6] B. Aharmim et al. (SNO Collaboration), *Phys. Rev. C* 88, 025501 (2013).
- [7] B. Aharmim et al. (SNO Collaboration), *Phys. Rev. D* 80, 012001 (2009).
- [8] K. Abe et al. [T2K Collaboration], *Nucl. Instr. Meth. A* 659, 106 (2011).
- [9] N. Abgrail et al., *Nucl. Instr. Meth. A* 637, 25 (2011).
- [10] P-A. Amaudruz et al., *Nucl. Instr. Meth. A* 696, 1 (2012).
- [11] K. Abe et al. [T2K Collaboration], *Phys. Rev. Lett.* 107, 041801 (2011).
- [12] M. Apollonio et al., *Euro. Phys. J. C* 27, 331 (2003).
- [13] K. Abe et al. [T2K Collaboration], *Phys. Rev. D* 85, 031103(R) (2012).
- [14] N. Ackerman et al. [EXO collaboration], *Phys. Rev. Lett.* 107, 212501 (2011).
- [15] M. Auger et al. [EXO collaboration], *Phys. Rev. Lett.* 109, 032505 (2012).
- [16] P.T. Winslow, K. Sigurdson and J.N. Ng, *Phys. Rev. D* 82, 023512 (2010).
- [17] Y. Cui, D.E. Morrissey, D. Poland and L. Randall, *JHEP* 905, 76 (2009).
- [18] H. Davoudiasl, D.E. Morrissey, K. Sigurdson and S.Tulin, *Phys. Rev. Lett.* 105, 211304 (2010).

- [19] H. Davoudiasl, D.E. Morrissey, K. Sigurdson and S. Tulin, Phys. Rev. D 84, 096008 (2011).
- [20] A.K. Ichikawa, Nucl. Instr. Meth A 690, 27 (2012).
- [21] K. Abe et al. [T2K Collaboration], Nucl. Instr. Meth. A 694, 211 (2012).
- [22] S. Aoki et al., Nucl. Instr. Meth. A 698, 135 (2013).
- [23] S. Assylbekov et al., Nucl. Instr. Meth. A 686, 48 (2012).
- [24] K. Abe et al. [T2K Collaboration], Phys. Rev. D 87, 012001 (2013).
- [25] R. Neilson et al. [EXO collaboration], Nucl. Inst. Meth. 608, 68 (2009).
- [26] A. Dobi et al. [EXO collaboration], Nucl. Inst Meth. A 659, 215 (2011).
- [27] M. Montero Diez et al. [EXO collaboration], Rev. Sc. Instrum 81, 113301 (2010).
- [28] D. Sinclair, J. Phys C S203, 012062 (2010).
- [29] D. Sinclair, J Phys. C S309, 12005 (2011).
- [30] A. Dobi et al. [EXO collaboration], Nucl. Inst. Meth. 675, 40 (2012).
- [31] M. Auger et al. [EXO collaboration], JINST 7, 05010 (2012).

4.2.1.3 FUNDAMENTAL SYMMETRIES

Symmetries play a central role in particle physics and our understanding of the basic building blocks of the universe. In addition to space-time symmetries that give rise to fundamental laws like the conservation of energy and gauge symmetries which produce the fundamental interactions, there are the discrete symmetries of charge-conjugation (C), which exchange particles and antiparticles, parity (P), the reversal of spatial coordinates, and time-reversal (T).

The foundations of physics were shaken to its core in 1957 with the discovery of the violation parity symmetry of violation in beta decay, which has since been incorporated into the Standard Model of weak interactions. The combined charge-parity symmetry (CP) was also found in 1964 and has since been explained by the presence of a complex phase in the mixing of quarks. The combination of all three discrete symmetries (CPT) is an intrinsic outcome of the quantum field theories that are the foundation of the Standard Model of particle physics. An observation of CPT violation would require radical reworking of our understanding of particles and interactions.

The question of CPT violation remains a crucial question, as the known sources of CP violation in the Standard Model, an essential ingredient in generating a matter-dominated universe, are insufficient to create the observed asymmetry in our universe. Further sources of CPT violation can be studied by comparing matter/antimatter counterparts of the same system, or through T violation, which is related to CP violation through CPT symmetry.



MAKOTO FUJIWARA WINS JOHN DAWSON AWARD

04 April 2012

TRIUMF scientist and ALPHA-Canada spokesperson, Makoto Fujiwara, was awarded the 2011 John Dawson Award by the American Physical Society. Dr. Fujiwara was recognized for his role in the introduction and use of innovative plasma techniques which produced the first demonstration of the trapping of antihydrogen inside the ALPHA experiment at CERN. The award is bestowed upon scientists that make breakthroughs in the field of plasma physics. Dr. Fujiwara was the sole recipient from TRIUMF and the only Canadian to win the award in 2011.

This award was specifically given for the trapping of antihydrogen, which took place in November 2010. Since that time, there have been a number of important breakthroughs involving ALPHA. In the middle of 2011 Dr. Fujiwara was the lead author of a paper that appeared in Nature Physics, which revealed that the ALPHA team had trapped antimatter atoms for 16 minutes. In March 2012, another paper was published in Nature, revealing that ALPHA, with leadership from Canadian researchers, had measured for the first time an intrinsic property of antimatter atoms.

Probing Matter/Antimatter Asymmetry with ALPHA

Atomic hydrogen is one of the best-studied systems in all of physics and has played a central role in establishing quantum physics from the Bohr model to the theory of quantum electrodynamics. A comparison of properties of hydrogen and its antimatter counter-part antihydrogen addresses the validity of a fundamental symmetry, CPT, which occurs in quantum field theories that are relativistic, local, and unitary.

CPT symmetry violation is a possible explanation for how our universe comes to be composed almost entirely of matter. The ALPHA (Antihydrogen Laser Physics Apparatus) at CERN has achieved trapping of antihydrogen in 2010 [1]. In 2011, ALPHA reported confinement of antihydrogen for nearly 1,000 seconds [2], an increase by a factor more than 5,000 from the initial result. Most recently in 2012, ALPHA performed the first spectroscopic measurement on antihydrogen atoms by driving its hyperfine transitions with microwaves, an initiative led by Canadian scientists on the experiment [3]. Canadian physicists were the principal authors of two [2, 3] of the three papers published in Nature journals.

Between 2008 and 2010, ALPHA developed techniques to prepare and measure the plasmas needed to enable trapping of antihydrogen. A novel diagnosis for antiproton plasma radial profile using annihilation detection was reported [4]. Rotating RF fields were used to compress multi-component charged plasmas to the required densities [5]. A new mode of particle transport in a Penning trap was observed [6]. Formation dynamics of antihydrogen were studied in detail in a multipolar neutral antiatom trap [7]. Evaporative cooling, a common method for cooling neutral atoms, was applied for the first time to cold plasmas, achieving antiproton temperatures as low as 10 K [8]. Autoresonant injection of the antiprotons into the positron plasmas enabled the mixing of these plasmas with minimal heating [9]. Direct observation of centrifugal separation allowed detailed studies of equilibration dynamics in electron-antiproton plasmas [10]. These developments involving innovative plasma techniques were made possible by the use of antiproton annihilation detection, together with plasma imaging with multi-channel plates [11]. Microwave probing and manipulations of trapped charged plasmas provided useful information about their properties and allowed a precise measurement of the magnetic field in the trap centre. Its position-sensitive annihilation detection capability distinguishes ALPHA from its competition.

In 2009 ALPHA achieved plasma conditions that produced very cold antihydrogen atoms and reached detection sensitivity which allowed detection of trapped antihydrogen. The first six candidate events for trapped antihydrogen were observed that year, with a statistical significance sufficient to reject the dominant cosmic background [12]; however, it was not possible to experimentally rule out a background process from annihilations of magnetically trapped bare antiprotons. In 2010, new techniques were proposed and developed to experimentally eliminate the possibility for bare antiproton background [13]. This led to a definitive proof of trapping [1]. Subsequently, ALPHA increased the trapping yields, and by introducing a delay between the time when the antihydrogen atoms are synthesized and their release time from the trap, the collaboration ascertained that antihydrogen remained trapped for at least 1,000 seconds [2] (see Figure 1), which was sufficient to enable spectroscopic studies on single antiatoms. This was the major milestone required to proceed with spectroscopy.

Techniques to irradiate plasmas in the ALPHA trap with microwaves have been developed at the University of British Columbia and Simon Fraser University since 2005, and in 2011 the first experiments with high-power microwaves were performed. Irradiating the

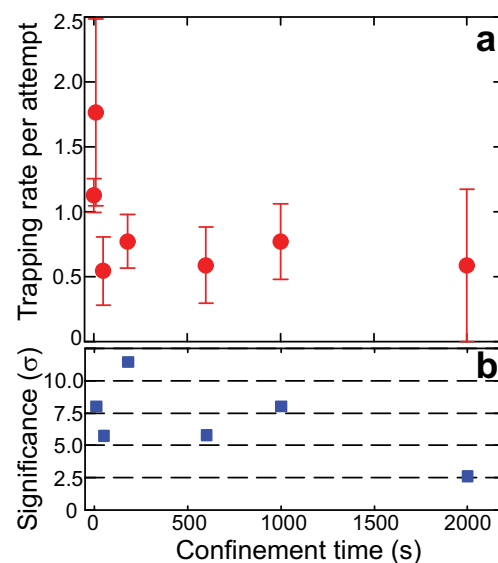


Figure 1: Antihydrogen trapping rate as function of confinement time. From Ref. [2].

antihydrogen atoms at the resonant frequency of the positron spin resonance transitions at 28 GHz drives the transition from a trappable to a non-trappable state, expelling it from the trap. An excess of annihilation events during the irradiation (see Figure 2) and a strong decrease of these events when the trap was subsequently emptied were seen, setting bounds on the antihydrogen resonances within 100 MHz of the corresponding hydrogen resonances [3]. Highly sensitive annihilation detection capability was a key to both of these measurements.

Following the success in initial microwave spectroscopy, the collaboration has taken on a major upgrade project, ALPHA-2, to enable laser spectroscopy of trapped antihydrogen, and to provide improved and more flexible magnetic field configuration for microwave spectroscopy and anti-atom manipulations (see Figure 3). Recent theoretical simulations suggest that such an extension would allow laser cooling of antihydrogen to temperatures as low as 20 mK [14].

Electric Dipole Moments

An electric dipole moment (EDM) of a system is the projection of its charge distribution along the total angular momentum vector J . Thus $D=dJ$. Under parity transformations (P), D changes sign, but J does not, and under time reversal (T), J changes sign, but D does not. Thus d must be odd under both P and T transformations. We can think of the EDM as arising from an electrical polarization of the system that is induced by elementary particle interactions that violate P and T, and, assuming CPT invariance, must violate CP.

Among the most interesting contemporary motivations for the measurement of EDMs is the connection to baryogenesis laid out in the Sakharov criteria requiring (1) baryon number violation, (2) CP violation, and (3) non-equilibrium expansion. Standard Model sources are not sufficient to generate even the observed baryon asymmetry of the universe; thus new forms of beyond-Standard-Model physics CP violation are expected. Most significant extensions of the Standard Model introduce additional phases that could produce the baryon asymmetry and lead to an EDM many orders of magnitude larger than those through quark mixing in the Standard Model [5]. For example, supersymmetric models introduce phases that could produce the baryon asymmetry at the electroweak scale and produce EDMs of atoms or the neutron close to the current limits of sensitivity. CP violation is also a valuable observable for probing physics beyond the

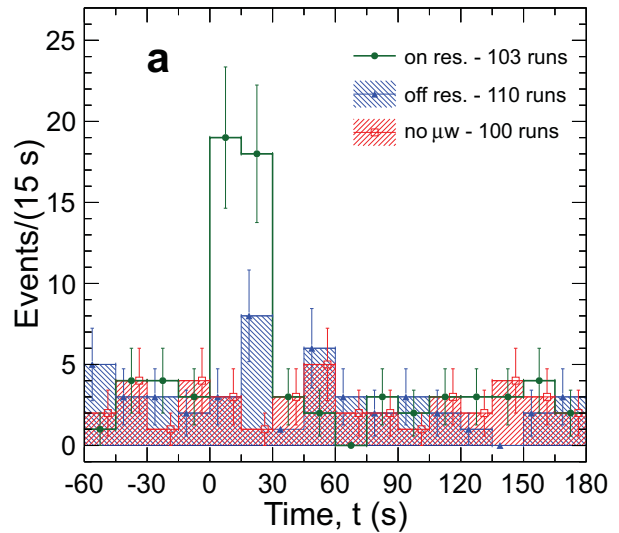


Figure 2: Antihydrogen annihilation time distribution as a function of time, for microwave on resonance, off resonance and no microwave dataset. Microwaves are applied at time 0, and the annihilation peak at that time indicates the induced spin flip of antihydrogen. From Ref. [3].

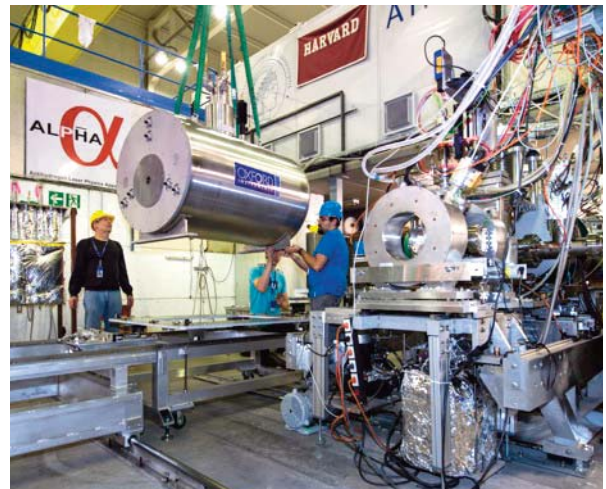


Figure 3: The ALPHA-2 apparatus is the major upgrade project currently in progress. The most recent addition has been the atom-trap cryostat built at TRIUMF. Together with the new superconducting solenoid (built by Oxford Instruments in the UK and financed by the Danish Carlsberg Foundation), they join the catching trap and the existing positron accumulator from ALPHA to make up the complete chain of apparatus. Photo © 2012 CERN

Standard Model more generally, i.e. CP violation can be used to reveal a weaker interaction in the presence of the dominant strong and electroweak interactions of the Standard Model.

There have been a number of measurements of EDMs in systems that have strong sensitivity to the electron EDM (paramagnetic systems) and EDM in hadronic systems (diamagnetic atoms, the neutron and future storage-ring experiments with nuclei). There are also several ways in which beyond-standard-model physics can contribute to the EDM of a system: θ_{QCD} , electron EDM, intrinsic quark EDMs, and EDMs induced by hadronic currents (chromoEDMs- $d_{w,d}$), 4-quark interactions, and 3-gluon interactions. In fact, there are three dominant contributions in paramagnetic systems and at least ten independent parameters in hadronic systems. This means that it will be crucial to push ahead with EDM measurements in a number of systems, particularly hadronic systems.

Neutron EDM

Measurements of the neutron electric dipole moment (nEDM) d_n are sensitive probes of quark EDMs, or quark chromo-EDMs. New physics scenarios seeking to describe the baryon asymmetry often generate nEDMs of $O(10^{-27})$ e-cm, just beyond the current experimental limit of $d_n < 2.9 \times 10^{-26}$ e cm. The nEDM tends to be more sensitive to the EDMs of the constituents (quarks and gluons) than the atomic and molecular systems because there is no electron cloud in the system to screen the EDMs.

The next generation of nEDM experiments worldwide aims to constrain the d_n $O(10^{-27}-10^{-28})$ e cm. The goal of the first experiment at the TRIUMF Ultra-Cold Neutron (UCN) Source is to reach a precision corresponding to $d_n < 1 \times 10^{-27}$ e cm by 2017. Further improvements to the apparatus, and to the UCN facility itself, are planned for after 2018, with the eventual goal of achieving $d_n < 1 \times 10^{-28}$ e cm. A basic overview of the physics behind our nEDM concept is presented in Ref. [17]

The basic design of the TRIUMF nEDM experiment calls for a room temperature EDM experiment to be filled with ultra-cold neutrons (UCN) by our cryogenic UCN source, which is based on the design successfully deployed by our Japanese collaborators, led by Y. Masuda [17,18]. Neutrons are moderated, and then converted into UCNs by down-scattering in superfluid helium (see Section 5.5.3.2). The EDM experimental apparatus to be used at TRIUMF has several unique features and improvements with respect to other EDM experiments. The cell size is reduced, anticipating the gains in UCN density. Both the active and the passive magnetic shielding are improved, as are the control and characterization of the magnetic field, and a new Xe-129 comagnetometer technology is used.

The UCN source and a prototype EDM experiment will be developed and operated at the Research Center for Nuclear Physics (RCNP, Osaka) at low luminosity until 2014. Relevant apparatus for the eventual experiment at TRIUMF will be moved in 2015 for integration with subsystems now being developed in Canada, with first operations in 2016.

Further experiments on the neutron lifetime in a magnetic trap, and on quantized energy levels of neutrons confined above a mirror by Earth's gravitational field are considered, among others, as candidates for the long-term physics program.

Canadian involvement in the nEDM experiment has now expanded to include research and development on key components, and construction of new equipment. The main components are the comagnetometer and the UCN detector. The University of British Columbia (UBC) and the University of Winnipeg are completing new systems to develop the xenon comagnetometer concept. At UBC, a system to study direct two-photon optical pumping of xenon has produced its first results. At the University of Winnipeg, a xenon polarizer system has been developed based on spin-exchange optical pumping with rubidium. They are also investigating a new UCN detector concept for sensing the high count rate expected in the EDM experiment, based on lithium-loaded glass scintillator and possible pulse-shape discrimination to reject gamma-ray backgrounds. Figure 4 displays some detector prototyping and fabrication process steps at the Nanosystem Fabrication Laboratory at the University of Manitoba.

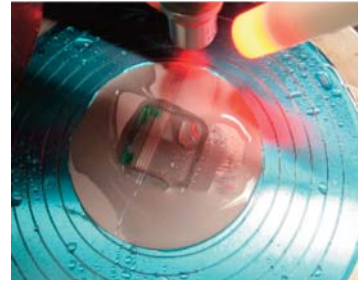
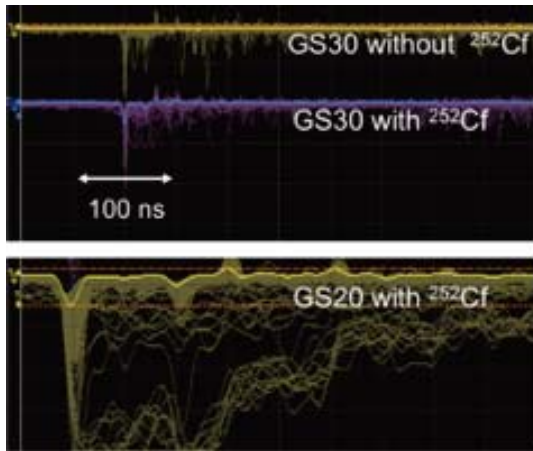


Figure 4: Left: Oscilloscope traces of PMT outputs showing neutron captures on GS20 (Li-6 enriched) and GS30 (Li-6 depleted) glass scintillator. Right: Cutting glass scintillator at UM

TRIUMF is developing a new high-voltage system to study EDM cell geometries and leakage currents in xenon and other gas environments, and the University of Winnipeg group is developing a prototype magnetic shield for the nEDM experiment. Both will eventually come together at TRIUMF to combine shielding, the Xe comagnetometer, and high voltage into one apparatus before the first experiments with ultra-cold neutrons. Figure 5 displays a test apparatus at the University of Winnipeg for active magnetic compensation of environmental fields in the laboratory, using a fluxgate magnetometer within a box coil. The group is also conducting detailed Monte Carlo studies of cold neutron moderators, and spin evolution in the EDM experiment due to magnetic field inhomogeneities (resulting in a variety of systematic effects). These studies include estimates of thermal transport in the UCN source, in particular, heat transport through the superfluid helium.

Active research and development on most of these topics is in progress at this time. The xenon work has produced some first results on spectroscopy of the relevant levels and magnetic sublevel effects.

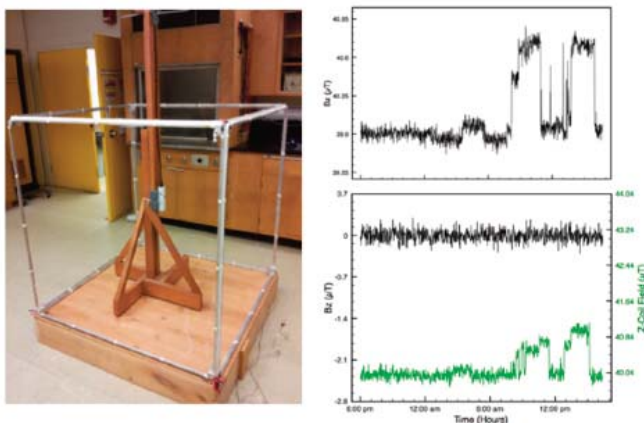


Figure 5: UW test apparatus (left) with three-axis fluxgate magnetometer on wooden stand at centre of x-, y-, and z-compensation coils. Results showing the $\sim 1 \mu\text{T}$ field perturbation (top right) that occurs during working hours due to opening/closing of shipping bay doors one floor below; the same time period on a different day with active compensation running (bottom right), the compensating field is shown in green.

Atomic EDM using Radon

In octupole-deformed nuclei, collective effects produce higher order vibrations and deformations that can lead to a large intrinsic dipole moment, and a T-violating interaction can align this moment with the nuclear spin. The result is an expected enhancement of the Schiff moment (effectively the RMS of the dipole moment distribution) by factors of several hundred to a thousand with respect to Hg-199. Two different systems provide experimental opportunities to extend the sensitivity to T violation: laser cooled Ra-225 in an optical trap and spin-exchange polarized Rn-223 in a cell, both of which are investigated by TRIUMF experiment S929. For Ra-225, calculations combined with well-established spectroscopy of nuclear levels provide confidence that the enhancement relative to Hg-199 is a factor of several hundred; however, the

nuclear structure information on radon isotopes is meager, and establishing a confident estimate of the octupole enhancement requires nuclear structure measurements as input to theoretical calculations. We have therefore set the primary initial goals of the RadonEDM program as technical developments essential to the EDM measurement, with nuclear structure measurements as the secondary goal.

The radon nuclei will be polarized by spin exchange with laser-polarized rubidium in cells with N₂ buffer gas. The technical developments for the RadonEDM experiment, which are detailed in Section 5.5.1.9, include measurements of the rubidium polarization [19] and developments of the EDM measurement cell.

The RadonEDM apparatus was moved to TRIUMF from Stony Brook and set up in dedicated space on the floor of ISAC-I. [20] The beam line was extended to a new, dedicated end station and beam optics were developed to deliver beam to the foil and transfer apparatus. A test run in July 2008 had the following goals: (1) to use short-lived (i.e. about a 20-minute half-life) noble gas isotopes to perfect the online transfer techniques; (2) to set up the laser optical pumping apparatus that satisfy lab safety requirements; (3) to observe gamma-anisotropies in noble gas isotopes with a nuclear spin greater than 1/2; and (4) to measure rubidium polarization online. The experiment was successful, to some degree, in all four goals.

During a 2004 run, the technique was sufficiently developed to efficiently transfer noble gas atoms into a cell using a buffer gas. The half-life of Xe-120 was also measured. The transfer technique was about 50% efficient, so a goal was set to improve this significantly. M. Hayden of Simon Fraser University developed a cold finger (that could be rapidly heated and cooled), as well as efficient gas transfer geometry. The efficiency was tested with Xe-123 ($I = 1/2$), which could be produced in quantities sufficient for accurate efficiency measurements. Transferring a known amount of xenon from the measurement cell to the cold finger and back to the measurement cell provided a self-calibrated measurement, showing that the transfer efficiency is consistent with 100%. The process of heating and cooling takes about 5 minutes, or 1/6 of a half-life, leading to minimal loss of activity due to decay.

We also measured gamma ray anisotropies for transitions populated by the decay of polarized Xe-121. Unfortunately the production rate of Xe-121 was very low due to ion source problems, and the count rates were correspondingly low.

Currently there are essentially no data on excited states of the radon isotopes of interest. Study of nuclear structure of Rn-221 and Rn-223 is essential, and the group at TRIUMF has established an attack on several fronts. The current focus of the group is to make measurements that will establish energy levels, spins and parities of excited states through astatine decay; in contrast, at ISOLDE, radon isotopes are excited by Coulomb exchange on medium-mass targets and gamma-ray angular distributions are used to establish spins and parities, while at Michigan State University's National Superconducting Cyclotron Laboratory, gamma ray spectroscopy is used in coincidence with particle identification for fragments of a U-238 beam to identify gammas and excited states in a number of neutron-rich heavy isotopes.

The scheme at ISAC is to study astatine β -decay with a uranium carbide target operating at 2 μ A of proton current. Beam time in December 2010 led to a new and efficient three-step laser ionization process for identifying astatine isotopes by the TRILIS group at ISAC using the α decay of At-199 detected in the PACES Si(Li) detectors of the 8π spectrometer as the optimization signal. Moving to neutron-rich astatine beams, isotopes up to At-219 were delivered to, and identified with, the 8π spectrometer. This was possible because of the limited beam contamination from the surface-ionized francium and actinium isobars due to their short α -decay half-lives (e.g., 20 ms for Fr-219 and 12 μ s for Ac-219). However, for the isotopes of specific interest to the RadonEDM program, the much longer francium and actinium half-lives (4.8 minutes and 22 minutes for Fr and 52 ms and 2.1 minutes for Ac) led to a large surface-ionized contamination of the beam that completely masked any potential signal from the much less intense laser-ionized At isobars. A major effort has since been made to suppress surface-ionized beam contamination by combining the TRILIS ion source with a new RFQ system, which will be tested online at ISAC in early 2013. Based on the current conservative estimate of a roughly 1% efficiency associated with the RFQ, the predicted rates of beams delivered to the 8π spectrometer for 10 μ A of protons on a uranium carbide production target

are 10 pps and 0.1 pps for At-221 and At-223, respectively, with negligible isobaric surface-ionized contamination. While the expected At-223 intensity is below the useful threshold for coincidence spectroscopy and will require further development through, for example, implementation of thorium carbide targets at ISAC concentrating on the higher yield At-221, it will provide sufficient coincidence data to elucidate the structure of the low-lying levels of the essentially unknown Rn-221, daughter nucleus. This will also complement work at ISOLDE and NSCL described below.

At ISOLDE a Coulomb excitation experiment, led by P. Butler of the University of Liverpool, was carried out to measure octupole collectivity in Ra and Rn isotopes [21]. The initial goal has been study of the neighbouring even-even Rn and Ra isotopes with radioactive beams of Rn-220 and Ra-224 accelerated to ~ 2.8 MeV/u. Gamma decays following Coulomb excitation in Ni, Cd, and Sn targets were detected in the MINIBALL array and analyzed using the GOSIA code to determine octupole collectivity. The conclusion is that Rn-221 is most consistent with an octupole vibrator, while Ra-224 is consistent with permanent deformation. The trends in these two species suggest that Rn-221 is not permanently deformed, but may have comparable octupole moments to Ra isotopes. If this is the case and the splitting of parity-coupled states is ~ 400 keV in Ra-221 compared to ~ 40 keV in Ra, the EDM enhancement may be a factor of ten less for radon. A paper has been recently submitted. In 2012, an attempt was made to continue these studies with Rn-221. A low-current beam was eventually used to observe gamma rays associated with Rn-221 decay. However it was not possible to further identify these levels.

Recently a successful experiment was carried out at NSCL in which a 80 MeV/u U-238 beam was incident on an active diamond target. Gamma rays detected with GRETINA are correlated with fragments detected in the S800 magnetic spectrometer. The systems worked as designed and analysis is underway with the goal of identifying gammas and thus levels in the isotopes of interest along with the very large number of neutron-rich isotopes in the mass range near $A = 238$.

Electron EDM Experiment Using a Fountain of Francium

An experiment to discover or rule out an electric dipole moment (EDM) of the electron, as small as a factor of 100 below the present limits, is being developed. Francium has the highest sensitivity to an electron EDM of any atom studied and Fr-211 is the least sensitive to systematic effects. The experiment is done on atoms in free space and free fall, with no confining lasers, gasses or walls, and with no applied magnetic fields.

Discovering an electron EDM would prove the existence of a new source of CP violation, new TeV-scale physics, and undiscovered particles. Finding no EDM would, for example, constrain supersymmetric models by raising the minimum superpartner masses and lowering the maximum CP-violating phases, making supersymmetry a less plausible solution to the hierarchy problem (please see Section 4.2.1.1). Electron EDM experiments, sensitive to lepton-sector CP violation, are complementary to neutron EDM experiments, which are sensitive to new sources of quark sector CP violation and to the strong CP phase, θ_{QCD} .

A proof-of-principle, laser-cooled cesium atom electron EDM experiment was conducted in 2007, and identified areas needing further development [22]. They were: preventing loss of atoms, reducing magnetic field noise, and further understanding and controlling systematic effects. The TRIUMF experiment will look for an electric dipole moment in the valence electron of the francium atom by comparing the interaction energy (phase advance) of the francium atoms with their spin aligned and anti-aligned with an applied electric field.

Atoms in a francium fountain (a cloud of cold atoms launched upward by laser beams, similar to an atomic clock) will enter an electric field produced by parallel conducting plates 1 cm apart at about ± 50 kV. Under the influence of gravity, the atoms, which enter at about 3 m/s, slow, turn around, and fall out of the electric field plates, having spent about 0.7 s in the electric field. The atomic state is prepared by laser light before entering the electric field and is analyzed after leaving the electric field. The measurement is thus done in free space and free fall, with no confining lasers, gasses, or walls.

The slow-moving neutral atoms, however, will experience forces in an inhomogeneous field region as they enter and exit the electric field, which will cause them to defocus. Without some form of focusing, almost all of the atoms would be lost. To avoid magnetic fields, the required focusing is provided by a pair of electrostatic triplet lenses upstream of the electric field plates. The shape of each triplet lens provides a combination dipole and sextupole electric field that acts as a transverse defocusing-focusing-defocusing lens combination, resulting in net focusing of the atoms in both transverse directions.

A linear optics solution has been completed for the transport of the francium atoms through the fountain. In addition, the optimum shape for the entrance field has been modeled [23]. With the current design, most of the atoms launched into the fountain will return and be detected.

To reach the required experimental sensitivity, magnetic noise between the state preparation and analysis needs to be 5 ft or less. Electron EDM experiments are sensitive to magnetic noise (principally along the electric field direction) through the interaction of the magnetic moment of the valence electron with the changing magnetic field. Magnetic noise was measured at a possible experimental site on the TRIUMF ISAC facility experimental floor during machine operation on May 25, 2011. To reduce the fluctuations to below 5 ft, a shielding factor of about 6.6×10^6 is needed along the quantization axis. Both time varying magnetic fields, and the Earth's static magnetic field can in principle be shielded with mu-metal although a shielding factor of such a large magnitude must be demonstrated.

To test shielding calculations, design, and assembly, a half-scale prototype magnetic shield was constructed consisting of four layers of 3.17 mm-thick Carpenter HyMu 80 alloy. It was constructed at LBNL and tested in a three-axis vertical test stand designed and constructed at TRIUMF (see Figure 6). A known external field was applied and the field inside the shields was measured to determine the transfer function. Three layers provided a radial shielding factor in excess of 10^7 , in agreement with calculations. Because the shielding factor decreases with size, the full-size shield will have four layers.

The most complete calculations of EDM-mimicking effects in any system have recently been completed for francium and cesium [24]. Control of systematic effects is the main obstacle to improving the electron EDM limit. The use of electric field quantization, in which the ratio of electric field splitting of levels of different $|m_F|$ to the Zeeman splitting is about 100, suppresses the EDM-mimicking effects of motional magnetic fields seen by the atoms moving through the electric field. The calculation expands the complete time evolution operator in inverse powers of this ratio. For a specific set of coherent states, potential systematic errors enter only as even powers of the ratio, making the expansion rapidly convergent. The use of Fr-211, which has large electric field splittings, and the nulling of remnant magnetic fields, can keep false EDMs below the experimental goal.



Figure 6: The magnetic shielding test stand with Ben Feinberg. The shields are inside the central cylinder and are positioned vertically as in a fountain. Magnetic fields in both transverse directions are produced by long rectangular coils wound on the wood forms seen prominently in the photograph. Axial fields are produced by solenoid coils wound on a fiberboard cylinder.

MTV: Test of Time Reversal Symmetry Using Polarized Unstable Nuclei

The MTV (Mott polarimetry for T-Violation) experiment searches for violation of time reversal symmetry in a nuclear beta-decay using a new type of particle position detection device. A test experiment in 2008 at KEK in Japan confirmed 10% precision [25] by precisely measuring the polarization of electrons emitted in the beta decay of polarized Li-8. A demonstration of the existence of electron polarization perpendicular to the electron momentum direction would signal the violation of time reversal symmetry. The world's highest precision of 0.1% can be achieved at TRIUMF, thanks to the large intensity and high polarization of the Li-8 beam produced at ISAC.

A first test experiment in 2009 demonstrated that 0.1% statistical precision can be achieved to 10^7 polarized Li-8 particles per second from ISAC, at around 80% polarization, a marked improvement over the 10^5 particles per second and 8% polarization at KEK. A physics run in 2010 accumulated sufficient statistics for a 0.1% result [26,27]. Further improvements of the sensitivity can be achieved with a new Cylindrical Drift Chamber (CDC) that was developed in Japan, and successfully tested at ISAC in November 2012. The physics dataking with the new CDC setup will start in 2013. The Standard Model of particle physics predicts negligible signals for the MTV experiment, thus any evidence of a T-violating effect in MTV would constitute evidence for new physics beyond the Standard Model. MTV expects to eventually achieve 0.01% precision to T-violating effects.

Selected References

- [1] G.B. Andresen et al., *Nature* 468, 673 (2010).
- [2] G.B. Andresen et al., *Nature Physics* 7, 558 (2011).
- [3] C. Amole et al., *Nature* 483, 439 (2012).
- [4] G.B. Andresen et al., *Phys. Plasmas* 15, 032107 (2008).
- [5] G.B. Andresen et al., *Phys. Rev. Lett.* 100, 203401 (2008).
- [6] G.B. Andresen et al., *Phys. Plasmas* 16, 100702 (2009).
- [7] G.B. Andresen et al., *Phys. Lett. B* 685, 141 (2010).
- [8] G.B. Andresen et al., *Phys. Rev. Lett.* 105, 013003 (2010).
- [9] G.B. Andresen et al., *Phys. Rev. Lett.* 106, 025002 (2011).
- [10] G.B. Andresen et al., *Phys. Rev. Lett.* 106, 145001 (2011).
- [11] G.B. Andresen et al., *Rev. Sci. Instr.* 80, 123701 (2009).
- [12] G.B. Andresen et al., *Phys. Lett. B* 695, 95 (2011).
- [13] C. Amole et al., *New Journal of Physics* 14, 105010 (2012).
- [14] P.H. Donnan, M.C. Fujiwara, F. Robicheaux, *J. Phys. B* 46, 025302 (2013).
- [15] G.B. Andresen et al., *J. Phys. B: At. Mol. Opt. Phys.* 41, 011001 (2008).
- [16] G.B. Andresen et al., *Nucl. Instrum. Methods A* 684, 73 (2012).
- [17] Y. Masuda et al., *Phys. Lett. A* 376, 1347 (2012).
- [18] Y. Masuda et al., *Phys. Rev. Lett.* 108, 134801 (2012).
- [19] E.R. Tardiff et al., *Phys. Rev. C* 77, 052501(R) (2008).
- [20] T. Chupp, *Nucl. Phys. A* 827, 428 (2009).
- [21] L.P. Gaffney et al., *Nature* 497, 199 (2013).
- [22] J.M. Amini, C.T. Munger Jr., and H. Gould, *Phys. Rev. A* 75, 063416 (2007).
- [23] B.J. Wundt, C. T. Munger, and U. D. Jentschura, *Phys. Rev. X* 2, 041009 (2012).
- [24] J.G. Kalnins, *Phys. Rev. ST Accel. Beams* 14, 104201, (2011)
- [25] H. Kawamura: Study of time reversal symmetry in nuclear beta-decay using tracking detector. (D.Sc. Thesis, Rikkyo University, 2010).
- [26] J. Murata et al., *J. Phys. CS* 312, 102011 (2011).
- [27] J. Onishi et al., *J. Phys. CS* 312, 102012 (2011).

4.2.1.4 WEAK INTERACTION STUDIES

Of the three fundamental forces described by the Standard Model (SM) of particle physics, the weak interaction is the least well understood. The relative weakness of the weak force at low energies, compared to electromagnetism or the strong force, makes it more challenging to study experimentally. The weak force is also very different in its structure from the other known forces in that it violates the parity (P), charge conjugation (C), and flavour symmetries. Precision studies of the weak force at TRIUMF seek to improve our understanding of the weak interaction, and to investigate the origin of P-, CP-, and flavour-symmetry breaking.

Fundamental forces in the SM are induced by the exchange of vector boson particles. The electromagnetic force is mediated by the massless photon and the strong force is mediated by the massless gluon. In contrast, the weak force arises in the SM from the exchange of massive $W^{+/-}$ and Z^0 vector bosons. The large masses of these mediators compared to the proton ($m_p = 0.938 \text{ GeV}/c^2$), $m_w = 80.4 \text{ GeV}/c^2$ and $m_z = 91.2 \text{ GeV}/c^2$, are the reason why the weak force is so weak at low energies. At higher energies, approaching m_w , the SM describes how the weak force grows to be of comparable strength to the other forces and unifies with the electromagnetic force to form a single electroweak force. The splitting of the weak and electromagnetic components is called electroweak symmetry breaking, and is caused by the Higgs field in the SM. Studies of the weak force at high energy seek to test this unification and to probe the underlying cause of electroweak breaking.

In addition to testing the SM, precision measurements of the weak force at both low and high energies also offer the exciting prospect of discovering new particles and forces beyond the SM.

The many possibilities for this new physics can be classified according to the mass scale Λ of the new particles. Energies larger than Λ are needed to create the new particles directly; however, the effects of exotic particles can also make themselves felt at much lower energies by inducing new interactions among SM particles suppressed by the large mass Λ (in direct analogy to how the weak force operates at energies below m_w). By looking for deviations from the SM in weak-interaction processes, lower-energy experiments with high precision can detect indirectly the existence of new physics. Low- and high-energy tests of the weak force therefore play a complementary role in the search for new particles and forces, and TRIUMF has been and continues to be involved in a number of world-leading efforts through its in-house program (TWIST, PIENU, TRINAT, 8π , FrPNC) as well as through external efforts with ATLAS (please see Section 5.5.5.2 (LHC/CERN), and Qweak (JLAB)).

The simplest and best-studied weak interaction process is the decay of the muon into an electron and a pair of neutrinos, $\mu \rightarrow e\nu_e\nu_\mu$. This decay is induced by the exchange of a W vector boson.

The TRIUMF Weak Interaction Symmetry Test (TWIST) made a detailed study of the decays of positively charged spin-polarized muons. By measuring the angle and momentum distributions of the positrons (e^+) emitted in these decays, the experiment obtained the most precise determination ever of the muon decay parameters ρ , δ , and $P_\mu\xi$, as shown in Figure 1.

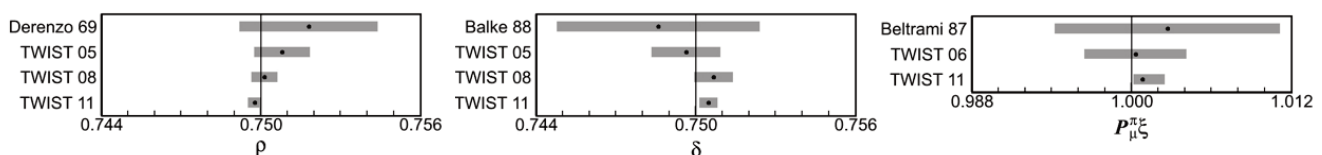


Figure 1: TWIST measurements of the muon decay parameters ρ , δ , and $P_\mu\xi$ relative to previous determinations. In each plot, the vertical line shows the Standard Model prediction and the grey bars show the total uncertainty.

The TWIST measurement relied on an intense high-quality TRIUMF muon beam and used a high-precision positron tracking spectrometer to measure the decay products, together with the extensive computational resources of WestGrid Canada for data analysis. A first intermediate result was published in 2008 [1] demonstrating an understanding and control over the dominant systematic uncertainties. Some data were also obtained for negative muon decay in orbit around a nucleus, with a precision that required the inclusion of radiative corrections for the first time in that system [2]. The summary of the final results from a blind analysis of billions of muon decays was released in early 2011 [3]. As with most precision experiments, the final uncertainties were dominated by systematic effects whose magnitudes had to be assessed and verified carefully [4,5].

The final TWIST result improved the measurement of the muon decay parameters ρ , δ , and $P_{\mu\xi}$ by approximately one order of magnitude compared to the previous Particle Data Group world-average. These results are consistent with the predictions of the SM, and they place a strong limit on many types of new physics. For example, in the case of left-right symmetric models, the masses of exotic charged scalars or vectors coupling to leptons are constrained to be larger than thousands of GeV in some cases. These limits are comparable to those obtained by direct high-energy searches (such as the LHC) if the new particles also couple to quarks, and much stronger if they do not [3].

The PIENU experiment at TRIUMF is studying this decay channel with the primary goal of measuring the decay rate of charged pions to electrons relative to the much more common decay to muons, $R_{e\mu} = \Gamma(\pi \rightarrow e\nu(\gamma))/\Gamma(\pi \rightarrow \mu\nu(\gamma))$, to a precision better than 0.1%. This measurement will provide the best test of electron-muon universality in weak interactions and test the Standard Model (SM) prediction of $R_{e\mu} = 1.2353(1) \times 10^{-4}$.

The branching ratio $R_{e\mu}$ is obtained comparing the positron yield from the $\pi^+ \rightarrow e^+\nu$ decay ($E_e = 69.8$ MeV) to the yield from the $\pi^+ \rightarrow \mu^+ \rightarrow e^+\nu\nu$ decay chain, where $\pi^+ \rightarrow \mu^+\nu$ is followed by the decay $\mu^+ \rightarrow e^+\nu\nu$ ($E_e = 0.5 - 52.8$ MeV). To reduce positron contamination in the pion beam, the M13 channel was upgraded [6] and the detector system was installed in 2008 for an engineering run. After many improvements in the detector and data acquisition system in 2009, smooth data taking started in 2010. Although the sample size was ultimately limited by short beam periods, a few million clean $\pi^+ \rightarrow e^+\nu$ events were accumulated by the end of 2012, and this reduced the statistical uncertainty to below 0.1%. Extensive Monte Carlo simulation and data studies are expected to reduce the systematic uncertainties significantly below this level as well.

A measurement of $R_{e\mu}$ to a precision of 0.1% will represent an improvement by a factor of four relative to the current world-average. At this level, deviations from the SM due to new pseudoscalar particles with masses up to 1,000 TeV can be probed, as can charged Higgs bosons with masses up to 500 GeV [7]. Data from PIENU can also be used to search for exotic massive neutrinos N emitted in $\pi^+ \rightarrow e^+N$, as these would modify the energy spectrum of the emitted positron. An analysis of preliminary data has been used to improve the limit on massive neutrinos in the mass region $m_\nu = 65-130$ MeV, where the limit on mixing with SM neutrinos $|U_{ei}|^2$ has been constrained to a level of ten parts in a billion [8,9].

Weak interactions also play an important role in atomic nuclei. The best-known example is beta decay where a neutron decays to a proton, an electron, and a neutrino through the exchange of a W boson, $n \rightarrow p e \bar{\nu}_e$. Precision measurements of beta decays have been made at TRIUMF by the 8π , GPS, TITAN, and TRINAT experiments.

The TRIUMF 8π experiment has measured the half-life of Fermi-type beta decays in Ga-62, K-38m [10], and Al-26m [11,12], obtaining world-leading precision branching ratios in each case. Also half-life measurements with GPS and 8π on O-14 [13], Ne-18 [14], Ne-19 [15] achieved world leading precision. These results have been combined with other experiments to obtain a world-best determination of V_{ud} , the first element of the Cabibbo-Kobayashi-Maskawa matrix that describes the coupling of the W boson to quarks and a fundamental constant of the SM. The result for V_{ud} , together with the world averages of V_{us}

and V_{ub} provide the most stringent test of the unitarity of the CKM matrix. Detailed measurements of the energy released in these decays also give the best existing limits on new scalars that couple to normal-chirality leptons. Measurements in Al-26m give a sensitive test of isospin mixing, a vital input needed to determine the potential accuracy of future isospin-mixing calculations. Related measurements of the beta decay, mass, and structure of Rb-74 have been made by GPS, 8π , collinear laser spectroscopy, and TITAN [16,17].

Beta and Nuclear-Recoil Asymmetries

Beta decays provide another access to weak-interaction physics. The TRINAT collaboration studied Rb-80 and K-37 using a neutral atom trap. The recoil asymmetry with respect to the spin in the decay of Rb-80 improves the bounds on non-standard four-fermion couplings to exotic neutrinos [18]. These measurements are limited by the 1% systematic theory uncertainty on the corrections from nuclear structure effects. To improve this, TRINAT has begun to study K-37 decays to its isobaric analog Ar-37, which has much smaller corrections that can also be calculated more accurately. Measurements of K-37 were made in an upgraded apparatus in December 2012, reaching a statistical error below 2%. Eventual goals are to reach 0.1%, a level at which several types of new physics, such as supersymmetry, can potentially produce observable effects.

The weak processes discussed so far have all been induced by the charged W boson. Significant effects can also be generated by the neutral Z boson. An example studied at TRIUMF is the violation of parity in atoms, where the exchange of Z bosons between orbital electrons and the nucleus allows atomic states with different parities to mix with one another and induces transitions that would otherwise be forbidden. The goal of the Francium Parity Non-Conservation (FrPNC) experiment [19] is to measure these effects in francium (Fr) atoms. As the heaviest alkali, francium is particularly well suited to this type of study; the single valence electron implies the atom is simple enough in structure to be understood theoretically, while its large mass produces a strong overlap of the electron wave-function with the nucleus, enhancing the effects of the short-ranged weak interaction. While francium has no stable isotopes, it has now been produced at rates of $5 \times 10^8/s$ from ISAC, making precision measurements possible.

In fall 2012, the FrPNC collaboration measured the atomic hyperfine splitting in francium atoms using collinear and in-trap laser spectroscopy, and detected the next higher magnetic moment beyond the nuclear dipole in Fr-207 and Fr-213. These isotopes show similar behaviour to that previously measured in Fr-208-212, suggesting regular single-particle behaviour for the valence nucleons. Such measurements will be essential for interpreting future atomic parity violation experiments at TRIUMF, which will be sensitive to the spatial distribution of neutrons in the nucleus.



DNP THESIS PRIZE AWARDED TO ROB MACDONALD

27 January 2010

Rob MacDonald of the University of Alberta was this year's winner of the 2008-2009 Division of Nuclear Physics (DNP) Thesis Prize. This prize is given in Experimental or Theoretical Nuclear Physics to a student who is obtaining his/her Ph.D. degree from a Canadian University. MacDonald's thesis "A Precision Measurement of the Muon Decay Parameters Rho and Delta" was based on doctoral research performed at TRIUMF with TWIST, under the supervision of Art Olin.

MacDonald's thesis reported intermediate results for the TWIST experiment. It was the quality of his analysis and dissertation that brought attention to his work. The thesis was not only useful for committee members, but also served as a useful reference document for the TWIST group as the experiment continued.

MacDonald commented, "Good science and good communication are very important to me. The last stages of my thesis work were devoted to checking every corner of our analysis and turning over every rock, looking for potential problems and making sure we accounted for every possible source of error." The result was a measurement Rob was confident he could support and defend.

The ultimate goal of the FrPNC experiment is to measure the weak charge, the effective coupling of the nucleus to the Z boson, of several Francium isotopes to better than 0.1%. A determination at this level will be sensitive to new vector bosons with masses up to several TeV, comparable to the sensitivity of direct searches at the LHC. These measurements will also be sensitive to the hypothetical exchange of much lighter bosons that violate parity and couple only very feebly to the Standard Model.

Parity violation can also be induced in scattering processes by the exchange of Z bosons. The Qweak experiment is studying this effect in the scattering of polarized electrons on a liquid hydrogen target by measuring the change in the scattering rate when the electron spin is reversed. The Qweak experiment is based at JLab (Jefferson Laboratory), but many of the key components including the electron detector and the electronics for the data acquisition system were built at TRIUMF. Installation of the experiment in Hall C began in December 2009 and was completed in May 2010, and commissioning took place from October 2010 until February 2011. During this commissioning phase, some 4% of the anticipated total data were obtained in 2,500 hours. Further data are being taken and considerable progress has been made analyzing them. It is anticipated that when the full data set is analyzed in 2013 and 2014, a statistical error close to the design goal of 6×10^{-9} will be achieved.

The SM prediction for the scattering asymmetry is approximately -250×10^{-9} , while the goal of the Qweak experiment is a precision of 6×10^{-9} (combined systematic and statistical) [20]. A measurement of this accuracy would determine to 0.3% the weak mixing angle $\sin^2\theta_w$ at low momentum transfer, which describes the relative strength of the weak and electromagnetic forces. The precision of this result relative to measurements of the weak mixing angle at other energies is shown in Figure 2. This level of precision also makes the Qweak experiment sensitive to many types of new physics with masses up to the TeV scale, such as an extra neutral vector boson or supersymmetry.

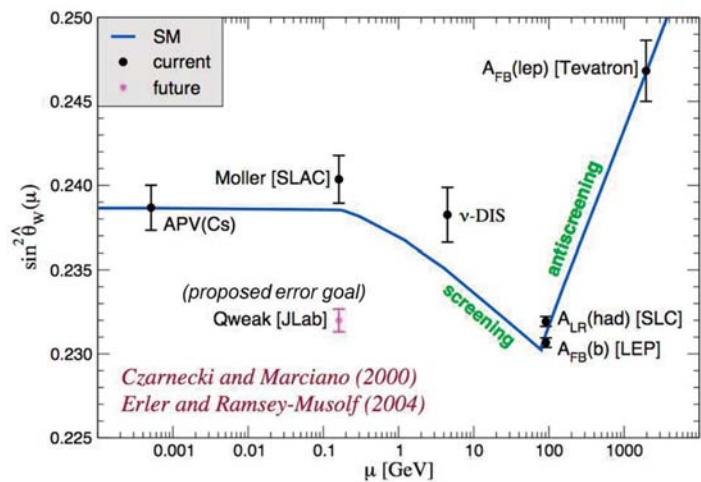


Figure 2: Estimated precision of the Qweak determination of the weak mixing angle $\sin^2\theta_w$ relative to other measurements at different energies.

A sensitive test of both the W and Z contributions to the weak force and of new physics is the anomalous magnetic moment of the muon $(g-2)_\mu$. The Brookhaven E821 experiment has already measured $(g-2)_\mu$ very precisely, and the value they obtain differs by more than three standard deviations from the theoretical prediction of the Standard Model. To confirm this result, TRIUMF is involved in a program at J-PARC (Japan Proton Accelerator Research Complex) to measure $(g-2)_\mu$ with a different approach, with independent systematic uncertainties, using the acceleration of muons following the laser ionization of muonium in vacuum [21].

In collaboration with KEK and RIKEN, a TRIUMF group has measured and characterized the emission of muonium (μ^+e^-) into vacuum following muon thermalization in silica aerogel. This is an important step in developing the high-intensity muon beam needed for the J-PARC $(g-2)_\mu$ measurement. Following an initial μ SR experiment at M20 to identify promising materials, silica aerogel samples were studied further via imaging of muon decay positrons from vacuum near the aerogel surface. Two experimental periods at the M15 muon channel allowed the characterization of muonium emission from several types of aerogel. This input was crucial to the J-PARC evaluation process that resulted in the $(g-2)_\mu$ project receiving Phase 1 approval in early 2012.

Higher-Energy Probes

Studies of the weak force at higher energies, near or above m_W , seek to probe directly the W and Z bosons that mediate this interaction. The Collider Detector at Fermilab (CDF) experiment at the Tevatron measured the mass of the W boson to a very high precision by studying proton-antiproton collisions at 1.96 TeV in which a W boson was created. In the subset of these events, where the W boson decayed to an electron or a muon and a neutrino, the particle momenta were measured and combined to form a quantity called the transverse mass m_T . The W boson mass was extracted by fitting the predicted shape of the distribution of m_T values to the data.

Applying these methods to 2.2 fb^{-1} of collision data, the W boson mass was measured to a precision of 19 MeV [22]. This single experimental measurement improves significantly on previous Tevatron and LEP combinations, which had precisions of 31 MeV and 33 MeV respectively, and dominates the new world-average W boson mass, $m_W = 80385 \pm 15 \text{ MeV}$. This improvement in the measurement in the W mass is significant because its value is sensitive to the mass of the Higgs boson and any other new particles that might be present. Applying the measured W mass to the global fit to electroweak observables gives a prediction for the Higgs boson mass of $m_H = 94^{+29}_{-24} \text{ GeV}$, consistent with the mass of the Higgs boson discovered at the LHC [23].

The ATLAS experiment at the CERN Large Hadron Collider (LHC) has studied the collisions of protons at centre-of-mass energies of 7 and 8 TeV (please see Section 5.5.5.2). With this much energy, ATLAS is able to probe both the W and Z bosons that mediate the weak force as well as the underlying structure of electroweak symmetry breaking. With the 25 fb^{-1} of proton collision data obtained so far and the exquisite sensitivity of the ATLAS detector, these studies may be done to a very high precision.

The large collision energy of the LHC means that it is a veritable factory for the W and Z weak bosons, and for top quarks (which decay by the weak interaction without first hadronizing). New results from studies of W and Z boson production include: W and Z cross-section measurements [24,25,26,27] and transverse momentum distributions [28,29]; WW [30,31,32], WZ [33,34], ZZ [35,36], $W\gamma$ and $Z\gamma$ [34,37,38] cross-section measurements; triple-gauge-boson coupling measurements for all combinations of W and Z bosons and photons; and measurements of W polarization [39] and W charge asymmetry [40] in proton collisions. There are also many new results from top quark studies, including measurements of W boson polarization in top decays [41], and measurement of the t-channel single top-quark electroweak production cross-section [42] as well as evidence for the associated production of a W boson and a top quark [43]. Many of these results are shown in Figure 3, 4, 5.

This diverse range of studies provides a strong test of the underlying electroweak structure of the weak force predicted by the SM, and so far the measurements made by ATLAS are consistent with the SM. The SM description of electroweak symmetry has also received further experimental support from the discovery of a new bosonic particle at the LHC whose properties agree with those of the SM Higgs [43]. ATLAS searches for new physics constrain the direct production of additional new particles with masses up to several TeV. These direct limits are complementary to those obtained by lower-energy precision tests. A more detailed description of these studies can be found in Section 4.2.1.1.

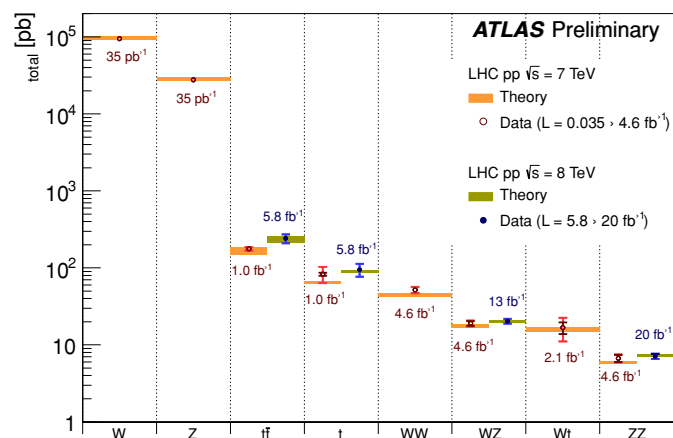


Figure 3: Measurements of weak boson production cross-sections by the ATLAS experiment.

Selected References

- [1] R.P. MacDonald et al. (TWIST Collaboration), Phys. Rev. D 78, 03201 (2008).
 - [2] A. Grossheim et al., Phys. Rev. D 80, 052012 (2009) [hep-ex/0908.4270, TRI-PP-09-28].
 - [3] R. Bayes et al. (TWIST Collaboration), Phys. Rev. Lett. 106, 041804 (2011).
 - [4] J.F. Bueno et al. (TWIST Collaboration), Phys. Rev. D 84, 032005 (2011).
 - [5] A. Hillairet et al. (TWIST Collaboration), Phys. Rev. D 85, 092013 (2012).
 - [6] A. Aguilar-Arevalo et al., Nucl. Instrum. Method A 609 (2009) 102.
 - [7] D. Bryman, W.J. Marciano, R. Tschirhart and T. Yamanaka, Ann. Rev. Nucl. Part. Sci. 61, 331 (2011).
 - [8] A. Aguilar-Arevalo et al., Nucl. Instrum. Method A 621, 188 (2010).
 - [9] M. Aoki et al., Phys. Rev. D 84, 052002 (2011).
 - [10] G. Ball et al., Phys. Rev. C 82, 045501 (2010).
 - [11] P. Finlay et al., Phys. Rev. Lett. 106, 032501 (2011).
 - [12] P. Finlay et al., Phys. Rev. C 78, 025502 (2008); P. Finlay et al., Phys. Rev. C 85, 055501 (2012).
 - [13] A. Laffoley et al., Phys. Rev. C 88, 015501 (2013).
 - [14] G.F. Grinyer et al., Phys. Rev. C 87, 045502 (2013).
 - [15] S. Triambak et al., Phys. Rev. Lett. 109, 042301 (2012).
 - [16] E. Mane et al., Phys. Rev. Lett 107, 212502 (2011).
 - [17] S. Ettenauer et al., Phys. Rev. Lett. 107, 272501 (2011).
 - [18] R. Pitcairn et al., Phys. Rev. C 79, 015501 (2009).
 - [19] S. Aubin, et al., Nuovo Cim. C 035N04, 85 (2012).
 - [20] D.S. Armstrong et al., [arXiv:1202.1255 [physics.ins-det]].
 - [21] H. Iinuma, J. Phys. Conf. Ser. 295, 012032 (2011).
 - [22] T. Aaltonen et al. [CDF Collaboration], Phys. Rev. Lett. 108, 151803 (2012).
 - [23] ATLAS Collaboration, Phys. Lett. B716, 1 (2012).
 - [24] G. Aad et al., Phys. Rev. D 85, 072004 (2012).
 - [25] G. Aad et al., JHEP 1012, 060 (2010).
 - [26] G. Aad et al., Phys. Lett. B706, 276 (2012).
 - [27] G. Aad et al., Phys. Rev. D 84, 112006 (2011).
 - [28] G. Aad et al., Phys. Rev. D 85, 012005 (2012).
 - [29] G. Aad et al., Phys. Lett. B705, 415 (2011).
 - [30] G. Aad et al., [arXiv:1210.2979] (submitted to PRD).
 - [31] G. Aad et al., Phys. Lett. B712, 289 (2012).
 - [32] G. Aad et al., Phys. Rev. Lett. 107, 041802 (2011).
 - [33] G. Aad et al., Eur. Phys. J. C 72, 2173 (2012).
 - [34] G. Aad et al., Phys. Lett. B709, 341 (2012).
 - [35] G. Aad et al., [arXiv:1211.6096] (submitted to JHEP).
 - [36] G. Aad et al., Phys. Rev. Lett. 108, 041804 (2012).
 - [37] G. Aad et al., [arXiv:1302.1283] (submitted to PRD).
 - [38] G. Aad et al., Phys. Lett. B717, 49 (2012).
 - [39] G. Aad et al., Eur. Phys. J. C 72, 2001 (2012).
 - [40] G. Aad et al., Phys. Lett. B701, 31 (2011).
 - [41] G. Aad et al., JHEP 1206, 088 (2012).
 - [42] G. Aad et al., Phys. Lett. B717, 330 (2012).
 - [43] G. Aad et al., Phys. Lett. B716, 142 (2012).
-

4.2.2 STRONGLY INTERACTING SYSTEMS: FROM NUCLEI TO STELLAR EXPLOSIONS

The strong interaction is one of the four known fundamental interactions of nature. It is responsible for a broad range of bound states between quarks and gluons. Protons and neutrons, the basic building blocks of atomic nuclei, are most commonly known representatives of strongly bound systems, jointly referred to as nucleons. Nuclei are the core of atoms and account for essentially all the mass of the matter known in the universe. The interactions between nucleons inside atomic nuclei determine the properties of atomic nuclei, for example if a nucleus is stable or is transformed through radioactive decay into another nucleus. Reactions between atomic nuclei govern the energy production in stars and the synthesis of heavier elements from the primordial fuel of stellar burning, hydrogen and helium. The elements from carbon to iron, with 26 protons, are predominantly produced in stellar interiors while we know that about half of the elements heavier than iron, up to uranium with 92 protons, are created in cataclysmic events in the universe.

Thus the study of nuclear physics connects the building blocks of life on Earth with the life and death of stars and history of the early universe back to first few minutes when the first helium and lithium were created.

The strong interaction is remarkably complex at the low energies (1 GeV) and long distance scales (1 fm = 1 millionth of a billionth of a meter) relevant for the binding of quarks into nucleons. The force between nucleons can be studied through scattering experiments with high precision. However, it remains impossible to derive the interaction between two and more nucleons in an analytical way from the underlying interaction of quarks through the exchange of gluons, the force carriers of the strong interaction. Effectively the nucleon-nucleon interaction can be viewed as a kind of Van-der-Waals interaction that leaks out of the nucleons, similar to the molecular binding of neutral molecules.

The study of the atomic nucleus has undergone a major re-orientation in the last decades and has seen the emergence of new frontiers. In particular the availability of energetic beams of short-lived (radioactive) nuclei, in the following referred to as rare isotope beams or beams of exotic nuclei, has opened the way for the exploration of the structure and dynamics of complex nuclei in regions far away from stability, where very limited information is available. Among the exciting new topics emerging from this research are, for example, the appearance of single- and double-nucleon (Borromean) halo nuclei, the increasing ability to describe nuclear properties from first principle using ever more realistic forces, as well as the breakdown of the magic numbers, the long-standing benchmark for structural evolution, and the emergence of simple patterns in the complex nuclear many-body system.

TRIUMF is at the forefront of this quest with world-leading expertise both in the theoretical and experimental investigations. The TRIUMF Theory Group is carrying out leading edge research on the properties of heavy bound mesons using lattice QCD and the application of *ab initio* theories to describe light nuclei and their reactions using realistic forces, based on chiral effective field theory. The TRIUMF rare isotope facility ISAC is using the isotope separation online (ISOL) method to produce and deliver intense rare isotope beams to a suite of world-class experiments that study the properties of ground states and excited states of nuclei, and study nuclear reactions with the aim to map out nuclear properties and determine reaction rates relevant for the understanding of nuclear burning stars and star explosions. ISOL RIB facilities like ISAC at TRIUMF, which is the ISOL facility with the highest power in the world, enable not only the precision study of nuclear properties but are also able to deliver sufficiently intense beams of species that allow the direct measurement of the very low reaction rates of nuclear reactions occurring in various astrophysical environments.

During the past five years the ISAC facility has further developed its spectrum of available beams, in particular taking advantage of laser ionization, as well as its operational reliability, enabling the new and existing experimental facilities, some of which recently expanded their capabilities, to carry out forefront research on the structure and dynamics of exotic nuclei and their role in the universe.

4.2.2.1 FROM QCD TO NUCLEAR FORCES

Quantum Chromodynamics (QCD) is a microscopic theory of strong interactions, formulated at the level of the quark substructure of matter; it specifies how the six fundamental quarks interact by exchanging gluons, the force carriers of the strong interaction. This theory can in principle explain a diverse range of phenomena, from the nature and distributions of new particles produced in the highest energy collisions at the Large Hadron Collider (LHC), to the properties and structure of known particles, stable and unstable atomic nuclei as studied at ISAC. Indeed, the development of QCD and the confirmation of its role as a microscopic description of strongly interacting matter has been a major success of the Standard Model.

Progress is advancing on a number of fronts, and TRIUMF scientists have had key roles, with seminal contributions. On the theoretical side, a method known as lattice field theory allows for a non-perturbative calculation of properties of strongly interacting quark and gluon systems. In this method, space-time is represented as a discrete lattice in a numerical procedure that can be controlled systematically. This allows for a computation of the quantum field theory equations and the prediction of a wide range of phenomena. Lattice QCD has been a long-standing research topic in the TRIUMF Theory Group, and some recent results are presented here. On the experimental side, predictions of lattice QCD, and of QCD-inspired effective field theories, can be tested by comparison with data. Precise measurements using polarized beams to study the spin structure of the proton and neutron are powerful tools to advance our progress in this challenging field. TRIUMF's contributions here have been focused on the G0 experiment at the Thomas Jefferson National Accelerator Facility (JLab) in Newport News, VA, USA. The G0 experiment probed the strange quark contributions to the nucleon electric and magnetic moments via scattering of spin polarized high-energy electron beams (see Figure 1).

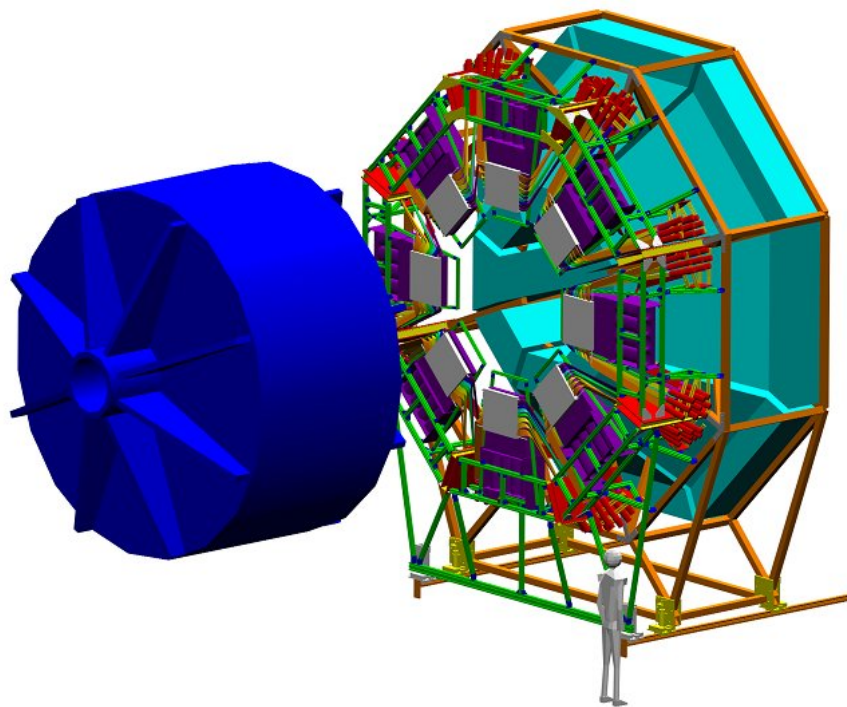


Figure 1: Detectors fabricated and tested at TRIUMF for the G0 backward angle measurements at JLab. The 8-fold symmetry of the detector system is matched to that of the superconducting magnetic spectrometer. Visible are the supports for the scintillation detector arrays (white), in front of the aerogel Cherenkov detectors, whose magnetically shielded photomultiplier tubes are visible in yellow.

The theory of QCD is studied at TRIUMF by means of numerical simulations using the techniques of lattice field theory. Understanding the strong force among quarks and gluons is a very difficult problem. The strong force bears some resemblance to the electromagnetic force between a proton and an electron, which produces the hydrogen atom with its large number of possible energy levels, but the strong force presents additional unique challenges. First the underlying theory of low-energy QCD has no small parameter in which to make an expansion, so theorists have developed a computer simulation method called lattice QCD. Secondly, there

are several flavours of quarks in nature (u,d,s,c,b,t), and their range of masses (a few MeV/c² to 170 GeV/c²) exceeds the ability of present-day computers for computation unless specific lattice QCD methods are developed and tuned to each quark flavour. Recent lattice QCD research from the TRIUMF group has produced valuable progress in the theoretical understanding of physics involving two of the heavier quarks: the charm quark and the bottom quark. A few major research highlights, where TRIUMF personnel played a primary role, are presented in this plan.

The bound state of one quark and one antiquark is called a meson. Because additional quark-antiquark pairs can appear and disappear at any time in nature, a lattice QCD study will find that two-meson states can mix with single-meson states. To deal with this significant complication, an advanced lattice algorithm called distillation has become available recently. This has been applied to the calculation of the mass and decay rate of the ρ meson (made of u, d light quarks), a benchmark problem that provides a good test of the simulation methods.

A novel application of distillation has been the ongoing study by TRIUMF scientists of mesons containing a charm quark. The goal of this work is a unified description of the energy levels within the whole family of charmed mesons, whether the second quark is up, down, strange or charm. Mesons with and without angular momentum (S and P waves) have already been studied successfully [1] and state-of-the-art lattice methods, including a large set of basis operators and the variational analysis method, were invaluable in achieving these results.

A subsequent study examined two charmed mesons, the D_0^* and D_1 mesons, in particular detail [2]. These two mesons are experimentally broad (i.e. they decay rapidly) and thus are particularly affected by nearby two-meson states. This lattice study used the distillation technique to include the coupling of D_0^* with its two-meson state ($D\pi$) and the coupling of D_1 with its two-meson state ($D^*\pi$). The calculation was done on a rather small lattice and with up and down quarks somewhat heavier than their true masses so it should be considered an exploratory study, but it stands as the first time that the D_0^* and D_1 mesons were calculated as resonances in lattice QCD. Overall, this study gave a good description of the charmed meson spectrum, including some excited states that are compatible with recent results from the BABAR experiment.

Work is ongoing to implement an even more powerful method, called stochastic distillation, which should allow simulations to be done on lattices of larger volume with lighter up and down quark masses. A goal is to extend the inclusion of two-meson operators to the charm-antistrange meson (D_{s0}^*), which still represents a puzzle for the physics community.

Lattice QCD simulations of bottom-antibottom mesons were also carried out. In familiar quantum language, one would expect to see energy levels that can be categorized as radial excitations and orbital excitations. This study observed orbital excitations (S, P, D, F and G waves) beyond the reach of any previous lattice results [3]. Radiative transitions from a radially-excited S-wave state to a lower state (by photon emission) were also observed for the first time in any lattice study of bottom-antibottom mesons [4].

A major effort was undertaken to calculate the masses of b-quark baryons (i.e. three-quark objects) using lattice gauge field configurations to contain the effects of quark vacuum polarization due to up, down, and strange quarks (provided by Japanese collaborators) [5]. In a separate effort, the bottom quark was described by a nonrelativistic expansion in the lattice simulation and tested by applying it to the bottomonium and B mesons [6].

After using known meson masses to determine all required parameter values, the baryon masses emerged as predictions from the lattice QCD simulation. When this study was published, only four of the baryons had already been seen experimentally (Λ_b , Σ_b , Σ_b^* , and Ξ_b) and there was an experimental prediction for the Ω_b that differed significantly from the lattice QCD prediction. As Figure 2 indicates, a subsequent experimental measurement produced a new value for Ω_b that is very close to the lattice QCD prediction, and another experiment published a measurement of the Ξ_b^* mass in perfect agreement with the lattice QCD prediction.

The other two baryons in the figure remain as lattice QCD predictions, awaiting experimental confirmation. To date, this is the most complete study of bottom baryons that has been done using lattice QCD.

Jefferson Laboratory (JLab) is North America’s premier electron beam scattering facility for nuclear physics. Located in Newport News, VA, the CEBAF accelerator at Jefferson Lab supplies intense beams of high-energy electrons to experiments that probe the quark substructure of the proton. The G0 experiment is a multi-year, international effort utilizing JLab’s unique spin-polarized electron beams, aimed at unraveling the strange quark contributions to the proton’s electric charge and magnetization structure. The experiment was first proposed in 1993; custom apparatus was installed in Hall C at JLab in 2003, and data taking took place in 2004 and 2006/7. Data analysis and publications commenced in 2004 and continue to the present.

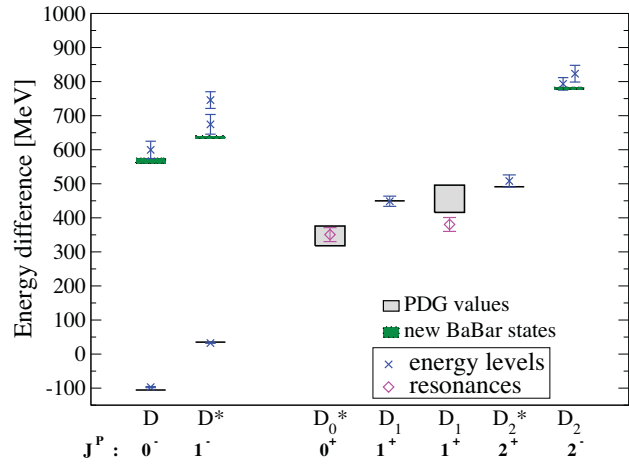


Figure 2: A study depicting two charmed mesons, D_0^* and D_1 .

In QCD, the proton is predominantly a bound state of the lightest quark constituents, two “up” quarks, and one “down” quark, and its properties are mainly determined by these. However, due to transient quantum fluctuations, heavier quarks—mainly the “strange” quark, may contribute to the proton’s properties, e.g., its charge and magnetic moment distributions.

Suggestions that strange quark quantum effects could be responsible for relatively large effects, on the scale of 15% or more of the proton’s magnetic moment [7], motivated several experiments to probe these effects. G0 is arguably the most ambitious and comprehensive of these efforts from the standpoint of kinematic coverage and instrumentation.

The G0 experiment was designed to shed light on possible strange quark contributions by using the weak interaction as a probe of the proton’s structure. Much of the G0 detection system and corresponding support structures were designed and fabricated at TRIUMF. The weak interaction has a unique feature that it is not mirror-symmetric; this feature is referred to as its parity-violating property. By combining existing measurements from “ordinary” (parity-conserving) electron scattering with a set of new parity violating electron scattering measurements obtained with the G0 apparatus, it is possible to disentangle the individual quark contributions to the proton’s electric charge and magnetization distributions. Thus, the strange quark contributions, predicted for example from lattice field theory, could be quantified for the first time by experiment.

In order to use the weak interaction as a probe of the proton structure, its parity-violating property had to be invoked. This meant that the basic electron-proton scattering process had to be compared in two distinct states related by a mirror reflection. This was achieved by manipulating the spin direction of the high-energy electron beam incident on a liquid hydrogen target. With the electron spin direction rapidly reversed with respect to its direction of motion parallel and antiparallel, a tiny change in the scattering rate results from the weak interaction (the dominant effect in this case is the electromagnetic scattering rate, which is mirror symmetric). Comparing this rate difference to its average value results in a scattering asymmetry. The scattering asymmetries in the G0 experiment were inherently very small, and high statistical precision was required in order to achieve adequate sensitivity to the suggested strange quark effects; typical asymmetries amounted to 5 parts per million, with required sensitivity at the 5% level.

The G0 apparatus used a cryogenic liquid hydrogen target, a superconducting magnetic spectrometer, and a segmented detector system to measure parity-violating asymmetries in electron-proton elastic scattering at a wide range of scattering angles, yielding information that could be related to the momentum transfer “ Q ” in the scattering process [8]—a key kinematic quantity that is needed to characterize the distributions comprising the proton’s structure.

In order to disentangle the strange quark contributions to the proton electric and magnetic moment distributions, half of the data were taken in “forward angle” mode, and the second half in “backward angle” mode. In the forward angle mode, the recoiling protons from the e-p collision were focused through the 8-sector superconducting toroidal magnet onto arrays of scintillation and Cherenkov detectors; in backward angle mode, the entire apparatus was rotated and the scattered electrons were detected. Additional detectors were added to assist with particle identification, and some data were also acquired with a liquid deuterium target, to support the main physics analysis.

Data analysis of the first phase of G0, the forward angle measurement, constrained the strange quark contribution to a linear combination of electric and magnetic form factors of the proton [9]. Additional physics results based on measurements of asymmetries with the electron beam polarized transverse to its direction of motion were also extracted from the forward angle data set [10]. These latter effects are not parity-violating, but are extremely small, and are a sensitive probe of two-photon exchange contributions to the scattering process, which is normally neglected.

The second-phase of G0, the backward angle measurement, completed data-taking in 2007, and the analysis of these data was completed in mid-2009. Efforts then focused on computing the relevant radiative corrections, which needed to be applied before the forward and backward angle results could be properly combined and the strange quark effect contributions to the electric and magnetic distributions of the proton could be extracted separately and thus achieve the full physics goals of the G0 program.

The final results (see Figure 3) showed that strange quarks make small ($< 10\%$) contributions to the ground state charge and magnetic form factors of the nucleon [11]. These results are consistent with lattice QCD simulations carried out in collaboration with the TRIUMF Theory group [12] and attracted considerable interest in the subatomic physics community. Additional physics results involving transverse beam spin asymmetry data were also extracted from the backward angle measurements [13]. As well, a description of the G0 apparatus was summarized and published [14] in 2011. In 2012, analysis and extraction of physics results involving pion electroproduction asymmetries was completed [15]. Present efforts are focused on the analysis and extraction of further physics results involving inelastic electron asymmetries. It is anticipated that these data will be released for publication in 2013.

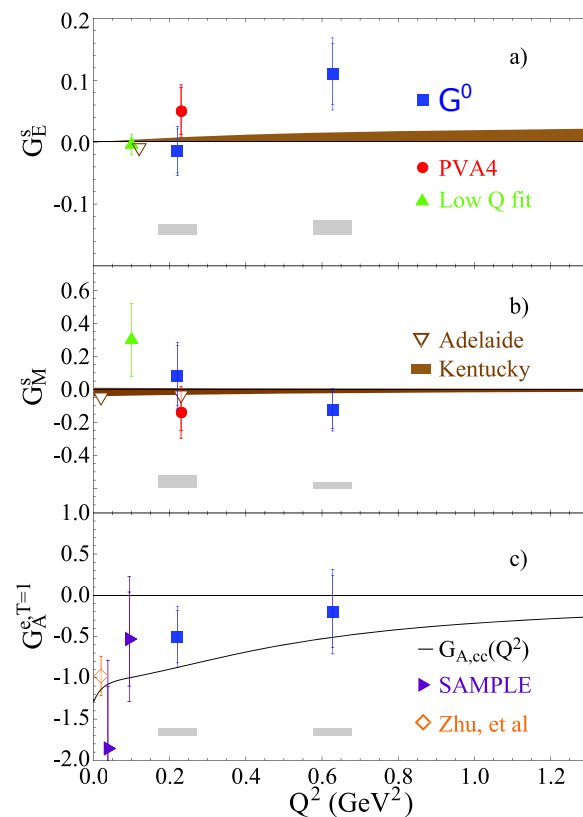


Figure 3: The form factors a) G_E^s b) G_M^s and c) $G_A^{s,T=1}$ determined by the G0 experiment and others. Error bars show statistical and statistical plus point-to-point systematic uncertainties (added in quadrature); shaded bars below the corresponding points show global systematic uncertainties (for G0 points).

Selected References

- [1] D. Mohler and R. M. Woloshyn, Phys. Rev. D 84, 054505 (2011).
 - [2] D. Mohler, S. Prelovsek and R. M. Woloshyn, Phys. Rev. D 87, 034501 (2013).
 - [3] R. Lewis and R. M. Woloshyn, Phys. Rev. D 85, 114509 (2012).
 - [4] R. Lewis and R. M. Woloshyn, Phys. Rev. D 86, 057501 (2012).
 - [5] R. Lewis and R. M. Woloshyn, Phys. Rev. D 79, 014502 (2009).
 - [6] T. Ishikawa et al., Phys. Rev. D 78, 011502 (2008).
 - [7] C.V. Christov et al., Prog. Part. Nucl. Phys. 37, 91 (1996).
 - [8] C.V. Christov et al., Prog. Part. Nucl. Phys. 37, 91 (1996).
 - [9] D.S. Armstrong et al. (G0 Collaboration), Phys. Rev. Lett. 95, 092001 (2005).
 - [10] D.S. Armstrong et al. (G0 Collaboration), Phys. Rev. Lett. 99, 092301 (2007).
 - [11] D. Androic et al. (G0 Collaboration), Phys. Rev. Lett. 104, 012001 (2010).
 - [12] R. Lewis, W. Wilcox, and R. M. Woloshyn, Phys. Rev. D 67 013003 (2003).
 - [13] D. Androic et al. (G0 Collaboration), Phys. Rev. Lett. 107, 022501 (2011).
 - [14] D. Androic et al. (G0 Collaboration), Nucl. Inst. Meth. A646, 59 (2011).
 - [15] D. Androic et al. (G0 Collaboration), Phys. Rev. Lett. 108, 122002 (2012).
-

4.2.2.2 NUCLEAR FORCES AND EXOTIC NUCLEI

Atomic nuclei are fascinating objects made up of protons and neutrons (called nucleons) and surrounded by electrons. Recent theoretical investigations predict the existence of roughly 7,500 different atomic nuclei (or isotopes) both stable and unstable ones.

Unstable nuclei have lifetimes that can be as small as a fraction of a second. The nucleons are held together, even if only for a short time, by effective forces originating from the fundamental theory of quantum chromodynamics (QCD). At the low-energy regime relevant to nuclear physics, QCD is highly non-perturbative and thus intricate. These diverse phenomena observed in nuclear physics have their roots in the complex nature of nuclear forces. As one moves away from the so-called valley of stability and investigates neutron-rich nuclei, new phenomena or structures emerge, and their interpretation is crucial to our understanding of nuclear physics. This poses one of the most challenging intellectual questions. What are the limits of nuclear existence? The intellectual challenge lies in being able to describe the nature of the atomic nucleus as a many-body system.

The following discussion will present experimental efforts and state-of-the-art theoretical methods to further our understanding of the complex interaction that holds nuclei together. The examples are taken from light nuclei, where the most extreme ratios of neutrons-to-protons can be reached. The reason for investigating those isotopes is two-fold. First, in order to probe neutron-proton interactions, one needs to understand the effects that a very asymmetric nucleon composition would have, hence comparing a He-4 nucleus (with 2p and 2n) or C-12 (with 6p and 6n, and an n-to-p ratio of 1) to a nucleus like He-8 (with the same 2p but 6n, and an n-to-p ratio of 3). Secondly, light nuclei are accessible theoretically in a very fundamental manner, because their total nucleon numbers are small enough for first-principle calculations to be performed, the last from the most neutron-rich calcium isotopes investigated to date. It is, in fact, crucial to extend theories and computational methods to heavier and heavier nuclei that also exhibit larger n-to-p ratios.

The first example of new and unexpected behaviours is the appearance of halo structures in light neutron-rich nuclei, where loosely bound neutrons surround a tightly bound core. He-6 is the lightest known halo nucleus. The configuration to form such a nucleus is approximated with a three-body problem, where all the three possible two-body subsystems (the di-neutron and the helium-5-core) are unbound, but the combination of three-body system is bound. Another striking feature is the fact that both He-5 and He-7 do not have bound ground states, but He-8 exists again, and is a so-called a two-neutron halo.

One powerful way to test nuclear theories is through precision mass measurements. The mass provides direct access to the total binding energy of the system, which in turn reflects the forces and hence gives fingerprints of the nuclear interactions. The measurement of masses is not limited to halo-nuclei and, in fact, over the past two decades, the high-precision direct mass measurements of short-lived nuclei have provided valuable information on a wide range of topics. The atomic mass is an important quantity for the determination of the neutron separation energy, the energy needed to liberate one or two neutrons, or, in other words, the quantity which describes how tightly the last neutron(s) is (are) bonded to the core. The neutron separation energy depends on the difference in mass of neighbouring isotopes.

An equally important way to probe our understanding and the description of the nuclear system comes from a measurement of the charge radius. The charge radius is defined as the extent of the proton distribution within the nucleus. The other key measure to describe the nucleus is the matter radius. If the hypothesis of extra neutrons outside the core is true, then there would be a difference in the neutron and proton distribution of the nucleus, with more neutrons outside the proton distribution, but all nucleons obeying the rules of quantum mechanics. The charge radius of atoms is typically determined in electron scattering experiments, which are difficult for short-lived isotopes. The neutron distribution is derived from total cross-section measurements, a method that is applicable to short-lived exotic isotopes.

An alternative approach for the charge radius measurement comes from atomic physics, where the determination of atomic electron transitions provides a sensitive tool for probing the charge distribution in the nucleus via the hyperfine interaction. The atomic transitions are investigated with sophisticated laser spectroscopy. In fact, recent advances in online laser spectroscopy, in combination with precision atomic calculations, have allowed a precise, model-independent determination of the charge radius. However, these calculations have to take into account that the variation of the electronic transitions is caused in part by the change in the centre-of-mass movement when adding neutrons. In some cases, the largest source of uncertainty in these calculations stems from the knowledge of the actual atomic mass used to determine this so-called mass-shift.

One of the most effective ways to measure atomic masses is with ion trap techniques [1], and one of the most advanced systems in the world utilizing this method is TITAN (TRIUMF's Ion Trap for Atomic and Nuclear Science).

JOINT PUBLICATIONS DEMONSTRATE LABORATORY SYNERGY

July 1 2009

Two recent publications by the TRIUMF Theory Group highlight the great strides the group has made toward understanding the structure of light nuclei, and demonstrate the dynamic relationship between theoretical and experimental science.

The first, "Role of the Final-State Interaction and Three-Body Force on the Longitudinal Response Function of He-4," was published in *Physical Review Letters*. This work is triggering new experimental activity in Mainz (Germany) and it is relevant for the experimental program at Jefferson Lab (USA).

The second, "Helium halo nuclei from low-momentum interactions", will soon appear in the *European Physical Journal*. Here, the group's new first-principles (ab-initio) methods for solving the quantum many-body problem are used to derive theoretically the properties of halo nuclei. The results are then compared to experimental data from the TRIUMF ISAC program. These recent publications solidify the Theory Group's strong theoretical efforts, sustaining TRIUMF's world leadership role in nuclear physics.

Recently, the first direct mass-measurement of the two-neutron halo nucleus He-6 was carried out at TITAN together with a more precise measurement of the value for the four-neutron halo He-8 mass [2]. Measurements were performed using the TITAN Penning trap mass spectrometer.

In the Penning trap, a single ion (with mass m and charge-state q) is trapped in a combination of electric and magnetic (B) fields, and the characteristic cyclotron frequency is given by $\omega_c = q/m \cdot B$. The precise determination of the cyclotron frequency then allows the extraction of the atomic mass of the ion.

TITAN is currently the only system in the world where such measurements can be performed, due to its rapid measurement capabilities while preserving the required precision. The results of the new masses lead to improved values of the charge radii and the two-neutron separation energies, which combined provide the most stringent tests for three-body forces for neutron-rich isotopes, with n-to-p extremes. State-of-the-art *ab initio* calculations for He-6 performed at TRIUMF were compared to these findings and co-published with the new experimental data [3]. Due to the particular extended structure of the wave functions, taking into account that the halo neutrons are very far away from the core, these nuclei are difficult to investigate theoretically. The new calculations performed at TRIUMF were obtained with the so-called effective interaction hyperspherical harmonics (EIH), which is a few-body method mostly used for lighter nuclei. Binding energies and charge radii were calculated together for the first time using chiral (low-momentum) potentials, which is explained in the following paragraph. Effective field theories are a modern theoretical instrument to construct interactions among nucleons. Starting from point-like nucleons as effective degrees of freedom and imposing chiral symmetry, which is found in the fundamental theory of strong forces (QCD), one can derive nuclear forces in a systematic way. They are the Goldstone bosons of this theory, where chiral symmetry is spontaneously broken. All the different diagrams can be ordered according to a power expansion in Q/Λ , where Q is the relevant scale of the low-energy physics one wants to describe and Λ is a breakdown scale, ~ 11 GeV. Beyond this scale the inner structure of the nucleons cannot be neglected and such expansion would break down. For low-energy observables instead, the relevant momenta involved are such that $Q \ll \Lambda$, and the expansion is expected to converge. Binding energies and charge radii are such low-energy observables.

One observes the appearance of nucleon-nucleon (NN) interactions, where only two nucleons are present, at the leading order of the expansion, i.e. $(Q/\Lambda)^0$. Three-nucleon (3N) forces, where three nucleons interact simultaneously and four-nucleon (4N) forces instead appear at higher order in this expansion, namely at $(Q/\Lambda)^3$ and $(Q/\Lambda)^4$, respectively. In other words, there is a natural hierarchy among nuclear forces, where NN interactions are more important than 3N forces, 3N forces are more important than 4N forces etc. Because the theory can be worked out at different orders, this approach is systematic and theoretical error bars can be assessed, for example by comparing calculations at different orders.

The theoretical calculations performed at TRIUMF for the He-6 nucleus used only NN forces, neglecting 3N forces, as a first step towards a complete investigation. The two-neutron separation energy (energy necessary to remove two neutrons) and the charge radius were calculated. Results are shown in Figure 5 together with the TRIUMF experimental measurements and with other theoretical calculations based on more phenomenological approaches to nuclear forces. Evidently, all theories, except for the Green's function Monte Carlo (GFMC) red points fail to reproduce the data. This is due to the fact that three-nucleon forces have been neglected. In fact only the GFMC calculations include 3N forces. Thus, precise experimental data such as those on He-6 provide very stringent tests on modern calculations and will be crucial to test chiral 3N forces in the future.

The He-6 example described above shows how experiment and theory could work in synergy to advance our understanding of nuclear forces. Theoretical efforts are in fact directed towards utilizing chiral effective field theory to predict the properties of halo nuclei and other isotopes and will need to be tested against experiment. This should ultimately lead to an extension of the theoretical predictability of nuclear properties to all isotopes.

Another way to look at the charge distribution of the nucleus is by measuring its quadrupole moment. Recently a new, more precise technique was developed to measure ground state quadrupole moments using β -NQR [4]. This was applied to the halo nucleus Li-11 resulting in the best measurement so far for the ratio of quadrupole moments of Li-11 and Li-9 [5]. This ratio is reliably predicted by *ab initio* theory, while the theory is challenged to reproduce the absolute values. The charge radius of Li-11 was previously measured at TRIUMF using laser spectroscopy [6].

Further studies, which were aimed at beryllium isotopes, made use of a different experimental technique but also aimed at providing two independent experimental observables. These could then be compared to theoretical prediction.

In these studies of the neutron-rich nuclei Be-10,11,12, one finds a unique nexus between TRIUMF ISAC's unsurpassed light-mass intensities and the unique experimental facilities available at TRIUMF. All of these experiments used the high-resolution, highly segmented germanium detector area TIGRESS for gamma ray detection in combination with the particle detector BAMBINO (please see Section 5.5.2.1). The experiments were carried out by accelerating the beryllium isotopes to a 2-3 MeV and then impinging on a target inside the BAMBINO detector. The beryllium isotopes react with the target atoms and excited states are generated.

The first excited state of Be-10 is a gamma-emitting 2^+ state that decays to the 0^+ ground state. This 2^+ state exhibits quadrupole deformation, the magnitude of which has been deduced from lifetime measurements. *Ab initio* calculations with local two-body forces, however, disagree on the sign of the deformation, that is, whether it is prolate or oblate. Other calculations, which include three-body forces, result in a predicted shape change from oblate to prolate, while another calculation by a group at TRIUMF using non-local two-body forces consistently calculates a prolate shape.

The sign of the deformation was measured by the reorientation effect of Coulomb excitation (Coulex) experiments [7]. Radioactive Be-10 beam produced by ISAC, ionized by the resonant laser ionization technique, and accelerated by ISAC-II to the TIGRESS beam station, have been scattered off a high-Z target foil and detected with BAMBINO silicon detectors. In inelastic scattering, the Be-10 2^+ state is excited by the electric field of the target nuclei and then decays by emitting gamma rays, which are detected with TIGRESS high-purity germanium detectors as shown in Figure 1. The excitation yield cross-section depends not just on the magnitude of the deformation but also its sign; when the measured yield is compared with lifetime data, it is concluded that the sign of the transition matrix element must be that of a prolate deformation (see Figure 2).

In the case of the one-neutron halo nucleus Be-11, the transition strength between the $\frac{1}{2}^+$ ground state and $\frac{1}{2}^-$ excited state is the strongest E1 electric dipole transition known. The strength of this transition and the structure of E1 strength in continuum states is a challenge that modern theory is able to address with accuracy. However, there is a troubling 10% discrepancy between lifetime and high-energy inelastic scattering measurements of the reduced matrix element. At TRIUMF the Coulex cross-section has been measured at low bombarding energies (below the Coulomb barrier to avoid additional production channels and keep the final states well defined), so that one key source of systematic uncertainty, the contribution of nuclear interference to the

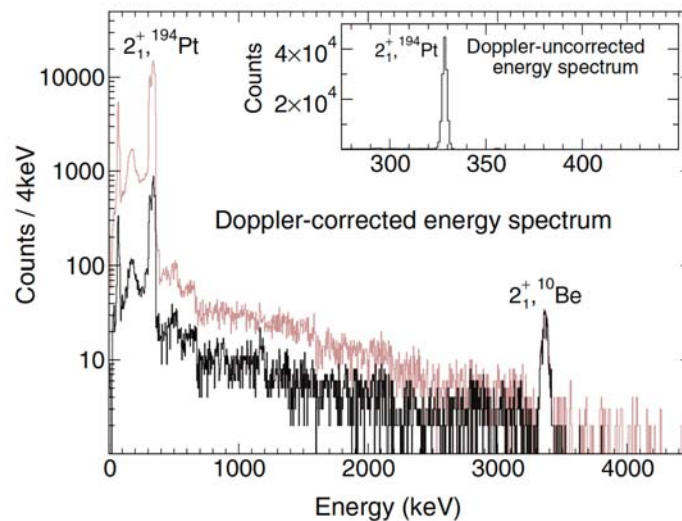


Figure 1: Gamma-ray spectrum from [7]. Brown, total spectrum; black, spectrum gated by the inelastic scattering peak in Bambino

excitation probability, is eliminated to the 1% level. Again, the scattered radioactive ions were detected with BAMBINO, and gamma rays emitted after inelastic excitation were detected with TIGRESS (see Figure 3). The new measurement has an uncertainty of 2%, which is both consistent with all the other inelastic scattering measurements and which is almost four times more accurate than the world average.

Both described cases in beryllium, Be-10 and Be-11, take advantage of TRIUMF's intense radioactive species production, efficient ionization, and acceleration and transport of high-quality low-mass beams to allow for precise measurements of nuclear properties for comparison to state-of-the-art models. The last example in this isotopic chain, Be-12 pushes the limits of sensitivity to provide qualitative insight into the properties of this nucleus. In this case, the BAMBINO detectors were used to measure reaction cross-sections and angular distributions, which can be compared to theory. The $^{11}\text{Be}(d,p)$ reaction populated [8] both the ground and several excited states in Be-12 (see Figure 4). Analysis of the transfer reaction angular distributions showed that the s-wave component of the excited 0^+ was in fact much larger than that of the ground state. In combination with low neutron binding, these are considered key parameters of a halo behaviour, which means that in this case the excited state is a halo state, i.e. the valence neutrons have a large spatial extent, as in the well-known case of the Li-11 ground state.

These findings were compared to theoretical calculations performed at TRIUMF, using the No-Core Shell Model (NCSM) with the so-called CD Bonn 2000 two-body force. The theoretical results obtained are in agreement with other *ab initio* calculations performed within the Green's function Monte Carlo (GFMC) with local two- and three-body forces. This fact is interpreted as such due to the stronger spin-orbit component present in the non-local CD Bonn potential, which accounts for the additional spin-orbit effects obtained from the Illinois three-nucleon force used in the GFMC calculations.

In all effects, calculations agree with TRIUMF experimental data in assigning a negative sign to the quadrupole moment of the first excited state in Be-10. Hence, in order to clearly separate the validity of two- or three-body forces, additional experiments are needed; they should provide the resolution to distinguish between applications of the theoretical approaches. But, as seen in the case of helium, there is more and more evidence for the need to include three-body forces in describing very neutron-rich isotopes, hence atoms with extreme n-to-p ratios.

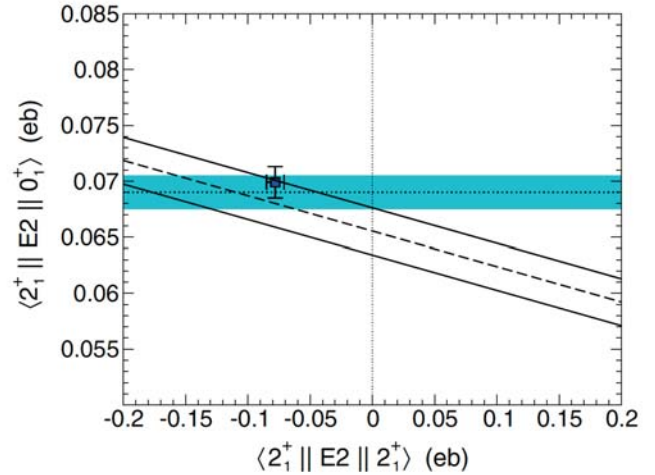


Figure 2: Exclusion plot combining lifetime and Coulex data, indicating a prolate shape. Data point is a calculation based on the methods of Navratil et al.

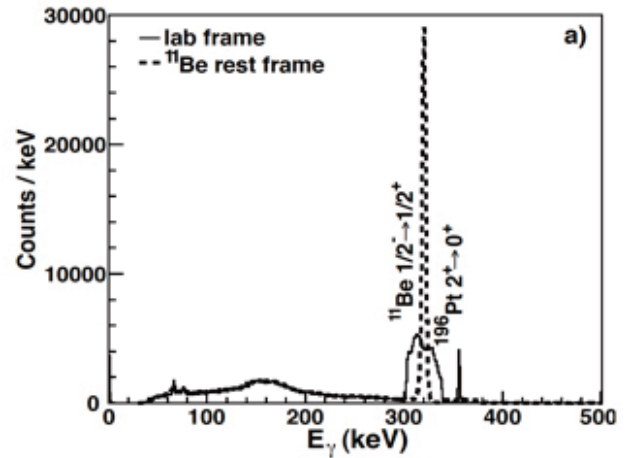


Figure 3: Gamma-ray spectrum with and without Doppler correction from the Be-11 high-precision B(E1) measurement.

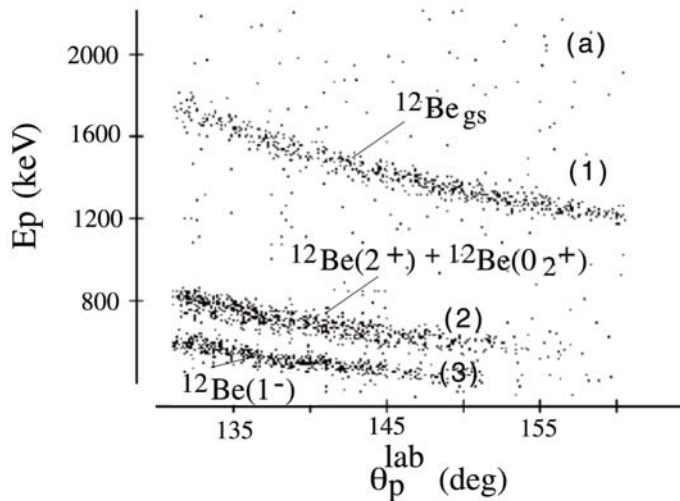


Figure 4: The kinematic loci of the protons identified in the upstream silicon detector in coincidence with Be-12 in the downstream silicon detector. The band identified with (2) was analyzed to extract a large s-wave component for the excited 0^+ state, leading to the conclusion that this is a halo state

Further reaction studies were carried out in light nuclei, such as inelastic deuteron scattering of Li-9 [9] as well as reaction studies using Li-11 to study various aspects of the interaction between a halo nucleus and Pb-208, such as elastic scattering below the barrier [10], inelastic break-up [11], and sub-barrier fusion [12].

As an extension of theoretical approaches developed for lighter isotopes, the case was made to try to describe, theoretically, neutron-rich calcium isotopes, which were chosen because a full body of data exists near the stable Ca-48, and because a promising theoretical framework was developed, based on the *ab initio* calculations for light nuclei, which has the potential to be further extended to even heavier nuclei. For this reason, calcium isotopes, Ca-49-52, were measured at ISAC to study the effect of three-nucleon forces in medium-heavy nuclei.

Neutron rich calcium isotopes are of keen interest to theorists. The calcium isotopic chain is the only chain that has two stable doubly magic isotopes, Ca-40 and Ca-48. Magic nuclei occur when a nucleus has a closed nuclear shell of protons or neutrons. These magic nuclei are remarkably stable hence they have extra binding compared to their neighbours and can be compared to a noble gas configuration in the periodic table of elements. The magic numbers for nuclei are 2, 8, 20, 28, 50, 82 and 126. These magic numbers have been of immense help in describing the physics of nuclei; however, it has been found that “new” magic numbers can arise, and the well-known magic numbers can disappear or migrate. This is in contrast to the noble gases in the chemical periodic table, which are always at the same number of closed atomic shells, throughout the entire periodic table. In the calcium isotopes it has been predicted that new magic numbers can appear at neutron numbers 32 or 34. The exact location of the predictions depends on what kind of nuclear interaction

INTERNATIONAL TEAM CONVENES TO STUDY SODIUM-26

20 October 2009

During the month of August, an international team of researchers assembled at TRIUMF to run the first of a series of experiments in nuclear structure and astrophysics using neutron transfer reactions with neutron-rich sodium isotopes. The experiment was run using the new SHARC (Silicon Highly-segmented Array for Reactions and Coulomb) detector, which had been integrated into the existing TIGRESS (TRIUMF-ISAC Gamma-Ray Escape Suppressed Spectrometer) apparatus. The goal of the experiment was to investigate the changes in shell structure in exotic nuclei (in particular sodium-26) through a reaction where a neutron is transferred into the already neutron-rich sodium-25 nucleus.

It was originally thought that the shell model used to describe nuclear structure would be the same for exotic nuclei as it is for stable nuclei. However, researchers have come to find that these shell structures change in exotic nuclei as the ratio between the number of protons and neutrons changes. Using the SHARC-TIGRESS detector system, experimenters are better able to probe the structure of these exotic nuclei.

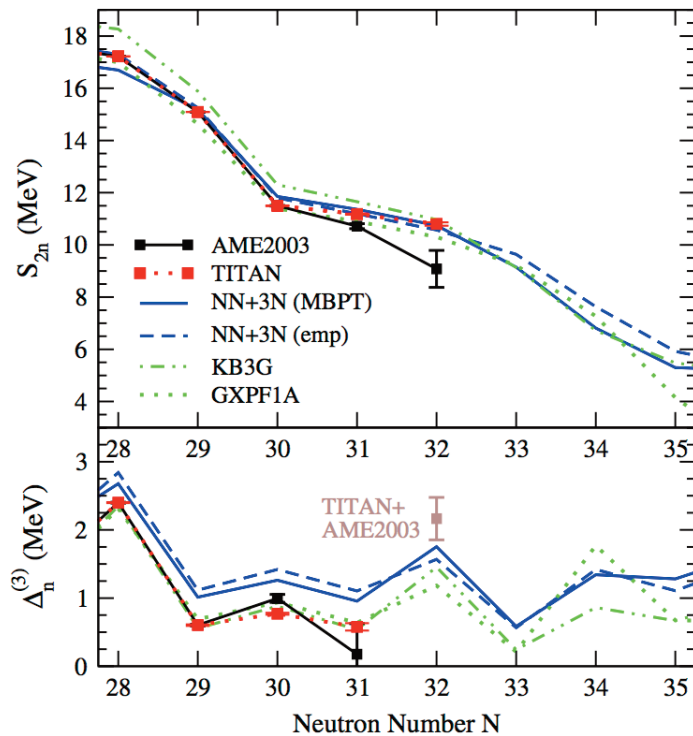


Figure 5: The new TITAN mass values for the neutron separation energies in calcium isotopes agree extremely well with theory, and show a large deviation from the values in the literature.

is used in the calculation. The verification of the theoretical prediction is possible by measuring the binding energies, or separation energies (via a mass measurement), and extra strong binding compared to the more n-rich neighbour isotope, would indicate a closed shell.

The calcium isotopes for the experiment were produced by bombarding a high-power tantalum target with a 70 μ A proton beam of 480 MeV energy and using a resonant laser ionization scheme to enhance the ionization of the beam. The calcium isotopes were sent to the TITAN precision measurement Penning trap, where the mass of all isotopes was determined with unprecedented precision [13,14]. The agreement between experiment and theory is remarkable and is shown in Figure 5. While older phenomenological theories (green lines) also agree very well with the new experimental values, it is important to remember that they are based on interaction parameters adjusted to experimental inputs from nearby nuclei in order to give accurate predictions. The three-body (blue lines) have not had the same tweaking, and are equally as good at predicting the observed trend but are completely based on unadjusted interactions.

Selected References

- [1] K. Blaum, J. Dilling, and W. Nörtershäuser, *Physica Scripta* T152, 014017 (2012).
- [2] M. Brodeur et al., *Phys. Rev. Lett.* 108, 052504 (2012).
- [3] S. Bacca, N. Barnea, A. Schwenk, *Phys. Rev. C* 86, 034321 (2012).
- [4] A. Voss et al., *J. Phys. G: Nucl. Part. Phys.* 38, 075102 (2011).
- [5] A. Voss et al., *J. Phys: Conf. Ser.* 312, 092063 (2011).
- [6] W. Nörtershäuser et al., *Phys. Rev. A* 83, 012515 (2011).
- [7] J.N. Orce et al., *Phys. Rev. C* 86, 041303(R) (2012).
- [8] R. Kanungo et al., *Phys. Lett. B* 682, 391 (2010).
- [9] H. Al Falou et al., *Phys. Lett. B* 721, 224 (2013).
- [10] M. Cubero et al., *Phys. Rev. Lett.* 109, 262701 (2012).
- [11] P. Fernandez-Garcia et al., *Phys. Rev. Lett.* 110, 142701 (2013).
- [12] A.M. Vinodkumar et al., *Phys. Rev. C* 87, 044603 (2013).
- [13] A. Lapierre et al., *Phys. Rev. C* 85, 024317 (2012).
- [14] A. Gallant et al., *Phys. Rev. Lett.* 109, 032506 (2012).

4.2.2.3 COLLECTIVE STATES IN NUCLEI

The emergence of simple patterns in the behaviour of atomic nuclei, associated with collective behaviour such as rotational and vibrational motion, out of the underlying complex single-particle motion of protons and neutrons remains a fascinating area of nuclear physics. Why are there almost degenerate energy states of very different shapes (shape-coexistence) in nuclei and how does the nuclear many-body system transition between different shapes? Are there collective states in which protons and neutrons do not act in phase and what can one learn about the proton-neutron interaction from their study? How do collective degrees of freedom (rotational, vibrational) compete with single-particle motion? These are some of the questions currently driving the research on collective states.

The widely occurring manifestation of shape coexistence in nuclei leads to low-lying 0^+ states that have a very different shape than the ground state of the nucleus. The shape-coexistent state involves typically pair excitations across energy gaps that result from shell structure. This has led to the question of the role of pair excitations across energy gaps resulting, not only from shell structure, but also from subshell structure. Very little is known even about the occurrence of subshell gaps across the nuclear mass surface, let alone their involvement in nuclear collective behaviour.

While some low-lying 0^+ states are due to shape-coexistence the nature of other 0^+ states remains mysterious. While originally identified as vibrational states build on spherical or deformed ground states, more precise measurements have put this simple interpretation into question. This is also connected to the question to what extent multi-phonon states are realized in nuclei

Guided by the questions above there have been, two major lines of investigation have been carried out using the 8π spectrometer at TRIUMF in the past few years. The first has focused on detailed spectroscopy to resolve fundamental issues of collectivity in the Cd isotopes, long thought to be the best-known examples of quadrupole vibrational behaviour in spherical nuclei anywhere on the nuclear mass surface. This has led to published results on Cd-110 [1,2] and Cd-112 [3]. By using the sensitivity of the 8π spectrometer to measure weak γ -ray decay branches from highly excited states (see Figure 1), highly collective transitions predicted by sophisticated Interacting Boson Model-2 (IBM2) calculations were sought. These calculations were able to reproduce the decay of the second and third excited $0^+_{2,3}$ levels by assuming strong mixing of the spherical phonon and deformed intruder states (the latter based on $2p-4h$ states involving a proton pair excited across the $Z=50$ gap). In Cd-112, the 0^+_4 level was reassigned from a 3-phonon vibrational state to an excitation based on the intruder configuration due to its lack of an observed decay to the 2^+ 2-phonon level thus removing any possible candidate for the 0^+ 3-phonon state (see Figure 2). Using the high-sensitivity achieved in the decay of In-110 feeding levels in Cd-110, it was determined that the mixing of intruder and vibrational states was weak, thereby negating this mechanism as the explanation of the decays of the $0^+_{2,3}$ levels. Reconsidering the properties of the 0^+ states, it was suggested that the underlying structure of the non-intruder states in Cd-110 was γ -soft, not spherical vibrational [2], raising the possibility that none of the

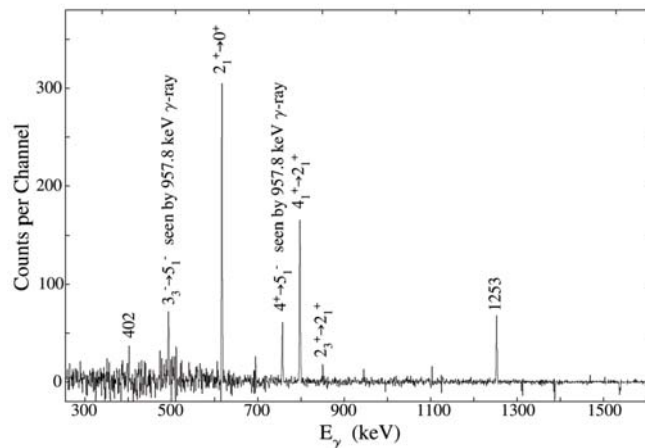


Figure 1: γ -ray spectrum gated by the 958.0-keV transition feeding the 1871-keV 0^+_4 level in Cd-112. The energies of the γ -ray transitions from the 0^+_4 level are labeled in keV, with the remaining transitions labeled with their placements in the level scheme [3].

stable Cd isotopes possess spherical vibrational multi-phonon states. The program has expanded to include detailed investigations of Sn-116 and Xe-124, with the ultimate goal of establishing the nature and evolution of low-lying collectivity in the $Z=50$ region by establishing detailed systematics of the structures of the Cd, Sn, Te, and Xe isotopes.

The second line of investigation has focused on initiating detailed studies of possible shape coexisting structures where subshells may be playing a role. Conventionally, nuclear collectivity has been regarded as weak or absent at closed shells and strong far away from closed shells. A few exceptions have been found in the form of shape coexistence. In general, evidence for such structures has been indirect, e.g., from the observation of excited rotational energy patterns in nuclei with spherical ground states, where there is a lack of direct evidence of quadrupole deformation.

The zirconium isotopes span a range of masses from a mid-open-shell deformed region (Zr-80), through a closed neutron shell (Zr-90), to a closed neutron subshell (Zr-96), and then to a sudden reappearance of deformation (Zr-100), which persists to a mid-open-shell region (Zr-108).

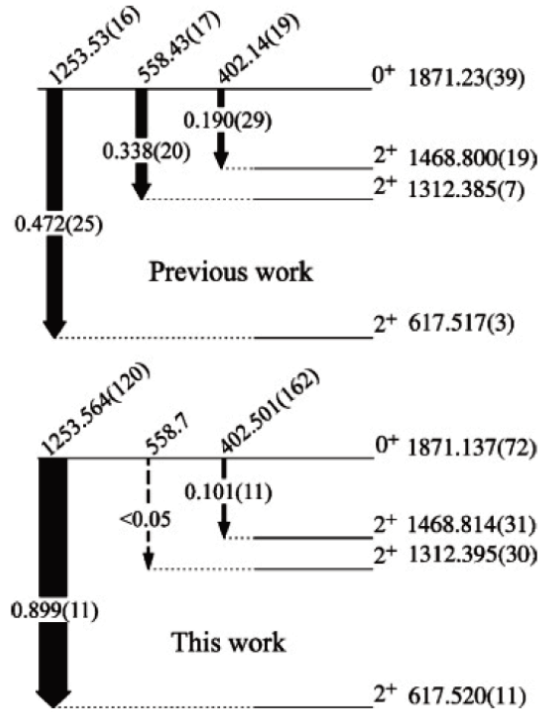


Figure 2: Previous and current level schemes for decays from the 1871-keV 0_1^+ level in Cd-112 [3].

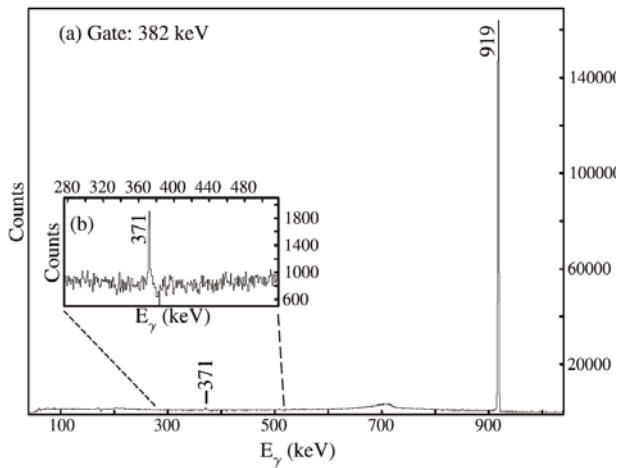


Figure 3: (a) Portion of the γ -ray spectrum gated on the 382-keV gamma ray in Zr-94 following the decay of Y-94. (b) Confirmation for the placement of the deexciting 371-keV 2_2^+ to 0_2^+ gamma ray is evident [4].

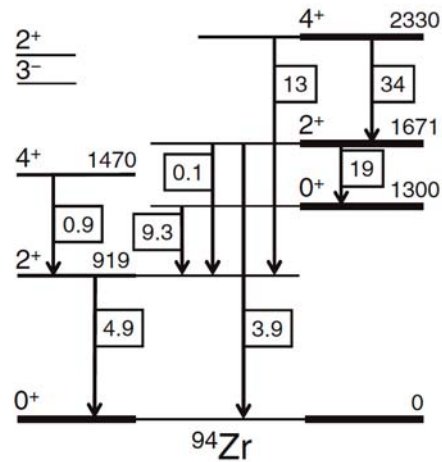


Figure 4: Levels of Zr-94 below 2350 keV, with the band based on the 1300-keV 0_2^+ state emphasized. The $B(E2)$ values in W.u. are given in boxes [4].

This behaviour is unprecedented anywhere on the nuclear mass surface. Earlier hints of shape coexistence in the zirconium isotopes existed; however, these suggestions depended on the indirect evidence from rotational band energy patterns and electric monopole transition strengths. In a study with the 8π spectrometer, lifetime data obtained with the $^{94}\text{Zr}(n,n'\gamma)$ reaction were combined with a detailed study of Zr-94 (see Figure 3, 4) from the decay of Y-94 to form a consistent picture of shape coexistence in Zr-94 based on the direct evidence provided by electric transition strength $B(E2)$ [4]. This observation raises the possibility that similar structures may have been overlooked due to the lack of knowledge of weak transitions amongst highly excited states, and that shape coexistence can be manifest in nuclei with closed subshell structure, rather than being present only in nuclei with closed major shells.

On the theoretical side, the investigations by the TRIUMF Theory Group into collective excitations are focused on the origin of alpha clustering in light nuclei. Starting from the realistic nuclear forces derived within the chiral effective field theory from the QCD, the theory group is developing and applying many-body methods that describe the structure, scattering and reactions of nuclei. Bound and resonance states of light systems with dominant alpha-cluster structure such as L-6i (*d*-alpha) [5,6], Be-7 (alpha-He-3), Li-7 (alpha-H-3) were investigated recently. A formalism to calculate alpha-alpha scattering from the first principles and, eventually, the collective Hoyle state (alpha-Be-8) and O-16 alpha-cluster states (alpha-C-12) is underway. Understanding of the emergence of collectivity in medium mass nuclei from the first principles can be facilitated by *ab initio* techniques such as Coupled-Cluster Method or the Self-Consistent Green's Function method applied recently to isotopic chains near oxygen and calcium using the chiral nucleon-nucleon and three-nucleon forces [7-9].

Selected References

- [1] P.E. Garrett et al., Phys. Rev. C 78, 044321 (2008).
- [2] P.E. Garrett et al., Phys. Rev. C 86, 044304 (2012).
- [3] K.L. Green et al., Phys. Rev. C 80, 032502 (2009).
- [4] A. Chakraborty et al., Phys. Rev. Lett. 110, 022504 (2013).
- [5] P. Navratil and S. Quaglioni, Phys. Rev. C 83, 044609 (2011).
- [6] S. Quaglioni et al., Journal of Physics: Conference Series 402 012037 (2012).
- [7] R. Roth et al., Phys. Rev. Lett. 109, 052501 (2012).
- [8] S. Binder et al., Phys. Rev. C 87, 021303(R) (2013).
- [9] A. Cipollone et al., Phys. Rev. Lett. 111, 062501 (2013).

4.2.2.4. NUCLEAR ASTROPHYSICS

Our current understanding of the universe puts the formation of the very lightest chemical elements just minutes after the Big Bang, with nearly all other naturally occurring elements arising from stellar mechanisms. These include quiescent nuclear burning in stars as well as explosive events occurring in stellar binary systems on compact objects such as white dwarfs. The heaviest elements are believed to have originated in energetic explosions such as merging neutron stars or core-collapse supernovae. Although the main processes leading to the formation of the elements are known in general, the details are not known, nor are the exact stellar locations for some of the more exotic processes. In addition, the physics of stellar systems, especially the explosive ones, is not known in detail and modeling is hindered by incomplete nuclear physics information.

The availability of accelerated radioactive ion beams, of short-lived species likely only to be seen in explosive stellar scenarios, affords us the opportunity to recreate the microscopic conditions inside stars and measure nuclear properties which eliminate nuclear physics as a source of uncertainty in astrophysical models and further our detailed understanding of the origin of the chemical elements. The experimental nuclear astrophysics and theory groups at TRIUMF have made significant advances in this field through diverse experimental and theory programs pertaining to a variety of astrophysical scenarios.

At temperatures characteristic of the quiescent stellar fusion occurring in the sun and other stars, the relevant thermonuclear reactions generally proceed non-resonantly, with some important exceptions. In contrast, at the higher temperatures found in stellar explosions such as novae, X-ray bursts, and supernovae, the higher density of compound nuclear excited states leads to large resonant contributions to the relevant thermonuclear reaction rates. Resonant reaction rate contributions may be calculated precisely from the properties of the compound nuclear states that serve as resonances. The most important of these is usually the excitation energies of the states. The spins and parities of the states must also be known. Finally, the partial decay widths of the states that serve as resonances are needed to calculate their contributions. Non-resonant reaction rates are not so readily calculated, but rather require high fidelity nuclear structure models coupled to reaction theory to enable extrapolation from energies accessible in the lab to those relevant to the sun and other stars. The astrophysical S factor, which is obtained from the cross-section by factoring out the dominant energy dependences on the de Broglie wavelength and the Coulomb penetrability, is the most convenient quantity for such extrapolations.



TUDA COMPLETES FIRST FLUORINE-18 EXPERIMENT ON NOVAE REACTIONS

27 June 2008

On June 10, 2008, The TRIUMF-UK Detector Array (TUDA) collaboration celebrated as they completed a three-week run using the world's most

intense accelerated F-18 beam to investigate one of the most important nuclear reactions occurring in novae. The data obtained will aid in understanding observations made by satellite gamma-ray observatories such as the Gamma-ray Large Area Space Telescope (GLAST), which coincidentally blasted off from Cape Canaveral on the same day the TUDA experimental run finished.

The gamma-ray emission from novae is dominated by the beta-decay of the isotope F-18 (fluorine atoms, but containing one less neutron than usual). Scientists of the TUDA collaboration have been able to make a direct measurement of the fluorine-oxygen isotope reaction that is integral to understanding these cosmic events. The intensity of the beam reached about 10 million particles per second, making it the most intense beam of its type in the world. Such an achievement allows for first-time measurements at energies of particular interest for resolving astrophysical uncertainties.

For laboratory measurements using radioactive ion beams, reaction cross-sections can be measured directly when sufficient beam intensity exists. If not available, indirect experimental measurements can be combined to determine the relevant nuclear reaction rates. Finally, where no laboratory measurements exist, theoretical estimates must be used.

Big Bang Nucleosynthesis

The initial abundances of the lightest elements, H, He, and Li, were determined by the nuclear reactions that occurred in the first few minutes after the Big Bang. Precise knowledge of the rates of these reactions is needed for comparisons of the primordial elemental abundances predicted by theory and inferred from observations. Both nuclear experiment and theory are crucial.

The primordial abundance of Li-7 inferred from astronomical observations is roughly a factor of 3 below the abundance predicted by the standard theory of Big Bang nucleosynthesis (BBN) using the baryon-to-photon ratio determined mainly from measurements of the cosmic microwave background radiation. In contrast, there is good agreement for H-2 and He-4. Taking into account the estimated uncertainties on the observationally inferred and the theoretically deduced Li-7 abundances, the significance of the discrepancy is $(4.2-5.3)\sigma$. This constitutes one of the important unresolved problems of present-day astrophysics and is termed the cosmological lithium problem. Among other possibilities, the discrepancy could be due to new physics beyond the standard model of particle physics, errors in the observationally inferred primordial lithium abundance, or incomplete nuclear physics input for the BBN calculations. In a recent theoretical paper, Cyburt and Pospelov proposed that destruction of Be-7 via resonant capture of H-2 could resolve the discrepancy. TRIUMF scientists have used data from a recent ${}^9\text{Be}({}^3\text{He},t){}^9\text{B}$ measurement to definitively rule out this possible solution to the cosmological lithium problem [1].

With collaborators, TRIUMF's theory group has applied the *ab initio* No-Core Shell Model combined with the resonating group method (NCSM/RGM) to calculate the cross-sections of the ${}^3\text{H}(\text{d},\text{n}){}^4\text{He}$ and ${}^3\text{He}(\text{d},\text{p}){}^4\text{He}$ fusion reactions relevant to BBN and the future of energy generation on Earth [2]. Starting from a similarity-transformed chiral nucleon-nucleon interaction that accurately describes two-nucleon data, they performed many-body calculations that predict the cross-sections of both reactions. Virtual three-body breakup effects were obtained by including excited pseudo-states of the deuteron. The results are in satisfactory agreement with experimental data and will aid future microscopic investigations of polarization, electron screening, and other effects.

Quiescent Stellar Burning

In order to gain a detailed understanding of nucleosynthesis and stellar evolution, it is necessary to quantitatively understand the nuclear reactions that operate while stars are stably fusing hydrogen or helium in their cores. Among other things, the rates of these reactions determine the compositions of stars prior to supernova explosions, set the timescales of the longest phases of stellar evolution, and help determine the neutrino fluxes that can be used to infer the core temperature of the sun and test solar models.

The flux of high-energy solar neutrinos has now been measured with a precision of 5% or better. Since the decays of Be-7 and B-8 are the principal sources of this well-measured solar neutrino flux, the rates of the reactions that create and destroy these nuclides must be known with better precision to facilitate comparisons of predicted and observed solar neutrino fluxes.

The zero energy astrophysical S factor for the ${}^3\text{He}(\alpha,\gamma){}^7\text{Be}$ reaction, $S_{34}(0)$, is crucial for solar neutrino flux calculations because this reaction is the dominant means of producing the neutrino source Be-7 in the Sun and also because the neutrino source B-8 is formed by the capture of a proton by Be-7. In fact, the Be-7 neutrino flux is proportional to $S_{34}(0)^{0.86}$ and the B-8 flux is proportional to $S_{34}(0)^{0.81}$. Measurements at the relevant centre-of-mass energy (E_{cm}) of 23 keV are infeasible, so instead measurements at higher energies must be extrapolated with the aid of theory. To better constrain the extrapolation, the DRAGON group has begun a series of measurements of the ${}^3\text{He}(\alpha,\gamma){}^7\text{Be}$ cross-section at centre-of-mass energies between

1.5 and 2.8 MeV. These measurements are ongoing but the analysis of a preliminary run at 2.8 MeV is complete; in this run the beam suppression of the separator was found to exceed 10^{14} at the 90% confidence level, the highest value so far for any recoil separator [3].

As the only means by which the dominant high energy solar neutrino source B-8 is produced, the ${}^7\text{Be}(\rho,\gamma){}^8\text{B}$ reaction and its zero energy astrophysical S factor $S_{17}(0)$ are of great interest to solar modellers. In the latest evaluation of solar fusion cross-sections, the theoretical error assigned to the extrapolation of the S factor from experimentally accessible energies to zero energy dominated the error budget. Recently Navratil, Roth, and Quaglioni used the NCSM/RGM to calculate S_{17} [4]. Starting from a selected similarity-transformed chiral nucleon-nucleon interaction that accurately describes two-nucleon data, they performed many-body calculations that simultaneously predict both the normalization and the shape of $S_{17}(E)$. They also studied the dependence on the number of Be-7 eigenstates included in the coupled-channel equations and on the size of the harmonic oscillator basis used for the expansion of the eigenstates and of the localized parts of the integration kernels. Their result for $S_{17}(0)$ is lower than, but consistent with, the latest evaluation and reduces the extrapolation uncertainty.

An indirect alternative to measuring radiative capture reactions at high energies and extrapolating to stellar energies is studying the asymptotic normalization coefficient (ANC) of a valence nucleon via transfer reactions. Using the TUDA facility, experimenters at TRIUMF led by Howell and Davids have studied the elastic/transfer reaction ${}^7\text{Li}({}^8\text{Li}, {}^7\text{Li}){}^8\text{Li}$ for the first time. By measuring the angular distribution in which interference between elastic scattering and single neutron transfer produces characteristic oscillations, the ANC of the $p_{3/2}$ neutron in Li-8 was inferred. Invoking isospin symmetry, the experimenters then deduced the ANC for the corresponding proton in B-8, which is directly related to $S_{17}(0)$. This result, recently accepted for publication, is consistent with both radiative capture measurements and indirect determinations.

A number of reactions that proceed in stars that have reached advanced stages of stellar evolution are important for nucleosynthesis and for energy release. Steady-state stellar helium burning mainly produces C-12 via the triple- α process at typical temperatures between 0.1 – 0.3 GK. This reaction can in principle be followed by further α -capture reactions. However, the ${}^{16}\text{O}(\alpha,\gamma){}^{20}\text{Ne}$ reaction is very weak at these temperatures due to the lack of a suitable resonance in Ne-20. Its inverse reaction initiates the neon burning stage of stellar evolution. Most recent measurements determined only the S_2 component of the astrophysical S-factor (decay through the first excited state in Ne-20), with the S_0 component (directly to the ground state) derived from theory. In September 2010, Hager et al. carried out the first measurement of the total S-factor using DRAGON [5] at $E_{\text{cm}} = 2.26$ MeV, following up in April 2011 with additional measurements down to $E_{\text{cm}} = 1.69$ MeV [6]. Using the array of bismuth germanate detectors surrounding the DRAGON gas target to detect prompt γ rays from the reaction, it was possible to identify the contributions from the different decay cascades for all energies.

Up to half of the heavy elements were produced in stars by the capture of neutrons into intermediate mass nuclei. This so-called s -process can be inhibited if other nuclei capture the neutrons before they can participate in the heavy element building. At the time of formation of ancient massive stars, elements heavier than helium had not yet been synthesized in significant amounts. Consequently the neutron poisons usually present due to previous nucleosynthesis stages were absent. This lack of secondary neutron poisons, together with the large abundance of O-16, produced in situ during the helium burning stage, resulted in a high neutron capture rate on O-16. The O-17 thus formed could recycle the neutrons back into the stellar plasma, through the ${}^{17}\text{O}(\alpha,n){}^{20}\text{Ne}$ reaction, having little impact on the subsequent s process. The efficiency of this recycling depended on the rate of the competing (α,γ) reaction that produces Ne-21 without releasing the captured neutrons. Limited experimental data are available on these reactions and the two theoretical calculations of the reaction rates diverge significantly at stellar temperatures, resulting in predicted s -process abundances that differ by up to three orders of magnitude. To address this discrepancy, the ${}^{17}\text{O}(\alpha,\gamma){}^{21}\text{Ne}$ reaction was studied using DRAGON over a range of E_{cm} from 0.62 to 1.5 MeV. The resonance strengths of two states in Ne-21 were determined and off resonance data used to extrapolate the S-factor across the

Gamow window (the energy region of effective burning in the stellar environment). The calculated reaction rate indicates that sufficient neutrons are recycled and that *s*-process nucleosynthesis is not inhibited.

The bulk cosmic origin of fluorine is uncertain. Asymptotic giant branch (AGB) stars are the final phase in evolution for stars with an initial mass of approximately 2-8 solar masses. They are thought to be one of the main sites for the production of fluorine, but models do not produce enough F-19 to match observations. The $^{18}\text{F}(\alpha,p)^{21}\text{Ne}$ reaction rate is important in predicting the stellar abundance of F-19 in AGB stars as it competes with the $^{18}\text{F}(\beta^+\nu)^{18}\text{O}(p,\alpha)^{15}\text{N}(\alpha,\gamma)^{19}\text{F}$ reaction chain, reducing the number density of O-18 ($N_{\text{O-18}}$) but increasing the number density of protons (N_p). Effectively, as the reaction rate for $^{18}\text{F}(\alpha,p)^{21}\text{Ne}$ increases, the product $N_{^{18}\text{O}}N_p$ increases, producing more F-19 via the reaction chain $^{18}\text{O}(p,\alpha)^{15}\text{N}(\alpha,\gamma)^{19}\text{F}$. At energies relevant to helium shell burning in AGB stars the uncertainty in the measured cross-section of the $^{18}\text{F}(\alpha,p)^{21}\text{Ne}$ reaction is almost two orders of magnitude. A direct measurement of the reaction is not currently feasible due to the limited F-18 beam intensity available but information on the cross-section can be extracted from a measurement of the time-reversed reaction $^{21}\text{Ne}(p,\alpha)^{18}\text{F}$ at TUDA (see Figure 1), which was filled with hydrogen gas at 330 mbar creating an extended gas target. Two arrays of silicon detectors inside TUDA were then used to detect the F-18 and α in coincidence at $E_{\text{cm}} = 0.6 - 1.4$ MeV in the $^{18}\text{F} + \alpha$ frame.

The oldest stars in the Milky Way Galaxy fuse H stably into He via the CN cycle. Its slowest reaction, $^{14}\text{N}(p,\gamma)^{15}\text{O}$ controls the rate of energy release in the cycle and thereby determines the lifetimes of the ancient stars it powers. It is impossible to measure this reaction cross-section directly at the required astrophysical energy of 30 keV. The largest remaining uncertainty in the extrapolation to low energies is the width of the subthreshold 6.79 MeV state in O-15. At the DSL facility installed at ISAC-II, Galinski et al. have constrained the lifetime (and thereby the width) of this state using the Doppler shift attenuation method and the $^3\text{He}(^{16}\text{O}, ^4\text{He})^{15}\text{O}$ reaction.

Cataclysmic Binary Systems, Compact Objects, and Supernovae

Explosive nucleosynthesis under degenerate conditions occurs in a range of different systems from isolated massive stars to cataclysmic binaries in which matter is transferred from a relatively un-evolved star to a compact object such as a white dwarf or a neutron star.

Novae occur in cataclysmic binary systems in which hydrogen-rich material is transferred onto the surface of a white dwarf from the expanded envelope of a larger star. This material is compressed and heated, leading to the onset of nuclear burning, dumping more energy into the system and leading to a

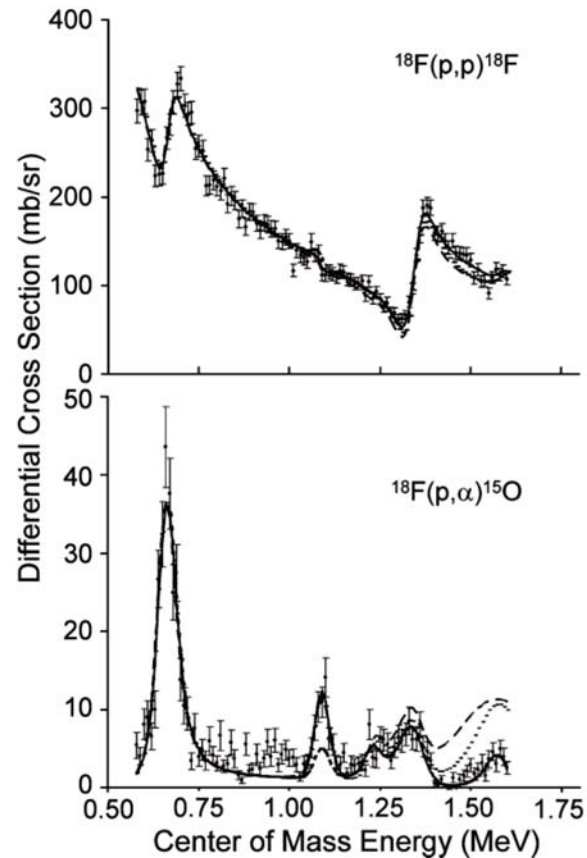


Figure 1: Differential cross-sections of the $^{18}\text{F}(p,p)^{18}\text{F}$ and $^{18}\text{F}(p,\alpha)^{15}\text{O}$ reactions as a function of centre-of-mass energy obtained using the TUDA array. A simultaneous R-matrix fit, calculated for a centre-of-mass angles of 156° for (p,p) and 151° for (p, α), is shown by the solid black line. The dashed and short-dashed lines show cross-sections calculated for different high lying resonance parameters, based on previous work.

thermonuclear explosion which ejects a large amount of material. If the environment grows hot enough, nucleosynthesis involving proton capture reactions can occur up to the calcium region. In addition, long-lived radioisotopes such as F-18, Na-22 and Al-26 are synthesized. Such isotopes are observation targets for current and future satellite γ ray telescope missions, and could provide a powerful tool to observe and understand nova explosions. Novae are the simplest and most common type of explosive stellar event, with some 30 per year predicted to occur in the galaxy, and therefore provide the best test for models of explosive stellar hydrodynamics and nucleosynthesis that can be improved by comparing to observations. Nuclear physics input is a crucial part of this understanding.

The initial 511 keV and continuum γ -ray spectrum emanating from novae hours to days after onset arises in part due to decaying F-18. The flux of this spectrum varies from model to model and due to the particular qualities of the individual nova, but estimates suffer from large nuclear physics uncertainties, particularly those from reactions which create and destroy F-18 in the thermonuclear runaway such as $^{18}\text{F}(p,\alpha)^{15}\text{O}$, $^{18}\text{F}(p,\gamma)$ and $^{17}\text{O}(p,\gamma)^{18}\text{F}$, with the first reaction being the most significant. At ISAC, the world's most intense accelerated F-18 beams of 10^7 s^{-1} have been demonstrated, enabling studies of reactions on F-18.

At the TUDA facility, a simultaneous measurement of $^{18}\text{F}(p,\alpha)^{15}\text{O}$ and $^{18}\text{F}(p,p)^{18}\text{F}$ was performed at E_{cm} between 0.6 MeV and 1.6 MeV [7]. Elastically scattered protons and coincident α -particles and O-15 recoils were detected in large area segmented silicon arrays, leading to the measurement of an excitation function showing several resonances. Simultaneous R matrix fits to the elastic and (p, α) channels confirmed some existing resonance parameters while identifying two new resonances and providing widths for all of them. A state predicted by theory that could have significantly affected the cross-section at low energies via interference with partner states, and thus affected the reaction rate, was not seen, and in general the level scheme was elucidated, leading to a better constrained $^{18}\text{F}(p,\alpha)^{15}\text{O}$ reaction rate.

In addition, a direct measurement of $^{18}\text{F}(p,\alpha)^{15}\text{O}$ at low energies was performed using the full beam intensity of $10^7/\text{s}$ [8]. Cross-section measurements were obtained at E_{cm} of 0.250, 0.330, 0.453 and 0.673 MeV. The 0.330 MeV and 0.673 MeV measurements were made at the peaks of known resonances as a check on the consistency of the experiment, while the other two points were made in lower cross-section inter-resonance regions where interference between resonances is difficult to determine theoretically. Most importantly, the 0.250 MeV measurement is the lowest determination of this reaction cross-section to date, and is right in the energy region which dominates F-18 destruction at peak nova temperatures. With this data point and the previous R matrix work, much better constraints can be put on the role of the $^{18}\text{F}(p,\alpha)^{15}\text{O}$ reaction in F-18 destruction, and thus the resultant 511 keV flux from nova explosions.

The rate of the $^{18}\text{F}(p,\gamma)^{19}\text{Ne}$ reaction also affects the final abundance of F-18 in hot oxygen-neon novae. Of the two resonances thought to play a significant role, one ($E_{\text{cm}} = 0.33 \text{ MeV}$) has a radiative width estimated from the assumed analogue state in the mirror nucleus, F-19. The second ($E_{\text{cm}} = 0.665 \text{ MeV}$) does not have an analogue state assignment so this information is lacking. At the DRAGON facility the first successful direct measurement of the $^{18}\text{F}(p,\gamma)^{19}\text{Ne}$ reaction was performed [9]. The strength of the 0.665 MeV resonance was found to be over an order of magnitude weaker than currently assumed in nova models as a result. Reaction rate calculations show that this resonance is now expected to play no significant role in the destruction of F-18 at any astrophysical energy.

F-18 nucleosynthesis in classical novae also strongly depends on the thermonuclear rate of $^{17}\text{O}(p,\gamma)^{18}\text{F}$, which is part of the hot CNO cycle; the relevant temperature range is between 0.1 and 0.4 GK. The literature on $^{17}\text{O}(p,\gamma)^{18}\text{F}$ gives conflicting information for the direct capture (non-resonant) component of the reaction rate. In August 2011, Hager et al. measured the $^{17}\text{O}(p,\gamma)^{18}\text{F}$ cross-section with DRAGON between $E_{\text{cm}} = 250$ and 500 keV [10]. A second set of measurements was performed at DRAGON in September 2012. During this time, the cross-section on and 10 keV below the resonance were measured. Most recently a direct measurement of the $^{18}\text{F}(p,\gamma)^{19}\text{Ne}$ reaction was performed at DRAGON [11]. The strength of the 665 keV resonance was found to be over an order of magnitude weaker than currently assumed in nova models. Reaction rate calculations show that this resonance therefore plays no significant role in the destruction of F-18 at any astrophysical energy.

Other important radionuclides present in nova ejecta are Na-22 and Al-26. In particular Na-22 is a promising astronomy target because it is thought to be produced in large quantities, delivering a strong flux of 1.275 MeV γ rays. However, despite predictions to the contrary, none of these γ rays have been observed from an individual nova. Part of the problem again is nuclear physics uncertainties in Na-22 production and destruction reactions. Al-26 is unsuitable for observation from a single source because of its long lifetime, but novae are thought to produce up to 20% of the Al-26 observed in the galaxy, with the rest coming from massive stars.

A reaction that affects the abundance of both Na-22 and Al-26 in novae is $^{23}\text{Mg}(p,\gamma)^{24}\text{Al}$. This reaction had never been measured and thus contributed a large uncertainty to the final Na-22 and Al-26 predicted yields in nova models. With the highest intensity ^{23}Mg -23 accelerated beam in the world, some $5 \times 10^7 \text{ s}^{-1}$, the $^{23}\text{Mg}(p,\gamma)^{24}\text{Al}$ reaction was measured directly for the first time at the DRAGON facility to a precision sufficient for nova yield purposes [12]. This experiment challenged the DRAGON facility due to the Mg-23 beam being embedded in a more intense Na-23 beam, such that the facility had to separate not only Al-24 recoils from Mg-23 and Na-23 beam background, but also from Mg-24 recoils from the $^{23}\text{Mg}(p,\gamma)^{24}\text{Al}$ reaction. Thus this was a successful experiment both in terms of scientific result and technical achievement.

The $^{22}\text{Na}(p,\gamma)^{23}\text{Mg}$ reaction directly destroys Na-22. Its cross-section had been measured over the years using chemically prepared targets, but recently a new excited state in Mg-23 was measured in γ decay studies that could significantly contribute to the reaction rate at nova temperatures. In a collaborative project with the Centre for Experimental Nuclear Astrophysics (CENPA) at the University of Washington, Seattle, the experimental nuclear astrophysics group at TRIUMF designed an experiment to measure the strength of this possible new resonance using Na-22 targets produced at ISAC by implanting a very pure and intense (10^9 s^{-1}) ^{22}Na beam into a pure copper backing. Subsequently the $^{22}\text{Na}(p,\gamma)^{23}\text{Mg}$ reaction was measured using this target and a proton beam from the accelerator at CENPA [13,14]. Strengths of all known resonances were re-measured, as was the potential new resonance. It was found that some of the previously measured resonances were in fact some 2.5-3 times stronger. All known contributing resonances were measured with the highest precision to date. The end result is a Na-22 destruction rate that is larger than previously thought, leading to smaller predictions of Na-22 1.275 MeV γ -ray flux from oxygen-neon novae or equivalently, an decrease in the maximum detectability distance for nova-produced Na-22. This is an important result that is being checked by other laboratories using different methods, as well as using indirect methods at TRIUMF such as lifetime measurements in Mg-23.

The CENPA and earlier Bochum experiments conclude that at nova temperatures the reaction rate is dominated by a resonance about 206 keV above the $p + \text{Na-22}$ threshold, corresponding to an excitation energy of 7.786 MeV in Mg-23, but the resonance strengths reported differ substantially. By measuring the spin, lifetime, and proton decay branching ratio of the 7.786 MeV state, one can derive its resonance strength. A recent β -decay experiment performed in Jyväskylä, Finland provides compelling evidence for the spin assignment and determines the proton branching ratio to be 0.037(7). At TRIUMF Kirsebom et al. have recently carried out a Doppler shift attenuation method measurement using the $^3\text{He}(^{24}\text{Mg},^4\text{He})^{23}\text{Mg}$ reaction to determine the lifetime of the 7.786 MeV level in Mg-23.

Another reaction that strongly affects the abundance of Al-26 in nova ejecta is $^{26}\text{Al}(p,\gamma)^{27}\text{Si}$. Having previously measured $^{26}\text{Al}(p,\gamma)^{27}\text{Si}$ at the DRAGON facility, attention turned to the role of the short-lived isomer, Al-26m in the destruction of Al-26 in novae. Since Al-26m beam intensity is much lower than the ground state intensity at ISAC, direct measurements of the lower energy resonances important at nova temperatures have been impossible. Therefore indirect studies are required to determine the $^{26\text{m}}\text{Al}(p,\gamma)^{27}\text{Si}$ reaction rate. Such a study was performed at the TUDA facility using the $^{26\text{g}}\text{Al}(d,p)^{27}\text{Al}$ reaction at 6 MeV/nucleon in order to populate states in Al-27 that are the mirror states of the ones of interest in Si-27 for novae. The experiment was able to achieve an excitation energy resolution of around 56 keV and populated many states of interest, enabling the identification of these states with their associated analogue states in Si-27. This will allow more precise calculation of resonance parameters for those Si-27 states where laboratory measurements are still lacking.

Presolar grains are micrometer-sized grains of material that are fossils of stars and stellar explosions, and remained unchanged during the formation of the solar system. These grains, found in meteorites, carry signatures of the nucleosynthesis processes that occurred in the environment in which they were formed. By measuring the ratios of different isotopes of certain chemical elements the origin of these grains can be determined. While grains from AGB stars and Type II supernovae are common, only a few grains from novae have been discovered to date, and their classification as novae grains is still under debate. There is one isotope that, if measured, has the potential to be a ‘smoking gun’ for nova origin, S-33. The current models of oxygen-neon novae predict 150 times more S-33 in these environments than is found in our solar system. However, the uncertainty of this overabundance is 200+ 200%, -99% due to uncertainty in the $^{33}\text{S}(p,\gamma)^{34}\text{Cl}$ reaction rate. This uncertainty comes from the fact that there were several resonances in the relevant energy region (corresponding to temperatures of 0.2 to 0.4 GK) that had no measured resonance strengths. Thanks to the offline ISAC ECR ion source, intense beams of S-33 became available and these resonance strengths were measured using DRAGON. All of the known resonances within the relevant energy region and below what could be studied previously have now been measured. Even with up to 4×10^{15} beam ions on target, very few Cl-34 recoils from the reaction were seen for any of the previously unmeasured states. As a result these states do not contribute strongly to the reaction rate at and above 0.3 GK and the resonance at an excitation energy of 5576 keV in Cl-34 dominates the rate. The four lowest-energy resonances may contribute at temperatures of 0.25 GK and below. While further work will be required to determine the resulting S-33 overproduction factor, the rate of $^{33}\text{S}(p,\gamma)^{34}\text{Cl}$ reaction is not significantly changed over much of the oxygen-neon nova temperature range as a result of these measurements, though the uncertainty is reduced. This is good news for studies of presolar grains as this implies that the large S-33 overproduction factor is preserved, making it a good identifier for grains of nova origin.

Computational studies of novae have been performed at TRIUMF using the state-of-the-art stellar evolution code MESA and associated NuGrid code [15]. This is part of a joint project led by the University of Victoria, the Joint Institute for Nuclear Astrophysics, and TRIUMF. Models of CO and ONe white dwarfs were set up and used to investigate nucleosynthesis and convective boundary mixing in the subsequent novae explosions from accretion from a companion star for a wide range of parameters. Dedicated computational hardware belonging to the TRIUMF Nuclear Astrophysics Group was used for this. Eventually, the models will be used to determine nuclear reactions of astrophysical interest as well as evaluate the impact of existing measurements.

Neutron stars, which are formed in core collapse supernovae, are exotic end states of stellar evolution that play an important role in some cataclysmic binary systems and are of considerable interest in their own right as laboratories for high density, asymmetric nuclear matter.

Theorists at TRIUMF showed that microscopic calculations based on chiral effective field theory (EFT) interactions constrain the properties of neutron-rich matter at sub-nuclear densities much more strongly than is reflected in commonly used equations of state [16]. Combined with neutron star masses inferred from observations, their results lead to a radius of 9.7-13.9 km for a 1.4 solar mass neutron star, where the theoretical range is due roughly equally to uncertainties in many-body forces and to the extrapolation to high densities.

With collaborators, TRIUMF theorists formulated a low-energy effective theory describing matter in the inner crust of neutron stars [17]. This region consists of superfluid neutrons and a lattice of nuclei. The low-energy theory can be written using symmetry considerations and describes the dynamics of the Goldstone modes—the lattice and superfluid phonons that arise due to the spontaneous breaking of continuous space-time symmetries of the lattice and the condensate, respectively. They showed that the underlying interaction between the neutrons and the nuclei gives rise to entrainment and mixing between the Goldstone modes. This reduces the contribution of the superfluid phonons to the transport of heat in the inner crust. Currently Sharma, Forbes, and Bulgac are investigating the dynamics of vortices in the neutron superfluid, in particular focusing on a reliable estimate of the pinning force exerted by nuclei on the vortices. This is a key quantity required for the phenomenology of glitches in neutron star rotation.

Type I X-ray bursts (XRBs) are brief recurrent bursts of X-ray emission and are a frequent phenomenon in the galaxy. Our current understanding is that they originate in binary systems where material from a relatively un-evolved star accretes onto the surface of a neutron star, leading to an eventual thermonuclear runaway. The elevated temperatures achieved in XRBs are thought to allow nucleosynthesis up to the tin/tellurium region via the rapid-proton capture (rp) process. In order for this to occur, the thermonuclear runaway must start via a break out from the β -limited hot CNO cycles through the $^{15}\text{O}(\alpha,\gamma)^{19}\text{Ne}$ or $^{18}\text{Ne}(\alpha,p)^{21}\text{Na}$ reactions.

Both reactions are extremely difficult to measure directly, and are targets for future studies at TRIUMF. However, the value of the $^{18}\text{Ne}(\alpha,p)^{21}\text{Na}$ reaction rate at XRB temperatures has been constrained through a study of the inverse reaction $^{21}\text{Na}(p,\alpha)^{18}\text{Ne}$ at TRIUMF [18]. This was performed at the TUDA facility using Na-21 beams at ISAC-II of energies between 4.1 and 5.5 MeV/nucleon, and intensities of 10^6 s^{-1} . As depicted in Figure 2, this work shows that the contribution of the ground state component of the $^{18}\text{Ne}(\alpha,p)^{21}\text{Na}$ rate is lower than previously thought, requiring higher XRB temperatures before breakout can be achieved and the burst can ensue. Further work on the direct reaction is required to completely solve this problem.

Davids et al. performed a Monte Carlo calculation of the astrophysical rate of the $^{15}\text{O}(\alpha,\gamma)^{19}\text{Ne}$ reaction based on an evaluation of published experimental data. By considering the likelihood distributions of individual resonance parameters derived from measurements, estimates of upper and lower limits on the reaction rate at the 99.73% confidence level were derived in addition to the recommended median value. These three reaction rates were used as input for three separate calculations of Type I XRBs using spherically symmetric, hydrodynamic simulations of an accreting neutron star. In this way the influence of the $^{15}\text{O}(\alpha,\gamma)^{19}\text{Ne}$ reaction rate on the peak luminosity, recurrence time, and associated nucleosynthesis in models of Type I XRBs was studied [19]. Contrary to previous findings, no substantial effect on any of these quantities was observed in a sequence of four bursts when varying the reaction rate between its lower and upper limits. Rather, the differences in these quantities are comparable to the burst-to-burst variations with a fixed reaction rate, indicating that uncertainties in the $^{15}\text{O}(\alpha,\gamma)^{19}\text{Ne}$ reaction rate do not strongly affect the predictions of this Type I XRB model.

Core-collapse (or Type II) supernovae (CCSN) are perhaps the most familiar stellar explosions. They occur when massive stars run out of fuel after a series of core and shell burning processes and the resulting iron core collapses, electron degeneracy pressure being unable to resist gravity. The resulting explosion, reinvigorated by large neutrino fluxes, causes conditions of extremely high temperature, density, and free neutron and proton concentrations that may be suitable for rapid neutron capture or r -process nucleosynthesis, which is believed to produce about half of the elements heavier than Zn.

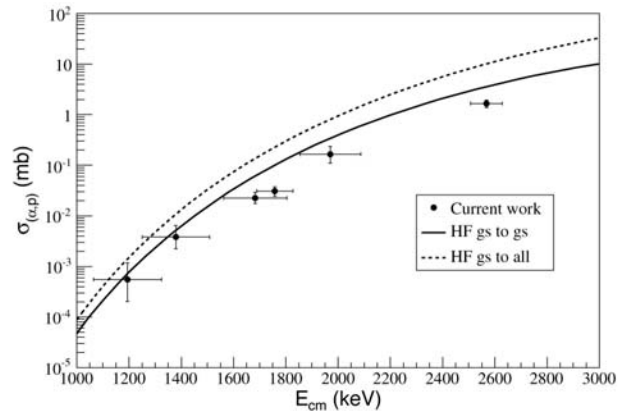


Figure 2: Experimental $^{18}\text{Ne}(\alpha,p)^{21}\text{Na}$ reaction cross section (black dots) as a function of centre-of-mass energy. Predictions based on Hauser-Feshbach calculations for ground-state to ground-state transitions (full line) and ground-state to all-states transitions (dashed line) are shown for comparison.

Neutrino interactions with nucleons are believed to play a critical role in the supernova explosion mechanism. Theoretical study of these interactions is necessary to quantitatively understand one of the most prolific nucleosynthesis sites in the universe. TRIUMF theorists investigated the neutrino response in pure neutron matter at sub-nuclear densities, estimating the neutrino-pair bremsstrahlung reaction rates based on modern EFT interactions [20]. In state-of-the-art supernova simulations, the standard rates for bremsstrahlung are based on the one-pion exchange approximation to the nucleon-nucleon interaction, corresponding to the leading order in EFT. When all orders are considered up to convergence, the neutrino rates are reduced significantly with respect to the standard rates.

With the new UC target capability at ISAC providing neutron-rich beams including some along the expected path of the r process, first experiments with heavy Rb and Sr isotopes have begun using TITAN, the 8π spectrometer, and the laser spectroscopy station. Masses are the most important nuclear quantities to measure in order to compute the nucleosynthesis expected under r process conditions, as they determine the neutron separation energies and thereby the path. Recently the TITAN Penning trap measured the masses of Rb-94,97,98 and Sr-94,97-99 with uncertainties of less than $4 \text{ keV}/c^2$, finding deviations of up to 11σ when compared to previous measurements and substantially reducing abundance prediction uncertainties [21].

CCSN are thought to be among the largest contributors to galactic Al-26. The actual galactic Al-26 abundance is known fairly well, and the Al-26/Fe-60 ratio is known very precisely. The CCSN models however suffer from considerable uncertainties in Al-26 production because of lack of experimental knowledge of the reactions that create and destroy Al-26 under CCSN conditions. In particular, The $^{26m}\text{Al}(p,\gamma)^{27}\text{Si}$ reaction plays a special role since Al-26m and Al-26g are in quasi-equilibrium in these conditions, and thus knowledge of both the destruction of the ground state and isomer is needed to determine the Al-26 effective half-life and ejected abundance. With the higher energy resonances that contribute to $^{26m}\text{Al}(p,\gamma)^{27}\text{Si}$ being significantly stronger than those for nova temperatures, direct measurements are within reach at the DRAGON facility, using the Al-26m intensities available. DRAGON recently performed the first measurement of a resonance in $^{26m}\text{Al}(p,\gamma)^{27}\text{Si}$ using a mixed Al-26g/Al-26m beam, with an isomer intensity of order 10^5 s^{-1} . This would represent the first ever measurement of radiative capture on a nuclear isomer, and constrain the $^{26m}\text{Al}(p,\gamma)^{27}\text{Si}$ reaction rate for CCSN.

Selected References

- [1] O. Kirsebom and B. Davids, Phys. Rev. C 84, 058801 (2011).
- [2] P. Navrátil and S. Quaglioni, Phys. Rev. Lett. 108, 042503 (2012).
- [3] S.K.L. Sjue et al., Nucl. Instr. Meth. Phys. A 700, 179 (2013).
- [4] P. Navrátil, R. Roth, and S. Quaglioni, Phys. Lett. B704, 379 (2011).
- [5] U. Hager et al., Phys. Rev. C 84, 022801(R) (2011).
- [6] U. Hager et al., Phys. Rev. C 86, 055802 (2012).
- [7] A. St. J. Murphy et al., Phys. Rev. C 79, 058801 (2009).
- [8] C. Beer et al., Phys. Rev. C 83, 042801 (2011).
- [9] C. Akers et al., Phys. Rev. Lett. 110, 262502 (2013)
- [10] U. Hager et al., Phys. Rev. C 85, 035803 (2012).
- [11] C. Akers et al., Phys. Rev. Lett. 110, 262502 (2013).
- [12] L. Erikson et al., Phys. Rev. C 81, 045808 (2010).
- [13] A. Sallaska et al., Phys. Rev. Lett. 105, 152501 (2009).
- [14] A. Sallaska et al., Phys. Rev. C 83, 034611 (2011).
- [15] P. Denissenkov et al., Astrophys. Journal 762, 8 (2013).
- [16] K. Hebeler et al., Phys. Rev. Lett. 105, 161102 (2010).
- [17] V. Cirigliano, S. Reddy, and R. Sharma, Phys. Rev. C 84, 045809 (2011).
- [18] P. Salter et al., Phys. Rev. Lett. 108, 242701 (2012).
- [19] B. Davids, R. Cyburt, J. José, and S. Mythili, Astrophys. Journal 735, 40 (2011).
- [20] S. Bacca et al., Astrophys. Journal 758, 34 (2012).
- [21] V.V. Simon et al., Phys. Rev. C 85, 064308 (2012).

4.2.3 NUCLEAR MEDICINE

Isotopes have critical uses in medicine for the diagnosis, treatment, and management of both acute and chronic disease. The cost to the economy of some of the more prevalent conditions affecting Canadians is staggering: 70% of Canada's healthcare budget is spent on chronic disease management with cardiovascular disease accounting for \$21 billion in lost economic activity¹, cancer for \$23 billion², and mental illness and neurodegeneration for \$51 billion³. All of these areas involve chronic care, affect many individuals, and draw substantial resources from a healthcare system trying to balance costs with demand for services. This balance will continue to remain a challenge for the foreseeable future, with expenditures expected to balloon as the Canadian population continues to age. One example is the cost of managing mental health, expected to grow to \$293 billion/year by 2040⁴.

During the 2008–2012 period, TRIUMF's Nuclear Medicine Program has evolved significantly. In addition to leadership of a national effort to develop accelerator-based production of key medical isotopes, the TRIUMF team has developed research thrusts in isotope-production target technology and radiopharmaceutical applications for advanced imaging of disease. Finally, TRIUMF's Proton Therapy Program has been pursuing improved analysis and control of exposure during the treatment process. This section reports on progress in these areas over the past five years.

4.2.3.1 INTRODUCTION

TRIUMF's Nuclear Medicine Division maintains core competencies in three key areas: (1) medical isotope production and isolation, (2) innovations in accelerator targets and nuclear chemistry for radiopharmaceuticals, and (3) radiopharmaceutical synthesis and application. The Nuclear Medicine Division continues to attract substantial funding from partners and these resources have been directed toward upgrades and research ranging from improving TRIUMF's aging chemistry facilities for radiopharmaceutical production under GMP (good manufacturing practice) guidelines, to leveraging TRIUMF's expertise in accelerator-based isotope production to address the recent medical-isotope crisis. Several of these opportunities provided a means to establish or enhance collaborations with new partners across the country.

Over the past five years, TRIUMF has emerged as a strategic centre for the innovation of novel isotope production technology and applications. The result has been the development of technology and training of highly qualified individuals for the Canadian and international cyclotron and radiopharmaceutical communities.

4.2.3.2 ALTERNATIVE PRODUCTION METHODS FOR TC-99M

The medical isotope technetium-99m (Tc-99m) is widely used in medical imaging (about 80% of procedures employ it), but in recent years its use has been beset by single-point-of-failure problems with the current reactor-based supply chain. That is, Tc-99m is conventionally produced in a handful of 50+ year old nuclear reactors that employ highly-enriched, weapons-grade uranium as the target material. Concerns about the reliability of these reactors as well as geopolitical pressure to restrict usage of fissile materials has generated considerable pressure to develop alternative production technologies.

North America is uniquely positioned to implement an alternative, large-scale Tc-99m production program by leveraging its existing fleet of hospital-based cyclotrons to produce this isotope on demand, where it is needed, when it is needed. By doing so, existing cyclotron centres will collectively showcase a decentralized Tc-99m production model to the world, ushering in a new paradigm involving multi-regional isotope production within a larger system capable of avoiding single-point-of-failures and the need to use enriched uranium of any grade.

One of the two reactors producing more than a third of the global supply of Tc-99m is the National Research Universal (NRU) reactor in Chalk River, Ontario. Recognizing the need for Canada to develop alternative sources not only for its citizens but also to retain a portion of the global market, Natural Resources Canada (NRCan) launched a series of competitive funding programs to support development and deployment of new technologies.

Building on its long experience with medical isotopes and cyclotrons, TRIUMF convened a national consortium consisting of a multidisciplinary team of physicists, engineers, chemists, and physicians from the British Columbia Cancer Agency (BCCA), Lawson Health Research Institute (LHRI), and the Centre for Probe Development and Commercialization (CPDC) to deliver an innovative solution to the medical isotope crisis. The consortium was awarded \$13M federal funds to pursue the development of cyclotron-based production of Tc-99m (under the 2010–2012 Non-reactor Isotope Supply contribution Program, NISP, and the 2012–2016 Isotope Technology Acceleration Program, ITAP).

To date, all institutions in the consortium have successfully demonstrated the feasibility of producing Tc-99m using machines found in Canada's existing medical cyclotron infrastructure. Efforts established the parameters for optimal irradiation of Mo-100 targets to obtain high-quality Tc-99m for clinical translation. Results allowed the team to understand the control parameters that influence reproducibility and predictability of Tc-99m yields and radionuclidic purity. The results, which can be used as a baseline to implement a decentralized production paradigm, include:

- Calculated theoretical yields for (p,x) reactions of the various molybdenum isotopes that could potentially be found in enriched Mo-100. This established theoretical Tc-99m yields and radionuclidic impurities [1,2].
- A manufacturing process for Mo-100 target plates using novel Mo-100 coating methods [3];
- Design, assembly, and installation of target stations at TRIUMF (using a CP42 cyclotron), the BCCA (operating an ACSI TR19), CPDC and LHRI (using GE PETtrace cyclotrons; Mitigated risks associated with unique specifications for various cyclotrons at various institutions. For example, the GE PETtrace cyclotrons at CPDC (vaulted) and LHRI (self-shielded) maintain the same capabilities, but exhibit unique specifications in their upgrades and operations;
- Design, assembly, and installation of target transfer systems to move solid targets from the cyclotron to a shielded workspace (hot cell) at BCCA, CPDC, and LHRI;
- The development of new, automated purification methods to extract and purify Tc-99m at greater than 90% efficiency from irradiated targets [4].
- Demonstrated that high (Curie-quantity) production yields are achievable with radionuclidic purity in excess of 99.7%;
- Reconstituted commercial technetium kits, and demonstrated that the resulting preparations were well within existing quality control (QC) standards. However, the presence of minute quantities of other Tc isotopes will require new USP/EP standards. Radionuclidic impurities can be controlled through the isotopic purity of the Mo-100 feedstock, cyclotron irradiation energy, irradiation time, and transport/distribution time.
- Calculated human dosimetry of cyclotron-produced Tc-99m based on theoretical yields of the various radioisotopes [5].
- Developed an efficient method to recycle Mo-100 with over 90% recovery in order to make the production process economically competitive.

The end result is that, in less than two years, the team of investigators advanced the idea of cyclotron-based Tc-99m production considerably and demonstrated a viable alternative for this important isotope. With proof of concept in hand, the team is now working toward validating the technology on a commercial scale, establishing the final production yields, and running clinical studies under stringent quality requirements in order to assess economic feasibility and to establish a mechanism, and the receptors needed, to transfer this technology to the private sector and the global market.

Selected References

- [1] A. Celler, X. Hou, F. Bénard, T. Ruth. *Phys. Med. Biol.* 56, 5469 (2011).
- [2] K. Gagnon et al.. *Nucl. Med. Biol.* 38, 907 (2011).
- [3] T.J. Morley et al., *Electrochemistry Communications* 15, 78 (2012).
- [4] T.J. Morley et al., *Nuc. Med. Biol.* 39, 551 (2012).
- [5] X. Hou et al., *Phys. Med. Biol.* 57, 1499 (2012).

4.2.3.3 MEDICAL ISOTOPE PRODUCTION

Thirty years ago, the University of British Columbia (UBC) Department of Medicine entered a pioneering collaboration with TRIUMF that began the Positron Emission Tomography (PET) Program. While this relationship is still at the core of the TRIUMF's Nuclear Medicine Program, significant expansion has taken place.

Today, in an era of constrained budgets and increasing regulatory oversight, TRIUMF, teamed with key members of the imaging community at the British Columbia Cancer Agency (BCCA) and several other institutions across Canada, to bring radiotracer production programs in line with the explosive demand for non-reactor sources of isotopes with applications in science and medicine.

During the past five years, TRIUMF produced medical isotopes for neurological (primarily UBC-based programs) and oncological (primarily BC Cancer Agency) use in the surrounding region. (This specific performance is discussed in Section 5.6.1.) With the acquisition, installation, and commissioning of a modern TR-19 cyclotron at BC Cancer Agency, TRIUMF remains as the primary radiopharmaceutical provider for the Parkinson's (neurological) research at UBC and serves as a back-up supplier for oncology studies at VGH. TRIUMF continues to produce isotopes for novel applications in chemistry, biology, oceanography, and medicine at UBC.

FIRST PATIENT SUCCESSFULLY SCANNED IN LUNG CANCER HYPOXIA CLINICAL TRIAL

11 July 2008

With help from a team of TRIUMF experts, the radiopharmaceutical known as [¹⁸F]EF5 is poised to take out the guesswork of deciding treatment for some cancer patients.

TRIUMF scientists delivered the first doses of [¹⁸F]EF5 to the UBC Hospital for a clinical study in patients with lung cancer hypoxia, an oxygen deficiency that, when present in cancer cells, indicates resistance to traditional radiotherapy cancer treatments. The first patient was successfully scanned on July 8, 2008 using a radiopharmaceutical traced with the fluorine-18 isotope.

This imaging represents the first successful clinical PET scan performed with [¹⁸F]EF5 in Canada. Currently, medical isotopes are used to image only the location and size of a tumor in the body. Now, with studies underway using [¹⁸F]EF5, medical practitioners will be able to detect the important cellular characteristic of hypoxia, allowing them to develop customized treatment plans for the cancer patient based on the information the scans provide. If successful, [¹⁸F]EF5 PET scans may be an important tool in the fight against cancer worldwide.

Radiometallic-Isotope Production in Liquid Targets

Nuclear Medicine at TRIUMF continues to focus on research to develop platform technologies that advance the field of accelerator-based medical isotope production and to better enable radiopharmaceutical development. The widespread acceptance of new and promising radioisotopes is typically challenged by their availability and accessibility, brought about by a need for solid target irradiation capabilities and/or the purchase of an appropriate isotope generator, if available.

Most medical cyclotron sites maintain an isotope production infrastructure that makes use of a pneumatic transfer of a liquid or gas from the cyclotron target to the radiopharmaceutical production workspace within a shielded hot cell, making solid target irradiation difficult. A need to install a solid-target transfer system necessitates a substantial technical and financial commitment by a facility in order to explore additional isotopes. Facility upgrades may prove to be cost prohibitive, especially if preliminary biological studies are required to warrant their purchase. These obstacles likely inhibit the development of novel tracers that may possess a better match between the physical half-life of a promising new radioisotope and the pharmacokinetic profile of the vector to which it is attached.

To enhance the availability of new and promising radiometallic isotopes, TRIUMF and BCCA are currently developing a platform technology to enable irradiation of select metal-salt solutions for the production of research quantities (or higher) of various radioisotopes using readily available liquid target equipment found in all cyclotron facilities. We are currently pursuing the production of Tc-94m ($t_{1/2}=0.87$ h), Ga-68 ($t_{1/2}=1.1$ h), Sc-44 ($t_{1/2}=4$ h), Cu-61/64 (Cu-61 $t_{1/2}=3.3$ h, Cu-64 $t_{1/2}=12.7$ h), Zr-89 ($t_{1/2}=78$ h) and/or Mn-52 ($t_{1/2}=134$ h) using the appropriate precursors in salt solution.

Tc-94m was produced by irradiating solutions of natural-abundance ammonium heptamolybdate tetrahydrate $((\text{NH}_4)_6\text{Mo}_7\text{O}_{24})\cdot 4\text{H}_2\text{O}$ on TRIUMF's TR-13 cyclotron in a standard liquid target at 5 μA for 1 hour [1]. Measured yields were sufficient to allow subsequent isolation and radiopharmaceutical chemistry. The purification chemistry applied was identical to that developed during the large-scale Tc-99m production effort discussed above.

To demonstrate the versatility of this approach, the same target system was used to produce Sc-44, an attractive isotope due to its 3.97 hr half-life and short positron range. Salt solutions of $^{nat}\text{Ca}(\text{NO}_3)_2$ were irradiated at low current (8 μA for 1 hour). Sc-44g was produced via the $^{44}\text{Ca}(p,n)$ reaction, isolated using commercially available ion exchange resins, and successfully used in radiolabelling experiments using established chelate systems. Studies toward new radiopharmaceuticals are currently underway. A new target design tested even makes it possible to irradiate the salt solution up to a beam current of 20 μA with an increased yield over the original target design. Moving forward, efforts will continue to demonstrate this technique for the production of Zr-89, Mn-53, Ga-67/68 and Cu-61/64. All will be generated and purified and put toward studies in which their use is deemed beneficial.

Given the low-current requirements and off-the-shelf availability of the hardware, the approach described here provides a simple method for most medical cyclotron facilities to produce useful quantities of radiometals by adapting liquid targets already in place for the production of other PET isotopes, such as F-18. The production of radiometals in liquid targets, as developed at TRIUMF, will allow many centres to produce a range of new and emerging isotopes without a significant investment in solid-target infrastructure, facilitating a quick turn-around for the investigation of these isotopes as alternatives for any imaging study.

Cu-64,67 Production for Oceanography Studies

Marine phytoplankton are estimated to reduce approximately 45 Gigatons of CO_2 from the earth's atmosphere to organic carbon each year, accounting for roughly half of the total carbon fixation on earth. A portion of the organic carbon sequestered this way is exported to the deep ocean as sinking particles. Variations in the magnitude of this macro-biological carbon pump affect the CO_2 content of the upper ocean, which in turn regulates atmospheric carbon dioxide levels and climate, on time scales ranging from hundreds to thousands of years.

In order to better understand the regulation of the global carbon cycle, Dr. Maite Maldonado at UBC has focused her research on determining the factors that control oceanic phytoplankton productivity. Research over the last several decades has revealed that the availability of certain micronutrients, such as the trace elements Fe, Mn, Zn, and Co may affect phytoplankton species composition, function, and community growth [2]. Copper (Cu) has been identified as a required redox element in enzymes involved in various metabolic pathways, such as respiration (e.g., cytochrome oxidase) in phytoplankton. Cu is also needed for the oxidation of organic nitrogen and the detoxification of superoxide radicals using a Cu/Zn superoxide dismutase in some phytoplankton. Most recently, Cu has been established as an important micronutrient for Fe-limited green algae and marine diatoms. This finding is important because 30% of the global ocean is Fe-limited. In Fe-limited waters, phytoplankton is observed to thrive and thus must have evolved either through a unique mechanism of Fe uptake and/or a lower Fe demand for growth. The replacement of Fe-containing enzymes with Cu-containing enzymes may explain the success of oceanic phytoplankton in open-ocean waters, where Fe concentrations are too low to support growth of coastal phytoplankton. To better understand the role Cu plays in phytoplankton subsistence and growth in low Fe waters, Dr. Maldonado has turned to radioisotopes of Cu to track and identify trace metal acquisition, metabolism and nutrition of marine bacteria and phytoplankton.

Typically obtained as a by-product of Ga-67 production, Cu-67 has recently experienced its own supply crisis as production emphasis at major commercial suppliers has moved away from both of these isotopes. In response, TRIUMF, in collaboration with Dr. Maldonado, mobilized to produce Cu-64 and Cu-67 for her studies as described above.

In summary, Dr. Maldonado's research aims to address fundamental questions in microbial physiology, ecology, and evolution in order to better understand how trace metal distribution and speciation may control global phytoplankton productivity in the present day and over glacial-interglacial cycles. In turn, these findings will elucidate how marine microorganisms may affect trace metal biogeochemical distribution and cycling in the ocean.

N-13 Nitrate Production for Botany Studies

A long-standing collaboration between TRIUMF and Dr. Tony Glass (UBC) utilized N-13 nitrate production capabilities at TRIUMF to enable studies on plant nutrition. Research in Dr. Glass's laboratory focuses on membrane transport processes responsible for transferring inorganic ions (particularly K^+ , NH_4^+ and NO_3^-) across the plasma membrane, from external (soil) solution, into the roots of higher plants. $^{13}NO_3^-$ and $^{13}NH_4^+$ transport processes have been studied at the molecular level in both wild type and mutant (gene deletion) genotypes of various plant species [3,4].

Genes encoding high- and low-affinity NO_3^- transporters and high-affinity NH_4^+ transporters were cloned by Dr. Glass's group and experiments were conducted to understand the manner in which the gene products (proteins) participate in transport processes, and the manner in which they are regulated. As a testament to the complexity of the studies involved, one species (*Arabidopsis thaliana*) was found to maintain a total of 11 genes encoding NO_3^- transporters and 5 encoding NH_4^+ transporters. In the case of NO_3^- substantial quantities of this ion were found to be transported to the leaves of many plants, where it is reduced to NH_4^+ and converted to amino acids and other N-containing compounds. Thus, ion uptake is not exclusively a function of root cells only, but leaves too must reabsorb nitrate from the xylem sap.

Selected References

- [1] C. Hoehr et al., Appl. Rad. Isot. 70, 2308 (2012).
- [2] J. Guo, S. Lapi, T.J. Ruth, M.T. Maldonado, Journal of Phycology 48, 312 (2012).
- [3] Z. Yong, Z. Kotru, A.D.M. Glass, Plant Journal 63, 739 (2010).
- [4] Y. Wang et al., Fungal Genetics and Biology 45, 94 (2008).

4.2.3.4 TECHNOLOGICAL INNOVATIONS

Despite over 80 years of cyclotron research and development, relatively little is understood about the environment within a cyclotron target during irradiation. Optimized irradiation conditions are typically deduced by indirect measurement of beam location, target body temperatures, vacuum levels, and other peripheral metrics of the cyclotron and target hardware. A better understanding of the conditions (beam energy, position and fluctuations, target temperature gradient, etc.) within the target will improve the reliability of cyclotron and target performance during isotope production. Knowledge of these parameters allows for the design and improvement of new cyclotron target technology as Canada shifts from relying on large-scale production and distribution of isotopes from the Chalk River nuclear reactor to widespread, routine, large-scale, reliable production of important isotopes in hospital-based medical cyclotrons.

During the past five years, target technology research and development has focused on enhancing cyclotron beam energy measurements, beam-profile monitoring, and radiometallic isotope production using liquid targets.

Fundamental Measurements of Cyclotron Energy

When used for medical isotope production, both new and old cyclotrons require periodic validation of beam energy to ensure optimal performance. This is not only part of good manufacturing practice and quality assurance but is necessary for optimizing target yields and minimizing the radiation dose overhead of radionuclide production. An example where such a validation is of particular importance is when undesired by-products result from competing energy-dependent reactions (e.g., production of I-123 via the (p,2n) reaction when producing I-124 from Te-124).

Although it is often claimed by cyclotron manufacturers that the energy of their machines never changes, field experience suggests that this assertion is not valid for the majority of present-day negative ion cyclotrons. The extraction of negative ion beams by a stripper foil can give useful beam on targets even with substantial orbit centre offsets. Changes in magnet shim or in distribution of the RF (radio frequency) field along the dees can cause the orbital centre to drift. Furthermore, the loss of position calibration or damage to extractors and stripper foils can also substantially affect the beam energy. While cyclotrons in nuclear physics institutions often have analyzing magnets with well-characterized energy definition, this diagnostic tool is not feasible for most medical cyclotron configurations because the production targets sit more or less straight on the beam port with little or no further collimation. As such, an off-line approach for evaluating the beam energy of a medical cyclotron is required.

For most applications the simple method of beam range determination will not be accurate enough due to straggling. Long stacks increase straggling, and it can be difficult by conventional “burn” methods to discriminate the Bragg peak end from thermal damage. For this reason, we investigated a new, simple-to-perform method for evaluating the cyclotron beam energy by exploiting the $^{nat}\text{Cu}(p,x)^{63}\text{Zn}$ reaction. By irradiating a stacked Cu-Al-Cu foil system and a universally available dose calibrator (a re-entrant ion chamber used in every nuclear medicine facility), TRIUMF, in collaboration with the Hevesy Laboratory at the Technical University of Denmark, developed a method sufficiently sensitive to achieve the necessary energy precision of a few tenths of an MeV. The proposed method was extensively evaluated and tabulated for protons in the 11-19 MeV energy range, but it can be straightforward to extend the general principle to protons, deuterons, and alphas of other energies that make it relevant to most modern cyclotron facilities. To facilitate the adoption of this technique into routine evaluation of the cyclotron beam energy, TRIUMF has published a list of recommended nominal aluminum degrader thicknesses as well as a list of the corresponding curve fit data for evaluation of the proton energy using the measured Zn-63 activity ratio [1]. Application of the proposed method to the monitoring of deuteron energies is a topic we plan to explore further in the near future.

Beam-Profile Monitors

Given the frequent (daily) and prolonged (~6 hour) irradiation times required for the production of Tc-99m on small medical cyclotrons, an ability to monitor cyclotron beam positioning in real time may become a crucial metric to ensure a reliable supply of medical isotopes for many Canadians. Three popular methods for determining the beam profile on a PET cyclotron have been: (1) using an autoradiography technique to measure the activity pattern induced in a target foil with a radiation sensitive film, (2) the remote movement of a wire through the beam, and (3) measuring the amount of current striking a set of collimators in front of the target. The drawback of these approaches is their inability to monitor the beam in real time at full beam power, which results in either an exhibiting non-linear correlation in signal response to the power deposited, or not being able to provide a two-dimensional beam profile.

Over the past five years, TRIUMF designed and successfully tested a beam-profile monitor that is able to withstand the high, absorbed power of a PET cyclotron and monitor the deposited energy linearly and in real time [2]. A prototype monitor, consisting of a water-cooled Faraday cup and two orthogonal rows of tungsten electrodes mounted on a water-cooled support frame and spaced closely together, was designed, built and tested. After applying a voltage potential to the electrodes, the beam current was measured using a custom electronic setup involving a current mirror and a current-to-voltage amplifier. With the growing prevalence of hospital-based cyclotrons, a real-time beam profile monitor will enable rapid and simple beam diagnostics, ensure optimal performance for isotope production, and reduce maintenance because of better beam alignment with the target port and hardware.

Miniaturization of Radiopharmaceutical Synthesis

Radiotracers such as [¹¹C]raclopride are produced in a process that can take between 45 and 60 minutes to complete. These conventional approaches can consume upwards of 75% of the ¹¹C ($t_{1/2} = 20$ min) due to radioactive decay alone, even more if synthesis losses are considered. To compensate, a large starting quantity of radioactive precursors such as [¹¹C]methyl iodide is required to produce an adequate amount of the tracer for injection. In this investigation, a continuous-flow microchip was explored for the purpose of synthesizing C-11 radiotracers in a shorter time by exploiting the favourable reaction kinetics of using smaller reaction volumes. To enhance the mixing of reagents within the microchannel, a micromixer “loop” design was used in fabricating various polydimethylsiloxane chip styles. With a loop design implemented in an abacus-style chip for the production of nonradioactive raclopride, shorter reaction times, reduced precursor use, and improved yields were possible when compared with the use of a simple serpentine design (no loop-style chip). However, when performing the equivalent radiochemical reaction, the results were not as favourable. Using the loop design in a full loop-style chip, parameters such as premixing the reagents, reducing flow rate, and varying reagent concentrations were explored to improve the yields of [¹¹C]raclopride (in terms of relative radioactivity) formed.

We have demonstrated that the use of a microchip maintains advantages through improved yields and shorter reaction times for the production of nonradioactive as well as [¹¹C]raclopride [3,4]. Microfluidic synthesis has improved the nonradioactive synthesis results in comparison with the conventional process by reducing the reaction time by ~33% and required ~5% of the MeI used in conventional preparation. The abacus microchip was found to be a better design than the no loop or serpentine chip to provide a better yield. For the [¹¹C]Rac synthesis, the full loop chip produced better results, demonstrating higher [¹¹C]Rac relative radioactivity and higher conversion of [¹¹C]MeI to [¹¹C]Rac than the abacus microchip. To evaluate the microchip method further, the reactants were premixed, and we found that the full loop chip still produced better results than the abacus chip, thus reinforcing the importance of a micromixer design for this process.

We have also improved the [¹¹C]Rac synthesis by reducing the flow rate to 2 μ L/min. Although we have demonstrated the advantages of lower precursor consumption and safer operation, this modification would not be the most efficient solution on a production scale because a lower flow rate will decrease production speed. The fabrication of a glass chip with the micromixer design is underway for the full investigation and optimization of the microchip radiosynthesis of [¹¹C]Rac and other labelled compounds. In addition, the behaviour of reagents in the microchannels is further explored in a computational fluid dynamics study.

Radiotherapeutic Isotopes

Beyond imaging, the radiometal family of isotopes is also home to a number of therapeutic β^- , α , conversion and Auger electron emitters. The short path length and high-LET particles are very effective in killing cells. Since the time of Marie Curie, use of radiation for the destruction of cancerous tissues has been recognized as a potential application, but it remains as an unoptimized science to date. The medical community has come to utilize wide-field, external beam radiation as a means to treat tumours in the hopes of delivering a fatal dose of ionizing radiation to the tumour volume while sparing the surrounding healthy tissue. There have been dramatic improvements in patient and tumour dose control over time; however, the concept continues to experience challenges associated with controlling radiation dose, side effects that include depressed immunity in patients making them susceptible to post treatment infections, and an increase in secondary cancers.

An alternative approach is to deliver a therapeutic radiation dose selectively to the tumour. By employing a similar strategy to that for molecular imaging, therapeutic isotopes can be incorporated into more complex pharmaceuticals for specific, targeted delivery of a potent radiation dose.

Successful radiotherapeutics developed to date have relied on the inherent biodistribution profiles of simple chemical salts: [^{131}I]NaI (thyroid treatment), [^{153}Sm]SmCl₂, [^{32}P]phosphates and [^{89}Sr]SrCl₂ for palliative treatment of bone metastases. More recent advances have seen a small degree of chemical complexity introduced into the final formulations. Examples include [^{131}I]mIBG for neuroblastomas, as well as [^{90}Y] and [^{177}Lu]-labelled peptides for neuroendocrine tumour treatment to [^{90}Y]glass microspheres (Theraspere™) injected directly into the liver for primary or metastatic liver tumours. It is reasonable to expect that radioisotope therapy will continue to require a greater availability of isotopes and more sophisticated biochemical approaches. To this end, radiotherapeutic isotopes have been growing in popularity despite challenges associated with their availability, distribution, and use.

Recent studies have shown that Rhenium-186 (Re-186) is emerging as an optimal candidate for radioimmunotherapy (RIT). This is mainly due to its nearly ideal half-life of 3.72 days as well as its decay properties (β^- , $E_{\text{max}}=1.07$ MeV and an imageable γ -ray at 137 keV with 9% abundance). The energy deposited to cells suggests that Re-186 is a promising candidate for therapy of tumours from millimetre to centimetre dimensions. Re-186 is currently available from neutron irradiation of Re-185 in low specific activity, although progress has been made toward improving this result. High specific activity Re-186 can be produced by proton bombardment of enriched tungsten targets. However, there are large discrepancies in the literature for the excitation function of the $^{186}\text{W}(p, n)^{186}\text{Re}$ reaction. In order to better assess the feasibility of producing multi-mCi levels of Re-186 for therapeutic applications via the $^{186}\text{W}(p, n)^{186}\text{Re}$ reaction, the excitation function was re-measured. Scientists at TRIUMF determined the cross-sections for the production of Re-181, Re-182m, Re-182g, Re-183, Re-184, and Re-186 from natural tungsten, using a stacked foil technique for proton energies up to 17.6 MeV. The results suggested that small quantities of Re-186 can be produced on TRIUMF's TR-13 cyclotron, but these quantities were insufficient to allow for a pre-clinical study to compare reactor-produced (low specific activity) with cyclotron-produced (high specific activity) Re-186. TRIUMF could explore this further with access to a higher energy, higher current cyclotron.

Selected References

- [1] K. Gagnon et al., Applied Radiation and Isotopes 69, 247 (2011).
- [2] C. Hoehr et al., AIP Conf. Proc. 1509, 41 (2012).
- [3] S. Haroun, et al., Can. J. Chem. 91, 326 (2013).
- [4] S. Haroun, Jour. Labeled Compounds & Radiopharmaceuticals 52, S503 (2009).

4.2.3.5 ADVANCING RADIOPHARMACEUTICAL SYNTHESIS AND APPLICATION

TRIUMF's Nuclear Medicine Division is built upon a long-standing symbiotic collaboration with the PPRC (under current Director Dr. Stoessl). This joint venture has led to one of the best PET brain imaging centres in the world, one flagship of TRIUMF's activity. Historically the radiotracer production and imaging had been headed by Dr. Ruth, a TRIUMF senior scientist. In light of the expansion of the TRIUMF Nuclear Medicine Program and UBC imaging capabilities (two clinical and two pre-clinical scanners), the position is now split between Dr. Schaffer (TRIUMF, Head Nuclear Medicine) and Dr. Sossi (UBC Physics and Astronomy, UBC PET Director). The tight collaboration between them is formalized by cross-appointments in their respective institutions.

While the main clinical research focus of the imaging program is Parkinson's disease (PD), an increased emphasis is being placed on other neurodegenerative disorders such as Alzheimer's. Achievements of the collaboration include pioneering work in discovering: mechanisms of PD pathogenesis, progression and treatment-related complications, the neurochemical basis of the placebo effect, establishment of neurochemical changes that precede the clinical symptoms of PD, development of novel data analysis methods and quantitative high-resolution imaging as well as significant optimizing dopaminergic tracer synthesis.

The program has generated well over 150 imaging-related peer-reviewed papers in the last five years and secured over \$15M CAD of funding.

Neurodegenerative Disease Imaging

Currently, seven compounds are produced on a routine basis using TRIUMF-designed automated synthesis equipment. Also, part of the radiopharmaceutical production lab was upgraded in 2010 with a contribution from Western Economic Diversification of Canada and PPRC, allowing the group to purchase new equipment and to better conform to GMP standards (see below).

Tracer demands are also changing as research at the PPRC and, more recently, the Centre for Comparative Medicine (CCM) at UBC evolves. Over the past two years, the core group has established the synthesis of [¹¹C] MRB (methyl reboxetine), a selective norepinephrine transporter (NET) blocker, for a collaborative study with Dr. Yu-Shin Ding, Departments of Psychiatry and Radiology, NYU Langone Medical Centre. [¹¹C]Yohimbine was developed for Dr. Doris Doudet for use in imaging noradrenergic receptors in the brain, and this was followed in early 2012 by [¹¹C] DASB, which will be used to assess the serotonin function in the brain, and by the inflammation tracer ¹¹C-PBR for Dr. Sossi's studies (in collaboration with Dr. Robert Mach, Department of Radiology, University of Pennsylvania Perelman School of Medicine) on the role of neuroinflammation in PD. [¹⁸F] EF5 was also resurrected for shipment to BCCA for a clinical trial on the use of PET in prostate cancer imaging. All tracer production is in the process of being transferred to the new GMP compliant facility.

In addition, a CFI-funded Milabs microSPECT/PET/CT camera was installed at the CCM. This camera will expand the pre-clinical imaging capacity of the existing Siemens microPET located at the UBC hospital and will provide novel opportunities to develop and use gamma-emitting radionuclide-labelled compounds, thus motivating further expansion of TRIUMF's Nuclear Medicine Program.

Clinical Studies of EF5 and FDOPA

Hypoxia in tumours is associated with genetic instability and increased resistance to radiation and chemotherapy, with previous work suggesting that hypoxia may be an important prognostic and predictive factor in non-small-cell lung carcinoma (NSCLC). In addition, antiangiogenic drugs and standard chemotherapy agents may alter tumour blood flow, resulting in changes in tumour oxygenation, but this has never been demonstrated in living patients or during treatment.

FIRST SUCCESSFUL SCAN OF PATIENT WITH F-DOPA ANNOUNCED

26 May 2011

TRIUMF's Mike Adam, along with Doctors Daniel Levine, Daniel Metzger, Helen Nadel, Angelica Oviedo, and Erik Skarsgard from BC Children's Hospital, used the radiopharmaceutical F-DOPA in conjunction with PET/CT imaging to diagnose a 16-year-old patient with a neuroendocrine tumour syndrome. Conventional magnetic resonance imaging showed three soft tissue tumours within the abdomen but this and conventional nuclear medicine imaging with Iodine-123 labeled MIBG failed to provide a unifying diagnosis. The F-DOPA PET/CT clearly depicted all three tumours and implied a common diagnosis, which was subsequently confirmed on genetic testing following successful surgical removal. This represented the first reported use of F-DOPA PET/CT for pediatric neuroendocrine syndrome imaging and was recently reported in the journal *Pediatric Radiology*.

The synthetic organic chemistry performed to add the Fluorine-18 isotope can only be done at a limited number of places, including BC Cancer Agency and TRIUMF. As a result, these two organizations have been receiving referrals from all over Canada. TRIUMF has been doing work in the field of nuclear medicine for approximately 30 years, and has become a driving force within it.

BCCA and TRIUMF have partnered to implement the production and use of radiotracer [¹⁸F]-EF5 (a nitroimidazole-containing compound) that is preferentially taken up by hypoxic tissues. EF5-PET thus allows clinicians to measure oxygenation, which can be compared to blood perfusion using complementary CT scanning (i.e. PET/CT), providing a quantitative, non-invasive means to quantify tumour blood flow and oxygenation before, during, and after chemotherapy (with and without the chemotherapeutic agent, bevacizumab) in patients with advanced NSCLC.

Patients with incurable stage III/IV NSCLC, who are to receive first-line platinum-based doublet chemotherapy alone or in combination with bevacizumab (as part of other clinical trials), were recruited for a study. All patients had quantifiable hypoxia in their primary tumours at baseline and notable changes in oxygenation and tumour perfusion. There was also some data to suggest that there had been a near doubling of blood flow to the central tumour mass over the course of treatment, with corresponding decreases in hypoxia. These scans demonstrated that antiangiogenic strategies, and chemotherapy alone, may significantly impact tumour oxygenation and blood flow. In the limited studies done so far there have been clear changes in tumour blood flow and hypoxia. Many more scans are underway. This study represents the first non-invasive documentation of lung cancer oxygenation and changes with therapy, suggesting that hypoxia may be an important predictive and prognostic factor for NSCLC.

Novel Small Molecular Tracers for Oxidative Stress Imaging

Until recently, the tracers produced are often literature-established, small-molecule pre-clinical and/or clinical imaging agents with a heavy focus on safety and good manufacturing practices. Further expansion in this area is planned for the next five years.

Cellular reactive oxygen species (ROS) can be generated from a variety of sources, both endogenous and exogenous, and play an important role in a number of cell signaling pathways. When ROS regulatory mechanisms become overwhelmed, the cellular antioxidant capacity is exceeded and oxidative stress can result. Tumour cells generate high amounts of ROS and respond by upregulating various detoxifying antioxidant systems. Glutathione is the predominant endogenous cellular antioxidant, and plays a critical role in the cellular defensive response to oxidative stress by neutralizing free radicals and reactive oxygen and nitrogen species. With cystine as the rate-limiting substrate in glutathione biosynthesis, the cystine/glutamate transporter (system x_c⁻) represents a potentially attractive biomarker for PET to enable *in vivo* quantification and functional assessment of x_c⁻ activity in response to oxidative stress associated with disease.

System x_c^- was first described by Banna and Kitamura in 1980 as a sodium-independent amino acid transport system with a very narrow natural substrate binding profile, especially when compared to other known amino acid transporters. x_c^- is a heteromeric protein composed of two subunits connected through a disulfide bridge; with 4F2hc as a heavy unit involved in trafficking the heterodimer to the plasma membrane, and a lighter subunit, xCT, conferring transport and substrate specificity. The level of x_c^- transporter activity/expression in normal cells is very low but is significantly upregulated in cells under oxidative stress. Upregulation of the transporter has been observed in tissues under oxidative stress and is implicated in a wide range of conditions including cancer, diabetes, cardiovascular and neurodegenerative diseases.

The ability to image x_c^- by PET means that it could be used to quantify oxidative stress as it is related to a particular disease state [1]. In collaboration with Dr. Jack Webster (GE Global Research), our team has established proof of feasibility for the use of ^{18}F -labelled aminosuberic acid (FASu) as an x_c^- binder. Preliminary data, using diethylmaleate (DEM)-treated EL4 lymphoma cell uptake studies and *in vivo* biodistribution and tissue uptake in mouse EL4 xenografts, demonstrate FASu as a potential novel agent for the *in vivo* assessment of the cystine transporter. FASu demonstrates 5-fold enhanced uptake *in vitro* under oxidative stress, with effective blocking using sulfasalazine, a known x_c^- inhibitor. FASu also shows *in vivo* uptake ratios exceeding 10:1 and 20:1 for tumour:blood and tumour:muscle, respectively, within two hours post injection. *In vivo* uptake was reduced when co-injected with unlabeled ASu, a structural analogue, suggesting specific uptake and competition between FASu and ASu.

With ^{18}F FASu, a tracer that binds x_c^- , we will enable real time, *in situ* information on oxidative stress activity at the site of disease with no perturbation of the biological system and without a need to rely on indirect *ex vivo* measurement of circulating systemic byproducts obtained through blood or urine analysis. This result represents an exciting opportunity for the TRIUMF molecular imaging community as a novel tracer with potential broad applicability across a number of diseases. The utility of ^{18}F FASu will be the subject of future studies between the division and its partners.

Mn-52 for Manganese-Enhanced MRI

PET and MRI are complementary techniques from an imaging perspective. PET is one of the most sensitive imaging methods in clinical use, capable of detecting trace (femtomolar/nanomolar) concentrations of injected tracers. An intrinsic trade-off in sensitivity involves image resolution, with modern PET scanners typically able to provide images with resolution in the millimeter range, making detailed anatomical studies difficult. To accommodate for this, the nuclear medicine community has been rapidly adopting multimodal imaging, in which one method, such as PET, is combined with another, such as CT or MR to afford co-registered images that map PET images on to those with greater anatomical detail.

MR allows anatomic imaging with exquisite resolution (sub-millimetre). In addition, the quantification reliability of MRI can be a challenge because the source of image contrast is complicated and depends greatly on details of image acquisition as well as the object being studied. MRI is also prone to spatial distortions from non-ideal magnetic field gradients as well as to localized susceptibility artifacts in image. Conversely, PET can provide quantitative and undistorted measurement of the spatial and temporal tracer distribution *in vivo* with a single image acquisition. PET is employed as a gold standard against which other potentially quantitative techniques, including MRI, are judged. In PET, concentrations of tracer are generally more easily related to biological function than are relaxivity parameters from an MRI experiment.

Mn-52 is a promising, yet poorly investigated, radionuclide for PET imaging. Mn-52 was selected primarily because of its low positron range and energy (0.63 mm, 244.6 keV), which is comparable to F-18 (0.62 mm, 250 keV) potentially preserving the spatial resolution of the proposed PET images. ^{52}Mn]MnCl₂ PET is particularly interesting because of the relatively novel MRI technique of manganese-enhanced MRI (MEMRI). In MEMRI, paramagnetic Mn²⁺ is used as a contrast agent *in vivo* that reduces T1 relaxation times and accumulates in areas of neuronal activity by uptake through voltage-gated calcium channels. MEMRI has been primarily used for imaging the brain of rats or mice and has also been employed for

neural tract tracing in mice. The radionuclide Mn-52 is expected to accumulate *in vivo* by the same biological mechanisms as nonradioactive Mn in MEMRI, providing the opportunity to study similar systems and processes as MEMRI with PET, to independently investigate the effects of Mn administrations needed for MEMRI studies on live animals, and to use the quantitative aspect of PET to validate MEMRI results. Mn-52 has previously been used to study Mn absorption in humans, but its use for PET-MR imaging has not been explored.

For Mn-52 PET to be a useful tool, it is necessary to establish that Mn-52 produces images of similar quality to established radiotracers and to demonstrate biological applications for which it is well suited. In collaboration with Dr. Sossi (UBC), Mn-52 was produced on TRIUMF's TR13 cyclotron via $^{nat}\text{Cr}(p,x)^{52}\text{Mn}$. PET images have been acquired with phantoms and rats, and similar images with F-18 have been acquired for comparison [2]. *In vivo* brain imaging after systemic injection in this work showed accumulation of Mn in the pituitary and ventricles, but did not observe Mn elsewhere in the brain in amounts distinguishable from background. This is inconsistent with published MRI signal enhancement, indicating that additional work is required to understand the biodistribution differences between tracer-level containing <240 ng of Mn to bulk level (non-radioactive) containing as much as 40 mg/kg of the metal. Despite this, Mn-52 has been established as a novel and potentially useful tracer for small animal PET imaging because of its manageable positron branching ratio and energy. With a longer half-life, Mn-52 remains detectable weeks after initial injection, allowing weeks-long study after a single injection.

Large Molecular-Weight Radiopharmaceuticals

There is an urgent need for companion diagnostics to provide detail on a person's predictive and prognostic markers so that physicians can diagnose disease while in a treatable state, select an optimal therapeutic course, and avoid ineffective drug treatment. Prognostic indicators of the long-term progression of a disease could also serve to enhance medical care for patients across a wide variety of indications. A growing number of experimental PET probes are being developed from peptide, protein, oligonucleotide and/or other large molecular weight platforms. Novel medical imaging (MI) probes are of paramount importance for elucidating the molecular origin of illness.

Having built a substantial program in the production and use of small molecule radiopharmaceuticals for *in vivo* analysis of the functional affects of disease, TRIUMF has been increasing research activity in the synthesis and radiolabelling of large molecular weight tracers with a goal of enabling *in vivo* analysis of changes in disease expression. With both small and large molecule labelling capabilities, TRIUMF maintains expertise and access to broadly enabling platforms for addressing a wide array of conditions.

Oligonucleotide (ODN) and Peptide Nucleic Acid (PNA) Labelling

There are approximately 200 different types of cancer, with some analyses suggesting that greater than five genes mutate in each tumour. With genetic heterogeneity across any given patient population, symptomatic diagnosis of cancer and/or classification of tumours are increasingly becoming insufficient means of dictating treatment and/or determining patient outcomes. Genetic profiling techniques have enabled the identification of specific genes that are over-expressed in various cancer types and, with that, the identity of unique gene clusters acting together in a specific subset of transformed cells driving disease forward. This knowledge offers a potentially powerful indicator of tumour function at the genetic level. Since individual gene alterations likely occur at too low a level to detect with existing imaging methods, mRNA over-expression resulting from gene modification could potentially serve as one of the earliest diagnostic indicators for the development of cancer in humans.

Genome BC has funded an effort through TRIUMF to advance the field of antisense PET. The effort involves conjugating peptide nucleic acids (PNAs) to cell penetrating peptides for enhanced access to the cellular interior. Specifically, the TRIUMF group will work progressively toward the proposed chimeras, first building complementary PNA constructs to known target sequences of two genes (GFP and HER2).

These sequences will be modified with a terminal azide to allow for “click” modification with a fluorescent dye or radiolabelling precursor followed by *in vitro* analysis. Once the selected PNA sequences have been validated, full construct synthesis will then be afforded by producing the CPP portion of the chimera on solid support. The conjugates will then be labelled using the radiolabelling methods discussed above. Once the *in vitro* work has been completed, the goal is to analyze the chimeras *in vivo*.

Aqueous Fluorination

Collaboration with Dr. Perrin (UBC) has seen the successful implementation of arylboronic acid bioconjugates as shelf-stable, stockable, precursors for one-step aqueous F-18 labelling of biomolecules. The feasibility of this approach was disclosed several years ago by examining the *in vivo* fate of F-18-labelled biotin-ArBF₃ and more recently with F-18-labelled marimastat-ArBF₃, a potent inhibitor of matrix metalloproteinases, which provided some of the first *in vivo* PET images of tumour-associated protease activity [3]. The synthetic advantages of this method, which include a one-step aqueous fluorination to provide radiochemically pure, labelled ligands, was detailed in a recent publication [4], conserving time and therefore the amount of F-18, radiochemical purity and higher specific activity. The team has recently overcome several issues in improving radiochemical yields, streamlining the experimental setup to work better with very small volumes and with low pH. Fluorinations can now be accomplished in ~25 minutes, with higher yields at lower fluoride concentration, therefore improving the specific activity. In a second effort, TRIUMF’s chemists have successfully extended this labelling technique to “click” chemistry, a labelling procedure via two steps in only one pot, resulting in a very quick and reliable generation of radiopharmaceuticals with high yield.

This project continues to receive accolades from the broader community with numerous conference presentations, invited lectures and publications in high-impact journals [5].

References:

- [1] M. Lo et al., J. Cell. Physiol. 215, 593 (2008).
- [2] G.J. Topping et al., Med. Phys. 40, 042502 (2013)
- [3] U.A.D. Keller et al., Cancer Res. 70, 7562 (2010).
- [4] Y. Li et al., Med. Chem. Comm. 2, 942 (2011).
- [5] Z. Liu et al., Angew. Chem. Int. Ed. 52, 1 (2013).

4.2.3.6 PROTON THERAPY

For large ocular melanomas or melanomas close to the optic nerve, the accepted best treatment choice is proton therapy. By the end of 2011, 20,761 patients, from all over the world, have been treated with proton therapy for ocular melanomas with 9 proton therapy centres using a dedicated beam line currently in operation. Here at TRIUMF, low energy protons (please see Section 5.6.3) from the main TRIUMF cyclotron have been used since 1995 to treat ocular melanomas [1]. By the end of 2012, the number of treated patients totals 170. The five-year local tumour control rate is 91%. The metastasis-free survival rate is an excellent 82% and the affected eye is saved in 80% of the cases. But there is always room for improvement, which translates into saving the lives of more patients.

Research during the past five years has focused on improving analysis and control of dose during the irradiation treatments. Simulations of the proton-therapy system have been improved and a novel approach to use PET scans immediately after treatment have been employed to analyze delivered dose profiles.

FLUKA Model of the Facility

In 2011, the computer program FLUKA [2], a particle physics Monte Carlo simulation package for simulating the interaction of particles with matter, was used to model the proton-therapy beam line. Figure 1 shows how the proton beam (in green) passes through the different elements in the beam line and the subsequent creation of secondary particles (in red and black). The simulation was verified against several sets of experiments. This computer model can now be used as a means to quickly and economically study changes to the beam line while avoiding significant disruptions in beam line operations. Modifications intended to improve beam characteristics can be tested experimentally with the goal of reducing patient dose from secondary particle emissions and as a direct consequence the occurrence of secondary cancer to the treated patient.

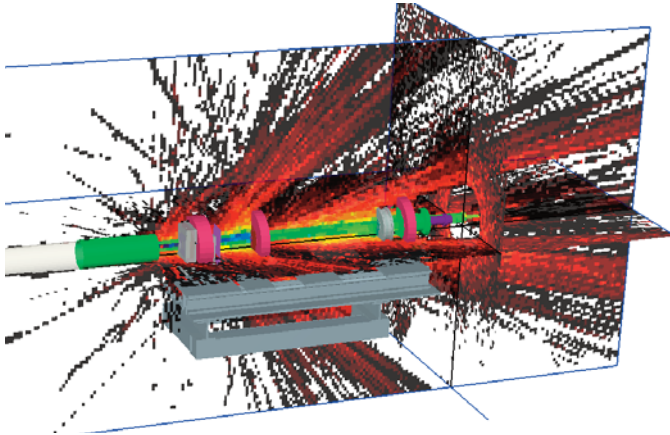


Figure 1: Simulation of the proton therapy beam line in 3D showing the incoming proton beam (green) and secondary particles (red to black).

PET after PT

The treatment plan for an ocular melanoma consists of four fractions administered on subsequent days. The dose planning involves measurement and marking of the tumour with tantalum clips and a sophisticated planning software to optimize the gazing angle, incoming beam energy and spread and the final patient collimator. Before each fraction, the patient is carefully aligned with the beam, an important step because proton therapy is a very precise form of radiotherapy with steep dose gradients at the target boundaries. Unfortunately, right now, there is no way to measure if the proton dose has been deposited exactly as planned. Currently, we are investigating the usefulness of position emission tomography (PET) after proton treatment (PT) as a way to visualize the proton dose deposited, since during proton irradiation, the PET isotopes O-15, N-13 and C-11 are produced. Several phantoms and one patient underwent a PET scan after proton irradiation [3] (see Figure 2). The production cross-section of the PET isotopes, produced during proton irradiation, will be included in the FLUKA simulation in the near future. The imaged activation profile will then be compared to the simulation and conclusions about the dose deposited by the protons will be drawn. The same technique will be applied to the patient data. If the resolution is sufficient, a

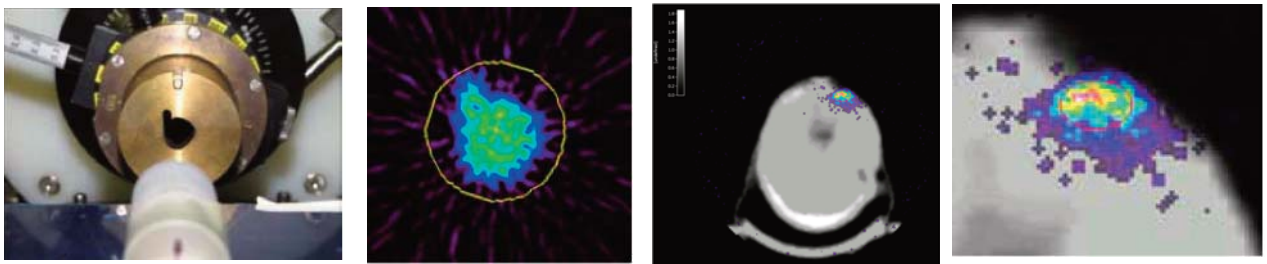


Figure 2: (a) The irregular collimator used for irradiation of a lucite rod phantom. (b) PET image of lucite phantom scan in the transverse plane. The outline of the phantom, determined from the transmission scan, is indicated by the yellow outline. (c and d) PET images of patient scan after proton treatment in the transverse plane. The activity in the tumor is clearly visible. The tumour size is indicated with the red outline. Scanning was performed at UBC PET Imaging Centre.

conclusion about the success of the patient alignment can be drawn. In the future, any misalignment could be compensated for in a subsequent fraction, avoiding missed dose to the tumour, and thereby reduced probability of local tumour control and excess dose to an adjacent structure with unnecessary collateral damage. This could ultimately lead to better patient care.

Selected References

- [1] E. Tran et al., *Int. J. Radiation Oncol. Biol. Phys.* 83, 1425 (2012).
 [2] www.FLUKA.org; G. Battistoni, et al., *AIP Conference Proceeding* 896, 31 (2007); A. Ferrari et al., *CERN-2005-10* (2005), *INFN/TC_05/11*, *SLAC-R-773*
 [3] C. Hoehr et al., *MIC 2012 Conference Record*, M22-3 (2012).

4.2.4 MOLECULAR AND MATERIALS SCIENCE

As Canada's accelerator laboratory, TRIUMF has been at the forefront of using particle beams as probes of chemistry as well as the structure and behaviour of materials. Beams of muons were first developed at TRIUMF to study subatomic physics by generating other secondary beams of more exotic particles. Muons are now generated and employed regularly to probe the origin and behaviour of magnetism in condensed-matter and gaseous systems. Several decades ago, Professor Jess Brewer (UBC), Don Fleming (UBC), Toshimitsu Yamazaki (Japan), and Ken Crowe (UC Berkeley) pioneered this line of investigation at TRIUMF.

TRIUMF has also developed a sensitive magnetic nanoprobe of materials that employs exotic isotopes of lithium. The isotope beams are generated within the ISAC facility and then deposited into thin structures to analyze the behaviour of magnetism at the interfaces between different types of materials. Called β -NMR, the technique is complementary to muon probes because it provides access to depth-dependent properties for materials that are too thin to stop a conventional muon beam or to carry out conventional NMR.

Beginning in 1995 TRIUMF has built up several beam lines that provide low-intensity, energetic proton and neutron beams to simulate natural-radiation exposures either in space or terrestrial environments; these facilities are called PIF & NIF.

4.2.4.1. BACKGROUND

Muons are elementary particles with a mass one ninth that of the proton (or 206 times the electron mass), a spin of $1/2$, and a magnetic moment 3.183 times larger than that of a proton. They are produced in the weak-interaction decay of pions (which are in turn produced from proton bombardment of a target material, typically beryllium or graphite, at 500 MeV), with a lifetime of 26 ns. These decay processes violate parity and result in an ensemble of muons being produced 100% spin polarized along (μ^-) or opposite (μ^+) to its momentum direction.

Though positive and negative muons have the same mass (105.7 MeV), their interactions in matter are quite different. The μ^+ has a lifetime of 2.197 μ s, regardless of the medium it is implanted in, and can be thought of as a light proton. In contrast, the μ^- is regarded as a heavy electron and, due to nuclear capture, its lifetime is strongly dependent on the atomic number of the material in which it is implanted, being as short as 80 ns in lead. The polarization of an ensemble of μ^+ or μ^- can be monitored by measuring the asymmetry in the muon's radioactive decay.

The decay of the positive (negative) muon violates parity and as a result the positron (electron) is emitted preferentially along the axis of the muon's spin. This anisotropy or "asymmetry" in the decay of an ensemble of polarized muons provides a convenient means of determining the direction of the muon's spin and is the key feature that makes the μ SR technique possible.



TRIUMF TO PLAY ROLE IN U.S.-FUNDED RESEARCH NETWORK

03 August 2010

The U.S. National Science Foundation (NSF) recently announced a \$2 million award for an international consortium aimed at probing novel superconductors with neutrons, muons, and photons through its Partnership in International Science and Engineering (PIRE) initiative. TRIUMF will play a unique and critical role in the network through its muon-spin resonance program at the Centre for Molecular and Materials Science (CMMS). The principal investigator is Dr. Yasutomo Uemura, a professor of physics at Columbia University, a core contributor to the CMMS, and a regular visitor to TRIUMF. The project began August 1, 2010, with funding for three years.

The NSF's PIRE program is designed to, "Support bold, forward-looking research whose successful outcome results from all partners—U.S. and foreign—providing unique contributions to the research endeavor." In this case, the consortium will focus on exploring novel superconductors using the combined power of muon, neutron, and photon probes along with scanning-tunneling microscopy.

The high intrinsic polarization of an ensemble of particularly positive muons, in marked contrast to its parent technique, nuclear magnetic resonance (NMR), is independent of temperature or magnetic field, which is highly important as it endows μ SR with a remarkable level of sensitivity in probing local magnetic environments that NMR simply cannot match. There is no need to first create spin coherence using a high-frequency preparation pulse, so the time resolution is significantly increased over that of conventional magnetic-resonance techniques. Thus, in a proton NMR experiment at 300 K and 9.4 T, the ensemble polarization is only $\sim 3 \times 10^{-3}\%$, which pales in comparison with the $\sim 100\%$ in μ SR. The result of this is that a clear signal can be obtained in μ SR from an ensemble of only about 10^8 stopping muons (measured, effectively, one at a time), whereas in NMR typically about 10^{19} polarized nuclei are required (produced from external RF pulse sequences), a succinct statement of the remarkably sensitive nature of the μ SR technique. A unique aspect of μ SR spectroscopy is that it can be performed routinely at very low (mK) temperatures and even in zero magnetic field, which is not possible in NMR (unless dealing with quadrupolar nuclei).

Muons can be implanted into solid, liquid, or gaseous samples. Implanted μ^+ initially have very high ("MeV") energy but are slowed down to near thermal energies on the nanosecond timescale. The final chemical environment of the muon depends on the chemical properties of the material in which it has been implanted. A fraction of the implanted μ^+ will end up in diamagnetic environments, as "bare" muons, solvated muons, or substituted for the proton of a diamagnetic molecule. The short lifetime of the muon limits the spectral resolution to ~ 70 kHz so it is not possible to resolve chemical shifts and distinguish between muons in different diamagnetic environments. Another fraction of μ^+ can pick up an electron during the slowing down process and form muonium ($\text{Mu} = [\mu^+, e^-]$), a one-electron atom with the positive muon as the nucleus. The fraction of muons observed as Mu depends strongly on the material and its physical state, ranging from 0 in most metals to 1.0 in gaseous Kr. Due to the μ^+ mass being 200 times that of the electron, the chemical properties of Mu are virtually identical to those of any hydrogen isotope, even though there are no protons or neutrons in the nucleus. Muonium chemistry extends the normal isotopic H atom mass scale to its lowest value, 0.113 amu. Muons can also be incorporated in free radicals, which are molecules with an unpaired electron. These are formed by the reaction of Mu with unsaturated molecules.

The μ SR techniques involve injecting a beam of spin-polarized positive muons into a sample and detecting the positron produced by the decay of each muon. The four techniques frequently used at the CMMS are: (1) transverse-field muon spin rotation (TF- μ SR), (2) zero-field muon spin relaxation (ZF- μ SR), (3) longitudinal-field muon spin relaxation (LF- μ SR), and (4) muon level-crossing resonance (μ LCR).

For TF- μ SR the basic experimental geometry is shown in Figure 1. The muon is injected into the sample with its spin perpendicular to the external magnetic field. Each incident muon passes through a muon counter, which starts a fast electronic clock that is subsequently stopped by the detection of the corresponding decay positron in a positron detector (in practice there can be arrays of several detectors). Events where more than one muon or positron is detected within the sample during a time window of several microseconds are discarded. The data are displayed as a histogram of the number of decay positrons detected in a given direction as a function of the lifetime of the corresponding muon and resembles the free induction decay that follows a $\pi/2$ pulse in nuclear magnetic resonance (NMR). The muon spin precesses about the transverse field, with a frequency that is proportional to the size of the magnetic field at the muon site in the material. The TF- μ SR configuration can be used to measure the magnetic field distribution of the vortex lattice in a type-II superconductor, the μ^+ Knight shift in metallic systems or the muon hyperfine coupling constant (hfcc) in a muoniated radical.

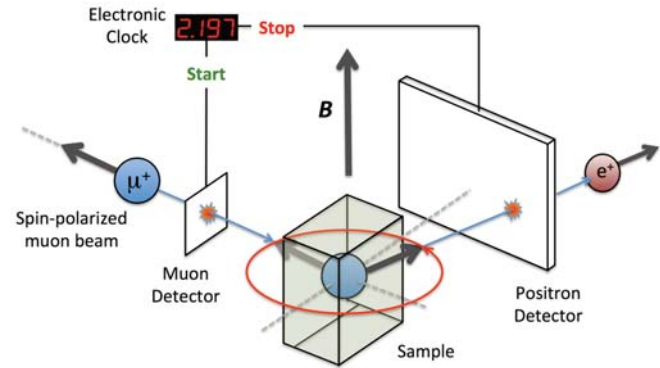


Figure 1: Schematic of the TF- μ SR experimental geometry.

The setup for the ZF- μ SR, LF- μ SR and μ LCR experiments is shown in Figure 2. The positron detectors are arranged in a way to measure the muon polarization along its original direction. The asymmetry parameter, $A(t)$, is defined as (5)

$$A(t) = \frac{N_B - N_F}{N_B + N_F}$$

where N_F is the total number of positrons detected in the forward counters and N_B is the total number of positrons detected in the backward counters, and is proportional to the muon polarization. In both the ZF- μ SR and LF- μ SR techniques the time dependence of the asymmetry is monitored. No field is applied in ZF- μ SR while an external magnetic field is applied parallel to the initial direction of the muon spin polarization in LF- μ SR. ZF- μ SR is a very sensitive method of detecting weak internal magnetism, that arises due to ordered magnetic moments, or random fields that are static or fluctuating with time. In μ LCR, it is the time-integrated asymmetry that is measured as the magnetic field is scanned in a series of small steps. Resonances occur where there is crossing of spin states due to hyperfine or quadrupolar interactions. It is frequently used to determine the nuclear hfccs of muoniated radicals.

There are only four μ SR facilities in the world, including CMMS, and of these only one other (Paul Scherrer Institute, PSI) provides continuous beams that are useful for studying materials with large magnetic fields and fast spin dynamics.

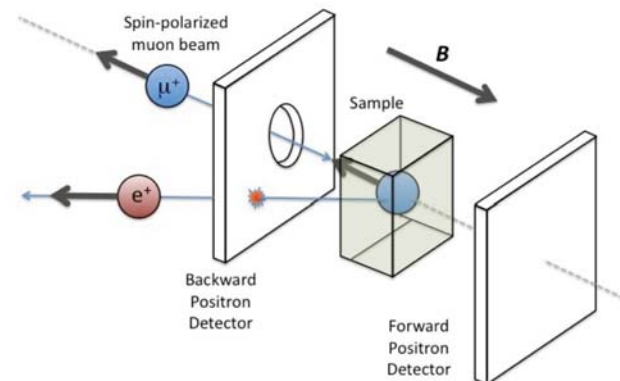


Figure 2: Schematic of the LF- μ SR or μ LCR experimental geometry. LF- μ SR is a time differential technique while μ LCR is a time-integral technique.

4.2.4.2. MAGNETISM

The application of μ SR to the study of magnetic systems continues to be of great interest. μ SR's utility stems from the sensitivity of the muon due to its large gyromagnetic ratio (more than 3 times that of a proton), and the fact that as a real space probe it complements reciprocal space probes such as magnetic neutron scattering. The volume sensitivity of μ SR makes it especially valuable for studying phenomena such as phase separation, while LF- μ SR is sensitive to a field fluctuation rate intermediate between inelastic neutron scattering and ac-susceptibility, making it especially well suited to studies of frustrated magnets.

Highly Frustrated Magnets

Frustrated magnetism is one of the most active fields in condensed matter physics as evidenced by the number of sessions devoted to it at the APS March Meeting and the rapid growth of participants in its major topical conference: Highly Frustrated Magnetism, held every two years, most recently in Hamilton, Ontario in 2012. The idea of frustration can be illustrated by considering three antiferromagnetically coupled spins on an equilateral triangle lattice. Satisfying the antiferromagnetic interactions between any two spins leaves the third spin unable to satisfy its interactions with the first two and as a result the system is unable to magnetically order at a temperature corresponding to the magnetic exchange interaction energy scale. The motivation for this interest is the now-realized expectation that frustrated magnetism provides a proving ground for discovering new states of matter; this concept of emergence is one of the most compelling paradigms in condensed matter research.

Pyrochlore are compounds of the general form $A_2B_2O_7$ that consist of two interpenetrating lattices of corner-sharing tetrahedra (for the A and B ions) that are a three-dimensional extension of the triangular lattice described above. The ability to place magnetic ions on either or both of the A and B sites provides considerable flexibility for exploring a wide variety of magnetic states. Miyazaki et al. studied a series of metallic ruthenium pyrochlores $Hg_2Ru_2O_7$, $Cd_2Ru_2O_7$ and $Ca_2Ru_2O_7$, finding a close relationship between the randomness of the frozen spin state with the degree of itinerance of the charge carriers [1]. Ofer et al. examined insulating $Y_2Mo_2O_7$, combining μ SR, magnetic resonance and neutron scattering to deduce the source of spin glass magnetism in this nominally well-ordered material finding evidence for local lattice distortions on setting around the spin freezing temperature driven by a strong magnetoelastic coupling [2].

$Dy_2Ti_2O_7$ has been widely studied as an example of so-called spin ice (see Figure 3). In this system, crystal field interactions force the magnetic Dy ions to point along the local $\langle 111 \rangle$ crystalline axes, either inwards or outwards from the centre of each tetrahedron as effective Ising moments. Ferromagnetic interactions between the Dy moments result in a ground state configuration for each tetrahedron consisting of two spins pointing in and two pointing out. The statistical mechanics of this arrangement are analogous to that of proton arrangement in water ice, where each oxygen has two covalently bonded and two hydrogen bonded protons. The elementary magnetic excitations consist of a single spin flip which results in two neighbouring tetrahedra having 3 spins in and three spins out respectively, creating an effective dipole with a pole in each of them. These spin flips can then move away from each other with zero energy

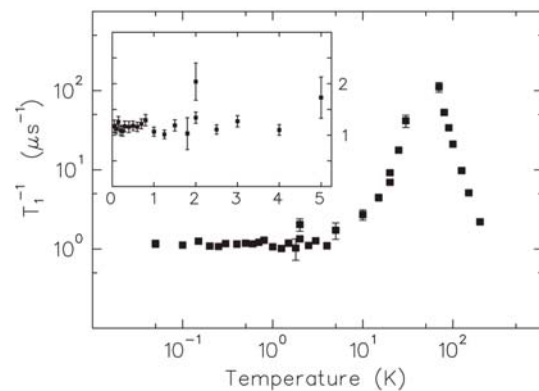


Figure 3: Muon spin relaxation rate in spin ice $Dy_2Ti_2O_7$. The low temperature behaviour of $1/T_1$ is shown in an expanded linear scale in the inset [3].

cost, giving deconfined monopoles. A μ SR study using pulsed muons claimed a direct detection of these deconfined monopoles, but Dunsiger et al. combined weak transverse field and longitudinal field μ SR measurements to demonstrate that the direct observation of monopoles by μ SR is impossible in principle, and that the measurements in the previously reported work reflected muons landing in the sample holder, rather than the $\text{Dy}_2\text{Ti}_2\text{O}_7$ sample under study [3]. Dunsiger et al. found that $\text{Dy}_2\text{Ti}_2\text{O}_7$ exhibited temperature independent spin fluctuations, which dominate any possible monopole signatures.

Fujihala et al. studied $\text{Fe}_2(\text{OH})_3\text{Cl}$ [4] and Hagihala et al. studied $\text{Co}_2(\text{OH})_3\text{Br}$ [5] where the magnetic ions lie on alternating triangular and kagome planes. These systems are strongly frustrated, although both compounds undergo magnetic ordering below 10K. In both systems strong fluctuations, detected by LF- μ SR, persist to very low temperatures; an example of persistent spin dynamics, a still to be understood hallmark of frustrated magnetic systems. Zig-zag magnetic chains exhibit strong frustration due to the competition between nearest and next-nearest neighbour interactions. Ofer et al. studied the evolution of incommensurate spin density wave order with charge doping in $\text{Na}_x\text{Ca}_{1-x}\text{V}_2\text{O}_4$ as the system varies from metallic (NaV_2O_4) to insulating (CaV_2O_4) [6] (see Figure 4). They found that a critical concentration, x_c , separated the insulating and metallic phases which possessed different magnetic ordering behaviour on the different sides of x_c . In a second study, Ofer et al. studied a series of zig-zag compounds EuL_2O_4 where L is the lanthanide Yb, Lu, Gd or Eu [7]. They found an evolution of the magnetic ground state from static antiferromagnetism to incommensurate spin-density-wave to a dynamic phase as the size of the lanthanide moment varies from 0 (Lu) to the largest value, giving maximum frustration.

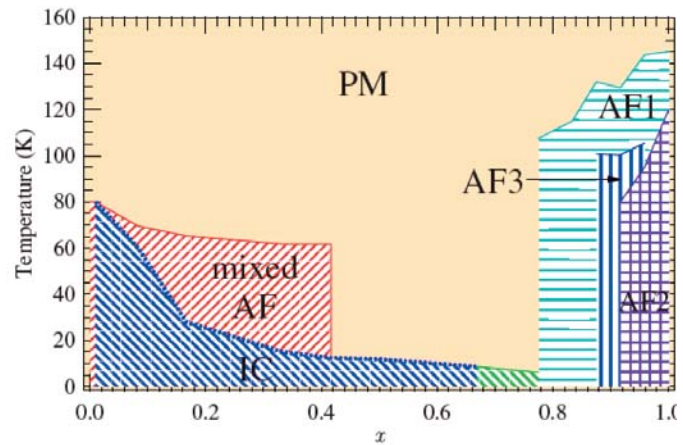


Figure 4: The phase diagram of $\text{Na}_x\text{Ca}_{1-x}\text{V}_2\text{O}_4$. PM: paramagnetic, AF: antiferromagnetic, and IC: incommensurate [2].

Low Dimensional Magnetic Systems

Low dimensional quantum magnets are of great interest due to the rich collection of behaviour they exhibit. Tsujimoto et al. reported the synthesis and magnetic properties of the two-dimensional quantum isostructural antiferromagnets $(\text{CuBr})\text{A}_2\text{B}_3\text{O}_{10}$ ($\text{A} = \text{Ca}, \text{Sr}, \text{Ba}, \text{Pb}$; $\text{B} = \text{Nb}, \text{Ta}$) which exhibit a $1/3$ plateau in their magnetization whose stability is largely controlled by the A ion size [8]. Using μ SR, they were able to identify two distinct phase transitions seen in specific heat as having magnetic and structural origins respectively. Uemura et al. studied the related $\text{Cu}(\text{Cl},\text{Br})\text{La}(\text{Nb},\text{Ta})_2\text{O}_7$ system and found that changing the Br concentration changed the ordering temperature without changing the size of the ordered moment and that the evolution of the system from a non-magnetic spin-gap state to one with magnetic order is associated with phase separation and/or a first order phase transition [9].

Magnetic Coordination Polymers

Coordination polymers are inorganic structures with metal cation centres connected by ligands forming an array. They are of great interest because of their potential for a variety of applications including molecular storage, optical materials and as sensors. Leznoff et al. have synthesized a variety of coordination polymers (see Figure 5) containing magnetic ions and have used ZF- μ SR to study the effects of varying the metal cation and geometrical frustration on their magnetic properties [10,11].

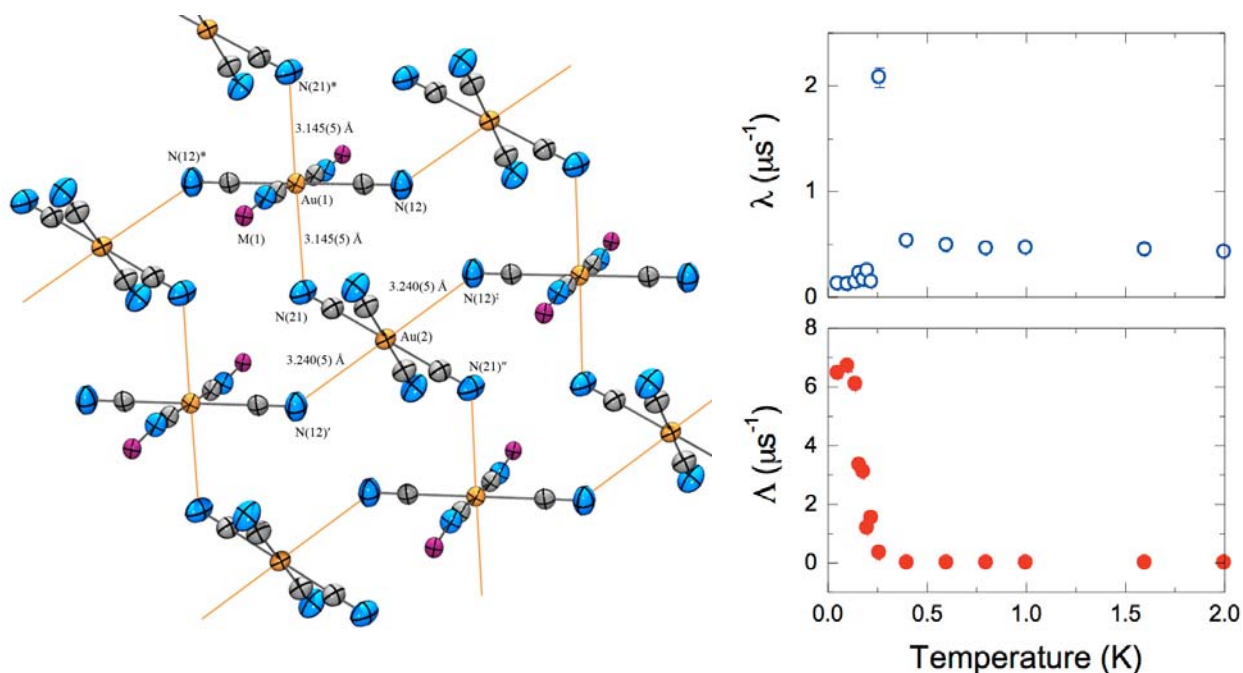


Figure 5: The $\text{Co}(\text{H}_2\text{O})_4[\text{Au}(\text{CN})_4]_2 \cdot 4\text{H}_2\text{O}$ coordination polymer consists of octahedrally coordinated metal centres with four equatorial water molecules and trans-axial $[\text{Au}(\text{CN})_4]^-$ nitriles, generating a 1D linear rod of $\text{M}(\text{H}_2\text{O})_4[\text{Au}(\text{CN})_4]$ -units. Only weak antiferromagnetic interactions along the rods are mediated by the $[\text{Au}(\text{CN})_4]$ -units. However, zero field μSR measurements indicate that there are also weak interchain interactions that yield a phase transition to a spin-frozen magnetic state below 0.26 K [11].

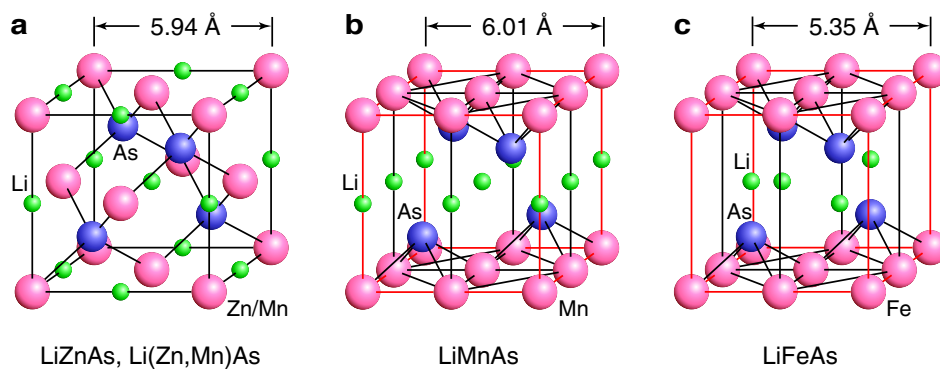


Figure 6: Crystal structures of cubic $\text{Li}(\text{Zn},\text{Mn})\text{As}$ (ferromagnet), tetragonal LiMnAs (antiferromagnet) and tetragonal LiFeAs (superconductor) [12].

Magnetic Semiconductors

Ferromagnetic systems created by doping transition metals into semiconductors have received considerable interest due to their potential use in spintronics devices. The limited solubility of divalent Mn atoms into trivalent Ga or In sites in $(\text{Ga},\text{Mn})\text{As}$ and $(\text{In},\text{Mn})\text{As}$ has resulted in these systems being chemically metastable and only available in thin film form. Deng et al. synthesized a new generation ferromagnet $\text{Li}(\text{Zn},\text{Mn})\text{As}$ based on the I-II-V semiconductor LiZnAs where the isovalent magnetic (Zn,Mn) substitution is decoupled from the carrier doping achieved with excess/deficient Li concentrations [12] (see Figure 6). Deng and collaborators used ZF- μSR and magnetization to detect and study the presence of ferromagnetism with critical temperatures as high as 50K. This ferromagnetic system contains square planar As layers, in common with antiferromagnetic LiMnAs and superconducting LiFeAs , which could lead to the development of new devices based on epitaxial junctions between these different compounds.

Materials for Battery Applications

The diffusion of Li^+ ions in solids is the underlying process in the operation of Li-ion batteries that are of enormous technological and economic interest. However, the diffusion coefficient of Li^+ ions (D_{Li}) has not been reliably determined for positive electrode materials because the most common technique for measuring D_{Li} , i.e. Li-7-NMR, is known to be unsuitable for materials that contain magnetic ions, due to the magnetic contribution to spin-lattice relaxation processes. Muons do not feel fluctuating magnetic moments at high temperature, but instead sense the change in nuclear dipole field due to Li diffusion. Even if magnetic moments still affect the muon-spin depolarization rate, such an effect can be distinguished by the application of a weak longitudinal field that decouples the magnetic and nuclear dipole interactions.

Sugiyama et al. have performed a series of studies of the magnetic and diffusive properties of a number of battery materials, starting with Li_xCoO_2 [13]. LiFePO_4 has many advantages as a practical battery material including high capacity and high stability during lithium extraction. Using ZF- μSR , they found antiferromagnetic order below $T_N = 52$ K in LiFePO_4 and by examining the temperature dependence of the field fluctuation rate they were able to determine $D_{\text{Li}} = 3.6 \times 10^{-10}$ cm^2/s at 300 K [14] (see Figure 7). Sugiyama et al. extended this study to other members of the LiMPO_4 family with $M = \text{Mn}$, Co and Ni , obtaining Li^+ diffusion rates for the $M = \text{Co}$, Ni versions [15].

Selected References

- [1] M. Miyazaki et al., Phys. Rev. B, 82, 094413 (2010).
- [2] O. Ofer et al., Phys. Rev. B, 82, 092403 (2010).
- [3] S.R. Dunsiger et al. Phys. Rev. Lett., 107, 207207 (2011).
- [4] M. Fujihala et al. Phys. Rev. B 82, 024425 (2010).
- [5] M. Hagihala et al., Phys. Rev. B, 82, 214424 (2010).
- [6] O. Ofer et al., Phys. Rev. B 82, 094410 (2010).
- [7] O. Ofer et al., Phys. Rev. B 84, 054428 (2011).
- [8] Y. Tsujimoto et al. Phys. Rev. B 78, 214410 (2008).
- [9] Y.J. Uemura et al., Phys. Rev. B 80, 174408 (2009).
- [10] J. Lefebvre et al., Inorg. Chem. 48, 55 (2009).
- [11] A.R. Geisheimer et al., Dalton Trans. 40, 7505 (2011).
- [12] Z. Deng et al., Nature Commun. 2, 422 (2011).
- [13] J. Sugiyama et al., Phys. Rev. Lett. 103, 147601 (2009).
- [14] J. Sugiyama et al., Phys. Rev. B 84, 054430 (2011).
- [15] J. Sugiyama et al., Phys. Rev. B 85, 054111 (2012).

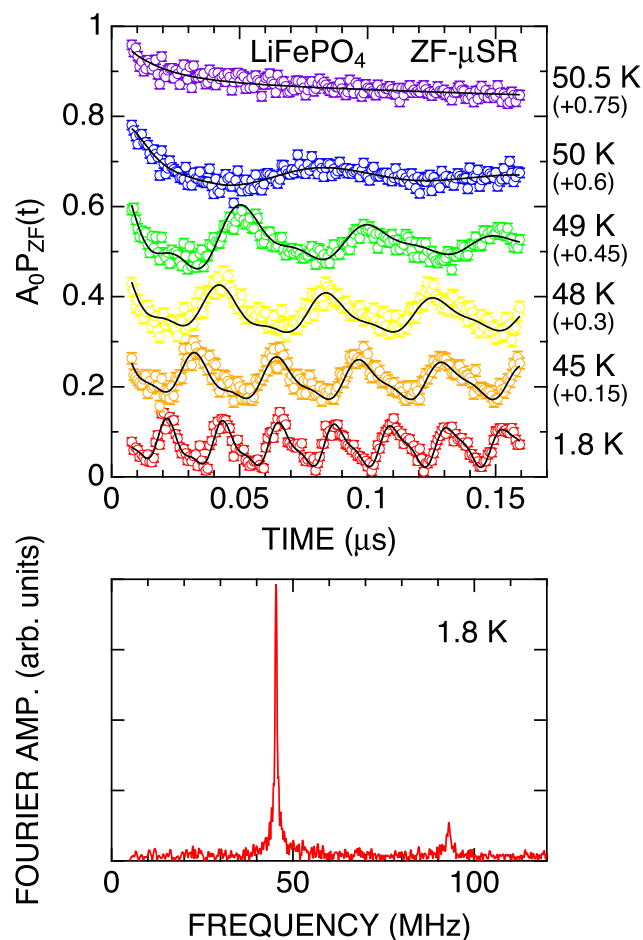


Figure 7: Temperature dependence of ZF- μSR spectra, showing precession in the spontaneous internal magnetic field and (bottom) Fourier transform of the time spectra measured at 1.8K [14].

4.2.4.3 SUPERCONDUCTIVITY

Superconductivity is at the forefront of modern condensed-matter physics and materials science. A steady stream of newly discovered superconductors over the past 25 years has fuelled continual interest in this fundamental, yet partially understood phenomenon. Over the past five years alone, the first evidence for the existence of topological superconductivity has emerged, and high-temperature superconductivity has been discovered in a variety of iron-based compounds. High-temperature superconductors have garnered considerable attention, as they offer a myriad of potential applications. Yet the microscopic mechanism(s) responsible for zero electrical resistance and perfect diamagnetism in these materials remains elusive. There are also numerous exotic low-temperature superconductors that defy understanding.

Condensed matter physics theorists have put forth various proposals for both mechanisms of superconductivity and competing phases, which are based on approximate calculations. Most often these calculations are guided by input from experiments that also serve the purpose of validating the theories. The μ SR technique has provided some unique insight into the role of magnetism in numerous novel superconductors, and has been widely used to investigate the local response of superconductors to an applied magnetic field.

Search for Loop-Current Order

A distinctive feature of high-temperature cuprate superconductors is the so-called “pseudogap” phase (see Figure 8), which exists at temperatures above the superconducting transition temperature (T_c) and over a wide range of doping (p). Prominent theories attribute the pseudogap phase to a “hidden order”, and in particular a time-reversal symmetry breaking phase characterized by ordered circulating orbital currents, which either breaks or preserves translational symmetry. The theoretical predictions have been bolstered by the finding, in polarized neutron diffraction studies, of unusual translational-symmetry breaking and preserving weak magnetic orders in the pseudogap region. While the observed magnetic orders bear some resemblance to the theoretical models, unlike μ SR, the neutron diffraction method does not provide information on the magnetic volume fraction.

In recent years, sensitive ZF- μ SR experiments have been carried out at TRIUMF to investigate the possible occurrence of weak orbital-like magnetic order in the mysterious pseudogap region. Two independent μ SR studies of $\text{La}_{2-x}\text{Sr}_x\text{CuO}_4$ show no evidence for magnetic order of any kind [1,2]. On the other hand, μ SR measurements on high-quality $\text{YBa}_2\text{Cu}_3\text{O}_y$ single crystals indicate the presence of magnetism compatible with the translational-symmetry breaking magnetic order detected by neutron diffraction [3]. However, the μ SR study shows that this magnetic order does not evolve with doping and, consequently, is unrelated to the pseudogap. Measurements on one of the samples studied by polarized neutron diffraction revealed a second kind of magnetic order, with characteristics in quantitative agreement with the translational-symmetry preserving magnetic order detected by neutrons (see Figure 9). However, the ZF- μ SR measurements clearly show that this form

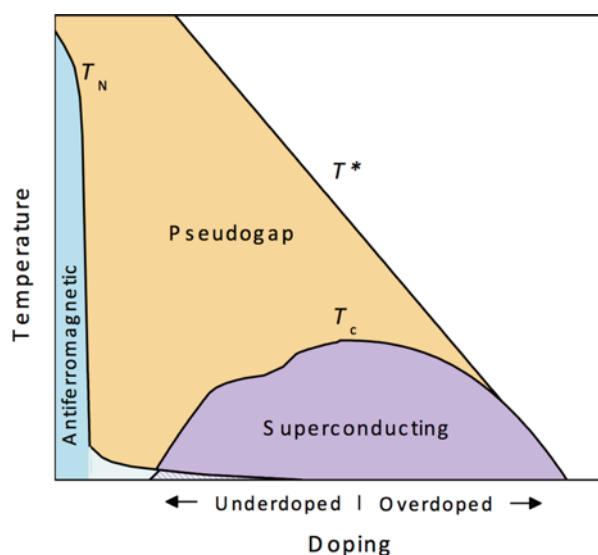


Figure 8: Generic phase diagram of cuprates. The undoped material is an antiferromagnetic insulator. The doping of holes in the CuO_2 layers destroys the antiferromagnetic phase, ultimately giving rise to a high-temperature superconducting state. Further doping eventually destroys superconductivity. Above the superconducting transition temperature (T_c) there is a highly anomalous “normal” state containing a so-called “pseudogap” phase. The pseudogap is believed to be either a precursor to superconductivity or a manifestation of a competing order. The relaxation rate Δ of the μ SR signal at zero field [34].

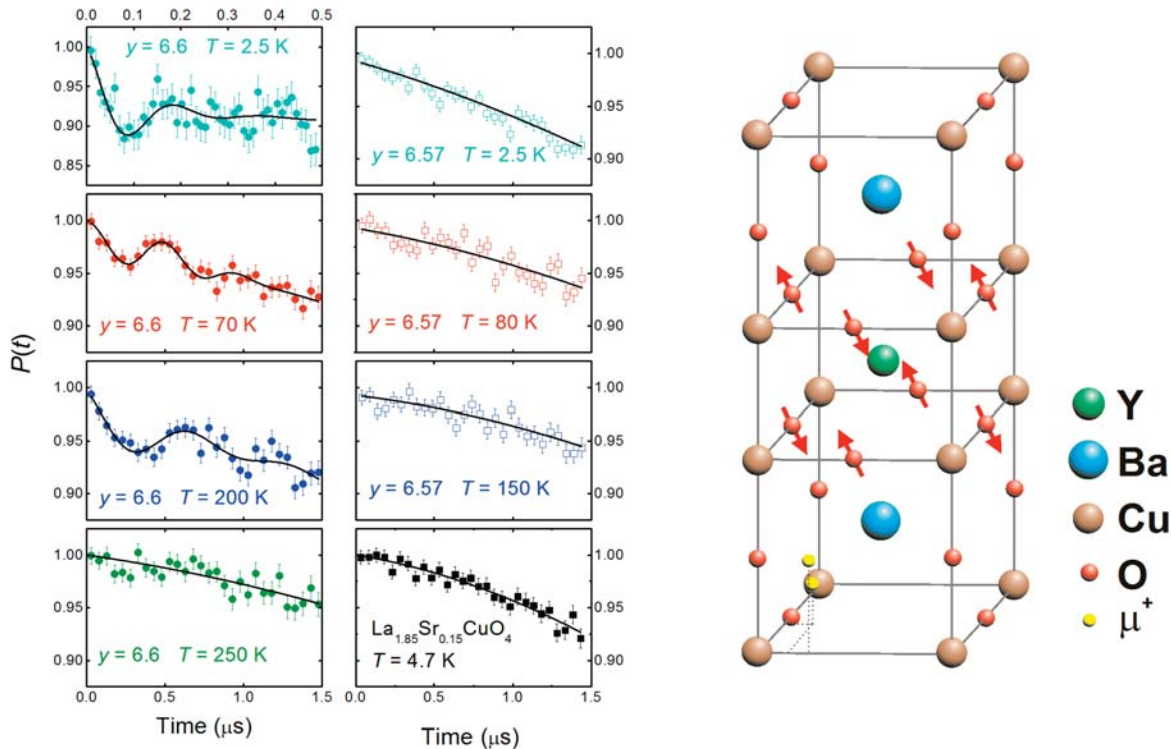


Figure 9: Search for loop-current order in the pseudogap phase of $\text{YBa}_2\text{Cu}_3\text{O}_y$ by ZF- μSR . A coherent oscillation indicative of magnetic order is observed only in a $\text{YBa}_2\text{Cu}_3\text{O}_{6.6}$ single crystal, which was previously identified as containing an unusual magnetic order by polarized neutrons scattering. However, as a local probe, the ZF- μSR measurements reveal that the magnetic order is present in only 3% of the sample, and can be explained by an impurity phase with local magnetic moments on the oxygen atoms in the CuO_2 layers [18].

of magnetic order exists in only about 3% of the sample, and hence is likely associated with an impurity phase. At present the evidence of absence of loop-current order from the μSR experiments is supported by nuclear magnetic resonance studies, but the issue is far from settled.

Magnetism Related to Superconductivity

Many exotic superconductors including high- T_c cuprates, iron pnictides, organics and heavy fermion systems have competing adjacent magnetic states, which has promoted pictures where the superconducting pairing is mediated by spin fluctuations. Carlo et al. combined μSR with magnetic susceptibility measurements to create a new magnetic phase diagram of $\text{Ca}_{2-x}\text{Sr}_x\text{RuO}_4$, which is a p-wave superconductor for the $x=2$ end-member [4]. They demonstrated that superconductivity in Sr_2RuO_4 occurs in close proximity to competing static magnetic order, providing strong evidence for the importance of spin fluctuations for superconductivity in this system.

Iron-Based Superconductors

Over the past five years, μSR has been widely applied to the study of recently discovered iron-based materials, which potentially offer a new path to room-temperature superconductivity. Superconductivity in these compounds is achieved by chemical doping of a magnetically ordered parent compound (similar to cuprates), and there is now strong evidence that Cooper pairing in the superconducting state is mediated by spin fluctuations. To date, the primary issues have been the symmetry of the superconducting order parameter, and the role magnetism plays in the pairing mechanism.

Shortly after the discovery of high-temperature superconductivity in iron-arsenic based compounds, and in parallel with μ SR studies elsewhere, experiments at TRIUMF demonstrated the coexistence of macroscopically separated superconducting and magnetic phases for a certain range of chemical doping [5-9]. The temperature and magnetic-field dependences of the superconducting carrier density were also investigated via measurements of the transverse-field μ SR line width [10-13] (see Figure 10). These studies contributed to the early understanding of the temperature-versus-doping phase diagram of iron-arsenic compounds, and placed limits on the possible symmetry of the superconducting order parameter.

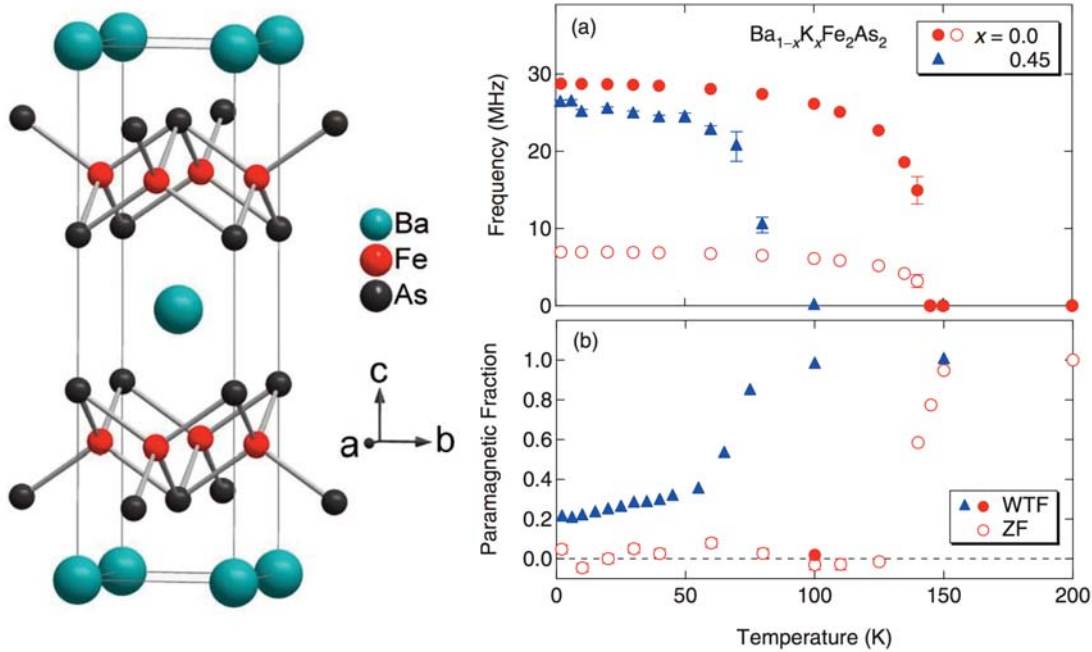


Figure 10: Magnetism and superconductivity in an iron based high-temperature superconductor [58]. An early μ SR study of the hole-doped iron arsenide $Ba_{1-x}K_xFe_2As_2$ shows the coexistence of phase-separated static magnetic order and nonmagnetic/superconducting regions. The latter is indicated here by the finite paramagnetic fraction [21].

Inhomogeneous Magnetic-Field Response of the Normal State

In recent years the unique high-magnetic-field μ SR capabilities of TRIUMF have been used to investigate the normal state of high- T_c cuprate superconductors. These studies have revealed an unexpected field-enhanced inhomogeneous line broadening persisting to temperatures high above T_c . Such measurements on heavily overdoped $La_{2-x}Sr_xCuO_4$ (see Figure 11) are dominated by an unusual Curie-like paramagnetism that grows with increased doping of charge carriers [14]. Recently it has been shown that this paramagnetic contribution to the μ SR detected distribution of internal magnetic field extends back into the underdoped regime, and also decreases beyond the superconducting “dome” in the temperature-versus-doping phase diagram [15]. These findings suggest that the paramagnetic component is caused by holes progressively entering the Cu $3d_{x^2-y^2}$ orbitals with increased doping.

In $YBa_2Cu_3O_y$ the normal-state inhomogeneous field response is observed to track T_c , indicating that the origin of the inhomogeneity is related to superconductivity [16,17]. This and other trends of the data can be explained by superconducting fluctuations that vanish inhomogeneously with increased temperature. While there is evidence for superconducting fluctuations persisting above T_c from other techniques, there is no consensus on the temperature and magnetic field range over which they persist. The μ SR experiments on $YBa_2Cu_3O_y$ provide evidence that superconducting fluctuations survive to higher temperatures than revealed by other methods, presumably reflecting the sensitivity of the muon. Furthermore, thus far only the μ SR

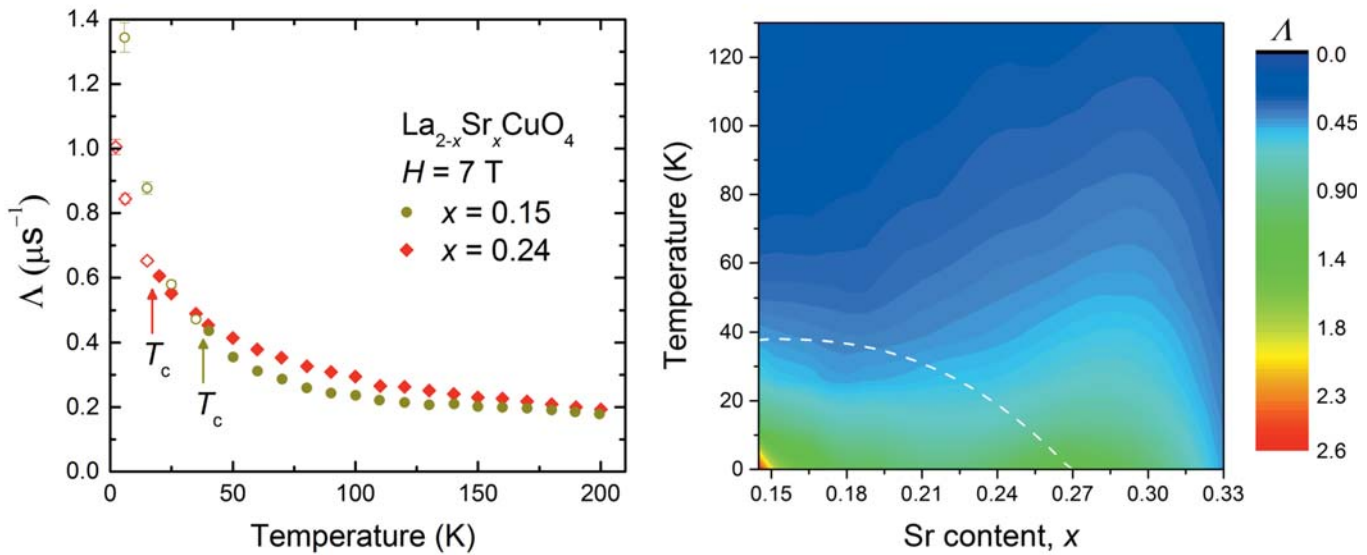


Figure 11: Inhomogeneous magnetic-field response of a high-temperature cuprate superconductor. The relaxation rate of the μ SR signal (Λ) of $\text{La}_{2-x}\text{Sr}_x\text{CuO}_4$ induced by an applied magnetic field exhibits an unexpected temperature dependence above T_c (In the temperature-versus- x phase diagram, T_c is indicated by the white dashed curve). The finite relaxation rate above T_c is indicative of a distribution of internal magnetic fields, which appears to originate from paramagnetic moments and fluctuation superconductivity [30].

results on $\text{YBa}_2\text{Cu}_3\text{O}_y$ have found evidence for fluctuation superconductivity being spatially inhomogeneous in the bulk. Ongoing studies of this kind are aimed at determining whether inhomogeneous superconducting correlations at temperatures above T_c are a universal property of cuprates.

Heavy Fermion Superconductors

Heavy fermion compounds are metallic systems having electronic effective masses that exceed the mass of the free electron by up two orders of magnitude. This is due to the interaction of the conduction electrons with localized f-electrons. One of the most fascinating and mysterious phenomenon that occurs in some of these materials is superconductivity. This is because localized f-electron magnetic moments are intrinsically harmful to the formation of a superconducting state.

As the only known Pr-based heavy-fermion superconductor, there has been a great deal of attention focused on $\text{PrOs}_4\text{Sb}_{12}$. Measurements of the magnetic-field response of the superconducting state of $\text{PrOs}_4\text{Sb}_{12}$ by μ SR at TRIUMF indicate that there is a complete energy gap that forms at the Fermi surface [18]. Moreover, the results are most compatible with the occurrence of two energy gaps on distinct Fermi surfaces, lending support to a body of evidence for multi-band superconductivity in this compound. The superconducting phase of pure $\text{PrOs}_4\text{Sb}_{12}$ at zero field is accompanied by the onset of a spontaneous static local magnetic field (revealed by ZF- μ SR), indicative of a state that breaks time reversal symmetry (TRS). The occurrence of TRS-breaking places significant constraints on the pairing symmetry of the superconducting state. More recently, broken TRS has been investigated in the superconducting state of the $\text{Pr}(\text{Os}_{1-x}\text{Ru}_x)_4\text{Sb}_{12}$ and $\text{Pr}_{1-y}\text{La}_y\text{Os}_4\text{Sb}_{12}$ alloy systems by ZF- μ SR [19]. This study shows that Ru doping is very efficient in suppressing TRS-breaking, whereas La doping is less so (see Figure 12). The results provide evidence for superconductivity mediated by itinerant crystal electric field excitations.

An interesting occurrence of the interplay between magnetism and superconductivity has been revealed in CeCoIn_5 . Although there is no static magnetism in CeCoIn_5 at zero magnetic field, a μ SR study at high magnetic field and low temperature has provided clear evidence for field induced magnetism [20]. This

result, which has been confirmed by NMR and neutron scattering experiments, provided initial support for a theoretically predicted coupled superconducting and antiferromagnetically ordered phase transition. However, the origin of this high-field-low-temperature state is a matter of current debate and investigation.

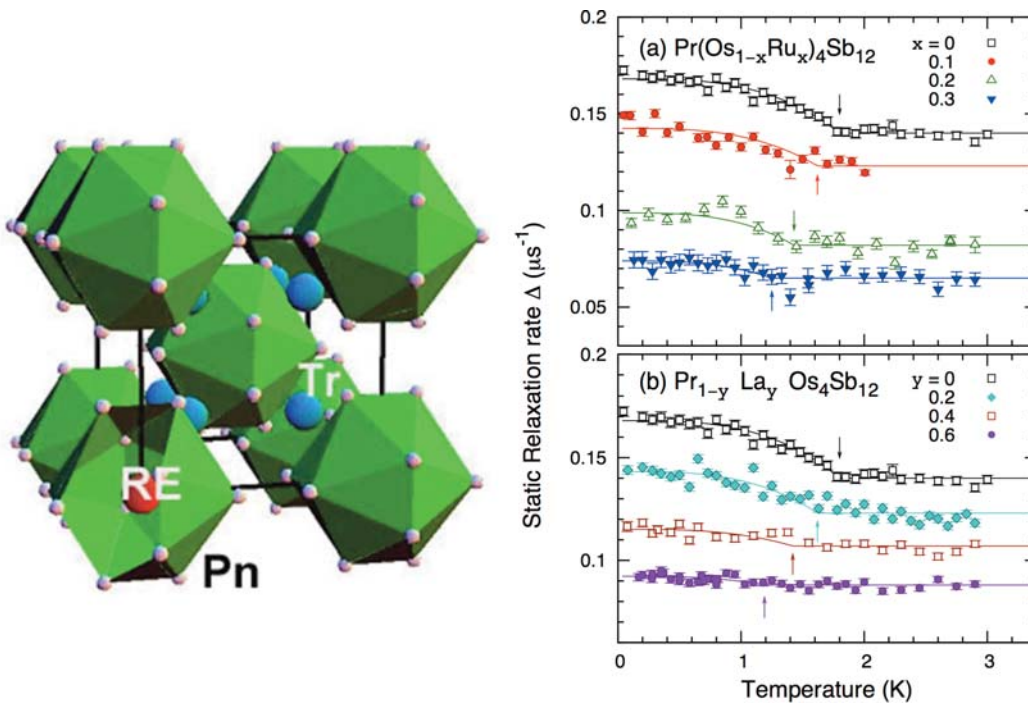


Figure 12: Effect of impurity doping on broken TRS in the superconducting state of $\text{PrOs}_4\text{Sb}_{12}$. The Ru or La ions substitute for the Os ions (blue spheres in the image). 12 Sb ions surround each Pr ion (red sphere). Broken TRS is signified by the onset of spontaneous magnetism, which enhances the relaxation rate Δ of the μSR signal at zero field [34].

Selected References

- [1] G.J. MacDougall et al., Phys. Rev. Lett. 101, 017001 (2008).
- [2] W. Huang et al., Phys. Rev. B 85, 104527 (2012).
- [3] J.E. Sonier et al., Phys. Rev. Lett. 103, 167002 (2009).
- [4] J.P. Carlo et al. Nature Mater. 11, 323 (2012).
- [5] S. Takeshita et al., J. Phys. Soc. Jpn. 77, 103703 (2008).
- [6] A.A. Aczel et al., Phys. Rev. B 78, 214503 (2008).
- [7] S. Takeshita et al., Phys. Rev. Lett. 103, 027002 (2009).
- [8] T. Goko et al. Phys. Rev. B 80, 024508 (2009).
- [9] J. Munevar et al., Phys. Rev. B 84, 024527 (2011).
- [10] M. Hiraishi et al., Phys. Soc. Jpn. 78, 023710 (2009).
- [11] T.J. Williams et al., Phys. Rev. B 80, 094501 (2009).
- [12] T.J. Williams et al., Phys. Rev. B 82, 094512 (2010).
- [13] J.E. Sonier et al., Phys. Rev. Lett. 106, 127002 (2011).
- [14] G.J. MacDougall et al., Phys. Rev. B 81, 014508 (2010).
- [15] C.V. Kaiser et al., Phys. Rev. B 86, 054522 (2012).
- [16] J.E. Sonier et al., Phys. Rev. Lett. 101, 117001 (2008).
- [17] A. Cho, Science 320, 42 (2008).
- [18] L. Shu et al., Phys. Rev. B 79, 174511 (2009).
- [19] Shu, L. et al. Phys. Rev. B 83, 100504(R) (2011).
- [20] J. Spehling et al., Phys. Rev. Lett. 103, 237003 (2009).

4.2.4.4 MUON CHEMISTRY

The muon chemistry program has been a part of the research enterprise at TRIUMF since the beginning, with the first chemistry paper published in 1978 on the subject of the $\text{Mu} + \text{F}_2$ chemical reaction rate in the gas phase. This program soon evolved into reaction rate studies in other environments, including pioneering work on the identification and molecular dynamics of muoniated transient free radicals, most of which cannot be identified by the long-standing technique of electron paramagnetic resonance (EPR). The μSR chemistry programs at CMMS are unique in the world.

Kinetic Isotope Effects in Chemical Reactivity

Low field TF- μSR is routinely used to measure the reaction rates of Mu with a variety of reaction partners and under a wide range of conditions. The μ^+ stop in a sample that is mounted in a weak transverse magnetic field (~ 5 G), which causes the muon spin in Mu to precess at a characteristic Larmor frequency of $\sim 1.4 \text{ MHz G}^{-1}$, which is approximately 100 times faster than the precession of diamagnetic muons. The pseudo-first-order reaction rate of Mu is determined from the damping of the Mu precession signal. A large number of chemical reactions have been studied at TRIUMF over the years and these studies have provided unique information about the effect of isotopic substitution, which in turn provides insight into the electronic properties of the reacting molecules.

A recent landmark study has looked at isotope effects on the simplest and most fundamental chemical reaction: the $\text{H} + \text{H}_2$ abstraction reaction. H and D atoms differ by only a factor of two in mass so they don't generally give rise to large isotope effects and they are also difficult to produce, while tritium is rarely used because it is dangerously radioactive. It has thus fallen to muon science to extend the experimental H atom isotopic mass scale, first to Mu, the lightest isotope of hydrogen, with a mass of 0.113 amu, and recently to muonic helium ($^4\text{He}\mu$), the heaviest isotope, with a mass of 4.11 amu, where the negative muon is captured by the helium atom and effectively "disguises" it as heavy H. It is now possible to compare isotopic mass effects in the chemical reactivity over a heretofore unprecedented factor of 36 in atomic mass. The $\text{Mu} + \text{H}_2$ and $^4\text{He}\mu + \text{H}_2$ reactions were studied at TRIUMF and a comparison between the experimental reaction rates and those predicted by fully rigorous quantum calculations are shown in Figure 13 [1,2]. The fact that the $\text{Mu} + \text{H}_2$ reaction is so much slower than the $^4\text{He}\mu + \text{H}_2$ reaction indicates the dominance of zero-point energy effects over quantum tunnelling and the quantitative agreement seen between quantum theory and experiment over the full temperature range of both data sets and over a remarkable range of a factor of 36 in isotopic mass is totally unprecedented and is the most definitive example of the utility of TRIUMF's muon beams in testing reaction rate theory. This is in fact the only reaction, still today, where the underlying potential energy surface is so accurate that such experimental tests are even possible.

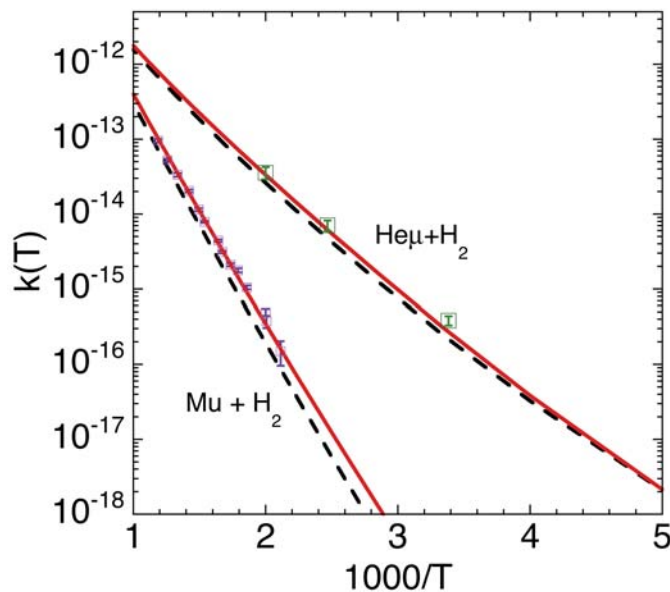


Figure 13: Muonic helium can be considered to be a super-heavy H isotope because the μ^- shields the charge of the nucleus. The measured reaction rates, shown in the above Arrhenius plot, are in quantitative agreement with fully rigorous quantum calculations and indicate that zero-point energy effects dominate over quantum tunnelling in the abstraction reactions [36].

Chemical Reactions in Extreme Environments

Canada is part of the Generation IV International Forum (GIF), which is a consortium of nations that have agreed to collaborate on research and development in support of the next generation of nuclear power systems. Experiments have been performed at TRIUMF in order to assist in the development of Supercritical-Water-Cooled Reactors (SCWRs). Existing pressurized water-cooled nuclear reactors (PWRs) operate at lower temperatures than a SCWR, and a major technology gap identified by the GIF is radiolysis and water chemistry under supercritical conditions. Accurate modelling of aqueous chemistry in the heat transport systems of pressured-water reactors requires data on the rate constants of reactions involved in the radiolysis of water and the action of water treatment additives (e.g., those used to suppress corrosion or the production of hydrogen). Unfortunately, most experimental data do not even extend to the temperatures used in current PWRs, typically around 600 K. Clearly, this is well short of the supercritical conditions (675–925 K) required by Generation IV designs. The data can be described empirically but with unphysical parameters such as negative activation energies. Given the higher temperatures envisaged in a SCWR, it would be dangerous to rely on extrapolation of data from the subcritical regime. Thus measurements of rate constants up to at least 875 K are needed.

It is technically very difficult to make direct kinetics measurements on reactive intermediates in superheated water but muon spin spectroscopy is well suited to study samples under extreme conditions, and TRIUMF researchers have many years of experience at studying muonium chemistry in water up to 725 K. Over the past decade a collaboration of researchers from Simon Fraser University and Mount Allison University have detected and characterized muonium in water from ambient conditions to supercritical, and measured the decay of the Mu signal in dilute aqueous solutions, thereby determining the rate constants for various muonium reactions. A common feature of the results is that Mu rate constants initially increase with temperature (the expected behaviour) but then go through a maximum, only to rise again at still higher temperatures. Given the similar behaviour for different types of reactions it was concluded that a key factor in the unusual temperature dependence seen is a “cage effect”, namely the number of collisions between a pair of reactants over the duration of their encounter. The model for Mu reaction kinetics may be extended to the reactions of other radiolysis transients, such as the $\cdot\text{OH}$ radical because the behaviour is characteristic of the solvent and depends only weakly on the nature of the reactants.

A good example where the simplicity inherent in Mu chemistry is an advantage is the controversy surrounding the importance of the $\text{H} + \text{H}_2\text{O} \rightarrow \text{H}_2 + \cdot\text{OH}$ reaction in the radiolysis of water (see Figure 14). Although very slow at low temperature, this reaction is a source of molecular hydrogen at high temperature, which is important because H_2 is added to the coolant in existing pressured-water reactors (including the CANDU models) to suppress O_2 production. Even if a different control strategy is used in the SCWR it will be necessary to model the H_2 yield as a function of temperature and density, both as a test of model accuracy and to produce data for input to other areas of the Generation IV project (safety and corrosion). Thus, determination of the rate constant for $\text{H} + \text{H}_2\text{O}$ is a high priority. Conventional radiolysis methods can only approach this problem via the rate of the reverse reaction, $\cdot\text{OH} + \text{H}_2$, and the equilibrium constant. Given the uncertainty in details such as the solvation energies of the transients under a variety of thermodynamic conditions, it is not surprising that there is disagreement on estimates of the rate constant for the forward reaction, $\text{H} + \text{H}_2\text{O}$. It can be measured directly for Mu. A preliminary analysis of TRIUMF results suggests that the competing reaction may be dominant below 575 K.

Probing the Structure and Dynamics of Free Radicals

Free radicals are species with unpaired electrons, which frequently makes them highly reactive and difficult to study. Moreover, they are often short-lived intermediates in chemical reactions, and it is necessary to determine their structure, dynamics and reactivity in order to fully understand the reactions in which they are involved (see Figure 15). The high reactivity of free radicals makes them difficult to study with most conventional spectroscopic techniques, including the principal method of electron paramagnetic resonance (EPR). EPR studies are frequently limited to conditions where the radicals are immobile. In contrast, muoniated radicals can be formed with high spin polarizations as a result of Mu addition reactions to

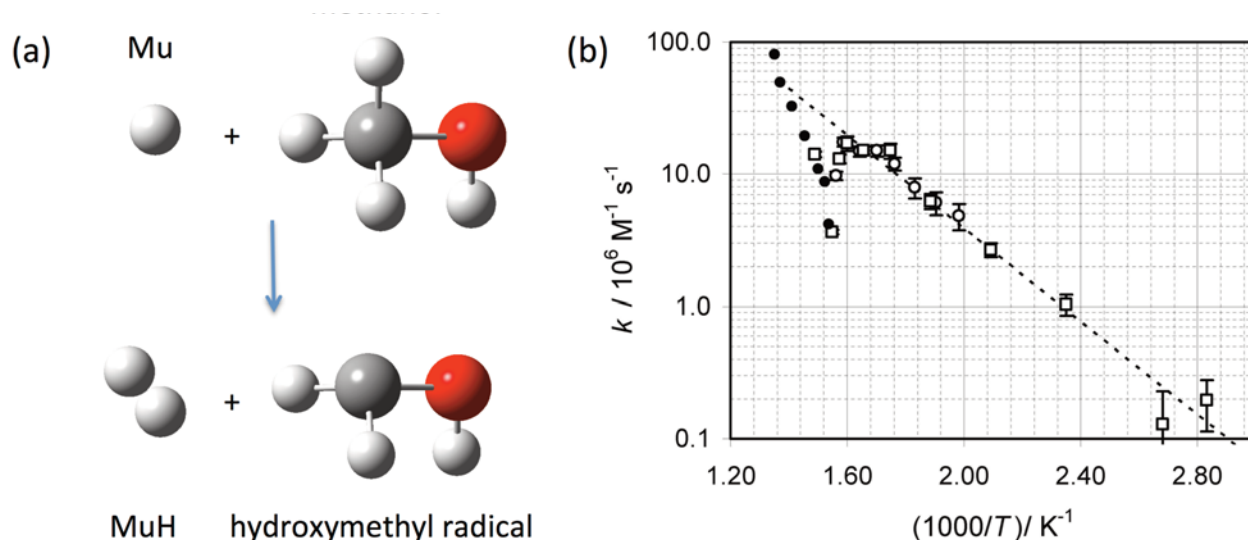


Figure 14: (a) The reaction of Mu with methanol proceeds by Mu abstracting an H from the methyl group of methanol (b) Arrhenius plot of the rate constant for the reaction of Mu with methanol in water. The rate constants deviate significantly from the Arrhenius behaviour (dotted line) near the critical point.

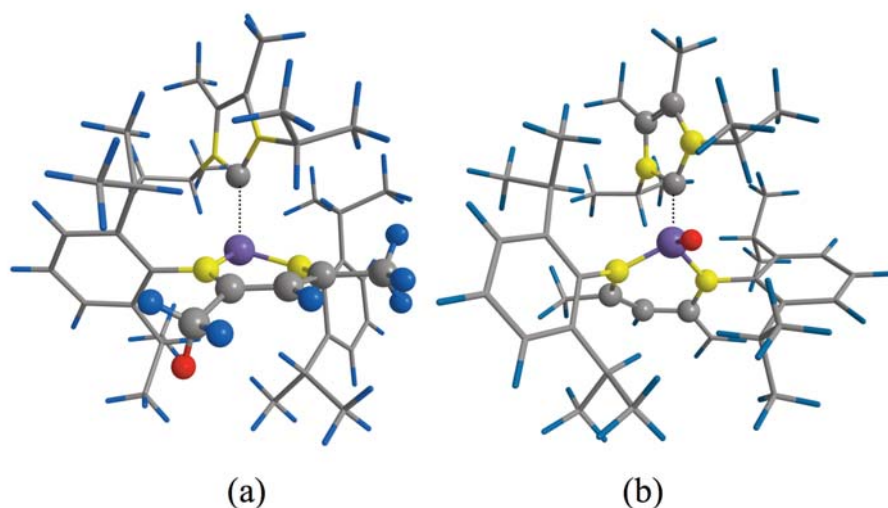


Figure 15: Muonium is an excellent, unbiased probe of reactivity, and using muon spin spectroscopy makes it possible to identify the site of Mu addition in quite complicated molecules. Two distinct free radicals were detected as a result of muonium addition to a silylene-carbene complex (Si violet, N yellow, C gray, H blue, Mu red) [42].

unsaturated bond systems in any environment and their time dependence studied. There are huge advantages in muon spin labelling over traditional labelling techniques and characterization using EPR spectroscopy.

As in EPR, the structure of muoniated radicals is inferred from the hyperfine coupling constants (hfccs), which map out the distribution of the unpaired electron. The magnitude and sign of the hfcc can provide information about the three-dimensional structure. Every muoniated radical has one muon hfcc but as many nuclear hfccs as there are different nuclei (mainly protons) in the radical, although in practice it is often not possible to observe all of them. The muon hfcc (A_μ) can be measured by TF- μ SR or μ LCR if the radical is undergoing anisotropic motion and the nuclear hfccs (A_X) are measured using μ LCR.

Hundreds of organic muoniated radicals have now been studied with the work performed on muoniated radicals over the last five years focused on determining the structure of main group and inorganic radicals. The structure is interesting in its own right but also provides information about how inorganic molecules react with Mu, and by inference H, the simplest free radical. There has also been a considerable amount of work on studying muoniated organic radicals in complex environments such as zeolites or in experimentally challenging environments such as supercritical water.

Novel Main Group Muoniated Radicals

An active area of research at TRIUMF is the study of the reaction of Mu with molecules containing Group 14 atoms (the column in the periodic table from carbon to lead) and the determination of the structure of the resulting radicals. The Percival-West collaboration has studied the radical produced by the reaction of Mu with silylenes and germylenes, which are heavier analogs of carbenes [3,4]. These molecules contain a divalent electron deficient Group 14 atom and are generally highly reactive. This work is unique in that no other groups have been able to study the reactions between such highly reactive species.

Percival and West found that in silylenes with small substituents on the nitrogen atoms, the initial silicon-centred α -muoniated radical, which was formed by Mu addition to the silylene and has Mu attached directly to the radical centre, reacts rapidly with another silylene to give a secondary α -muoniated, where Mu is attached to a silicon atom that is adjacent to the radical centre [5]. This reaction was done by obtaining TF- μ SR spectra of a mixture of two silylenes and observing that four types of radicals were formed by the coupling reaction. Silicon-centred α -muoniated radicals could be observed with sterically hindering groups on the nitrogen atoms to prevent dimerization [6]. Silylenes with tert-amyl and tert-octyl groups on nitrogen dimerized but the signal amplitude decreased due to the larger substituent groups on the silylenes slowing down the coupling reaction. The silicon-centred α -muoniated radicals have large A_{μ} values and this indicates the Si – Mu bond is oriented almost perpendicular to the ring. The Percival and West collaboration has gone on to study more complex silylenes with the results providing unique information about the reactivity of silylenes towards what is arguably the simplest free radical [7].

Experiments on germylenes have shown that Mu adds preferentially to the germanium atom to give a germanium-centred α -muoniated radical in which the germanium atom has a roughly tetrahedral configuration and that there is no dimerization as in the silylenes [3]. Percival and West have also studied muoniated radicals produced by Mu addition to silene (Si=C) bonds [4]. In some silenes Mu was observed to add to both sides of the Si=C bond while in others only addition at the carbon atom was observed. Further work is needed to determine what factors affect the reactivity of the Si=C bond.

Muoniated Radicals in Zeolites–Templates for Catalysis

Zeolites are basically aluminosilicate frameworks that have an ubiquitous presence in chemical industry due to their porous structure, both as molecular sieves and as heterogeneous catalysts, particularly in the petrochemical industry. Important in the latter case are the Y-faujasites (NaY, HY and USY) that consist of “supercages” (SC) with pore sizes of ~ 13 Å diameter and which are linked together by “windows” of mainly Si and bridging O atoms that have diameters of ~ 7.5 Å. Fairly large molecules like benzene (C_6H_6) can easily pass through these windows and reside at specific binding sites within the supercages. Though utilized by industry for many years, the understanding of the mechanisms of zeolite catalysis is still at a fairly rudimentary level. It is believed that protonation reactions involving H^+ transfer to adsorbed “guest” molecules in acidic “host” frameworks are important, but even so there is rather little detailed experimental evidence in support of this claim. Another possibility is H-atom transfer reactions to guest molecules for which there is even less evidence in the literature, partly because of the difficulty of identifying transient radicals by EPR in the geometric confines of zeolite frameworks and the limitations of studying the radicals far from the catalytically relevant temperature regime. This has prompted studies at TRIUMF by the Fleming group of Mu-substituted free radicals by the μ LCR technique, as a “template” for their H-atom analogs, exemplified by recent studies of the muoniated ethyl and cyclohexadienyl radicals in NaY, HY and USY (see Figure 16). This is the first evidence of molecular dynamics of free radicals in catalytically important zeolites by *any* technique, and represents another uniquely important aspect of the muon chemistry program at TRIUMF.

This work can be exemplified by the muoniated cyclohexadienyl radical, which has been extensively studied in several zeolites [8]. μ LCR studies of $C_6H_6\mu$ radicals in NaY zeolite with loadings of 2-3 benzenes per SC found the radical in two different environments; bound to the Na^+ with Mu of the CHMu methylene group either pointing away (exo) or toward (endo) the SII Na cation, or adsorbed at the window sites between the SCs. The interaction with the Na cation gives rise to unprecedentedly large ($\sim 20\%$) shifts in

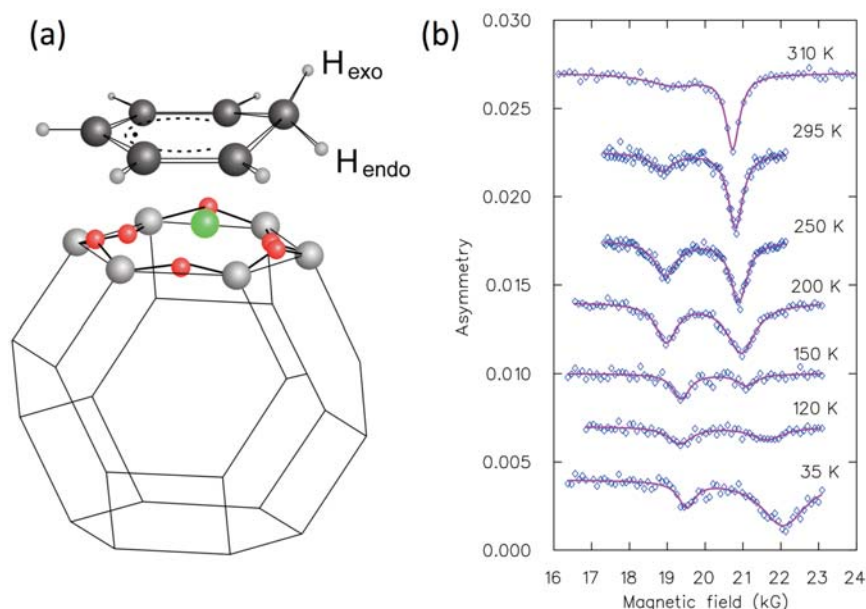


Figure 16: (a) Schematic diagram of the C_6H_6Mu radical interacting with the S_{II} cation in NaY (shown by the green circle), which causes distortion from planarity of the C-Mu bond above (*exo*) and below (*endo*) the plane, shown in the diagram as Hexo and Hendo, respectively. The Si atoms are shown by the light grey circles, with the O-atom bridges shown by the smaller red circles. Atom sizes are not to scale. (b) μ LCR spectra over a range of temperatures for USY at a loading of 2 benzenes/SC. The disappearance of the low field resonance by broadening with increasing temperature indicates the onset of isotropic reorientation motion above 310 K [37].

hyperfine coupling constants, indicating that a strong bond is formed with the π electrons of the C_6H_6Mu radical. The endo and exo orientations of the C_6H_6Mu radical give rise to two different muon hfccs because coupling to the Na^+ distorts the cyclohexadienyl radical from planarity and causes the muon and the methylene proton to be inequivalent. The cyclohexadienyl radical is essentially frozen on the time scale of 50 ns, complexing the $S_{II} Na^+$, which is unlike the behaviour of the benzene molecule in NaY and other faujasites where there is clear evidence for rotation about the six-fold axis as well as long-range diffusion from H-2 NMR spectra. This has been explained by the electric dipolar interaction of the C_6H_6Mu radical with the zeolite framework. Anisotropic motion of the C_6H_6Mu radical is observed up to 470 K, but the radical remains bound to the cation site even at the highest temperature, independent of benzene loading. In contrast, studies of the C_6H_6Mu radical in HY and USY, which are used frequently as heterogeneous catalysts in the petrochemical industry, over a range of benzene loadings and temperatures, have revealed substantially different results to NaY. First, a pronounced loading dependence was observed. At a loading of 2 benzenes per SC in HY and USY the μ LCR spectra of the C_6H_6Mu radical indicates it is in a polycrystalline environment over the whole temperature range studied, which includes data both above and below the bulk melting point of benzene. The magnitude and temperature dependence of the hfccs indicate that there is only a small amount of spin density transfer from the radical to OH binding sites with perhaps a slight distortion from planarity. Second, the μ LCR spectra of C_6H_6Mu radicals in USY zeolite with loadings of 2 benzenes per SC indicate that the cyclohexadienyl radical undergoes isotropic reorientation above ~ 310 K, where guest-host interactions are most important. This is probably due to its desorption from OH binding sites and its random reorientation within the volume of the supercage. Very similar behaviour is seen at a loading of 4 benzenes per SC at higher temperatures, but an additional resonance is observed at low temperatures in USY with 4 benzenes per SC and this is believed to result from benzene in intergranular regions. In USY at a loading of 6 benzenes per SC benzene resides primarily in intergranular regions, where it exhibits almost pure bulk-like behaviour. In contrast to NaY, this loading dependence indicates the importance of guest-guest interactions.

Supercritical water (SCW) has attracted much attention in recent years because of its unique properties, such as low viscosity, low density, low polarity and the high solubility of organic compounds and its potential use as a green solvent. Studying free radicals in SCW is technically challenging due to the high temperature and pressure of the critical point (647 K, 221 bar). There are no reports of radicals in SCW using EPR and only one report of the observation of the triphenylmethyl radical in subcritical water (at 573 K) using EPR [9]. SCW is an ideal system to study using mSR because the m^+ can penetrate a thick-walled vessel required to withstand the high pressures and stop in the fluid sample and the high-energy emitted positrons, which convey the spectroscopic information, can also penetrate the walls and be detected outside the container.

Numerous muoniated free radicals have been observed in SCW over the last twelve years. The first radicals to be observed were the cyclohexadienyl radical and the tert-butyl radical. The success of this study was due to a thorough understanding of some unusual features of SCW. Benzene is only sparingly soluble in water under standard conditions, so it is impossible to obtain TF- μ SR spectra of the $C_6H_6\mu$ radical in aqueous solution at room temperature. Percival et al. were able to obtain TF- μ SR spectra of the $C_6H_6\mu$ radical in SCW because benzene is completely miscible with water at elevated temperatures and pressures. The magnitude and temperature dependence of the muon hfcc of the $C_6H_6\mu$ radical provided information about the interactions between the radical and the surrounding solvent. The tert-butyl radical was produced by μ addition to isobutene, which was produced in situ by the counter-intuitive dehydration reaction of tert-butanol in SCW.

The Percival group has shown that the structure of a molecule can be changed in SCW by studying the μ adducts of acetone as a function of temperature. Acetone can tautomerize between the keto ($O=C(CH_3)_2$) and enol forms. The equilibrium constant for acetone at room temperature is firmly on the side of the keto form, with the enol content being approximately 6×10^{-7} %. Below ~ 520 K a single type of radical with a very small muon hfcc was observed. The magnitude of A_{μ} is consistent with the 2-muoxy-prop-2-yl ($\mu O-\dot{C}(CH_3)_2$) radical, albeit with a small shift that is consistent with the difference in solvent properties for different concentrations of acetone. This indicates that the keto form of acetone dominates in this temperature regime. Above 520 K the muon hfcc of the observed radical is much larger than that of the 2-muoxy-prop-2-yl radical. The muon hfcc of the observed radical is about 250 MHz and falls with temperature, which is typical behaviour for a β -muoniated alkyl radical. The radical was assigned as the 1- μ -2-hydroxy-2-propyl radical ($CH_3\dot{C}(OH)CH_2\mu$), which is formed by μ addition to the enol form of acetone and indicates the equilibrium constant has changed dramatically in SCW.

Supercritical CO_2 ($scCO_2$) has been found to be a useful “green” solvent for a wide variety of chemical applications and the supercritical region ($P_c = 7.38$ MPa and $T_c = 304.15$ K) is technically much easier to generate than SCW. The mSR experiments on $scCO_2$ are unique because CO_2 has no hydrogen atoms, so it is not possible to produce reactive species like H and OH, which are needed to create neutral radicals. The first muoniated radical to be observed in $scCO_2$ was the muoniated ethyl radical ($\mu H_2C-\dot{C}H_2$), which was produced by μ addition to ethane [10]. The identity of this radical was confirmed by measuring the muon and proton hfccs using TF-mSR and ALC-mSR, respectively. The magnitude of the hfccs indicates that the $\mu H_2C-\dot{C}H_2$ radical does not react with CO_2 as has been previously proposed. The temperature dependence of the hfccs may indicate clustering of the CO_2 molecules around the ethyl radical at some densities. Ghandi et al. studied the reaction of μ with vinylidene fluoride in $scCO_2$ and found that small changes in the temperature and pressure near the critical point could result in large changes in the reaction rate [11].

Selected References

- [1] D.G. Fleming et al., *Science* 331, 448 (2011).
- [2] D.G. Fleming et al., *J. Chem. Phys.* 135, 184310 (2011).
- [3] B.M. McCollum et al., *Chem. Eur. J.* 15, 8409 (2009).
- [4] R. West, P.W. Percival, *Dalton Trans.* 39, 9209 (2010).
- [5] B.M. McCollum et al., *Physica B* 404, 940 (2009).
- [6] A. Mitra et al., *Angew. Chem. Int. Ed.* 49, 2893 (2010).
- [7] P.W. Percival et al., *Organometallics* 31, 2709 (2012).
- [8] D.G. Fleming et al., *J. Phys. Chem. C* 115, 11177 (2011).
- [9] K. Kobiro, M. Matura, H. Kojima, K. Nakahara, *Tetrahedron* 65, 807 (2009).
- [10] P. Cormier et al., *J. Phys. Chem. A* 112, 4593 (2008).
- [11] K. Ghandi et al., *Phys. Chem. Chem. Phys.* 14, 8502 (2012).

4.2.4.5 β -NMR

All electronic, magnetic and structural properties of a material are altered near a heterointerface between two dissimilar materials due to the broken translational symmetry and the delocalized nature of electrons such that the character of the electronic wavefunction extends from one material to the other. In some cases, these changes are small and confined to just a few atomic layers while in other situations, the character of the collective behaviour is modified over many nanometers or even microns. An important implication of this behaviour is that thin films and interfaces have unique properties that are distinct from the bulk. This is analogous to a molecule in chemistry where the molecular properties are determined by, but are nonetheless distinct from, the atoms that form the molecule. Interfaces are extremely important in both pure and applied areas of condensed matter physics. The reason is simple to understand. Devices are made from materials and as these devices get smaller the interfaces and finite size effects play an increasingly important role in their function. Giant magneto-resistance in magnetic multilayers is one notable example that had a dramatic impact on magnetic storage. Virtually all the read heads for hard discs rely on the giant magneto-resistance effect in magnetic multilayers. Although the transport properties of a device are relatively easy measure, there are only a few experimental methods capable of probing local magnetic and electronic properties in a depth resolved manner. We have developed one of them here in Canada at TRIUMF called low energy beta-detected nuclear magnetic resonance (β -NMR). The TRIUMF/ISAC facility has unique capabilities that are designed to use implanted radioactive spins as a depth controlled probe of thin films and interfaces. Although many different isotopes made at ISAC can be used for β -NMR, almost all the experiments done so far use a beam of Li-8, which is produced in large quantities and is easy to polarize (so that all the probe spins are oriented in the same direction before introduction into the sample). It is also the lightest isotope suitable for β -NMR and has the special property that its daughter (Be-8) decays into two alpha particles, leaving nothing behind in the sample after the decay. This is similar to the positive muon (please see the discussion of muon spin rotation, mSR, in Section 4.2.4.1).

In fact the β -NMR technique is conceptually very similar to μ SR. A schematic of the experiment is shown in Figure 17. A beam of low-energy spin polarized radioactive spins is injected into the sample. The depth of implantation is controlled by placing the spectrometer on a high-voltage platform so that the radioactive ions must climb a potential hill to land on their way into the sample. The stopped radioactive nucleus acts as a probe of the local magnetic/electronic environment. All forms of nuclear magnetic resonance NMR, the basis of the medical imaging technique MRI, involve generation of a non-equilibrium spin polarization followed by observation of the time-dependent nuclear spin polarization. μ SR and β -NMR are distinct forms of magnetic resonance: a large non-equilibrium spin polarization is generated in a beam of particles before they are introduced into the sample. In addition, the polarization in such nuclear methods is detected through the anisotropic decay properties of the muon or nucleus. Consequently, a signal requires only about 10^7 spins, which is about a factor 10^{10} fewer than is required from conventional NMR.

β -NMR was invented in 1957, along with the discovery of parity violation in weak interactions; however, the particular variant developed at TRIUMF is relatively new. The key points are that, unlike conventional NMR, the signals in β -NMR are independent of sample size and can be monitored as a function depth on a nm length scale. Consequently, β -NMR is ideally suited to studies of thin films, heterostructures, and the near surface region of solids. One of the two main observables is the Larmor frequency, which is obtained most easily by measuring the time-averaged beta decay asymmetry as a function of the small RF magnetic field applied perpendicular to the initial polarization and large internal magnetic field. Some typical frequency spectra are shown in the top right of Figure 17. Alternatively, one can deliver short pulses of beam to the sample and measure the asymmetry as a function of time during and after the beam pulse. The resulting signal is a direct measure of the spin relaxation rate and temporal fluctuations of the local internal magnetic field. Some typical relaxation curves are shown in the bottom right of Figure 17. Both the Larmor frequency and spin-relaxation rate are sensitive monitors of the local electronic and magnetic properties in the thin film, interface or near surface region.

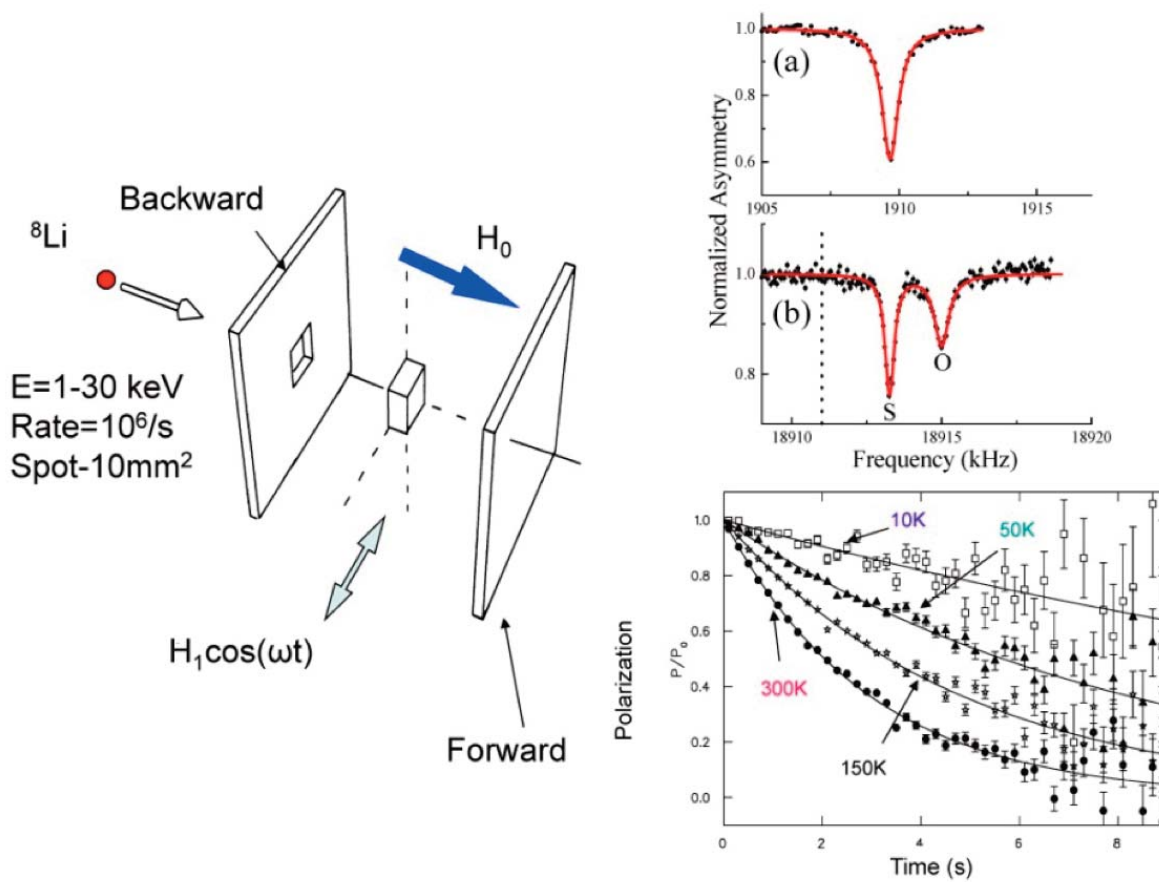


Figure 17: (Left) A schematic of a β -NMR experiment. The initial polarization can either be perpendicular to the beam direction or parallel and plastic scintillation detectors are used to detect the high-energy beta-decay electrons. (top right) The β -decay asymmetry can be measured as a function of a small RF magnetic field applied perpendicular to the main field. This results in resonances when the RF frequency matches the Larmor frequency of the Li-8 in the local magnetic field. The upper resonance corresponds to Li-8 in a thin 50 nm Ag film in a magnetic field of 0.3 T, while the lower spectrum was taken at 3.0 T, where signals from two different sites can be resolved. (bottom right) Alternatively one can pulse the beam with no RF field and simply measure the polarization decay as function of time. The observed relaxation in a 50 nm Ag film is due to Korringa scattering of conduction electrons at the Fermi surface [59].

β -NMR experiments at TRIUMF use the polarized low energy beam line at ISAC, which is a single user facility that can produce only one beam at a time, meaning that this experiment can only run when ISAC is not being used by another of the important experiments. For this reason, the amount of beam time that has been available to do these experiments is quite limited, amounting to a few weeks per year on average. In 2012, TRIUMF committed to providing five weeks of continuous beam time annually for the β -NMR program, making it one of the largest users of the ISAC facility. This is still a small amount of beam time relative to the muon beam lines that can be run in parallel, and one of the main limitations to growth of the technique is still the lack of available time. With the arrival of the ARIEL accelerator and planned photonuclear production of secondary radioactive ion beams, we anticipate another substantial increase in beam time available for these experiments in the coming five years.

While a few other laboratories are capable of β -NMR (notably ISOLDE at CERN), none have a dedicated facility to study materials science with depth-resolved capabilities, nor with the beam intensities and versatile spectrometers of CMMS. The TRIUMF β -NMR facility is a much needed complement to the low-energy μSR facility at the Paul Scherrer Institute due to the different timescales of the radioactive probes and this has resulted in a strong collaboration between TRIUMF and PSI.

Nature of Weak Magnetism in SrTiO₃/LaAlO₃ Multilayers

One of the most striking examples of how the electronic properties of an interface differ from bulk materials is in the case of simple SrTiO₃ (STO) and LaAlO₃ (LAO), both of which are nonmagnetic insulators; however, the interface of STO/LAO exhibits a wide variety of intriguing behaviours that include conductivity, superconductivity, and weak magnetism. The most direct evidence for the magnetism comes from β -NMR results at TRIUMF [1]. Figure 18 shows the spin relaxation rate in STO/LAO multilayers composed of alternating layers of STO (with a fixed thickness of 10 unit cells) spaced with LAO whose thickness can be varied. Note the spin lattice relaxation rate of Li-8 in superlattices with spacer layers of 8 and 6 unit cells of LAO exhibits a strong peak near ~ 35 K, whereas no such peak is observed in a superlattice with spacer layer thickness of 3 unit cells of LAO. The peak is attributed to weakly coupled electronic moments at the LaAlO₃/SrTiO₃ interface that are slowly fluctuating. These results show that the magnetism at the interface depends strongly on the thickness of the LAO spacer layer, and that a minimal thickness of ~ 4 -6 unit cells is required for the appearance of magnetism. The magnitude of the relaxation rate indicates the fluctuating moments are only 0.002 of a free electron in the two samples with a larger LaAlO₃ spacer thickness. The results are consistent with a dilute concentration of moments that are highly disordered as in a spin glass.

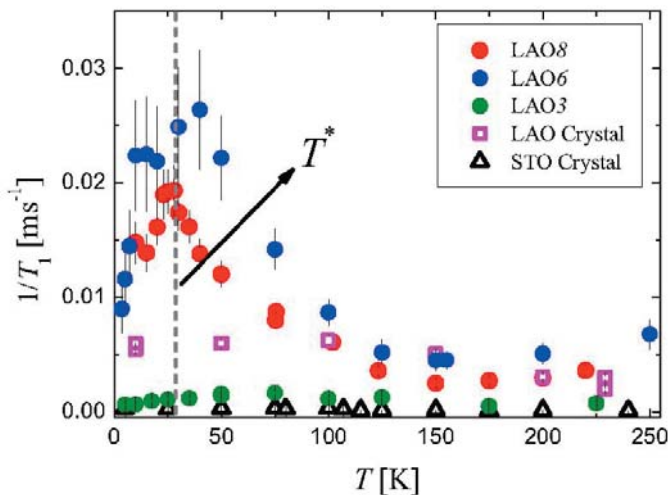


Figure 18: The spin lattice relaxation rate ($1/T_1$) as a function of temperature in 3 mT applied field. The red, blue and green circles are measurements in samples with 8 (LAO8), 6 (LAO6) and 3 (LAO3) unit cells of LAO, respectively. The squares and triangles are reference measurements in LAO and STO bare crystals [53].

Slow Order—Parameter Fluctuations in Superconducting Pb and Ag/Nb Films

In any superconductor, thermodynamic fluctuations of the order parameter are predicted to occur near the superconducting transition temperature. This leads to the appearance of superconducting correlations above T_c . Such fluctuations cause enhanced conductivity and diamagnetism above the critical temperature. The importance of fluctuations increases in systems of lower dimensionality (on the scale of the Ginzburg-Landau coherence length) such as thin films, wires, and small particles. Unconventional superconductors such as cuprates, with their quasi-two-dimensional (2D) electronic structure, low superfluid density, and short coherence length, are even more susceptible to fluctuations. In these systems superconducting fluctuations are thought to be largely responsible for a new phase called pseudogap regime and may be connected to the presence of a quantum critical point. In principle such fluctuations should also be observed in the NMR relaxation rate but until now have not been observed. Recently β -NMR has been used to observe critical fluctuations in a thin film of Ag on Nb and in Pb for the first time [2] (see Figure 19). This is possible because of the enhanced sensitivity of β -NMR to spin relaxation in low magnetic fields where measurements are not possible with conventional NMR. The amplitude of the fluctuations appears to be much larger than current theories predict.

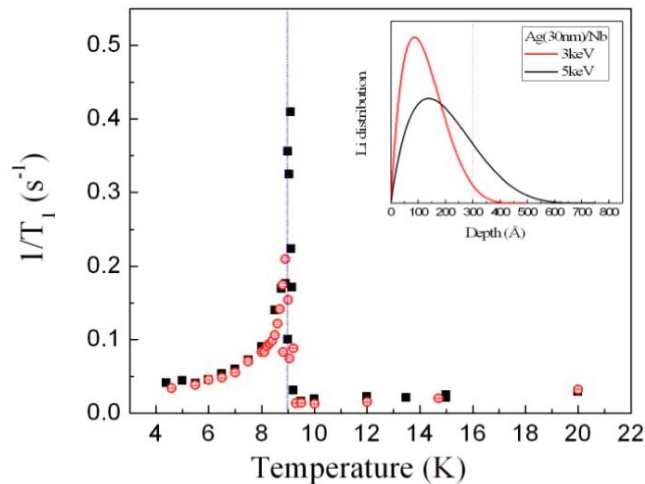


Figure 19: Nuclear spin relaxation rate of Li-8 in 30 nm of Ag on 270 nm of Nb. The signal comes entirely from the thin Ag film, which is not a superconductor. However the Nb with $T_c = 9.0$ K induces superconductivity in the Ag via a proximity effect. Note the sharp peak in the relaxation rate at the T_c . This is attributed to slow fluctuations in the induced superconducting order parameter in the Ag [54].

Interfaces of high- T_c superconductors (HTSC) are important from a fundamental viewpoint because they can be sensitive to fundamental symmetries, which may be regarded as the single most important observable in an unconventional superconductor. They may also have important applications because any device would involve such interfaces. While significant progress has been made in understanding the transport properties of such interfaces, very little is known about their magnetic properties, in part due to the lack of an appropriate local magnetic probe. A particularly unresolved issue is whether the superconducting order parameter (OP) breaks time-reversal symmetry (TRS) near the surface. A characteristic feature of TRS breaking (TRSB) is spontaneous magnetization; however, Meissner screening cancels this in the bulk, limiting the associated fields to within the magnetic penetration depth of defects and interfaces. To measure this magnetization directly, one requires a sensitive depth-dependent local magnetic probe. Recently Saadaoui et al. used β -NMR to perform a sensitive search for TRSB order near the surface of the high- T_c cuprate superconductor $YBa_2Cu_3O_{7-\delta}$ (YBCO) [3].

Low field resonance measurements were made on a thin Ag overlayer deposited on the surface of $\langle 110 \rangle$ oriented YBCO as shown in Figure 20. Note there is some additional line broadening at 4.3 K compared to 100 K; however, the observed line broadening scales with the applied magnetic field whereas line broadening from spontaneous TRSB should be field independent. Therefore, we do indeed observe weak magnetic fields at the surface, but they are attributed to vortices running along the surface. Any fields due to TRSB must be less than 0.2 G. This is much smaller than previous indirect studies based on tunneling.

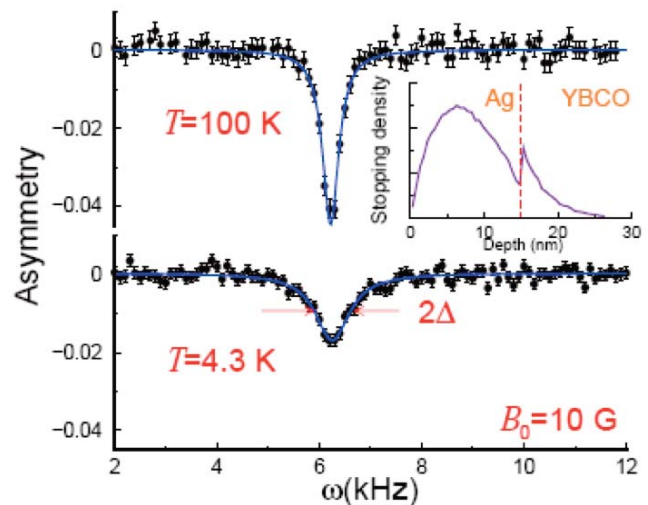


Figure 20: β -NMR spectra taken by implanting 2 keV Li^{8+} into 15 nm Ag/YBCO(110), in an external field of $B_0 = 10$ G applied along the surface of the film. Inset show the simulated implantation profile using TRIM.SP for Li^{8+} of 2 keV in 15 nm of Ag on YBCO [55].

Magnetic Properties of the Multigap Superconductor NbSe₂

One of the most important experimental observables in any superconductor is the magnetic penetration depth λ since it is directly related to the superfluid density $\rho \propto 1/\lambda^2$ and hence to the magnitude of the superconducting order parameter. Its variation as a function of temperature, composition, and magnetic field provides important tests for any model of superconductivity. Recently Hossain et al. have shown that β -NMR can be used to locally probe the Meissner and vortex phases of a superconductor [4]. Figure 21a shows the low field spin relaxation rate in the multigap superconductor NbSe₂ for the field parallel and perpendicular to the surface. In the normal state the relaxation rates are virtually the same indicating that the internal field seen by the Li-8 is the same. When the field is perpendicular to the surface, the sample is in the vortex state where the average internal field is almost the same as in the normal state. Note the observed Hebel Slichter peak in $1/T_1$ due to the opening of a superconducting gap just below T_c . However, when the field is parallel to the surface, there is a dramatic increase in the relaxation rate below T_c . This is due to Meissner screening of the applied field. The magnitude of the increase is a direct measure of the London penetration depth plotted in Figure 21. The temperature dependence of λ confirms the multigap nature of the superconducting gap.

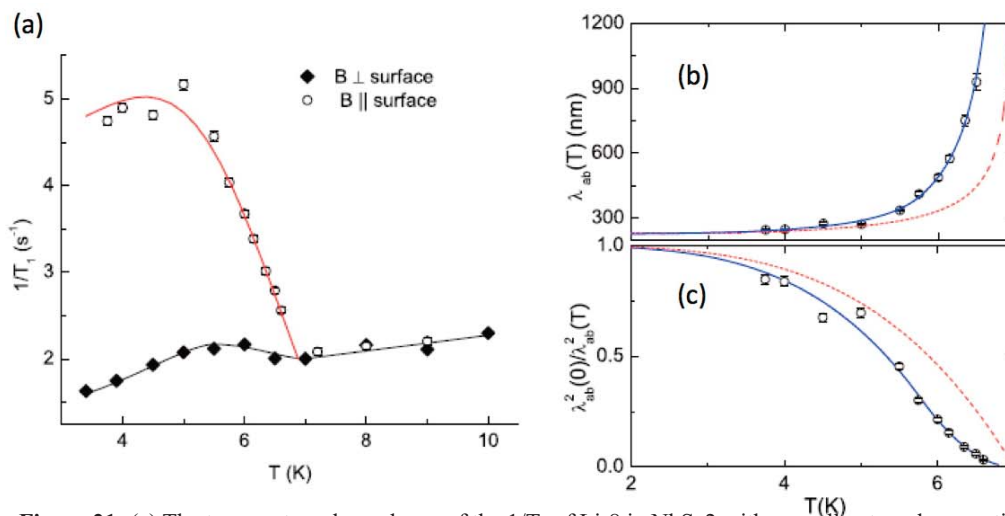


Figure 21: (a) The temperature dependence of the $1/T_1$ of Li-8 in NbSe₂ with a small external magnetic field of 30 G applied parallel to the surface (open circles) and with a 100 G applied perpendicular to the surface (filled diamonds). The fitted curve through the vortex state data filled diamonds is based on the Hebel-Slichter theory assuming a multigap model. The curve through the Meissner state data (open circles) is also derived from this model, taking into account the reduction in magnetic field from Meissner screening. (b) The magnetic penetration depth in the Meissner state of NbSe₂ as a function of temperature. The solid lines are a fit to the multigap model, whereas the dashed line is a fit to the single gap model. (c) The inverse square of the penetration depth versus temperature normalized the value at $T = 0$ [56].

Finite Size Effects in Metals

The metals platinum and palladium are well known as heterogeneous catalysts with chemically active surfaces that can dramatically increase the rates of important chemical reactions such as the reduction of oxygen (O₂) which is a key limiting step in such devices as hydrogen fuel cells. It is thus interesting to study the properties of these metals in the form of thin films and arrays of nanoparticles. While Pt catalysts have been studied by conventional Pt-195 NMR, the signal limitations of NMR entail the use of gram quantities of Pt catalyst, with significant polydispersity and a rather broad range of local behaviour. In the conceptually simpler geometry of a monolithic thin film or monolayer array of nanoparticles, we will be able to make much more detailed and careful studies that could then be used in advancing our fundamental understanding of the processes of catalysis, with the aim of designing cheaper and more effective catalysts, e.g., employing

transition metal oxides, rather than rare metals. In contrast to Pt, chemically similar Pd, which is also an important catalyst, cannot be studied effectively by conventional NMR because of the lack of any high sensitivity nucleus of Pd. We have established the sensitivity of Li-8 as a probe of the mobile d-electrons of Pt and Pd [5]. Figure 22 shows the large negative and temperature dependent Knight shift of the resonance in Pt. The role of the d-electrons is important in determining both the magnetic properties of these metals as well as their catalytic properties.

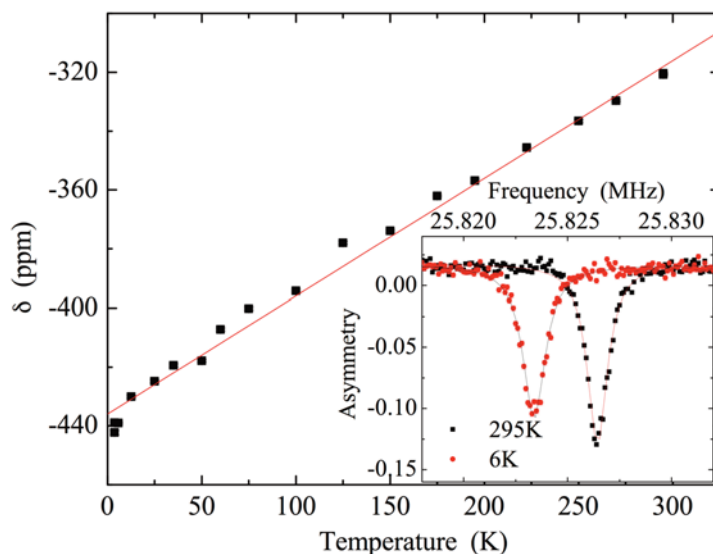


Figure 22: The inset figure shows the resonances of Li-8 in Pt together with the temperature dependence of the resonance shift. The negative, temperature dependent shift is characteristic of the mobile d-electrons of Pt [57].

Selected References

- [1] Z. Salman et al., Phys. Rev. Lett. 109, 257207 (2012).
- [2] E. Morenzoni et al., Phys. Rev. B 85, 220501 (2012).
- [3] H. Saadaoui et al., Phys. Rev. B 83, 054504 (2011).
- [4] M.D. Hossain et al., Phys. Rev. B 79, 144518 (2009).
- [5] O. Ofer et al., Phys. Rev. B 86, 064419 (2012).

4.2.4.6 RADIATION INDUCED EFFECTS IN MATERIALS AND ELECTRONICS

For many decades, research scientists and engineers have been battling to understand how to mitigate against the errors caused in electronic devices by naturally occurring ionizing radiation. Such radiation can lead to a degradation of expected performance, the loss of information or control, and even the failure or destruction of a device. Trying to understand the mechanisms behind radiation effects in matter has been of paramount importance to today's society. The study of new materials and the development of new technologies to allow faster, more compact, lower power, and inexpensive devices has demanded the availability of testing facilities to both investigate future solutions as well as to characterize and verify existing products. In typical years about 100 users from 25 to 30 companies in Canada, U.S., and Europe make use of these irradiation facilities.

PIF & NIF regularly make use of three beam lines at TRIUMF. Protons and neutrons are available at energies up to 120 MeV with BL2C1, which is shared with TRIUMF's Proton Therapy Centre for the cancer treatment of ocular melanoma. Higher energies, up to 500 MeV, are available with BL1B, a testing facility

truly unique to the world for both its broad range of energy and its intensity. More intense neutron irradiations can be done with the TNF location at the end of BL1A. Here, the “leftover” protons from the Meson Hall are converted to neutrons at the beam dump, yielding an energy spectrum well matched to that of atmospheric neutrons, ideal for testing avionics and ground-based electronic systems, such as network and power-distribution servers, automobile electronics, or even the latest cell-phone chips. As well, irradiations of microelectronics were also done using electrons from M11 and, more recently, muons from M20.

In addition to commercial electronics testing and qualification, fundamental research is also performed using PIF & NIF. Regular visits of researchers from several different institutes, laboratories, and universities happen each year to make use of the facilities and services offered at TRIUMF. The research is diverse and has impact. The data collected at TRIUMF are used in student theses, presented at international conferences, and are published in peer-reviewed journals and much of the research has won awards from the community both at the student and professional level.

For example, research supported by the Canadian Space Agency into reducing the increased incidence of cataracts in astronauts (and, to a lesser degree, pilots) has been done by examining the effects of dietary supplements; irradiations of pig eye lenses with protons and neutrons allow scientists to gauge progress. The different PIF & NIF beam lines have been used by several groups to characterize the design and performance of new detectors that need to survive in the harsh outer space environment.

Another impressive example is an in-depth, systematic program of study through modelling and measurement that has been undertaken by several leading groups to investigate the fundamental aspects of different electronic failures using irradiation from protons, neutrons, and now muons at TRIUMF. Experiments performed at TRIUMF have won the prestigious Outstanding Paper Award at the international IEEE Nuclear and Space Radiation Effects Conferences in 2008 (Enhanced Proton and Neutron Induced Degradation and its Impact on Hardness Assurance Testing) and in 2009 (Single-Event Upsets and Multiple-Bit Upsets on a 45 nm SOI SRAM).

Recent data have demonstrated that low-energy muons can cause direct ionization in specific types of electronic microcircuits just as has been found for low-energy protons. Leading-edge microelectronics exhibit sensitivity to lightly ionizing particles, such as protons, as the transport of a singly charged particle through semiconductor material generates sufficient charge in the device to result in an error. As the technology has moved to become more highly scaled and hence compact, less charge is required to potentially cause an error and the probability for an error increases significantly.

The first ever measurement of positively charged muons causing errors in electronics was performed at TRIUMF as part of the Ph.D. thesis of a student from Vanderbilt University, won the Top Student Paper at the 2011 IEEE International Reliability Physics Symposium, and has caused a stir in the microelectronics industry. The work demonstrated that a previously unobserved error mechanism could affect the latest devices. With the high reliability of equipment becoming ever more important, this work will have relevance to the design of data servers, medical equipment, and aerospace technology. The ultimate goal of this research is to understand if atmospheric or terrestrial muons will ever become a reliability issue for the semiconductor industry.

All of this research, enabled by PIF & NIF at TRIUMF, is allowing scientists and engineers to solve existing and minimize future problems, benefitting society with the training of highly qualified personnel and more reliable, better performing, more efficient and cleaner products as well technological advancement.

4.2.5 ACCELERATOR SCIENCE & TECHNOLOGY

TRIUMF is an exciting place to do accelerator physics: with primary beams of protons and electrons, and secondary beams of light to heavy ions for the rare isotopes program, and muons for the materials science program, there is present the complete range of accelerated particles. Each type brings different issues. For example, small permissible halo for the high power electron and proton beams; space-charge effects for the proton which is barely relativistic; high vacuum for the low energy electrons and for the high charge ion beams. The Accelerator Group's focus extends, also, outside the laboratory: there is active support for the LHC through lattice and beam-beam-effects studies, of accelerator simulation tools under the GEANT collaboration, and (to a lesser extent) of FFAGs under the Daresbury EMMA collaboration. All of these activities comprise reason for accelerator codes development and support.

The TRIUMF accelerators are varied: they range from the 40-years old maturity of the main cyclotron, through the decade of operation of the ISAC facility, to the e-linac still under construction. They span, too, a range of acceleration technologies: normal conducting structures in the cyclotron and ISAC-I, quarter-wave superconducting structures in ISAC-II, and elliptical SRF cavities for the e-linac. The main cyclotron has components at or reaching end of life, and there is an active program of refurbishment; with this comes the opportunity not just for replacement but for improvement of technology and of ideas. The refurbishment is supported by a proton beam development program that has as its second purpose the pursuit of 400 μA as a routine operations mode. Contrastingly, the e-linac generates the need and focus for design studies of beam optics in SRF linacs and beam lines; and ancillary studies of electron gun optics, wake fields and impedances, diagnostics, orbit correction, collimation, etc. Notably, these are not mere "paper studies", but rather must and have led to engineering design; and this commands an exacting degree of certitude.

An emerging imperative across the accelerator complex is for the introduction of more efficient and semi-automated tuning of the individual accelerators and beam lines. While the number of accelerators has increased, the overall size of the operations crews has not. Moreover, we recognize that the platforms and algorithms for beam-and-model-based computer control and tuning developed offsite have improved significantly; and the time is ripe to begin their deployment here. The e-linac injector, and particularly its low energy beam transport line, is identified as a rich and fertile testing ground for Accelerator Application Language (XAL) procedures.

The following tour of Accelerator Physics activity at TRIUMF begins with overall highlights and hands on development, and continues to design and modeling, and finishes with beam line technology advance and an account of work performed under external collaborations.

4.2.5.1 SYSTEM DEVELOPMENT AND UPGRADES

Over the past five years, a number of improvements to accelerator systems and operations were made—some refurbishments, some upgrades to modernize. Additionally, a test facility for electron beam optics was developed in cooperation with VECC in India.

New Cyclotron Vertical Injection Line Design and Design Methodology

After 36 years of continuous service, the original vertical section of the beam line that transports protons to the TRIUMF 520 MeV cyclotron has been decommissioned and replaced with a new one. The line's function is to transport the beam to and match into the electrostatic inflector. This line is 12 m in length, and consists of 26 electrostatic quadrupoles. The old line transported as much as 0.6 μA H-, but with bunching, this represents a peak current of 5 μA . The old line had issues with space-charge effects and voltage hold-off of the electrostatic optics.



DOUG STOREY RECEIVES PRESTIGIOUS NSERC AWARD

04 June 2013

The Natural Sciences and Engineering Research Council (NSERC) has announced the winners of this year's Alexander Graham Bell Canada Graduate Scholarship. One of them is a familiar face at the lab: accelerator physics Ph.D. candidate Doug Storey of the University of Victoria. Doug has worked closely with TRIUMF in both his graduate and doctoral research.

Storey's master's research has already proven highly beneficial to implementing safe operations procedures for the electron linear accelerator (e-linac) as part of the Advanced Rare Isotope Lab (ARIEL) that is currently under construction at TRIUMF.

For his doctoral research, Storey is developing a superconducting radio-frequency separator cavity for the e-linac that will become a crucial element in a future upgrade of the e-linac to include an Energy Recovery Linac and later a Free Electron Laser (FEL) which could be the first in Canada and a unique facility within North America.

Research such as Storey's will help Canadian and international scientists produce and study isotopes to advance our understanding of the nucleus, the origins of the chemical elements, and potential medical applications. Furthermore, the e-linac projects are driving new applications of accelerator technology for environmental remediation projects such as PAVAC Industries' pollutant scrubbing technology.

The new line optics were designed entirely using the TRIUMF code TRANSOPTR. This is first order and fully 6-dimensional; it can track all 21 second moments, and space charge is included by solving, at every integration step, the three elliptic integrals and rotating the forces to the lab frame. This is essential as the vertical injection line couples both transverse directions because of the axial magnetic field of the cyclotron, and subsequently couples completely to the longitudinal dimensions in the inflector. TRANSOPTR has been extended to include: varying axial magnetic fields, electrostatic spiral inflector, and motion through the first few turns of the cyclotron including acceleration effects.

Commissioning began in April 2011 and was very successful. Using settings derived purely from theory at start-up, the beam line reproduced the historical best transmission between buncher and cyclotron circulating beam (60%) after less than an hour of fine-tuning the steering correctors.

VECC Test Facility Commissioning

The VECC Injector test stand is a facility at TRIUMF-ISAC developed and implemented to prototype the injection complex for the e-linacs both at TRIUMF and at VECC in India. It provides a proving ground for the physics design and hardware/software developed for these applications. Equally important is the use of VECC to establish procedures before we move to routine operation.

The VECC test stand consists of an electron source, a beam transport system and infrastructure such as alignment, vacuum, power supplies, acceleration systems, electron beam diagnostic and control hardware and software. Through VECC commissioning from 2011 to 2013, we have validated design premises and principles of various components, used the test facility to pin down several design option issues such as beam loss monitors and element sequencing, established diagnostic and control procedures, characterized machine performance to some detail, identified areas for improvement such as dipole bipolar power supplies, and started the process of developing operational protocols and procedures.

4.2.5.2 IMPROVEMENTS TO MACHINE PERFORMANCE FOR EXISTING ACCELERATOR COMPLEX

Improved analytic and computational models, as well as physical control systems, of the accelerator complex have been implemented that allow operators and scientists to more precisely control and optimize the system.

Correction of Cyclotron Resonance

Imperfections in the TRIUMF cyclotron main magnet are a source of field errors which slightly violate the 6-fold symmetry. Among them, the third harmonic of the magnetic gradient drives the $\nu_r=3/2$ resonance; this results in a modulation of the current density versus radius observed from the resonance crossing (at 428 MeV) all the way to the extraction (480 MeV) (see Figure 1). The cyclotron has sets of harmonic correction coils at different radii, each set composed of 6 pairs of coils arranged in a 6-fold symmetrical manner, and designed to correct the first harmonic of the cyclotron magnetic field. The symmetry of this layout cannot create a third harmonic of arbitrary phase, and so a single set of harmonic coils cannot provide a full correction of third harmonic errors driving the $\nu_r=3/2$ resonance. However, the two outermost sets of harmonic correction coils are azimuthally displaced, and the $3/2$ resonance occurs where they overlap radially. By careful combination of the excitation amplitudes, it was possible to completely compensate the resonance. The feasibility of the idea was first demonstrated using simulations. Experimental measurements later demonstrated the full correction of this resonance. Operationally the advantage is that the ratio of extracted currents in the two high current beam lines, 1A and 2A, becomes insensitive to RF dee voltage.

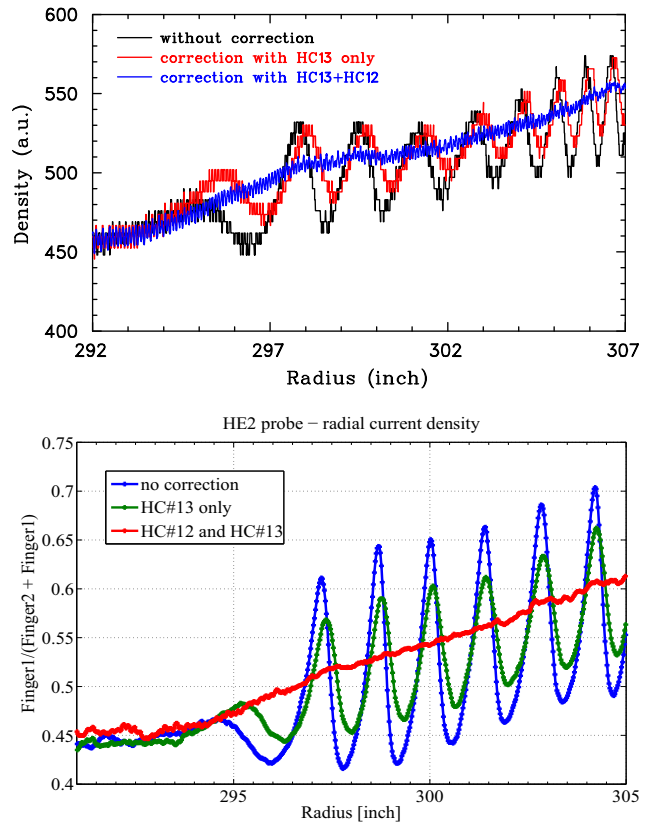


Figure 1: Suppression of the $\nu_r=3/2$ resonance: Radial beam density around extraction with 0, 1 and 2 correction coils. Top: simulation; Bottom: experimental results. The full correction results in greatly reduced fluctuation.

Cyclotron Beam Dynamics with Space Charge

The TRIUMF 500 MeV cyclotron accelerates H^- ions, and uses charge exchange extraction. No turn separation is required for extraction, leading to the very large phase acceptance of this machine (about 60°). Bunches are very long, and have a very large energy spread between the head and the tail. Each bunch therefore occupies a large volume in real space. Solving the Poisson equation in a particle-in-cell (PIC) code over such a large volume would require significant computation time. In addition, at high energy the turn separation is several times smaller than the radial beam size. It is therefore essential to take into account the effect of many neighbouring turns. The multi-bunch calculation in the commonly used simulation code is most appropriate when bunch length and width are comparable, whereas in TRIUMF's case the bunch length can be 400 times its radial width (see Figure 2).

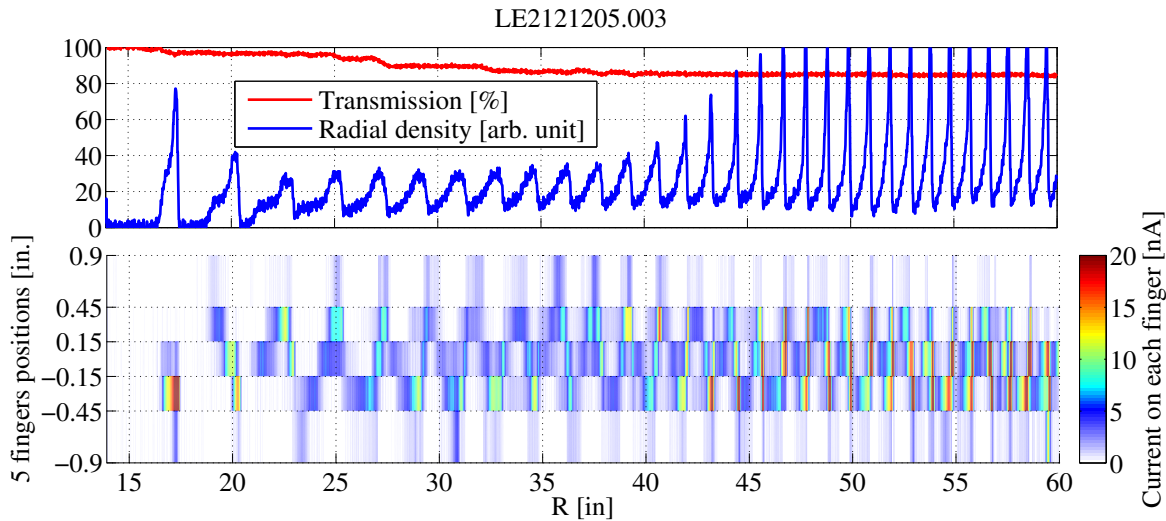


Figure 2: Top: turn pattern (from turn #2) seen by the LE2 probe. Bottom: detail of the signal on each individual finger.

To rise to the challenge of simulating space charge effects in the TRIUMF cyclotron we must take advantage of symmetries inherent in this problem: if we make the assumption that the beam shape evolves slowly compared to the turn-to-turn timescale, we can use periodic boundary conditions in the radial direction. This can reduce the computation time by orders of magnitude. The new code has just been benchmarked against results obtained with CYCO. Exciting outcomes are expected from this new simulation tool.

Improvement of Cyclotron Probes Data Processing and Visualization

New tools to process and visualize data from low-energy and high-energy cyclotron diagnostic probes using MATLAB® have been developed. Compared to the old VMS-based tools, we now benefit from a much larger library of modern data processing and visualization algorithms. We used these tools to improve our understanding of the beam dynamics in the cyclotron central region, and improve the accuracy with which we can measure the vertical position/size of the beam, its phase, and its radial density.

Tune Development for Primary Beam Lines

The TRIUMF cyclotron operated at 500 MeV for nearly four decades. Since 2010, the two primary beam lines 1A and 2A have been reconfigured for running at 480 MeV. The objective was to reduce by ~30% the beam losses caused by the electromagnetic stripping. New tunes were developed for 480 MeV and have performed smoothly. The loss reduction is confirmed both by online measurements and residual activation field mapping after eight months of beam production. In order to improve the stability of both primary beams, two of the harmonic coils were configured in Bz-mode to correct the $\nu_r=3/2$ resonance and stabilize the beam-split ratio fluctuations discussed above. The Br-mode of a harmonic coil plus two trim coils were used to correct the vertical position of the beam at extraction.

Tomographic Display of Beam Density Near Target

For ISAC at TRIUMF, radioactive isotopes are generated with proton beams of energy > 480 MeV. The beam power of up to 50 kW can easily melt the delicate target if too tightly focused. The target is protected by closely monitoring the distribution of the incident proton beam. There is a three-wire scanner monitor installed near the target; this gives the vertical profile and the $\pm 45^\circ$ profiles. Our objective is to use these three measured projections to find a 2D density distribution. We have developed a computer program to realize tomographic reconstruction of the beam density distribution by implementing the maximum entropy (MENT) algorithm. This program performs a calculation that is sufficiently efficient and robust that an operator can obtain the distribution within a few seconds of the scan. This program has become part of the routine operation of Beam Line 2A. In addition, we have developed the MENT technique to perform phase space reconstruction and have applied it to the injection line.

Beam Development at β -NMR

A polarized low-energy ion beam with a β -NMR/b-NQR spectrometer is one of the probes to study the magnetic properties of a material via radioactive decay. In this study one would typically need several million nuclear spins to generate a good NMR signal with stable nuclei. The β -NMR/b-NQR experimental setup at ISAC requires count rates in the range $1\text{--}2 \times 10^6/\text{s}$. In order to fulfill this requirement, production and transport of high intensity and high brightness beam to β -NMR/b-NQR is essential. In order to improve the transmission, systematic beam tuning was performed by using C-12, Li-7 and Li-8 beams with beam energy about 20 keV. We have established a reliable common tune between the β -NMR and β -NQR beam lines by using simulation and diagnostic tools. This work led to improved transmission by 20% and a significant gain in count rate. The results obtained in the β -NQR beam line show some room for improvement. In order to understand the transport properties through the β -NQR spectrometer we have initiated a full 3D simulation of ion beam transport through the β -NQR beam line.

Beam-Based Machine Characterization of VECC Test Facility

A comprehensive plan was completed at the VECC test facility to use electron beam to characterize the full phase space behaviours of both the beam and the machine transport. These data are then cross-compared to both the low- β empirical model for high-level applications and hardware bench data. The VECC diagnostic and control configuration has been designed, to the extent allowed by space and budget, to facilitate this program in both the main line and the spectrometer. As a by-product of this process, the performance of these diagnostic and control elements are also characterized. Longitudinal measurements benefited from the RF-deflecting cavity implemented in the spectrometer arm. A method developed using beam imaged from

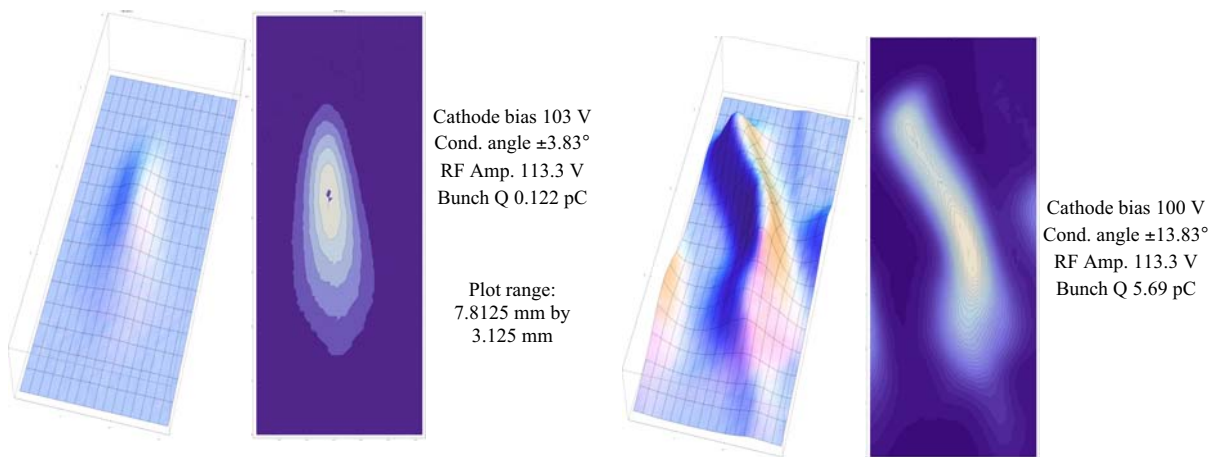


Figure 3: VECC Longitudinal beam phase space under two gun RF settings of a grid beamlet projected onto a screen in the spectrometer. The long dimension corresponds to the RF phase, with the full gun RF cycle spanning 13.08 mm. The short dimension corresponds to a momentum spread where dispersion is 2 m. Bunch lengthening, tail formation and time-momentum correlation as bunch charge increases can be directly seen from such plots.

the cathode grid to view-screens allowed direct and unambiguous measurement of intervening transport, as well as more accurate longitudinal beam determination from isolated grid beamlets (see Figure 3). Two major goals to be achieved from this program are accurately calibrated 6D beam and transport models, and completely debugged diagnostic and control procedures to be turned into high-level applications.

Study on Extraction Optics of H⁻ Ion Beams from a Negative-ion Source

Performance of an ion source is mainly validated by the extracted ion beam intensity and brightness. Also important is the ion beam matching to the transport line. Negative ion beam extraction is more complicated than positive ion extraction because of the co-extracted electrons and also the dynamics of the space-charge force. We have performed simulation and experimental study to understand the physics of negative ion beam extraction optics and to optimize the extraction system for higher beam intensity with better brightness. Based on simulation results, we have shown experimentally that the extraction system can be optimized for high-intensity, high-brightness beams by tuning the arc current along with the extraction voltage. Results are shown in Figure 4, projecting a gain of around 25% in beam intensity.

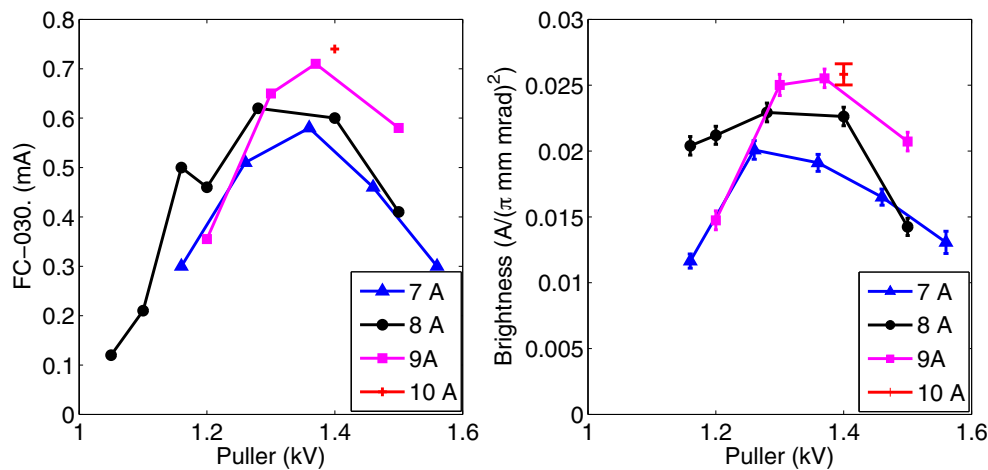


Figure 4: Beam intensity at the location of emittance measurement device (a) and beam brightness at the same location (b) for 294 kV H⁻ ion beam.

4.2.5.3 DESIGN AND MODELING

TRIUMF's accelerator team has improved the designs and working models of the accelerator complex to improve performance and contribute to the world-wide community. TRIUMF's involvement in the Geant4 collaborative software package has generated some of the most widely-cited scientific papers.

Geant4-based Tracking and Simulation

Geometries of TRIUMF beam lines have been simulated and studies conducted using the G4Beamline application, in particular modelling of losses in BL2A due to the cyclotron extraction foil, and simulations of the ISAC target module and the effect of the vacuum window on performance. We have also assisted the Muon Beam Lines group in their M9B study by making code modifications for muon spin tracking.

New applications have emerged with the ARIEL project, where the e-linac and beam transport lines have been simulated to study a momentum collimation device. The geometry of a novel design for the 100 kW beam dump has been constructed and used to estimate performance and heating effects. Initial optics results for simulating the entire system from the electron gun to the photo-fission target are encouraging and it remains to fill in more details to realize a comprehensive model.

TRIUMF-developed Codes

A number of accelerator-related codes developed at TRIUMF remain in frequent use both here and at other facilities. The Beam Physics Group continues to distribute, maintain, and support codes such as the tracking and simulation program Accsim, Long1d for longitudinal dynamics, Intran for beam line design, and Relax3d for static electric, magnetic and heat computations.

Design of Compact Dipole Magnets for the ARIEL Electron Beam Line

The main challenge was to design compact magnets to satisfy space constraints and minimize cost, while satisfying some field quality requirements. The quality of the field produced by a dipole magnet is usually expressed in terms of flatness of the field. Nevertheless, this notion is not easily translatable in terms of what really matters: does the magnet fulfill its role of steering (and focusing) the beam with a small enough impact on the beam quality? In this design study we have thus chosen to write the field quality requirements directly in terms of maximum emittance growth the electron beam may encounter due to non-linear field components.

The different beam lines comprise a total of fifteen dipoles, which have been divided into five different types, depending on the required integrated field and field quality. Five different magnet designs have been produced, based on magnetic modelling using OPERA-3D. To analyze the field quality, second order transfer maps were obtained from particle tracking with COSY-infinity.

E-Linac Beam Transport Line Design

Comprehensive beam dynamics studies as the foundation for the e-linac design were performed. This work included establishing the machine model from the electron gun to the acceleration and transport components through the entire line, purpose-built optimization platform for reaching best design parameters, and extensive configuration and tolerance analysis and operation scenario simulation. Our designs have anticipated that the facility will evolve over time. Phase One is an era in which the linac is operated solely for RIB production; this era begins with the injector and first accelerator cryomodule, and is completed by the addition of the second accelerator cryomodule. Phase Two anticipates that a recirculation ring is added between the exit and entrance of the accelerator cryomodules; this era would support either energy doubling for RIB production, or simultaneous beams for RIB on the straight-through path and an energy-recovered beam through the ring and linac for a FEL or other light source application.

Design of the entire Phase One e-linac beam line is complete, encompassing the electron gun, injection complex, low-energy, medium-energy and high-energy transport lines terminating at a 100 kW tuning dump, a 100 kW and a 500 kW convertor/target module, as well as the respective spectrometer arms. This design covers the magnetic optics, geometrical layout and element coordinates, and performance specifications for the dipoles, quadrupoles and correctors etc., in sufficient details for proceeding with engineering design.

RF Beam Separation Scheme and Hardware for E-Linac Multi-Pass Operation

The e-linac design work also covered Phase Two: future inclusion of a recirculating loop for energy doubling for RIB application, and high efficiency energy recovered beam for a free electron laser. A self-consistent beam separation configuration following the main linac, with RF separation for energy recovered operation and static magnetic separation for RIB energy doubling operation, was designed and incorporated into the e-linac baseline configuration. Multi-pass parameter and error tolerance studies were performed. Hardware design of the beam separation system was carried out in some detail. The extended optimization platform is expected to be useful in finalizing this design.

Beam Breakup Threshold for E-Linac Recirculation

In view of a possible future extension of the e-linac to include a recirculation ring for high-intensity energy-recovered free electron laser (FEL) applications, the beam breakup (BBU) threshold as a constraint on SRF cavity higher order modes becomes a deterministic factor in the cavity design. A comprehensive study was carried out to obtain this threshold covering a wide range of recirculation optics, operation scenarios, and beam parameters. A universal criterion relating higher-order modes was found necessary to ensure suppression of beam breakup modes in recirculation operation up to 20 mA, safely above the design FEL current. This HOM criterion was made into one of the requirements for the e-linac SRF cavity.

Generalized Global Optimization Platform

Building on the framework developed to optimize e-linac beam dynamics, a project was launched under partial NSERC funding to develop an integrated, general purpose optimization platform built to rigorous software standards, enabling the global optimization of a wide range of beam delivery systems of arbitrary topology as a unique accelerator design tool.

The optimization software is implemented and tested. It is parallel capable and works in a distributed computing environment such as WestGrid. The XML input file provides flexibility in defining the optimization variables, constraints, parameters, and also the tracking engine topology. The software was applied to the design of the beam transport of the VECC test stand. The next phase of VECC assembly is the installation of the cryomodule and the 10 MeV dump. We propose to increase the beam size at the dump to reduce heating and create a restrictive “neck” in the upstream beam pipe to prevent backscattering at the dump. The software was used to search for the optimal optics to satisfy the objectives, using a combination of ASTRA and MAD. The optimization results show that the beam at the neck can be squeezed to sub-mm while at the dump the beam can be blown up to 6 cm, satisfying all objectives. The software will be used on further problems for the e-linac. Another problem involving CSR is underway in 2013. The objective is to find the chicane design that produces the best beam characteristics. This design should be useful for DESY and also TRIUMF in preparation of the energy recovery linac (ERL) design. New features involving prototyping are also planned.

Low-b Empirical Model for Online Modelling and High Level Applications

An efficient but accurate beam dynamics model suitable for high level applications at low energy (< 10 MeV for electrons), despite its importance, has not been developed for machine control anywhere. We attempt to bridge this gap with an online empirical model through capturing tracking results into interpolatable and polynomial-expandable data as inputs to an online empirical model. This is more efficient than on-demand tracking but more accurate than analytical models over a considerable range of beam and hardware parameters. Optimal physical data formats and software structures have been worked out to take advantage of the mature XAL framework developed at SNS (at Oak Ridge National Laboratory). On this basis several high-level applications have been created as demonstrations, and beta-tested against data taken from the VECC test facility.

Geant4-Based Tracking and Simulation

An important development in the field of computational accelerator physics is the application of the Geant4 simulation toolkit to the study of beam lines and accelerators. Geant4 makes advances on several fronts. Its state-of-the-art models of particle interactions in matter contribute to our understanding of particle loss processes, foils, collimators, beam dumps and other vital components, but Geant4 also provides a powerful tracking and ray-tracing tool. Its 3D geometry builder allows modelling of accelerators and beam lines in far greater detail than traditional tracking and optics codes; there is great flexibility in defining electric and magnetic fields; and it provides high-precision tracking in these fields with user-settable error controls.

Start-to-end Tracking and Simulation Models of Accelerator Systems and Beam Lines

Construction of start-to-end computational models is driven by advances in accelerator codes which have become more accurate and comprehensive. For the ARIEL electron linac (from the electron gun to the photo-fission target) we plan to employ state-of-the-art codes such as GPT and ASTRA, together with fully 3D tracking and geometry provided by Geant4, via the G4Beamline application. This scenario allows accurate beam line element descriptions via detailed field data, as well as the treatment of overlapping and ambient fields. The extensive development of scripts, data converters, and modifications will be required to achieve full inter-operability between the primary codes, as well as optics and tracking codes such as TRANSOPTR, DIMAD, and Accsim which are essential for the configuration, data preparation, and test-case validations.

The use of Geant4 allows the simulation model to include particle interactions in matter, for studying beam losses, and also allows the extension to multiple beam paths and energies, such as in an ARIEL recirculating ring for ERL/RLA applications.

The same collection of codes, centred around Geant4/G4 Beam Line at the most accurate level, can be applied to other TRIUMF beam lines, in particular towards the redesign of Beam Line 1A, and to sub-systems such as collimators, beam dumps/stops, and diagnostic devices.

The versatility of Geant4 in terms of field descriptions, as well as precise control over error propagation, prompt its use in computational studies of isotope separation. In designing the CANREB facility it will provide a useful adjunct to traditional analysis and ray-tracing codes such as COSY-Infinity and Zgoubi.

Visualization of Beams and Beam Lines

An indispensable part of developing and employing 3D beam simulations is to be able to interactively visualize the geometry and particle trajectories from any viewpoint and at varying levels of detail. By leveraging the basic visualization platform provided by Geant4 we have produced a prototype Open Inventor viewer with features useful for beam lines or other extended structures and have used it extensively in daily work. TRIUMF plans to modernize the user interface and extend this viewer in a number of ways to support accelerator physics applications and Geant4 applications in general. This tool will be useful in educational and media applications as well.

4.2.5.4 ACCELERATOR SCIENCE

Over the past five years, researchers at science have contributed to key progress in several topics in accelerator science including quadrupole magnet design and novel accelerator designs.

Quadrupole Shaping

As originally conceived, the multipole elements commonly used to control charged particle beams are two-dimensional. They correspond to solutions of the Laplace equation $\nabla^2 V=0$, namely, in polar coordinates (r,θ) , $r^n \cos(n\theta)$ in the system where the potential on axis is zero. Thus $n=2$ for a quadrupole, 3 for a sextupole, etc. This implicitly assumes the elements are infinitely extended in the axial z direction, and of course in real beam lines, they are not. For $n=2$, the intended linear dependence of the fields upon transverse coordinate is thus broken by the finiteness of the quadrupole. This results in nonlinear force terms and aberrations, often incorrectly blamed on the fringe fields when in fact the real cause is simply the broken symmetry of being longitudinally finite.

It is not obvious how to terminate the poles of a quadrupole. Often, they are simply truncated. For very long quadrupoles, it can be argued that hyperbolic equipotential surfaces given by $r^2 \cos(2\theta)$ constant are optimal, but this is only true sufficiently far from the ends. However, for quadrupoles whose length is comparable to or shorter than the aperture, the 2D hyperbolic shape is clearly not optimal. We have analytically derived a new shape, and demonstrated that this shape yields smaller aberrations. Though the exact shape is impractical, for short quads it can be approximated with a simple spherical pole provided the sphere's radius is correctly chosen: it must be 1.54 times the quadrupole's aperture radius.

Quadrupoles with this spherical pole shape have been built and measured by Buckley Systems Ltd of New Zealand (see Figure 5). The field imperfections are found to be no larger than those of conventional long quadrupoles, and in some cases are significantly smaller.



Figure 5: Newly designed and built short quadrupole for ARIEL, as it arrived in its packing crate, February 2013.

Cyclotron Orbit Codes for FFAGs

In recent years fixed-field alternating gradient (FFAG) accelerator designs have generally been developed using synchrotron lumped element codes—or adaptations of them. But synchrotron codes are poorly adapted for use in accelerators with fixed magnetic fields, where the central orbit is a spiral rather than a closed ring, and the magnetic field must be characterized over a wide radial range. Cyclotron orbit-tracking codes, on the other hand, are specifically designed for such situations. We have evaluated the orbit properties of several proposed FFAG designs using two sister codes developed at TRIUMF: the equilibrium-orbit code CYCLOPS, and the accelerated-orbit code GOBLIN. A crucial preliminary stage in each case was the creation of a field grid in polar coordinates from the specified magnet positions, dimensions and strengths. We have also explored the potential of incorporating in cyclotrons the radial-sector-FFAG feature of reverse-bending magnets, in order to achieve maximum proton energies in the GeV region.

Poincaré Analyticity and the Complete Variational Equations

Work was done to generalize to all orders the usual first-order variational equations associated with any specific solution of any given (ordinary) differential equation. In so doing, it provides an explicit procedure for computing the Taylor map: the series that describe how the final conditions of a solution depend on the initial conditions and, if present, arbitrary parameters. Such Taylor maps are commonly used in accelerator design. They are expected to be of general utility for many other applications of ordinary differential equations including control theory. For example, it is illustrated that an eighth-order polynomial approximation (including parameter dependence) accurately reproduces the behaviour of the exact stroboscopic Duffing map including infinite period doubling cascades and strange attractors. This work has been published in *Physica D* with co-author A. Dragt.

4.2.5.5 EXTERNAL COLLABORATIONS

TRIUMF's success in accelerator science and technology is founded on a close collaboration with other key partners around the world. Several are mentioned here.

VECC Collaboration

The extensive collaboration with the Variable Energy Cyclotron Centre (VECC) in Kolkata, India, during the period of 2009–2013 is founded upon personnel exchange as a means to facilitate study of issues ranging from SRF system development to beam dynamics research and e-linac design optimization. In addition to SRF work, this sharing of skills and resources has greatly facilitated work on e-linac longitudinal and transverse dynamics optimization, electron gun beam dynamics modelling, beam breakup threshold studies, and beam-based measurements in the VECC test facility.

CERN Collaboration

The Canadian contribution to the LHC has continued in the form of beam dynamics studies, notably in beam-beam effects and their impact on LHC performance. For coherent beam-beam simulations TRIUMF is working with CERN physicists on developing a next-generation parallel code which can accommodate the complexities of the bunch population patterns in the counter-rotating beams and model their mutual electric-field effects in multiple interaction regions. An important step was to extend the electric field calculation from a soft-Gaussian model to a more accurate self-consistent model using a parallel grid-multipole method.

CERN is intensively pursuing plans for LHC future operations and upgrades, including the High-Luminosity LHC (HL-LHC). They wish to collaborate with us on studies of coherent beam-beam instabilities which may limit the LHC performance with increasing ranges of bunch populations, fill patterns, and active interaction regions. TRIUMF's part in this is the optimization and extension of our parallel self-consistent multi-bunch code COMBI to accommodate the operational scenarios and changes to interaction region components, together with the required output and analysis, as well as the validation of the COMBI code against LHC measurements.

When the LHC beams are brought into collision, a particle in one beam sees the Coulomb field of the other beam, which is strongly non-linear and repeats itself at every revolution. This unwelcome beam-beam effect is by design set at an unprecedented level in the present LHC. It also constitutes the largest obstacle for the High Luminosity LHC, planned for 2016. We have devised a mathematical model to describe incoherent (single particle) beam-beam effects of the more important, but difficult, long-range kind, the so-called parasitic encounters. The model was successfully applied to explain measurements made during dedicated Machine Development sessions at CERN, and promises to become an essential tool in designing the high-luminosity LHC upgrade.

Geant4 Collaboration

TRIUMF is a long-standing member of the Geant4 Collaboration devoted to developing, extending and supporting this software toolkit. The Accelerator Division contributes 0.25 FTE to the collaboration as part of our membership obligations. This work has focused on Hadronics, where we have developed and documented a process to extract cross-section data from the SAID interactive partial wave analysis facility and incorporate it into Geant4; and in Visualization, where we are developing a new visualization driver for Geant4 based on the Open Inventor (COIN3D) libraries and implementing features that are needed to streamline the viewing and navigation through beam line geometries or other extended structures.

XAL Collaboration

TRIUMF is a partner in the XAL collaboration in developing accelerator modelling and control infrastructure with the main purpose of self-contained and efficient online high level accelerator controls. This infrastructure is used worldwide in facilities such as SNS, SLAC, MSU-FRIB, ESS, GANIL, IHTP and other places. The collaboration aims to define a unified platform for all participant labs so that software developed for modelling and control can be shared. We requested and expect to take advantage of new models developed by the collaboration, such as electrical focusing elements. Tools developed at TRIUMF for XAL, on the other hand, including conversion between time-based and distance-based propagation modes, and low-b empirical model have been identified for inclusion in the next release package.

EMMA Collaboration

EMMA (Electron Model for Many Applications), funded for construction at the STFC Daresbury Laboratory in the UK in 2007 and completed in 2010, is a “non-scaling” FFAG accelerator designed to test the practicality of allowing particles to cross betatron resonances and follow a serpentine acceleration path in phase space (see Figure 6). TRIUMF contributions had been in three main areas: devising and analyzing the novel “serpentine” acceleration technique; choosing the basic design parameters for the ring and RF system, and setting equipment specifications for the RF system and beam diagnostics. This work culminated in tracking the electrons through the measured field of the prototype quadrupole magnets. This was carried out using the cyclotron equilibrium orbit code CYCLOPS, developed at TRIUMF, and confirmed that the orbit time and betatron tunes varied with energy in the ways anticipated. Further studies with its sister accelerated orbit code GOBLIN showed a small but acceptable growth in longitudinal beam emittance during acceleration. Since 2010 a series of experiments have been carried out by other members of the collaboration to evaluate the beam properties and behaviour. The main aims were to verify (i) that the beam could be accelerated through several betatron resonances without significant loss, and (ii) that TRIUMF’s proposed “serpentine” acceleration technique works. These aims have now been achieved, and a variety of more detailed information is emerging.

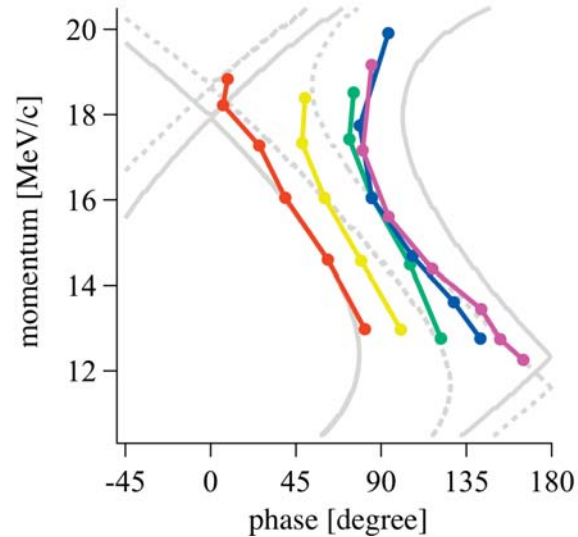


Figure 6: The observed serpentine behavior in momentum-phase space.

4.2.5.6 OTHER ACTIVITIES

Two undergraduate students at UBC plan to build a small (~1-MeV) cyclotron, emulating the successful efforts of a handful of North American students over the last 60 years. TRIUMF has agreed to provide laboratory space, redundant equipment and guidance. Once operational, this device will provide an ongoing resource for undergraduate experiments in accelerator and nuclear physics.

The project began in 2012 with a computer study of the pole shape needed to produce the desired magnetic field. The students are currently designing the vacuum chamber and investigating the RF requirements. They are also forming a Cyclotron Club at UBC, with the aim of involving more students in the project.

4.2.6 DETECTOR SCIENCE AND TECHNOLOGY

All experiments in particle and nuclear physics, as well as condensed-matter experiments at TRIUMF, require instruments to detect energetic subatomic particles. Detectors are required to measure various kinematic properties of each particle, such as its energy, momentum, the spatial location of its track, and its time of arrival at the detector. New scientific opportunities arise from advances in detector capabilities, such as enhanced precision in kinematic properties; the rate at which particles may be detected, which leads to improved statistical precision; and in reduced costs, which make possible larger systems with greater sensitivity to rare processes.

Over the last several decades, TRIUMF's Detector Group has established a strong international reputation for developing, designing and constructing state-of-the-art detectors, as well as developing new detector technologies. A steady progression of new instruments has been successfully deployed in measurements at TRIUMF and in collaborative projects elsewhere in Canada and abroad. As was typical in previous years, every detector or detector element produced by the Group during 2008–2013 has performed as required, with no disappointments. These successes are noted in the corresponding descriptions of those experimental activities elsewhere in chapters 4 and 5 of this document; the detector facilities are described in section 5.5.4.

The Detector Group has broad expertise in various detector technologies, in particular related to scintillation and gaseous detectors. The most prominent example of scintillator construction during 2008–2009 was a close collaboration with the T2K collaboration in the construction of two large fine-grained plastic scintillator arrays for the T2K neutrino experiment in Japan, as described in Section 5.5.5.3. This was a large and ambitious project, successfully employing a new photo-sensor technology on a large scale for the first time. The group also provided the design concepts and construction techniques for a potentially commercial application of scintillator technology on a substantial scale to the identification of subterranean ore bodies through the detection of cosmic-ray muons by scintillator assemblies deployed underground, as described in Section 4.4.1.

The largest gas detectors constructed during 2008–2009 were three large Time-Projection Chambers for precisely tracking charged particles produced by neutrino interactions in the T2K Experiment. This was the first large-scale application to TPCs of a recently developed technology for sensing clouds of electrons drifting in the gas.

The Detector Development Group is focused on the investigations and applications of new detector technologies, for example leading to the application of the new optical sensors to the T2K project, and the design and construction of the signal processing and digitization electronic system. Upon completion of T2K, solutions were developed to enable the use of SiPMs in other applications: positron emission tomography, muon spin rotation spectrometers for smaller samples, radiation monitoring and in particle physics experiments like TREK at J-PARC, Japan, and possible applications for anti-Compton shields for the gamma-ray spectrometer GRIFFIN (please see Section 5.5.1.3). The Detector Development Group has been promoting the development of a new photo-detector solution by providing expertise and resources, and applications in large underground experiments like nEXO will be investigated.

The activities of the Group in this five-year period include:

Design and/or construction of detector systems:

- time projection chambers and active target fine-grained detectors for T2K
- submerged optical test system for Super-Kamiokande PMTs
- precise mechanics and vacuum coupling, 110-element CsI micro-ball detector, and PIN-diode wall, CsI wall detectors for TIP (TIGRESS Integrated Plunger)
- in-beam multi-sampling ion chamber and associated low-pressure gas system, target vacuum chamber with multi-detector deployment (silicon-strip wheels and associated segmented CsI) for IRIS in ISAC-II
- focal plane vacuum vessels and detector vessels, low-pressure wire chamber, and low-pressure gas supply system for EMMA in ISAC-II
- 500-scintillating fiber active target in dark-box for TREK experiment at J-PARC
- 280 large light-guides DEAP (dark-matter search at SNOLAB)
- gas detector for NEURAL tracking detector for astrophysics
- prototype high-resolution detector for Liquid Xenon (LXe)-PET for medical imaging
- Muon Tomography scintillator arrays for underground mineral search
- SPICE (SPectrometer for Internal Conversion Electrons) for TIGRESS at ISAC-II
- diamond detectors ATLAS Upgrade including irradiation tests
- 25 rad-tolerant scintillator/PMT assemblies and 30 linear ion chambers for the ARIEL e-linac Machine Protection System

R&D on applications of silicon photo multipliers (SiPM):

- SiPM-based spectrometer for muon spin rotation
- SiPM-based solution for positron emission tomography

Detector electronics design and construction:

- trigger and readout electronics system for DEAP at SNOLAB
- amplifier/discriminator for diamond tracker of QWEAK at JLab:
- preamps for Silicon detectors of SHARC detector for TIGRESS
- preamps for silicon detectors, MCP readout for TRINAT
- front-end repeater upgrade and amplifier for microwave system for ALPHA
- modules for beam diagnostics of 500 MeV cyclotron vertical injection line

GEANT4 Collaboration for simulation of particle interactions and propagation:

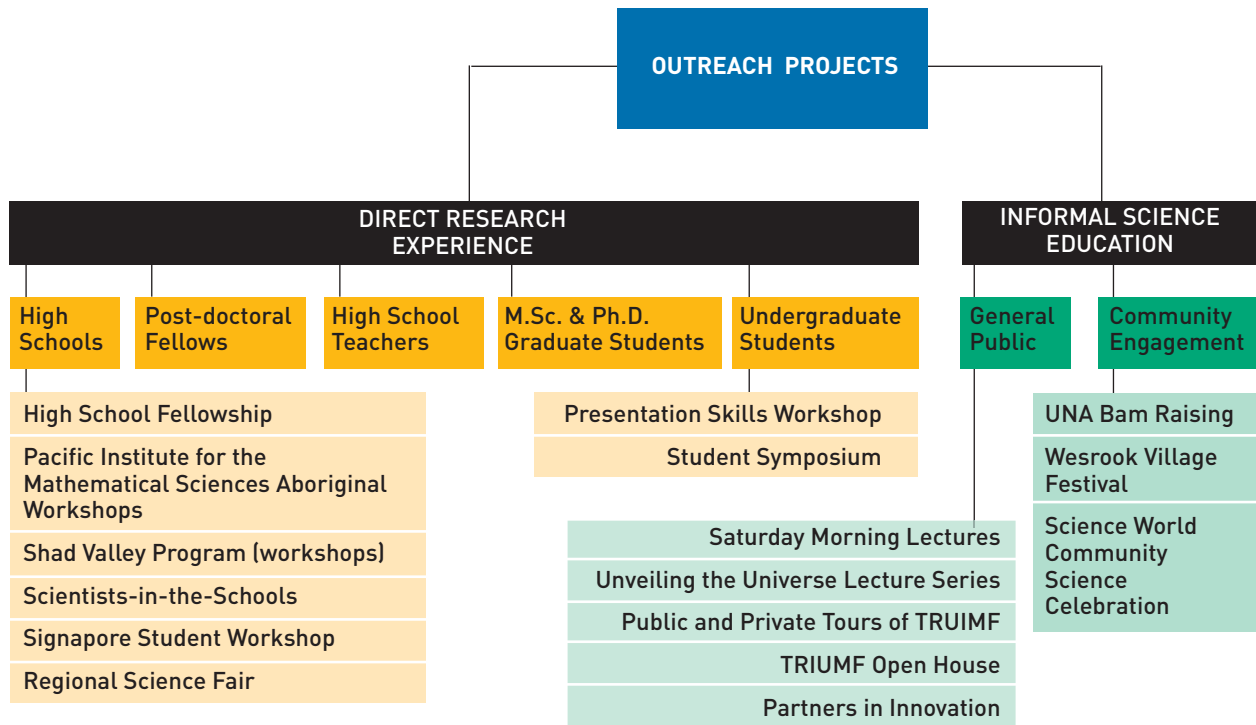
- Steering Board Member
- Deputy Working Group Coordinator (EM Physics, Basic/Extended Examples)
- Principal Developer: Optical Photon Physics and Fields Navigation
- System Testing Team and Publications Board Member
- User Consultation: HyperNews, Bug Report, User Requirements Report
- System Testing Team Member
- GEANT4 simulation support for experiments in the TRIUMF community: development of simulation code implementations
- Principle Developer: TWIST, PIENU, T2K/ND280 (TPC & FGD), Hyper-Kamiokande
- Team Developer: UCN/nEDM, ALPHA
- Consulting advice for a dozen experiments at TRIUMF

4.3 CREATING FUTURE LEADERS

The scientific enterprise generates three categories of benefit: advancing knowledge, creating future leaders, and generating societal and economic growth. This section discusses the second category: inspiring and attracting talent (see Figure 4.3-1 for an overview).

Sharing the process of research and development excites scientists and inspires participants, especially young students, to pursue training in science, technology, engineering, or mathematics (STEM). A solid STEM education in turn makes it more likely that such people will become leaders in research, business, social development, or public policy.

As a basic research laboratory, TRIUMF takes seriously its contribution to trained talent. The lab continuously seeks ways to enhance or adapt its practices to allow ever more students and members of the public to experience science, technology, and innovation activities. TRIUMF concentrates on those programs where its contributions can be unique and (increasingly) measured: offering direct research experiences for students (and sometimes teachers) and providing a number of informal science education activities. Strategic partnerships with other science promotion organizations are utilized to expand TRIUMF’s reach and impact.



4.3.1 DIRECT RESEARCH EXPERIENCES FOR YOUNG PEOPLE

TRIUMF is a unique environment, bustling with international activity as teams of multi-disciplinary scientists, technicians, and engineers collaborate to conduct world-class research using ultra-sophisticated technical infrastructure. Everyday-normal to scientists, this environment is breathtakingly inspirational to students and members of the public unaccustomed to science. As such, the unique value of TRIUMF's outreach activities is offering "direct research experiences" to high school, undergraduate and graduate students, as well as teachers.

High School Students

In 2004 TRIUMF created the High School Fellowship program with the Science Council of British Columbia (now BC Innovation Council). The Fellowship consists of a \$3,000 award and a six-week work term at TRIUMF, and attracts 60-100 applications from the very top high school physics students from across BC. One measure of the program's success has been the high return rate of Fellows as undergraduate co-op students, with several being taken on in their first year of university by former supervisors. The program now offers three Fellowship positions, and TRIUMF is actively coordinating with Science World at the Telus World of Science (including its Future Science Leaders program) to expand the Fellowships to even more deserving students.

TRIUMF also participates in the Shad Valley program and regularly hosts several young entrepreneurial students who assist with research and technology at the lab in multi-week work experiences.

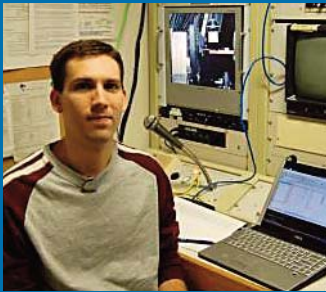
The laboratory worked with UBC, SFU, and UVic in launching ATLAS Master Classes in Canada (2011, 2012, and 2013). The program is spearheaded by CERN and creates daylong education and training sessions for talented high school students. The students learn about particle-physics data and analysis, work on real data from the ATLAS experiment, and then participate in an international videoconference to share their results with peers around the world.

The Vancouver School Board (VSB) and UBC established a working group dedicated to improving aboriginal educational opportunities. TRIUMF joined this group in 2008 and, for its initial pilot project in 2009, brought a Manitoba aboriginal high-school student, Dylon Martin, to TRIUMF for a six-week work experience. The goal was to inspire Dylon with a breadth of science outside his normal experience, and then have him share his experience with his peers. He spent a week each with five experimental groups and summarized his work in a weekly front-page web site story.⁵ Since then, each summer has brought one or two aboriginal high school students from the Pacific Institute for the Mathematical Sciences to TRIUMF to experience cutting-edge research and technology with different research groups.

TRIUMF also works with many local high schools to offer work experiences or job shadowing experiences for student in grades 10-12. The high school work experiences provide students an opportunity to experience a 'real world' employment environment as well as the experience of working in a research laboratory. Each experience lasts between one and three weeks and is part of their high school curriculum.

Undergraduate Students

TRIUMF is among the largest employers of undergraduate students in Canada, attracting students from university co-operative education programs across the country. The positions are in high demand; almost every single opening attracts 50-75 distinct applications. Students are hired three times a year, at the start of each school term and are employed for a minimum of four months. The work term may be part of their co-operative education program or a summer work experience. In addition, the TRIUMF Undergraduate Summer Research Award offers five \$2,000 scholarships every year to undergraduate students from each of Canada's five regions (Atlantic, Quebec, Ontario, Prairies, and BC) for summer research work. Students



STUDENTS DEMONSTRATION OF MUON-RELATED GLITCHES WINS AWARD

01 September 2011

Since 1995, the TRIUMF Proton and Neutron Irradiation facilities have delivered low-intensity, energetic proton and neutron beams to test sophisticated electronics, simulating years of natural-radiation exposures in space or terrestrial environments in just a few minutes.

Such tests probe the susceptibility of microelectronic devices to “soft errors” (switching a memory bit from 0 to 1, or vice versa). It has been known for over 30 years that natural proton and neutron radiation can cause such errors, but Brian Sierawski, a Ph.D. student at Vanderbilt University, reasoned that ever-smaller microelectronics might become susceptible to less-ionizing forms of cosmic radiation.

Sierawski and his Vanderbilt colleagues used TRIUMF’s M20 beamline to demonstrate that soft errors indeed could be induced by low-ionizing muons produced in cosmic-ray proton interactions in the upper atmosphere.

Demonstrating muon-induced soft errors earned Sierawski the Top Student Paper award at the 2011 IEEE International Reliability Physics Symposium. With ever-shrinking microelectronics, Sierawski’s work could impact the design of data servers, medical equipment, and aerospace technology. TRIUMF offers the only such muon beamline in North America for this research.

participate in activities as diverse as particle and nuclear physics research, nuclear medicine, engineering, accelerator operations, and communications and outreach. Some of their experiences were captured in blog posts and uploaded to the Quantum Diaries platform⁶ and to TRIUMF’s Headline News on its web site as well as several YouTube videos.

Undergraduate students are offered activities to enhance their experiences, including social events, weekly lectures, a Presentation Skills Workshop (with UBC), and the Student Symposium, where students give 10 to 15 minute talks to their peers for a chance to attend the Winter Nuclear and Particle Physics Conference in Banff. As a result, students consistently rank their TRIUMF experience very highly and many undergraduate students later return to TRIUMF as graduate students.

To fine-tune TRIUMF’s involvement in high school and undergraduate education, TRIUMF’s outreach coordinator began teaching entry-level university physics at UBC in 2011. Not only did he receive the highest ratings from students across the department, but he now determines what types of events and information are shared with students when they visit TRIUMF.

Funding Source	NRC		NSERC		CIHR		Other		Totals
	CAN	FOR	CAN	FOR	CAN	FOR	CAN	FOR	
Foreign Status									
FY2008–2009	56	3	5	1	0	3	4	0	72
FY2009–2010	53	5	2	1	0	5	2	0	68
FY2010–2011	60	6	3	1	0	6	0	0	76
FY2011–2012	58	4	9	2	0	4	1	0	78
FY2012–2013	58	3	10	1	0	3	1	0	76
SUBTOTALS		285	21	29	6	0	21	8	0
TOTALS		306		35		21		8	370

Table 1: Undergraduate students who worked at TRIUMF (and received stipends via TRIUMF) during the 2008–2012 period. Also shown is the source of funding and whether the students came to TRIUMF from Canada or abroad. Informal surveys of TRIUMF supervisors suggest that at least another 75 undergraduates worked at TRIUMF during this five-year cycle but were not paid through TRIUMF and therefore not tracked.

Graduate Students

TRIUMF's primary impact in university education is through graduate students, who come to TRIUMF from universities where they are participating in a degree program. Once at TRIUMF, each student works with a local supervisor to ensure that his/her learning and research are on track and will fulfill the requirements of their degree.

During the 2008-2012 period, graduate students working at TRIUMF completed 85 M.Sc. and Ph.D. theses. Two graduate students working at TRIUMF were also selected for the prestigious Vanier Canada Graduate Scholarships: Stephan Etteneuer (UBC) in 2009 for work in nuclear physics and Simon Viel (UBC) in 2011 for work in particle physics. In 2011, Patrick-Rey de Perio (Toronto) also received a Vanier Scholarship for work related to the T2K experiment, spearheaded by TRIUMF.

Funding Source	NRC		NSERC		CIHR		Totals
	CAN	FOR	CAN	FOR	CAN	FOR	
FY2008–2009	3	6	12	14	0	6	41
FY2009–2010	7	5	13	9	0	5	39
FY2010–2011	3	6	17	10	1	6	43
FY2011–2012	5	5	8	13	1	5	37
FY2012–2013	4	4	8	14	1	4	35
SUBTOTALS	22	26	58	60	3	26	
TOTALS	48		118		29	195	

Table 2: Graduate students who conducted research at TRIUMF and received stipends processed through TRIUMF's finance office. Students arriving from outside Canada are denoted as well, based on their residency status (SIN number).

Post-Doctoral Fellows

TRIUMF hosts advanced post-graduate training for many people. In the physical sciences, post-doctoral research experiences are an invaluable component of pursuing an academic career, a position in industry, or just in broadening one's research skills independent of career endpoint. Post-doctoral fellows (PDFs) at TRIUMF are usually supported with NRC or NSERC funds that focus the research contributions on specific topics. PDFs usually work on research in subatomic physics theory, experimental particle and nuclear physics, nuclear medicine, or accelerator physics and engineering. The experience at TRIUMF propels these researchers to become leaders in their field. For instance, Carleton's Dean of Science Malcolm Butler, Manitoba's chair of the physics department Peter Blunden, York University's Randy Lewis, former president of the Canadian Association of Physicists Shelley Page at Manitoba, and UBC's Javed Iqbal were all PDFs at TRIUMF.

	PDFs
FY2008–2009	40
FY2009–2010	44
FY2010–2011	44
FY2011–2012	46
FY2012–2013	49

Table 3: Post-doctoral fellows at TRIUMF. Six to eight PDFs each year are funded through the NRC Contribution Agreement.

High School Teachers

TRIUMF works with the BC Association of Physics Teachers to host a biennial professional development day for BC high school teachers. The event is at capacity every time with more than 75 teachers coming to TRIUMF for a full day to attend lectures, conduct hands-on experiments, and participate in teaching and instruction learning sessions. Over the five-year period 2008–2012, TRIUMF hosted the event three times (2008, 2010, 2012) and interacted with more than 225 teachers.

From time to time, TRIUMF also provides hosted internships for high school teachers to spend a week or two in the summer at TRIUMF during which they contribute to an active research project. Funding constraints and teacher availability have restricted the uptake of this offering.

TRIUMF also sponsors the Canadian Association of Physicists High School Teacher Award to promote and encourage enthusiasm for physics at the high school level. This award recognizes excellence in teaching physics in Canadian high schools and is awarded annually to four teachers across the country.



TRIUMF ALUMNUS RECOGNIZED FOR MO-99 PAPER

01 September 2010

On August 4, the TeraChem 2010 Committee awarded a Marino Nicolini Prize to Dr. Suzanne Lapi and her collaborators for their paper titled, “An alternative route to the production of High Specific Activity Mo-99”. The paper is based on the MoRe isotope-separation project, sponsored by Advanced Applied Physics Solutions, Inc., located at TRIUMF.

Dr. Lapi was a graduate student at Simon Fraser University working at TRIUMF and is now an Assistant Professor at the Washington University, St. Louis Campus. The Nicolini Prize is dedicated to the memory of Professor Marino Nicolini, awarded based on innovation in the proposed work, principal applications foreseen, and beneficial impact on society. MoRe [Molybdenum-Rhenium] technology aims to purify Mo-99 by mass separation of a Mo-98,99 source mixture created from a nuclear reaction on stable Mo-98. Radioactive decay of the purified Mo-99 leads to ^{99m}Tc , the most widely used medical imaging isotope. The MoRe project is under active development, but once operational, it could have a significant impact on the “isotope crisis” currently facing hospitals and cancer patients.

4.3.2 INFORMAL SCIENCE EDUCATION

Informal science education has been identified as one of the crucial drivers of a modern, sophisticated society.⁷ Informal science education, such as that conducted at zoos, museums, and research institutes, develops out-of-school learning that encourages lifelong learning, both “life-wide” (occurring across multiple venues) and “life-deep” (occurring at different levels of complexity). TRIUMF supports informal science education through a number of programs that provide public lectures, tours of the laboratory, and community engagement activities.

Public tours, educational programs, and outreach activities in the schools help guide young minds towards promising careers in science, technology, engineering, and medicine. In fact, informal science education targets all levels of curiosity and education backgrounds. At TRIUMF, the focus is programs that appeal to high school students and early university or college students. A side benefit is that these programs also attract the interest of mature adults interested in science and technology.

Saturday Morning Lectures

For over a decade TRIUMF has offered the Saturday Morning Physics Lectures in conjunction with the UBC and SFU Departments of Physics and Astronomy. These lectures are free and held one Saturday monthly, between October and April (except December). Guests are treated to two talks on topical subjects at a level suitable for a lay audience. The lectures have grown in popularity over time, so much so that the 100-seat auditorium was filled over capacity for most of the 2008–2009 and 2009–2010 series. Guests come from all over Vancouver and nearby municipalities and as far away as the Fraser Valley. Consequently the Lectures were expanded to include a second monthly presentation at SFU Surrey to better service guests from the east. The Lectures have attracted a devoted following of about 75% high school students and 25% adults. Future Lectures will be webcast with the new MediaSite system (operated in partnership with UBC) in an effort to extend TRIUMF’s reach into communities further afield.

Partners in Innovation

In 2011, TRIUMF entered into a five-year cooperation agreement with Telus World of Science, British Columbia’s leading science outreach agency for children from kindergarten through ninth grade. The Partners in Innovation program now combines TRIUMF’s high school focus with Telus World of Science’s younger-student focus to provide an additional opportunity for students to engage with and consider science, technology, engineering, and mathematics as a potential career path. Examples of new initiatives under this framework include: gallery space at the Telus World of Science building for student artwork generated after tours and studio time at TRIUMF; evening lectures for the public, featuring speakers such as CERN’s Director-General; and summer camps for “future science leaders.” The collaboration saw the outreach and communications groups from both institutions working together on a number of different facets of the program, ranging from facility coordination to social media marketing.

Unveiling the Universe Lecture Series

These at-your-doorstep lectures remain immensely popular, selling out in just a couple days and attracting curious minds to the OMNIMAX Theatre at the Telus World of Science, filling the 400-seat capacity. The demand for seats at these talks is so great that simulcasts of the talks are made available. One reason that the demand is so high is that the talks are given by leading scientists in their fields, working on some of the most exciting research and development currently taking place. Four examples are:

- Dr. Hitoshi Murayama, theoretical physicist and director of Japan’s Kavli Institute of Physics and Mathematics of the Universe, discussed anti-matter, neutrinos, and (the still-elusive) dark matter, explaining how these enigmas fit into our understanding of the Universe.
- Professor Gino Segrè, physics professor emeritus at the University of Pennsylvania and author of three popular science books, presented “Physics in Florence from Galileo to the Higgs Boson” in which he charted the history of physics as it grew from the influence of Galileo, his disciples, and the spirit of exploration in 17th-century Florence, to the present day, with the most dramatic event being the recent discovery of the Higgs boson. This event was co-hosted by the Italian Embassy.
- Rolf-Dieter Heuer, the director-general of CERN, delivered an illuminating talk called “Unveiling the Universe.” Heuer addressed why the search for the Higgs boson is so important and why the search for antimatter and dark energy are so integral to understanding the Universe, and our place within it.
- Dr. Lyn Evans, project leader for the Large Hadron Collider (LHC) construction, detailed some of the design features and technical challenges that make the LHC such an awe-inspiring scientific instrument. He discussed recent results from the LHC and what is next in the world of high-energy physics.

After each lecture, TRIUMF and Telus World of Science co-host an evening reception for community leaders to meet the speaker and local scientists and ask further questions. Where appropriate, these events have been co-hosted by the foreign consulates in Vancouver (e.g., German Consulate in Vancouver for Rolf Heuer, the Italian Embassy for Gino Segrè, the British Consulate in Vancouver for Lyn Evans).

Public Tours of the Laboratory

TRIUMF’s public tours, which are typically led by selected TRIUMF staff or trained students, continue to attract nearly 3,000 people per year. Working with results from surveys as well as updated best practices from the expert science outreach and engagement community, the laboratory is presently revising its tours program to tailor tours more closely to the interests of schools and the community.

Category	2008-09	2009-10	2010-11	2011-12	2012-13
General Public					
# of people	475	1845	616	820	891
# of tours	143	150	179	208	214
Science					
# of people	666	1004	1581	1184	1089
# of tours	45	55	83	91	78
Students					
# of people	491	574	952	844	751
# of tours	23	26	37	47	35
VIP					
# of people	356	198	190	97	99
# of tours	72	54	38	28	41
Total					
# of people	1988	3621	3339	2945	2830
# of tours	283	284	337	374	368

Table 4: History of public tours at TRIUMF. Note that the Community Open House in 2009 elevated the results for that year.

Engagement with Formal Education

TRIUMF has explored contributing expert materials for high school curriculum usage. One foray has been the *Physics in Action* educational videos series. These videos relate and demonstrate the work TRIUMF does with high-school physics concepts being taught. The first pilot video (on relativity) was done on a small budget but in 2006 TRIUMF was granted funds by NSERC’s PromoScience to create three new videos. In 2009, the relativity pilot video was re-edited to bring the look and production up to the standard of the second video, “Electromagnetism and Circular Motion in a Cyclotron,” which was also completed in late 2009. This video’s scope was the biggest project of its kind attempted at TRIUMF and has been enthusiastically received by teachers. The free DVDs, which included the new video, and the relativity re-edit, began shipping in early 2010 and to date almost a thousand copies have been distributed to teachers across Canada and around the world.

TRIUMF staff is also involved in the Canadian “Let’s Talk Science” and “Scientists in the Schools” programs that send trained scientists into school classrooms. Since 2009, TRIUMF has also participated in Virtual Researcher on Call, which uses modern-day videoconferencing to connect classrooms with scientists for hour-long discussions on breaking news topics.

The BC Science Fair Foundation organizes elementary school science fairs in BC, with support extending to local, regional, national and international science fairs. TRIUMF annually supports travel expenses to the national science fair for regional winners.

American Association for the Advancement of Science (AAAS) Annual Meeting

The annual meeting of the American Association for the Advancement of Science (AAAS) was held in Vancouver during February 2012, marking the first time in 30 years that the meeting was held outside the U.S. TRIUMF was heavily engaged in the local organizing activities and was an active coordinator of national involvement. Working with the BC Innovation Council and the Government of British Columbia, TRIUMF organized the BC AAAS Student Scholar program that provided scholarships to 200 high school students from across the province. These scholarships allowed students to register for the conference and become members of the AAAS for a year. Students attended science sessions, met the Governor General of Canada, pressed speakers with questions about the forefronts of research, and contributed to the record-breaking attendance at the AAAS conference. TRIUMF also partnered with the UBC Department of Physics and Astronomy to host a double-wide booth at Family Science Days. Nearly 5,000 visitors dropped by the booth to talk about the Higgs boson, medical isotopes, and radiation.

Community Engagement and Participation

TRIUMF is regularly involved in several local neighbourhood festivals and at community picnics such as the University Neighbourhood Association's Annual Barn Raising and the local Wesbrook Village Festival, TRIUMF and the community get to know one another. TRIUMF wants to inspire confidence and pride in people living near and around TRIUMF and make them feel comfortable and safe and so far it's working.

TRIUMF also participates in the Community Science Celebration organized by Telus World of Science each year and contributes programming to Canada's autumnal National Science and Technology Week. Finally, TRIUMF was heavily involved in the BC Year of Science celebration in 2011 and organized an exhibit on science and art at the Royal BC Museum.

To reach larger audiences, TRIUMF has piloted a number of events to “meet people the lab wouldn't ordinarily meet.” For instance, TRIUMF's communication team worked with theory post-doc Abishek Kumar on a dark-matter public talk that was featured in TEDxStanleyPark in early 2013. And research scientist Anadi Canepa was nominated and selected to participate in the Global Civic Society's Public Salon evening in April 2013 that featured short talks by “amazing individuals” in the Vancouver metropolitan area. Anadi's presentation received thunderous applause and generated new contacts and interest in TRIUMF, particle physics, and science.

Community Open House

The largest recent public outreach event was undoubtedly the 40th Anniversary Open House on August 8th, 2009, where over 1,300 enthusiastic adults and children took part in self-guided tours and physics demos and enjoyed free food. The Open House also demonstrated TRIUMF's community spirit—around 100 staff volunteered their time and energy to make the event a big success. TRIUMF is readying its staff for another open house in September 2013 which promises to attract more people than ever.



TIM MEYER RECOGNIZED AS TOP 40 UNDER 40

14 December 2011

TRIUMF's own Tim Meyer, Head of Strategic Planning and Communications, has been recognized as one of the Top 40 Under 40 by Business in Vancouver. Those who work with him at the laboratory know he is very deserving of this honour in recognition of his hard work and leadership.

Dr. Don Brooks, a member of TRIUMF's Board of Management, remarks that Tim "is one in a million and we are delighted to have him with us. This is a richly deserved award." Since

beginning at TRIUMF, Tim has made great contributions to the lab's outreach, long-term planning and partnership efforts.

After earning his Ph.D. in experimental particle physics from Stanford University, Meyer Meyer worked for the National Academies in Washington, D.C., where he was a senior program officer on the Board of Physics and Astronomy. Arriving in Vancouver in 2007, at TRIUMF he focuses on public and internal relations, and oversees the scientific publication and outreach programs.

Artist in Residence Program

As the practice and inquiry of science becomes more integrated into contemporary culture, TRIUMF's Artist in Residence (AIR) program has become more and more relevant. The program—managed day-to-day by a pair of TRIUMF co-op students—exists to generate a broader interest in the imaginative and inspirational side of scientific inquiry through the impressions of visiting artists.

Through an initial partnership with faculty at the Emily Carr University of Art + Design, TRIUMF regularly hosts classes of artists-in-training who learn about black holes and other transformations of energy and then spend studio time at the laboratory generating new artwork. Building on these initial forays, TRIUMF has now developed collaborations with the School of Art and Design in Berlin, Germany (a partnership that successfully obtained funding from the Goethe Institute) as well as advanced programs of study at the University of British Columbia and Simon Fraser University.

The Global Particle-Physics Photowalk in August 2010 attracted more than 200 photographers around the world to behind-the-scenes tours of the participating laboratories around the world. A local Vancouver photographer was awarded first place by an independent jury of experts for his photograph of the 8π nuclear physics experiment. Output from the AIR program now graces the walls at TRIUMF as well as several buildings in the community.

In summary, TRIUMF's informal science education programs touched the lives of many people during the 2008–2012 period:

- 350 undergraduate and high school students participated in Virtual Researcher on Call, Scientists in the Schools, and Let's Talk Science programs involving TRIUMF scientists;
- 2,500 people attended public science lectures as part of programs at Telus World of Science, British Columbia, Global Civic Society's Public Salon, and TEDxStanleyPark; and
- 25,000 people interacted with TRIUMF booths and activities at events such as the University Neighbourhoods Association Annual Barn Raising, Westbrook Village Festival, Telus World of Science Community Science Days, BC Year of Science exhibitions, and the American Association for the Advancement of Science Family Science Days.

4.3.3 OUTCOMES

Evaluating the impact of its direct research experiences for students as well as its informal science education activities is important to TRIUMF. Although the lab has several indicators that measure throughput and surveys to measure immediate satisfaction with events; longitudinal studies suffer from resource constraints. An informal survey of supervisors revealed, however, that students working in the TRIUMF environment tend to continue their success in academia, business, and beyond. For instance, after studying at CERN, students via TRIUMF end up at Canadian universities (25%), foreign universities (25%), government labs (25%), or in the private sector (25%).

Several young people participating in TRIUMF's direct research experience programs have received national and international recognition. For instance, Nick Zacchia was an undergraduate co-op student at TRIUMF in the Nuclear Medicine Division and ended up building a small electron accelerator for his Capstone project in Mechanical Engineering at Concordia University. As a result, he was selected to give the opening keynote address at TEDxKids@BC.⁸ Elsewhere, Brendan Baartman at Simon Fraser University received the Coryell Award in Nuclear Chemistry from the American Chemical Society for his contributions at TRIUMF under the tutelage of Professor Kris Starosta. Similarly, Eric Price, a graduate student with UBC's Chris Orvig in the Department of Chemistry won the U.S.-based Society of Nuclear Medicine Berson Yalow award in mid-2013. Eric was a co-op student with TRIUMF senior scientists Mike Adam in the Nuclear Medicine Program a few years earlier, an example of how TRIUMF inspires students in multiple areas of scientific research and development.

Finally, the Subatomic Physics Long-Range Plan "Canada in the Age of Discovery" (2012) did some investigations into the career paths of undergraduate and graduate students working in subatomic physics. The overwhelming findings of that report indicate that these graduates have found careers broadly distributed through the Canadian economy, including:

- Business entrepreneur (software and engineering companies);
- Electronics and engineering;
- Finance (quantitative analysis, financial risk management);
- Geophysics
- Government (radiation standards, radioactive threats, defense);
- Medical imaging;
- Nuclear power (reactor design); and
- Software (web applications, data mining, programming).

Not all of these students were influenced by TRIUMF, but as one of the major engines of subatomic physics in Canada, TRIUMF finds itself in a unique position. With even more resources for more outreach programs, the lab could build on its successes and attract new generations of scientists (and science followers) to the wonder and excitement of scientific research and development.

4.4 GENERATING SOCIETAL AND ECONOMIC BENEFITS

The public at large, via taxes and support for the government, invests in scientific research. Around the world, the level of public investment in science continuously exceeds that of the arts and traditional cultural expression. The implicit assertion is that science generates an additional stream of benefits that merit these additional resources beyond the intrinsic cultural and aesthetic appreciation of knowledge. Traditionally, we associate this additional level of impact with the societal and economic growth that arises from the practice of science: both in terms of trained and motivated personnel and short- and long-term economic impact. In this report, the inspiration and attraction of youth to science is discussed separately and provided in Section 4.3.

“Research in the sciences is fundamental to a 21st century economy. It underpins the continuing improvements in living standards that Australians expect and deserve.”

Australian Department of Industry, Science, and Research, Oct. 2011

This section discusses TRIUMF’s economic and societal impact over the past five years. It is organized to present results related to the activities of Advanced Applied Physics Solutions, Inc. (AAPS) followed by a report on innovation and industrial-partnership activities based at TRIUMF. The final topic examines models for measuring economic impact and presents results from a recent independent assessment.

TRIUMF & LOCAL FIRM JOIN ELITE LEAGUE ABLE TO PRODUCE SUPERCONDUCTING CAVITIES

14 April 2008

A team of B.C. scientists and engineers drawn from the TRIUMF laboratory and PAVAC Industries, Inc., announced today they have entered into an elite league of worldwide groups able to manufacture ultra-sophisticated superconducting accelerator technology. The B.C. team was able to fabricate, assemble, and test a high-tech device known as a “superconducting radio-frequency cavity” or SRF cavity. The modules are so technologically sophisticated that until now, only four other industry-based groups in the world have had the capability to produce them. These superconducting devices are assembled into modules to form next-generation accelerators with applications in health care, environmental mitigation and remediation, advanced materials science, and high-energy physics.

“This milestone is truly significant,” said TRIUMF director Nigel S. Lockyer. “The push for this technology started in particle-physics research but is growing in demand all over the world. And Canada now has the ability to compete for and contribute to that market.”

This technology is at the leading edge and rapidly expanding; laboratories around the world are lining up to incorporate it into their future projects. Literally tens of thousands of the devices will be needed over the next decade.

4.4.1 RESULTS FROM ADVANCED APPLIED PHYSICS SOLUTIONS, INC.

AAPS was created as a Centre of Excellence for Commercialization and Research (CECR) in February 2008 with initial support of \$14.95M from the Networks of Centres of Excellence program of the Government of Canada (see Section 5.10 for a complete discussion). AAPS provides business-management and market-analysis expertise to TRIUMF and actively maintains a broad network of contacts and takes note of commercialization opportunities that may be relevant for TRIUMF and its partners (see Figure 4.4-1).

AAPS was the only physical sciences based CECR funded in the original tranche of 11 CECRs created in February 2008. The five-year award was scheduled to expire in early 2013. In summer 2012, AAPS was invited to apply for an extension of the performance period and to apply for additional funding. Results of the competition were communicated in December 2012 and the NCE Secretariat indicated that the CECR performance period for AAPS would be extended without adding new funds. Two considerations were (a) the level of unspent funds at AAPS at that time (close to \$5M) and (b) the observation that AAPS might achieve self-sufficiency without needing new CECR investment.

The AAPS executive team has negotiated a new agreement with the CECR program that extends the performance period to 2017. The present governance structure (e.g., Board of Directors, NCE ex officio status, CEO & President) will continue.

AAPS expects to exhaust the CECR funds by 2015 and would then move out of that program. The extension decision has triggered several adjustments to AAPS and especially its interactions with TRIUMF. It is expected that this relationship will evolve further in 2015 when AAPS transition out of the CECR program. Briefly, AAPS and TRIUMF are moving toward improved synergies and cost-saving measures.

At end of FY2012–2013, AAPS has continued to maintain strong relationships with 23 partners this year and initiated new relationships. NDAs were signed with 6 companies to facilitate discussions on potential collaborations. Six MOU / Collaboration agreements were signed, 3 of which generate revenue. An inaugural “Innovations and Industrial Partnerships Workshop” was jointly organized by TRIUMF and AAPS in July 2012, where the directors and senior managers of TRIUMF’s member universities’ university-industry liaison offices came together to share best practices and explore collaborative opportunities.

Deal flow to AAPS comes from three areas (entrepreneurs who approach AAPS, TRIUMF’s network of industrial contacts and partners, and from within TRIUMF or its academic-research network). The ripest opportunities arise from TRIUMF’s relationships with existing vendors and its academic-research network.

IKOMED Technologies, Inc.

AAPS scouts for externally generated opportunities to incubate in the TRIUMF environment. Local Vancouver entrepreneurs generated an invention that would reduce the radiation exposure during standard medical fluoroscopy procedures, for example, inserting stents into the heart. AAPS recognized that the early stages of prototyping, software testing, and radiation modeling could benefit from a partnership with TRIUMF.

IKOMED Technologies, Inc. was launched as a start-up company in 2010, using a loan from AAPS, Inc., and floor space in the AAPS wing of TRIUMF’s main building. In June 2011, IKOMED secured its first round of private sector funding. This round enabled IKOMED to develop and test its technology for fluoroscopy radiation reduction. IKOMED has been granted the first of a series of patents by the U.S. Patent and Trademark Office and establish IKOMED’s intellectual-property position. Following

AAPS: TAKING CANADA'S EXTRAORDINARY INNOVATIONS IN PHYSICS TO THE MARKETPLACE



AAPS is INNOVATION.
Our goal is to help Canadian researchers develop and market physics-based technologies.



AAPS is PARTNERSHIP.
AAPS accelerates innovation by linking academic, industry and government stakeholders with common goals.



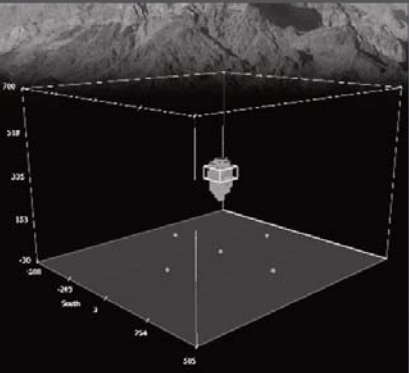
AAPS is COMMERCIALIZATION.
AAPS has experienced science and business advisors who can create successful marketing strategies.

Even genius needs a little help.

Innovation. Partnership. Commercialization.




AAPS: ADVANCING IMAGING TECHNOLOGIES FOR MINING EXPLORATION



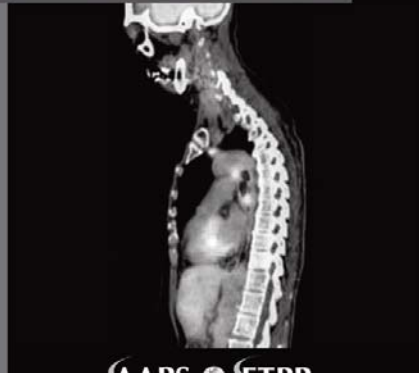
What if...

We could see inside mountains the way we see inside the human body?

AAPS has developed a precise, cost-effective and environmentally-friendly technology to image underground mineral deposits.

Through AAPS, an investment and market-ready company is being launched to commercialize this technology.

See www.crmgtm.com



AAPS  **ETPP**
Advanced Applied Physics Solutions Exploitation des Techniques de Physique en Physique

Innovation. Partnership. Commercialization.

www.aapsinc.com

AAPS: WORKING TO ADVANCE NUCLEAR MEDICINE IN CANADA







AAPS is ... working to secure Canada's supply of medical isotopes
 ... working to ensure all cancer patients have access to PET imaging – the most powerful tool for detecting and managing cancer. www.triumf.ca/pet-report
 ... a nationally-designated Centre of Excellence for Commercialization and Research

www.aapsinc.com

Innovation. Partnership. Commercialization.




Figure 1: AAPS, Inc. serves as TRIUMF's key commercialization partner.

Figure 2: CRM Geotomography Technologies, Inc. is a recent spin-out from AAPS that seeks to use cosmic-ray muons for underground imaging of candidate ore bodies.

Figure 3: AAPS builds on TRIUMF's expertise in nuclear medicine to create new markets and opportunities.

successful demonstration of IKOMED's patented X-ray radiation reduction technology with commercial fluoroscopy imaging equipment, the start-up finalized its second round of private-sector financing totaling several million dollars. Led by a group of Canadian private investors, this latest round of investment will enable IKOMED to expand its product offering and build manufacturing capability for its X-ray radiation reduction system. AAPS provides incubator facilities throughout these initial start-up phases.

IKOMED has recently signed a terms sheet with GE Healthcare and will become a preferred provider of their proprietary dose-reducing shutter systems that integrate with existing fluoroscopy machines as well as new ones. Discussions with other fluoroscopy-system manufacturers are in progress.

CRM Geotomography Technologies, Inc.

In 2013, AAPS spun off a wholly owned for-profit company to commercialize intellectual property developed at AAPS with a TRIUMF/UBC inventor. The technology uses cosmic-ray muons, particle detectors underground, and proprietary electronics and software to identify ore bodies that lie underground between the surface and the detectors (see Figure 4.4-2). CRM is expected to be transferred to a third party for remuneration (i.e., the company will be sold for a combination of cash and long-term royalties subject to negotiation).

Geotomography detector units were installed at Nyrstar Price 13 mine on Vancouver Island, survey data collected at 12 locations and inverted using AAPS proprietary software, and images created of the rock density above the detectors. Units were installed in November at TECK Resource's Pend'oreille mine in Washington State with survey completion in June 2013. CRM will continue to pursue contract revenue from other partners.

GPN Petroleum Technology, Ltd.

In early 2013, AAPS signed a Memorandum of Understanding and has just signed a Cooperative Research and Development agreement with GPN to develop an advanced neutron well-logging system for use in detecting oil in underground deposits. GPN is investing \$800k in the joint venture and AAPS in investing \$400k (in August 2013, the first \$400k from GPN was received). Upon successful completion of this project a Canadian controlled company will be established to manufacture and market the product.

Advanced Cyclotron Systems, Inc. High-Resolution Separator

A key element of TRIUMF's future success in rare-isotope physics is the ability to select and separate out rare isotopes from a milieu of products generated in a target. One tool of the trade is a high-resolution magnetic separator (HRS). TRIUMF may have built one of these devices on its own as part of the ARIEL project; however, AAPS recognized that a niche, global market existed for these devices.

AAPS put together a business framework that proposed the transfer of HRS technology from TRIUMF to a Canadian company as part of a deal to deliver the first HRS magnet to TRIUMF and to make future sales to laboratories in Switzerland, France, Germany, Japan, and India. The framework was approved by the AAPS Board of Directors. After scanning the industry, Advanced Cyclotron Systems, Inc. (ACSI) of Richmond, BC, expressed serious interest in the core technology and the future business opportunity.

AAPS is now assisting ACSI with developing and delivering a high-resolution magnetic separator valued at ~\$2.5M to TRIUMF while building capacity for worldwide sales of the technology. AAPS will invest \$1.2M and ACSI is investing several hundred thousand dollars. When complete, ACSI will be able to market and deliver these high-precision magnets for isotope separation to dozens of major research laboratories around the world. AAPS will recover its initial investment and TRIUMF will provide technical back-stopping to ACSI with an ongoing service and royalty model. The final details are presently being worked out.

PAVAC Industries, Inc.

AAPS guides TRIUMF on opportunities to convert industrial R&D relationships into protected, licensed, royalty generating partnerships. As mentioned earlier, TRIUMF has been working with PAVAC Industries, Inc. to manufacture SRF cavities for advanced accelerators. When PAVAC indicated an interest to move from manufacturing and selling SRF cavities valued at a few hundred thousand dollars to manufacturing and selling the full cryomodule system valued at a few million dollars, AAPS proposed a structure for developing and licensing this know-how and intellectual property to PAVAC in a way that was transparent and offered downstream revenues. The first cryomodule manufactured by PAVAC will be sold in India. The company is presently negotiating contracts with Korea as well.

The world market for these superconducting devices is expected to grow, and quite dramatically, well into the next decade with applications in healthcare, environmental mitigation and remediation, advanced materials science, and high-energy physics. With an international interest in developing applications for this technology and building the industrial capacity to supply the demand, Canadian capability assures the country a good share of the global market since there are a limited number of companies capable of producing these devices.

Through its involvement with TRIUMF, PAVAC has expanded from 9 to 55 employees in five years and has tripled its floor space at its Richmond plant.

Tc-99m Target Commercialization Company

The advent of the medical-isotope crisis in late 2007 triggered TRIUMF's participation in a national effort to develop cyclotron-production of Tc-99m (see Section 4.2.3.2). AAPS is playing a key role in developing business plans, assessing market conditions, and advising on where to "monetize" this disruptive technology (see Figure 4.4-3). AAPS is providing seed capital to launch a company (ARTMS, Inc.) that will commercialize the intellectual property associated with the new supply chain (i.e. target manufacture and recycling). TRIUMF's intellectual property is rooted in the challenge of target geometry including fabrication, mounting, and recycling after production. A provisional patent has been issued.

4.4.2 RESULTS FROM TRIUMF'S INNOVATION AND INDUSTRIAL PARTNERSHIPS

In addition to direct commercialization opportunities pursued with AAPS, TRIUMF engages in innovation and industrial partnership activities that generate commercial revenues and build powerful relationships.

Commercial revenues flowing to TRIUMF during the 2008–2012 period are shown in Table 1.

	Total	2012–13	2011–12	2010–11	2009–10	2008–09
Royalties						
Nordion	4,879,360	580,745	999,812	1,546,033	1,019,872	732,898
D-Pace, Other	87,655	9,233	13,713	24,924	24,965	14,820
Subtotal	4,967,015	589,978	1,013,525	1,570,957	1,044,837	747,718
Other Income						
PIF & NIF	1,720,768	204,753	330,451	451,837	733,727	0
F-18 Production	1,688,320	39,600	3,300	493,760	490,196	661,464
Miscellaneous	689,886	293,134	94,652	112,114	69,447	120,539
Subtotal	4,098,974	537,487	428,403	1,057,711	1,293,370	782,003
Grand Total	9,065,989	1,127,465	1,441,928	2,628,668	2,338,207	1,529,721

Table 1: Commercial revenues flowing to TRIUMF for the past five fiscal years.

Nordion, Inc.

Every year Nordion, Inc. produces 2.5 million patient doses of medical isotopes from its TRIUMF-based manufacturing facility and its three dedicated medical cyclotrons. Headquartered in Ontario and with sales of \$15M–\$20M each year from this plant, Nordion is a successful publicly traded company. Nordion co-located its cyclotron-production facilities with TRIUMF because of the laboratory's national and globally unique expertise in cyclotron maintenance, repair, operation, and development. A dedicated Applied Technology Group of about 30 FTEs operate Nordion's cyclotrons at TRIUMF and funded by Nordion. This group provides an extraordinary level of reliability and performance for Nordion's machines. This activity generates a royalty revenue stream for TRIUMF as well as enormous value to patients around the world. Nordion and TRIUMF received the 2004 NSERC Synergy Award for Innovation that recognized “best practices” between the commercial and public sector.

In other examples, TRIUMF produces specific isotopes under contract, such as silicon-32 for the U.S. labs at Oak Ridge and Los Alamos.

PIF & NIF

TRIUMF's PIF (proton irradiation facility) and NIF (neutron irradiation facility) represent a competitive option for computing, networking, and aerospace companies seeking irradiation testing of their equipment. Companies pay TRIUMF for the right to access of beam and technical staff time and leave with enhanced understanding of their products, or even with certification of their products to operate in a radiation environment.

Over the past few years, many PIF & NIF customers have requested more and regular access to our high-energy facility BL1B because, while the peak of the energy distribution of protons in space is at roughly 100 MeV, the distribution does extend as high as 500 MeV. This makes testing with higher energy protons crucial.

There are very few places in the world that can offer such high neutron energies for testing; alternatives include the facility at the Los Alamos National Laboratory in the U.S. and the Svedberg Laboratory in Sweden. With access to Los Alamos sometimes difficult, a shutdown of the Swedish facility a possibility, some customers began looking for a replacement testing facility. In particular, Cisco Systems, Inc. approached TRIUMF with the idea of performing all of its focused neutron-beam testing using BL1B. TRIUMF management agreed to proceed, and the upgrade began in 2012 with Cisco Systems investing \$150k. This arrangement was brokered by AAPS, Inc. Table 2 summarizes industrial use of PIF & NIF over the past five years.

PIF & NIF Commercial Use	Number of Companies	Beam Time
2008	42 companies	737 hours
2009	39 companies	610 hours
2010	39 companies	711 hours
2011	36 companies	589 hours
2012	43 companies	667 hours

Table 2: Industrial use of PIF & NIF irradiation services at TRIUMF for the past five years.

As discussed in Section 4.2.4.6, PIF & NIF also provides beam time for academic research.

Training and Transfer of Skilled Personnel

Although difficult to model and predict, certain individuals trained at TRIUMF (either as students or as professionals attending workshops and conferences) will go on to develop technologies, start businesses, and pioneer disruptive technological advances. In the absence of a key metric, several examples are reported here.

D-Pace, Inc. is one example of the highly qualified personnel aspect of TRIUMF’s impact. D-Pace was co-founded by Morgan Dehnel in 1995 after he earned his Ph.D. from UBC based on his doctoral studies at TRIUMF. The company started as a specialized contract engineering design firm catering to research facilities and private companies in the accelerator industry. Dehnel says that his company “owes its existence and almost all of its knowledge base to TRIUMF. This includes Ph.D. training, intellectual technology transfer in accelerator-related physics and engineering, technology license agreements, and business advice related to the licensed technology items. TRIUMF and D-Pace work together in a truly team effort.” In 2007, the TRIUMF and D-Pace partnership was celebrated with an NSERC Synergy Award for Innovation.

Another example is Moe Kernani. Trained by TRIUMF as a physics Ph.D. at UBC, Kernani is Vice President of NetApp, Inc., a leading provider of enterprise data storage solutions. Prior to that Kernani was President and CEO of Bycast Inc., the world leader in storage virtualization software for large-scale digital archives and storage clouds. Bycast was acquired by NetApp in the spring of 2010. Kernani currently serves on the board of directors of the British Columbia Technology Industry Association. He is a recipient of the *Business in Vancouver* “Forty under 40” award and was named the BC Technology Industry Association’s Person of the Year for 2011.

A final example is Juergen Wendland, a 2003 particle physics Ph.D. student who worked on HERMES at Simone Fraser University and TRIUMF and later was a post-doctoral fellow on T2K and SNO. He currently leads a group of quantitative analysts in a financial software company in Surrey, BC, called FINCAD.

During the 2008–2012 period, TRIUMF organized several dozen conferences in Canada that resulted in 39,000 person-days of visitors spending funds on lodging, food, and entertainment. The result is a five-year economic impact of about \$9.8M. Given that most people attending such international conferences are from outside of Canada, the money they spend on food, lodging, and other purchases is an economic benefit to the region and to Canada. This has had a high degree of success given the international scientific reputation of TRIUMF.

Societal Benefits

TRIUMF provides research experiences and informal science education activities for students, teachers, and the public. As part of the “STEM to STEAM” movement (Science, Technology, Engineering, and Mathematics to S,T,E, Arts, and M), TRIUMF has an arrangement with Emily Carr University of Art + Design that created an Artist in Residence at TRIUMF and a Scientist in Residence at Emily Carr. This team coordinates science-art interactions students and faculty (see Section 4.3). In August 2013, the director of TRIUMF and the president of Emily Carr conducted an evening debate in downtown Vancouver discuss the role of the “creative economy” in driving progress and growth; the event launched a one-year program that will place TRIUMF research scientists in student art studios at Emily Carr on a regular basis.

TRIUMF uses beams from the main cyclotron to provide proton therapy for ocular melanoma patients primarily from across Western Canada (see Section 5.6.3 for details). Since 1995, patients with ocular melanomas have come to TRIUMF to receive treatment, achieving a local tumour control of 91%. Between April 1, 2008 and April 1, 2013, 40 patients were treated with protons during five scheduled treatment sessions each year. This brings the total number of patients treated with protons at TRIUMF since the start of the program to 170.

After ARIEL is commissioned, TRIUMF’s cooling-water plant will be regularly discharging 8-10 MW of waste heat from the main accelerator facilities at the laboratory. The nearby UBC campus has made a public commitment to sustainability and is exploring options to develop a district-energy system for pooled and shared heating and cooling for a complex of residential housing of several million square feet. The heating requirements for this neighbourhood would vary seasonally but would be less than 10 MW at peak times. The estimated savings in carbon emissions is expected to be in the order of 13,000 ton per year.

Laboratories in Europe, particularly the European Spallation Source (ESS), are pioneering efforts to connect these “suppliers” and “consumers” of heat energy. The ESS has committed to operating as a carbon-neutral research-intensive facility. In Switzerland, the PSI laboratory already provides some heating of the local neighbourhood by repurposing waste heat from its research facilities.

Together, TRIUMF and UBC are exploring the feasibility of a pilot project that would use the waste heat from TRIUMF’s cooling systems to generate heat and/or energy for the nearby residential areas. This district-energy system would be the first of its kind in North America and would demonstrate a new level of energy efficiency and innovation as well as the value of partnering to achieve greater level of sustainability.

A process is now in motion to select the private partner that would work with UBC and others including TRIUMF to deliver a viable neighbourhood utility using the district-energy concept. UBC will with the selected partner to perform due diligence on project feasibility and enter a period of exclusive negotiation in order to prepare Definitive Agreements. These Agreements would then be submitted to the BC Utilities Commission for regulatory approval, if UBC decided to move forward with development of the system with that partner. A Request for Information was issued in early 2013 and Project Information Sessions were held in March 2013. Shortlisted candidates have been interviewed and negotiations are being completed with the successful company.

TRIUMF has already made some adjustments to ARIEL infrastructure in order to accommodate this opportunity.

4.4.3 RESULTS FROM MODELING ECONOMIC IMPACT

Several approaches are used to measure the impact of scientific research, although none purport to capture it in a systematic and conclusive way. “Narrative summaries” of technological advancement arising from scientific research often focus on conjectures and reports of active exploration of potential applications. Some use “input/output models” that are indexed by spending via the laboratory—sometimes separating out labour and sometimes lumping direct capital with labour—include direct, indirect, and induced economic impacts of the spending. Others include opportunity costs, social safety nets, and/or open/closed models for induced economic impacts. At other times, these input/output models are parameterized with a representation of a laboratory’s activities, one that uses a proportional combination of existing multipliers based on the sectors in which the laboratory operates (e.g., higher education, forestry, pharmaceuticals, and contract research services) or by directly inputting the laboratory’s spending patterns into an economic model of regional economic activity. The “data collection model” uses analysis and interpolation of sample economic activities (e.g., spin-off companies and sole-source consulting/service contracts). Yet another model measures “talent” and/or activity concentration in terms of uniqueness, value added, or development/maintenance of an absorptive capacity for scientific developments.

Approaches and Limitations

One limitation to these present-day economic impact models is their limited utility in capturing and projecting the powerful underlying contributions of science-driven breakthroughs. No contemporary economic impact study is able to project which developments in science will generate whole new industries and technologies akin to quantum mechanics, transistors, computers, and e-commerce although some economists say they are able to measure retroactively the inputs that led to these outputs.⁹

TRIUMF itself has not developed a model of economic impact; that is, the laboratory does not maintain a system of “mechanisms” that relates specific activities and decisions to future impacts, nor does it maintain a matrix of metrics or indicators that images these impacts. Instead, we rely on the opinions, models, and assessments of other experts for authoritative statements of TRIUMF’s economic impact. Two such examples are 2009’s “Economic and Social Impacts of TRIUMF” by MMK Consulting, and, more recently, the May 2013 “Return on Investment in Large Scale Research Infrastructure,” by Hickling Arthurs Low (HAL).

With respect to measurement in general, the HAL study makes the following observations:

This raises an important question: “If fundamental, curiosity-driven, research is economically important, why should it be supported from public, rather than private, funds?” There are a number of classic economic arguments for why government should support basic research, all based on the concept of “market failure”, the idea that the free market, if left to itself, will under-invest in science. These arguments are founded on the belief that science is in the public interest and therefore is deserving of pursuit.

...

Because basic science is in the public interest, and because it is supported by the public, there is a strong rationale for making scientific information freely available. Because no one is excluded from using the information, and it is freely available, scientific information is, in economic terms, a “public good”.

[HAL, p18]

This observation records what is considered to be conventional wisdom: Science is good the economy, but the challenge is how to measure and manage that benefit for optimal returns. TRIUMF is no exception, and in this discussion, we press on both the academic approach as well as where conventional wisdom tells us to look for impacts.

One of the difficulties in assessing TRIUMF’s benefits is finding a way to measure downstream, value-added benefits are hard to capture in present-day modeling. HAL explicitly notes that while TRIUMF derived technologies have, for example, created Advanced Cyclotron Systems, Inc., a 110-employee company that manufactures and sells compact medical cyclotrons, the downstream impact of these sales and their subsequent operation (e.g., the Edmonton, AB, acquisition of a TR-24 device from ACSI that will generate medical isotopes and directly impact the quality of healthcare for tens of thousands of Alberta patients dealing with cancer over the next decade) is something that cannot be measured and is therefore discarded as a measure of output value and impact [HAL, p61]). In another recent example, TRIUMF has agreed to provide radiotracers via the BC Preclinical Research Consortium for use at the Centre for Comparative Medicine for two separate companies to benchmark their drug-development processes (one of Lou Gehrig’s disease, the other for protein markers associated with neurodegeneration). This involvement is critical for those business but has not yet created measurable, independent benefits.

In addition, the HAL study notes explicitly that, the “...return from a million dollars worth of technology development is essentially the same as from a million dollars worth of road building (or any other activity)” [HAL, p10]. This statement sets aside the challenge of understanding the distinct difference in economic value of labour-driven activities and high-technology goods and services activities. Put another way, quantification of the difference in value between digging trenches and manufacturing high-technology devices for international sales and distribution is difficult for present-day economic models.

Perhaps one of the largest challenges in prospective studies of economic impact is attribution, i.e. what proportion of Company X’s true value and revenues is directly attributable to its interactions with Scientific Research Establishment Y? Some studies use surveys and interviews to try and measure this attribution; others use document reviews and direct observations from investors or valuers. In reality, however, cause and effect is a human-perception phenomenon. The real world is more arbitrary and complex.

.....

“**The outputs of basic research rarely possess intrinsic economic value. Instead, they are critically important inputs to other investment processes that yield further research findings, and sometimes yield innovations.**”

P.A. David, D.C. Mowery, and W.E. Steinmueller,
Center for Economic Policy Research, Stanford University

.....

Finally, the ultimate challenge for economic impact models is establishing causation. In the simplest sense, “Which investment at what moment of time will give rise to what economic impact?” The economic impacts of science are often expected to accrue over the course of a decade, even of a complete generation. In this manner of speaking, it would seem most appropriate to consider economic inputs to TRIUMF from 1995–2005 to be cross-correlated with output measures in the 2005–2015 timeframe.

Moreover, the HAL study notes,

Despite the difficulties in quantifying the social and economic benefits, the basic policy rationale for supporting research is now effectively beyond political debate, with relevant policy discussions concerned not with whether to fund research, but how best to support research to achieve maximum benefit.”
[HAL, p17]

In short, “everybody knows” that basic research is good for the economy, but a systematic framework to monitor and manage these impacts is still missing. Nevertheless, and despite all these challenges, HAL collected considerable data from TRIUMF and contacted several leading industrial partners. The HAL analysis was based on three inputs: expenditures by TRIUMF and AAPS in Canada, revenue by Canadian businesses attributable to their relationship with TRIUMF, and spending by delegates to scientific conferences located in Canada as a result of TRIUMF’s hosting role.

Results

HAL found that four Canadian businesses have significant revenues that are attributable to their relationship with TRIUMF: Nordion, ACSI, D-Pace, and PAVAC. The value of these revenues was adjusted to prevent double counting by accounting for royalties paid to TRIUMF, contracts with TRIUMF, and fees for services from TRIUMF. The adjusted total of these revenues is \$249.7M over the last decade.

Combined with a narrative that addresses disciplinary metrics, cross-disciplinary metrics, and strategic metrics, the study reported the following:

TRIUMF has received \$630 million over the last ten years, of which \$541 million was grants from public sources and \$16 million was commercial revenue. The remaining \$73 million was flow-through transfers from other organizations. During that time, TRIUMF spent \$622.4 million on operating and improving its facilities, realizing an increase to fund balances of \$7.3 million. AAPS has received \$12.4 million since it was created four years ago, of which \$11.3 million was grants from public sources, and \$1.1 million was commercial revenue. During that time, AAPS spent \$11.8 million on its operations, realizing an increase in balances of \$0.6 million.

As a result of that investment, TRIUMF and AAPS had a direct GDP impact of \$424.9 million for the study period; the total GDP attributable to TRIUMF and AAPS was \$941.1 million. British Columbia has received 80% of this total [Hal, pg. iii].

Over the past decade, direct economic impact totaled \$424.9M; indirect economic impact totaled \$181.3M; and induced economic impact was \$334.7M. These values come from an input/output economic model developed by HAL. The total impact for Canada from TRIUMF over the last ten years was 11,733-person years of employment. About 82% of this was in British Columbia, and 45% was a direct effect.

In addition, HAL examined TRIUMF’s return on investment from five perspectives: the return to British Columbia, the short-term return to Canada, an investment choice return, the long-run return to Canada, and the return to government.

Return to British Columbia

All but \$27.3 million of \$552.2 million, or 95%, of TRIUMF's and AAPS's public funding has come from federal sources. Given that British Columbia's GDP is about 12% of the Canadian total, BC's total involvement in the economic model for TRIUMF can be estimated at \$90.3 million, with the remainder coming from the rest of Canada. For this, BC received an increase in its GDP of \$752.3M; a return of 8.3 times their investment.

Short-Term Return to Canada

In the short-term, public spending on TRIUMF is a stimulant to economic activity. The \$552.2M of public spending resulted in an increase of \$940.9M in the country's total GDP for a return of 1.7 times the investment. Note that the MMK 2008 study reported on this same indicator and found a similar multiplier of 1.91.

Investment Choice Return

Investment in TRIUMF creates indirect and induced economic impacts, but then so does most other investments of public money. Therefore, under this model, the indirect and induced impacts are irrelevant; the direct impacts are the ones that should be used to compare investment choices. From this point of view, the \$552.2M of public spending resulted in an increase of \$424.9M in direct GDP for a return of 0.77 times the investment.

Long-Run Return to Canada

In this perspective, HAL narrows the economic model to pure loan and return-of-principal economics, ignoring societal benefits altogether. Accordingly, they say that public spending on TRIUMF contributes to the nation's debt, which in the long run must be paid back. From this point of view, the public expenditures should not be considered as contributing to the benefit. This leaves \$291.1M of the increase in the country's total GDP, for a return of 0.53 times the investment.

Return to Government

From one view of government, the return on investment in TRIUMF comes from the increase in taxes generated. From this perspective, the \$552.2M investment of public money resulted in an increase of \$252.3M in tax revenues for a return of 0.46 times the investment.

It should be noted at this point that TRIUMF generates economic benefits that were not included in the HAL return-on-investment calculations, including:

- Future business revenues: technologies developed which have not yet been commercialized;
- Past business revenues: prior to the last 10 years;
- Consumer surplus benefits: some firms will receive additional benefits and stimulus from interactions beyond the specific services they charged for;
- Technology diffusion benefit: those benefits attributed to personnel trained at TRIUMF who went on to achieve benefits elsewhere; and
- Skills improvement benefits: the improvement in a company's expertise and competitiveness as a result of working with TRIUMF.

4.4.4 CONCLUSION

TRIUMF has had definitive successes in stimulating societal and economic growth, and documenting these impacts is an active challenge. Be it the patients who have retained their eyesight by proton therapy to treat their ocular melanoma or the jobs created by ACSI's success in selling TRIUMF-designed cyclotrons around the world, the laboratory is fueling the innovation chain.

Salter and Martin paraphrase the OECD: "Knowledge and information abound, it is the capacity to use them in meaningful ways that is in scarce supply." Therefore, as they say:

"No nation can "free-ride" on the world scientific system. In order to participate in the system, a nation or indeed a region or firm, needs the capability to understand the knowledge produced by others and that understanding can only be developed through performing research. [HAL, p19]

With TRIUMF's network of international connections (see Section 3.2.2), the laboratory ensures that Canada stays abreast of key science and technology developments in subatomic physics and nuclear medicine around the world, thereby contributing to overall competitiveness and, more importantly, the ability to absorb and distribute breakthroughs for Canadians.

¹ Source: Heart and Stroke Foundation

² Source: Charity Intelligence Canada

³ Source: Canadian Mental Health Association

⁴ Source: Alzheimer's Society of Canada

⁵ See, for example,

<http://www.triumf.ca/research-highlights/student-stories/dylons-corner-where-physics-medicine-collide>.

⁶ See <http://www.quantumdiaries.org>, a globally shared blogging platform organized by the InterAction Collaboration of communications leaders at the world's major particle-physics laboratories.

⁷ National Research Council, *Surrounded by Science: Learning Science in Informal Environments*, Washington, D.C.: National Academies Press, 2009.

⁸ See <http://www.triumf.ca/research-highlights/student-stories/former-student-builds-mini-accelerator> and <http://www.triumf.ca/headlines/current-events/past-triumf-student-tedxkidsbc>.

⁹ See, for example, B. Godin and C. Doré, "Measuring the Impacts of Science: Beyond the Economic Dimension," retrieved from URL <http://www.csiic.ca> on 01 Aug 2013; R. Solow, "Technical Change and the Aggregate Production Function," *Review of Economics and Statistics*, 39, August, pp. 312-320; and Smith, Llewellyn (1997) "What's the Use of Basic Science?" http://www.jinr.ru/section.asp?sd_id=94.